5-1-2016

Physiology and Genetics of Starvation-Selected Drosophila melanogaster

Christopher Michael Hardy
University of Nevada, Las Vegas

PHYSIOLOGY AND GENETICS OF STARVATION SELECTED *DROSOPHILA MELANOGASTER*

By

Christopher M. Hardy

Bachelor of Science – Biological Sciences
University of California Irvine
2008

A dissertation submitted in partial fulfillment
of the requirements for the

Doctor of Philosophy -- Biological Sciences

School of Life Sciences
College of Sciences
The Graduate College

University of Nevada, Las Vegas
May 2016

UNLV | GRADUATE COLLEGE

Dissertation Approval

The Graduate College
The University of Nevada, Las Vegas

April 5, 2016

This dissertation prepared by

Christopher M. Hardy

entitled

Physiology and Genetics of Starvation Selected *Drosophila melanogaster*

is approved in partial fulfillment of the requirements for the degree of

Doctor of Philosophy – Biological Sciences
School of Life Sciences

Allen Gibbs, Ph.D.
Examination Committee Chair

Kathryn Hausbeck Korgan, Ph.D.
Graduate College Interim Dean

Laurel Raftery, Ph.D.
Examination Committee Member

Andrew Andres, Ph.D.
Examination Committee Member

Martin Schiller, Ph.D.
Examination Committee Member

Amei Amei, Ph.D.
Graduate College Faculty Representative

ABSTRACT

Physiology and Genetics of Starvation-selected *Drosophila melanogaster*

By

Christopher M. Hardy

Dr. Allen G. Gibbs, Examination Committee Chair
Associate Professor of Biological Sciences
University of Nevada, Las Vegas

In nature, organisms have evolved to survive in stressful environments. This has driven organisms to adopt a wide range of unique adaptations. Investigating the mechanistic basis of these adaptations is an important tool for discovery that has led to major advances in science and medicine.

We study how organisms survive life without food, or starvational stress. Environmental stressors have shaped the quantity and quality of food sources across the globe. This has led to vast differences in the ability of some organisms to tolerate starvation over others. Many researchers have used *Drosophila melanogaster* as a model to study global patterns of variation in starvation resistance. We complement this approach by experimentally evolving populations of *D. melanogaster* to become starvation resistant in the laboratory.

Starvation-selected *D. melanogaster* are ~3-4 times more resistant to starvation than their unselected controls. They do this primarily through an increase in stored lipids. Excess fats provide an abundant source of energy that can be metabolized to fuel all aspects of life when nutrients are scarce. However, the enhanced ability to survive starvation and store high levels of body fat comes at a cost to many other aspects of fitness. These evolutionary tradeoffs include a developmental delay, decreases in fecundity, metabolic

rate, activity levels and flight performance and disrupted sleeping patterns. Because some of these phenotypes are characteristic of metabolic disorder in mammals, we use starvation-selected *D. melanogaster* as a model to study the physiological and genetic basis of obesity.

Obesity is one of the leading risk factors for heart disease. Here, we tested the hypothesis that heart function is an evolutionary tradeoff with starvation resistance. We found that the hearts of starvation-selected *D. melanogaster* were dilated and poorly contractile- a condition known as dilated cardiomyopathy. We observed that heart dysfunction was highly correlated with increased fat tissue located between the heart and dorsal cuticle. The excess tissue physically altered the gross anatomical placement of the heart. Further experiments led us to suspect that this physical interference was the primary source of dysfunction. During these analyses we also discovered that the starvation-selected flies avoided lipotoxicity in the heart. Lipotoxicity is a common mechanism of obesity-associated heart dysfunction where excess lipids are ectopically stored within the myocardium. Instead, we found that the fat body of the starvation-selected flies contained very large lipid droplets whose estimated increase in volume could account for the ~2-fold whole body increase in total lipids. We hypothesize that the increased lipid droplet volume in the fat body of the selected populations is an adaptive response to increase the amount of stored lipids for starvation resistance, while limiting the harmful effects of lipotoxicity in peripheral tissues.

We were next interested in exploring the genetic basis of adaptation to starvation selection. To do this, we resequenced genomic DNA from the starvation-selected populations and their fed controls after 83 generations of starvation-selection. In total we

found 1,046,373 polymorphic sites, with many loci diverging between selection treatments. We found evidence for genetic heterogeneity between the replicates of the selected populations. The relative genetic differences between the starvation-selected replicates were physiologically relevant, as they correlated with differences in starvation resistance. We surveyed the genome for signatures of selection and found many large troughs in heterozygosity that approached fixation within the selected populations. These regions were variable across selected replicates, consistent with hard selective sweeps. In addition to these extreme regions of reduced heterozygosity, we found many locations across the genome that differed in allele frequency between selective treatments. To identify which regions were divergent due selection, we generated a novel algorithm to filter the effects of genetic drift from the dataset. After applying our drift filter, we mapped SNPs within each population to sets of genes. We focused on the most conserved mechanisms across replicates and found 1,453 genes, which were associated with a SNP under selection in all three replicate populations. These genes were enriched for many biological processes, including many associated with the evolved physiologies of the starvation-selected populations, including regulation of metabolism. Many of the candidate genes were found within the insulin and adipokinetic hormone-signaling pathways. 542 of the candidate genes are previously uncharacterized in *D. melanogaster*. These genes can be functionally validated for their potential role in starvation resistance and lipid metabolism in future studies.

Finally, we performed experiments to investigate the mechanistic basis of the ~24 hour delay in larval development in the starvation-selection populations. This delay provides starvation-selected larva more time to feed and accumulate lipids that are then

used for adult starvation resistance. In *D. melanogaster* a large pulse of the steroid hormone 20-hydroxyecdysone (20E) occurs near the end of larval development. This late-larval 20E pulse initiates a transcriptional cascade that commits the animal to pupariation. Our preliminary data suggest that the developmental delay in the starvation-selected populations is the result of a delay in the timing of the 20E pulse. If this hypothesis is correct, 20E-induced gene expression should be similar in the selected populations and their unselected controls at the onset of pupariation. To test this we resequenced the transcriptome of the larval fat body in the selected populations and their unselected controls during and after the onset of pupariation. We found that a large fraction of differentially expressed genes had similar patterns of expression between samples of the selection treatments. These data suggest that 20E-signaling functions similarly in both groups, just at a different time point in response to selection. However, there was a smaller, yet significant number of genes which were differentially expressed in response to selection. Furthermore we found that expression profiles differed among replicate populations of the starvation-selected line. Taken together, these results suggest that selection may have altered the timing of the late-larval 20E pulse, as well as the tissue-specific response to the 20E signal. These findings provide further insight into the mechanistic basis of the ~24 hour delay in larval development, which will be explored in future studies.

.

ACKNOWLEDGMENTS

I am extremely appreciative for the tremendous amount of help that went into making this work possible. First and foremost I would like to thank my family. From an early age they taught me to work hard, be independent and think critically. However, most importantly, they taught me to love exploring the world. My family has grown during my time at UNLV to include my wife, Christensen Hardy and her beautiful family. My entire family has consistently, tirelessly and lovingly gone out of their way to allow me to pursue this work to the best of my ability. I am forever grateful.

From an academic standpoint I am thankful to both Michael Rose and Molly Burke, who first inspired me to pursue biology and mentored me along my path to graduate school. Through them I met my academic advisor, Allen Gibbs. Allen is a brilliant scientist. He is an even better person. He taught me to write short, declarative sentences. He never yelled at me more than he had to when I would set off the fire alarm, and he was always there to open my office door when I locked my keys inside. He gave me the freedom to study anything I was interested in and was *never* too busy to offer advice, or help me figure out a problem in the lab. I am honored to have worked with him over the past six years and know that I will never find a mentor that is more dedicated to his students than Allen.

I have repeatedly been overwhelmed by the support I have received from the science community. Often times if I had a question that could not be addressed with the resources at UNLV I would blindly reach out to other researchers in the field. Specifically, I would like to thank Ryan Birse and Rolf Bodmer from the Sanford Burnham Institute for teaching me new methods and lending me their facilities to perform the work. I would also like to thank Matthew Wolf from the University of Virginia School of Medicine and Lin Yu

from the Duke School of Medicine for their generous contribution of time and resources. Finally I thank Logan Everett from North Carolina State University for helping me develop computational solutions to improve our experiments.

Here at UNLV there have been countless people who have helped guide and support me through my graduate career. First I would like to thank my graduate committee. They held me to a high standard, which greatly improved the quality of the work. Outside my committee I would like to thank Mira Han who helped me develop my ideas for the genomic work and provided excellent feedback. I have also been supported by many other graduate students at UNLV. In particular, I would like to thank friend/collaborator Katie Lantz who was always there to help with experiments and keep me moving forward.

Science makes big progress in small, incremental steps. Thank you to everyone that has helped each step of the way.

DEDICATION

To my wife, Christensen-

I wouldn't be here without you,

And I wouldn't want to be anywhere without you.

TABLE OF CONTENTS

LIST OF TABLES

LIST OF FIGURES

CHAPTER 1

LABORATORY SELECTION FOR STARVATION RESISTANCE IN *DROSOPHILA MELANOGASTER*: OBESITY AT WHAT COST?

1.1 Experimental evolution is a powerful tool to test evolutionary theory and study how organisms adapt to stressful environments.

In nature, organisms must constantly adapt to a wide variety of stressors, which are dynamic and largely unpredictable. Adapting to these changing environments takes place on many different timescales ranging from daily or seasonal shifts in physiology to long-term evolution by natural selection. Evolution has generated a wide range of variation between organisms that allow them to thrive even in extreme environments. Examples from nature are diverse, from deer mice surviving in severely hypoxic mountain ranges (Carey et al. 2012) to thermophilic bacteria in hydrothermal vents (Brock and Freeze 1969). Investigating how organisms adapt to extreme environments is a powerful tool that has led to important advances in modern sciences and medicine. The long history of studying uniquely adapted organisms was popularized by the Danish physiologist, August Krogh, who stated, "For many problems there is an animal on which it can be most conveniently studied" (Krebs 1975). Application of the Krogh Principle in practice has led to important scientific advances including the use of highly metabolic pigeon breast muscle to uncover the tricarboxylic acid cycle (Krebs and Johnson 1980), the isolation of heat-stable DNA polymerase from the thermophilic bacterium *Thermus aquaticus* to facilitate

polymerase chain reaction (Chien et al. 1976) and the use of giant squid axons to determine the ionic basis of action potentials (Hodgkin and Huxley 1952).

A complimentary approach to studying uniquely adapted organisms in the wild is to perform evolution experiments in the laboratory, where environmental stresses can be mimicked by an investigator under highly controlled, replicated designs (Bennett 2003; Garland and Rose 2009). In such an experiment, a founding population is established then subjected to either an environmental stress or a control condition, which are handled in parallel for many generations. Populations exposed to selective pressures may then adapt and evolve mechanisms that enhance their fitness in the novel environment. Traditionally, experimental evolution has been implemented to both test theories of evolution and investigate the physiological basis of adaptation to novel environments (Garland and Rose 2009; Kawecki et al. 2012). Because these types of studies can be highly replicated, it is possible to distinguish random stochastic processes such as genetic drift from conserved mechanisms of evolution, which are difficult to differentiate in natural populations. Although in theory experimental evolution can be performed on any population, practical considerations have limited these studies to organisms with relatively short generation times and low cost of maintenance. Interpretations of these experiments are further limited by low population sizes and number of generations compared to macroevolutionary processes in the wild. Despite these limitations, evolution experiments afford the opportunity to directly test predictions and hypotheses derived from evolutionary theory to address a wide range of questions on the repeatability of evolution, mechanisms of speciation, life history tradeoffs and the maintenance of variation by disparate evolutionary

processes (i.e. genetic drift, mutation rates, ect.: reviewed in Kawecki et al. 2012 and the references therein).

Because of the dynamic nature of evolution, *a priori* expectations for adaptive outcomes in selection experiments are often misguided as organisms may adopt a variety of unanticipated solutions (Bennett 2003; Garland and Rose 2009). In many cases experimental selection generates biological novelty, resulting in organisms which are functionally enhanced over their unselected controls or similar organisms in nature (Bennett 2003; Garland and Rose 2009). Understanding the mechanistic basis of these improvements has the potential for translational impact (e.g. extended longevity in Drosophila: Rose 1984; improved running performance in mice: Garland Jr. 2003). Some of the best examples come from evolution experiments in microbes, which can evolve quickly and be maintained in large population sizes. Such studies have played important roles in vaccine development, particularly in serial passage experiments where pathogens are introduced into a novel species and allowed to adapt across multiple passages. After several passages the virulence of the pathogen increases as it adapts to the new host. These adaptations incur evolutionary cost, leading to attenuated pathogenicity in the former host. This approach has been used in the development of some live vaccines (Ebert 1998).

The capacity for experimental evolution to drive discovery has been further enhanced by the increased accessibility of genetic sequencing over the past decade. Some early studies were able to track the trajectories of adaptive alleles over the course of natural selection by looking at multiple genetic markers across a single chromosome in *Drosophila* (Teotónio et al. 2009). Since that time, exponential improvements in deep sequencing technologies have driven down costs and made whole-genome sequencing of

organisms under selection a powerful new paradigm in experimental evolution. In one study, a malaria inducing parasite, *P. chabaudi*, was selected for drug resistance against an array of common malarial medications (Hunt et al. 2010). The evolved strains were fully sequenced and genes that confer drug resistance were proactively identified before any such mutation had occurred in nature. This type of study could allow health industries to proactively develop diagnostic tests and therapeutic interventions.

Over the past several years, studies combining experimental evolution with whole genome sequencing have been called "Evolve and Resequence" experiments (E&R; Turner et al. 2011). While E&R experiments have been performed in many organisms (Johansson et al. 2010; Rubin et al. 2010; Parts et al. 2011; Kelly et al. 2013; Beissinger et al. 2014; Burke et al. 2014), they have paired particularity well with the *Drosophila* model largely due to its short generation time, fully sequenced reference genome and the wealth of genetic resources. This paradigm has been used to address fundamental questions about the evolutionary patterns of adaptation and to uncover the genetic basis of evolved physiologies. To date, many E&R experiments have been performed in *Drosophila*, selecting for a variety of different traits including hypoxia tolerance, longevity, courtship song, body size, development time, desiccation resistance, high temperature and resistance to both the parasitoid *Asobara tabida* and the *Drosophila* C virus (Burke et al. 2010; Turner et al. 2011; Zhou et al. 2011; Orozco-terWengel et al. 2012; Remolina et al. 2012; Turner and Miller 2012; Jalvingh et al. 2014; Martins et al. 2014; Kang et al. 2016).

While the field will continue to improve by refining design parameters to increase the power to detect rare variants (Baldwin-Brown et al. 2014; Kessner and Novembre 2015), studies in pre-existing evolved populations have made several exciting discoveries.

In particular they have found complex patterns of adaptation. For instance, most E&R studies in *Drosophila* have found that selection acts on standing genetic variation rather than *de novo* mutations (Burke 2012; Long et al. 2015; but see Kang et al. 2016). This leads to large numbers of polymorphisms that shift in frequency in response to the evolutionary treatment. However, the trajectories of adaptive alleles may vary across evolutionary time. For instance, one E&R study found that while some alleles rose quickly and plateaued, others steadily increased across generations (Orozco-terWengel et al. 2012). In any case, as an advantageous allele sweeps towards fixation within the population, it pulls along linked regions of flanking DNA (Smith and Haigh 1974). This process is known as genetic hitchhiking, and it results in localized areas of reduced heterozygosity across the genome. Genome-wide scans of heterozygosity are therefore useful in identifying signatures of selective events. E&R studies have identified genes in close proximity to these signatures of selection and in some instances discovered pathways involved in adaptation (Burke et al. 2010; Turner et al. 2011; Zhou et al. 2011; Orozco-terWengel et al. 2012; Remolina et al. 2012; Turner and Miller 2012; Jalvingh et al. 2014; Martins et al. 2014). An important limitation of this approach is that linkage disequilibrium (LD) has been found to increase in experimentally evolved populations of *Drosophila* (Teotónio et al. 2009; Franssen et al. 2015). High LD may artificially inflate the number of genetic variants associated with selection. Fortunately, there are many genetic tools within the *Drosophila* research community that can be used to functionally validate candidate loci.

Identifying the genetic basis of complex traits is a long-standing goal for many scientific fields and E&R studies will certainly be a powerful tool of discovery in future efforts. These studies will continue to achieve greater resolution by using larger population

sizes, increasing the number of evolutionary replicates, sequencing individual organisms at greater depths and improving techniques to functionally validate putative loci. To date, E&R studies are only scratching the surface of what will be possible as techniques improve and experimental evolution is paired with other "omics" methodologies. For instance, RNA-sequencing can be used on experimentally evolved populations to study how adaptive alleles lead to functional changes in gene expression within specific tissues. Furthermore, chromatin immunoprecipiation sequencing (CHIP-seq), can be used to test how the functional organization of the genome may respond to selection. These approaches will offer new insights into how organisms respond and adapt to evolutionary pressures on the cellular level. This will improve our ability to address fundamental questions of how organisms adapt to stressful environments.

1.2 Laboratory selection for starvation resistance in *Drosophila* shifts energetic homeostasis, leading to an obese phenotype with associated evolutionary tradeoffs.

Acquisition, storage and utilization of nutrients are fundamental processes of life, required to generate the energy necessary for development, maintenance and reproduction. However, nutritional resources are constantly changing in the wild as environmental stressors shape the quantity and composition of available food. When energy resources become scarce, organisms may adapt by increasing energy storage, decreasing energy utilization or lowering the amount of energy required to survive (Rion and Kawecki 2007; Gibbs and Reynolds 2012). These adaptations affect biological decisions on when and where to divert energy resources, which ultimately has a large impact on fitness. This makes the underlying processes subject to natural selection, which has led to evolved differences in the ability of organisms to survive starvation. Understanding the nature of energy resource allocation and how organisms cope with dietary stress is a topic of considerable interest to evolutionary physiologists and has been widely studied in *Drosophila*.

In natural populations extensive variation in starvation tolerance exists both within and among species of *Drosophila* across the globe (van Herrewege and David 1997; Gilchrist et al. 2008; Sisodia and Singh 2010). The differences in the ability to survive starvation between species can be quite dramatic. For example, *D. seschellia* from the tropical African Island of Seychelles can survive only a day without food, whereas *D. arizonesis*, which are endemic to the Sonoran Desert in the southwest United States, can live just over a week (van Herrewege and David 1997). Intraspecies differences are generally not as pronounced, however when species are distributed across a wide

geographic range, adaptation to local environments may drive differentiation. For example, French and Congolian populations of *D. melanogaster* were shown to differ ~1.67 fold in starvation survival (van Herrewege and David 1997). Regional differences in starvation resistance are likely genetic as hybrids of *D. melanogaster* from diverse habitats display intermediate levels of starvation resistance (Kennington et al. 2001). Despite intensive efforts to understand the environmental factors that influence the evolution of starvation resistance, there is still no clear explanation for the geographic patterns of variation observed in *Drosophila* (Gibbs and Reynolds 2012).

Experimental evolution for starvation resistance

In order to better understand the physiological basis of adaptation to starvation, many studies have simulated starvational stress in the laboratory and evolved populations of *D. melanogaster* to become starvation resistant (Rose et al. 1992; Harshman and Schmid 1998; Reynolds 2013). Because starvation resistance in *D. melanogaster* is extremely variable and highly heritable, adaptation occurs rapidly (Service and Rose 1985; van Herrewege and David 1997). Within as few as 5-10 generations, starvation survival in the selected populations significantly increases over the unselected controls (Rose et al. 1992; Harshman and Schmid 1998). Over many generations selection greatly exaggerates this difference, allowing some populations to survive 3 to 4 times longer without food (Chippindale et al. 1996). This amounts to an absolute starvation survival duration of ~220 hours, which is well outside the ~60-110 hour range measured from natural populations of *D. melanogaster* (van Herrewege and David 1997; Karan et al. 1998).

A common adaptation to starvational stress in both laboratory selection experiments and in wild populations is to increase the amount of stored lipids (Chippindale et al. 1996; van Herrewege and David 1997; Harshman et al. 1999; Schmidt et al. 2005; Ballard et al. 2008; Sisodia and Singh 2010; Schwasinger-Schmidt et al. 2012; Goenaga et al. 2013; Aggarwal 2014). Lipids are critical for surviving starvation, as they are more energetically dense than proteins and carbohydrates and are mobilized under chronic conditions to supply the energy required for survival (Marron et al. 2003; Lee and Jang 2014). The overall lipid content in starvation-selected populations is much higher than typically found in nature and may increase as many as 3-4 times over unselected control populations (Chippindale et al. 1996; Gibbs and Reynolds 2012). These evolved differences in body fat composition are primarily due to an increase in the amount of triglycerides (TG) and not other major classes of lipid molecules (Harshman et al. 1999; Schwasinger-Schmidt et al. 2012). The overall increase in stored TGs correlates with differential activity of several enzymes associated with lipid biogenesis (Harshman et al. 1999). This indicates that starvation selection may act on variation involved in controlling metabolic homeostasis.

In addition to increasing energy storage, adaptation to starvational stress may also include a decrease in energy utilization (Gibbs and Reynolds 2012). *Drosophila* species differ in their starvation resistance per microgram of lipid, which suggests that some species may have evolved mechanisms to utilize their lipid resources more efficiently than others (Sharmila Bharathi et al. 2003). One potential mechanism to decrease energy expenditure would be to reduce metabolic rate. This is a common physiological response to acute starvation in *Drosophila* (Djawdan et al. 1997). However, the effect of laboratory

selection for starvation resistance on metabolic rate remains unclear (Gibbs and Reynolds 2012). While some studies suggest that selection reduces the mass-specific metabolic rate per fly, the effect is abolished when the mass of the non-metabolically active lipids are removed from the equation (Djawdan et al. 1997; Harshman et al. 1999). Others have been unable to replicate these findings, reporting no difference in metabolic rate per fly (Harshman and Schmid 1998). In some instances, the effects of starvation-selection on metabolic rate differed between the replicated populations under selection within the same experiment (Baldal et al. 2006). This study by Baldal et al. found that males from some replicate starvation-selected populations had even evolved a slight *increase* in metabolic rate (Baldal et al. 2006).

In addition to a reduction in metabolic rate, energy utilization could be decreased by adaptations that disrupt locomotion or reduce physical activity. However these data have also varied by experiment. While one study reported that starvation-selected flies were ~3 times less active than their controls (Williams et al. 2004), another found only a non-significant trend towards lower activity levels (Schwasinger-Schmidt et al. 2012).

The ambiguous results from these studies on energy utilization may be the result of variations in experimental design and the evolutionary history of the founding populations. For example, genetic variation in the founding populations of each experiment may have predisposed selection to act on alternative adaptive pathways, some of which may have led to phenotypes of reduced energy utilization. Furthermore, each experiment differed in the strength of selection and the number of generations in which it was imposed. These differences in experimental design could have impacted the evolutionary trajectories of alleles involved in energy homeostasis. However, the experiments described here only

sampled phenotypes after a relatively low number of generations of selection. It is possible that genetic variation associated with energy storage evolves quickly, while adaptations to reduce energy utilization are a more long-term evolutionary response. This hypothesis could explain why increased lipid storage is commonly observed in starvation-selection experiments, while reduced metabolic rate and physical activity are more equivocal. There is evidence to support that energy storage may be a "quick" adaptive phenotype in natural populations of *Drosophila*. For instance, *Drosophila* evolve quickly in response to selective pressures imposed by seasonal variation, which can drive rapid allelic change (Bergland et al. 2014). Studies have found naturally occurring polymorphisms in key metabolic genes that affect lipid storage and starvation resistance, which fluctuate seasonally and directionally across latitudinal clines (Paaby et al. 2010; Paaby et al. 2014). When these natural polymorphisms were crossed into a wildtype genetic background, they led to significant changes in lipid weight and starvation resistance (Paaby et al. 2014). Energy storage may then be affected by alleles with relatively large effect sizes that may oscillate quickly within a population. This could explain how starvation resistance and lipid weight evolve in as few as 5-10 generations in starvation-selection experiments (Rose et al. 1992; Harshman and Schmid 1998). The phenotypes associated with energy utilization may be more genetically diverse with smaller effect sizes, which would be driven by long-term environmental pressures. Tracking the evolution of these adaptations over a longer evolutionary time frame may provide further insight in future starvation-selection experiments. Regardless of the underlying evolutionary forces, starvation-selected *Drosophila* consistently adapt through profound shifts in energetic homeostasis, highlighted by large increases in stored fats.

Evolutionary tradeoffs associated with starvation resistance

Lipids are a vital resource to survive periods of low nutrient availability in the wild. However, as energy resources are diverted towards lipid storage, energy needed for life history traits such as reproduction, development or longevity may be reduced. This can lead to evolutionary tradeoffs, where starvation resistance is gained at a cost to other important fitness parameters.

In *Drosophila* energy stores are largely accumulated throughout larval development and stored in larval fat cells. These resources are required for the growth of developing tissues during metamorphosis and persist throughout the first several days of adult life (Gibbs and Reynolds 2012). In the young adult fly, larval fat cells will undergo programmed cell death and release energy which may be used to promote reproduction or to resist starvation in nutrient poor environments (Aguila et al. 2007; Aguila et al. 2013). Selection for starvation resistance commonly leads to a delay in larval development (Chippindale et al. 1996; Harshman et al. 1999). This delay increases larval feeding time, leading to the acquisition of greater energy stores that can be used for adult starvation resistance (Chippindale et al. 1996; Harshman et al. 1999). Indeed, freshly eclosed starvation-selected adults are already 80% more starvation resistant than their unselected controls (Chippindale et al. 1996). One then might expect that under fed conditions, starvation-selected populations would have greater reserves to invest towards reproduction. However this is not the case, as starvation-selected populations display low fecundity (Wayne et al. 2006). This may suggest that starvation selection programs flies to resist allocating energy towards reproduction as a cost to improve starvation resistance. This tradeoff is also observed in natural populations of *D. melanogaster* where the amount of

ovarian lipids are positively correlated with fecundity and negatively correlated with starvation resistance (Kalra and Parkash 2014). While the mechanisms that drive this tradeoff are poorly understood, genetic manipulations that alter the accessibility of lipids from the larval fat body during either metamorphosis (*Ilp6*, Bai et al. 2012) or adulthood (*diap1*, Aguila et al. 2013) increase starvation resistance at the expense of fecundity.

Experimental selection for increased longevity leads to a correlated increase in starvation resistance, which may suggest that these traits share a common genetic basis (Rose et al. 1992). Therefore, experimental selection for starvation resistance should lead to a correlated increase in longevity. However the results from starvation-selection experiments are equivocal, with studies finding increases, decreases or no difference in the lifespan of starvation-selected populations (Rose et al. 1992; Harshman et al. 1999; Archer et al. 2003). This paradox was resolved by tracking both traits over the course of a starvation-selection experiment. It was found that while each trait initially improved in response to selection, longevity began to decline in later generations despite continued improvements in starvation resistance (Archer et al. 2003). The concurrent improvements in starvation resistance and longevity in the early generations may have been due to selection on genetic variation associated with generalized stress resistance. However after many generations of selection, loci that independently improve starvation resistance likely accumulated, some of which had a negative impact on longevity (Archer et al. 2003; Rion and Kawecki 2007).

In both natural populations and selection experiments, adaptation to low energy environments shifts genetic variation in energetic homeostasis in favor of storage and retention, which leads to evolutionary costs. In other words, flies can be genetically

predisposed to become obese and genes that favor fat storage can have a negative impact on fitness. Because energy allocation is important to all organisms, some thought starvation-selected *Drosophila* could be used as a model to address some of the basic questions related to obesity in humans. While this will be discussed in greater detail in a later section, the primary focus of this dissertation will be to use starvation-selected *Drosophila* as a model to understand the genes that contribute to obesity and how excess fats promote disease.

1.3 Obesity is a complex condition caused by interactions between many different environmental and heritable factors.

Global rates of human obesity are at an all time high. This is a major health concern because obesity is a leading risk factor for many preventable diseases, which impact the quality and duration of life. While the mechanistic basis of these associations is an area of intense research, studies have shown that increased body mass index (BMI; kg/m^2), is a risk factor for reduced lifespan and strongly associates with cardiovascular disease, type-II diabetes and certain types of cancer (Ng et al. 2014; Segula 2014; Arnold et al. 2016). Obesity is also a common feature of the metabolic syndrome, a multi-factorial clinical state, in which patients are at high risk for cardiovascular disease and type-II diabetes (Grundy 2015). In addition to its implications in human health, treatment of obesity and its associated disorders is expensive which has profound economic consequences. While the medical costs that are directly attributable to obesity may be challenging to assess, a comprehensive review of 33 independent analyses estimated the medical costs of overweight and obesity in the United States to be nearly 114 billion dollars in 2008 alone (Tsai et al. 2011).

Most countries around the world have reported exponential increases in the number of individuals with Body Mass Indices (BMI; kg/m^2) greater than thirty, since 1980 (Stevens et al. 2012; Ng et al. 2014). In 2008, the number of obese individuals worldwide increased to approximately 486-530 million with the total number of overweight (BMI>25) individuals projected to have reached 1.41-1.51 billion (Stevens et al. 2012). Despite these large global patterns, population-level obesity rates range drastically, with rates among age-standardized females as low as 1.4% in Bangladesh to 74.8% in Nauru in 2008

(Stevens et al. 2012). The acceleration of obesity rates also varies by nation. For example, in many developed nations the rates of obesity increase have slowed over the past 10 years, with childhood obesity rates beginning to stabilize in some of these countries as well (Olds et al. 2011; Ng et al. 2014). While it is likely that large-scale trends in global obesity are due to technological advances that promote calorie-rich diets and decreased physical activity (Malik et al. 2012), population-level differences and shifting growth rates in developed nations are largely unexplained. While further understanding of these complex patterns will assist epidemiological efforts moving forward, the total number of affected individuals remains exceptionally high and will only continue to grow as obesity rates are expected to rise in much of the developing world (Ng et al. 2014).

While human health concerns and staggering medical costs have driven research focused on understanding the etiology of obesity and its associated disorders, there is still much that remains unknown. It has become clear that obesity is a complex condition that is shaped by the interactions between many environmental and heritable factors. Fundamentally, obesity is an issue of energy imbalance. Factors that either increase energy acquisition and storage or decrease consumption will drive a positive energy balance and promote fat accumulation. However stored fats do not affect everyone equally. Individuals with similarly high BMIs may completely differ in their risk of developing metabolic disorders (Despres 2012). Complications arising from obesity are more dependent on *where* and *how* fats are stored than the total amount alone. Individual differences in body fat distribution play a critical role in the progression of many diseases with the main distinction made between subcutaneous and intraperitoneal (or visceral) fat stores. Studies suggest that subcutaneous adipose tissue generally provides a benign neutral reserve for

stored fats while visceral adipose tissue is highly associated with cardiometabolic risk (Shimabukuro et al. 2013). Subcutaneous and visceral adipose tissues have a fundamental limit on the amount of fat they can store. When this limit is exceeded, lipids become ectopically stored within the cells of the internal organs (Bastien et al. 2014). High levels of ectopic fat lead to a phenomenon called lipotoxicity, a toxic cellular state that is highly correlated with structural and functional deterioration of the organ (Bastien et al. 2014).

Genetics play an important role in the distribution of these fat depots. This is particularly apparent in individuals with lipodystrophic disorders, where low levels of subcutaneous adipose tissue lead to the accumulation of ectopic fats and severe metabolic disorders (Nelson et al. 2013; Nolis 2014). While lipodystrophic disorders highlight extreme perturbations of lipid homeostasis, a wide-range of genetic variation in human populations likely exists, generating a large distribution of individual susceptibilities.

Differences also exist in the cellular forms and function of adipose tissue itself as various factors may promote a shift in adipocytes favoring energy storage (white adipose tissue) to those capable of utilizing energy to generate heat (brown adipose tissue; Schulz and Tseng 2013). While white and brown adipose tissue mark the extreme cellular subtypes, an array of "beige" adipocytes lay in-between, increasing the potential for cellular variation (Harms and Seale 2013).

It has long been accepted that obesity is highly heritable, ranging from 20-80% across various studies (Maes et al. 1997). Over the past 15 years, a large number of genome-wide association studies have attempted to elucidate the genetic basis of obesity. While the number of identified candidates remains relatively low, we have learned more

about the genetic basis of obesity in the past 10 years than in any point in human history and have come to understand that it is an extremely polygenic condition.

Obesity may also be acquired through non-genetic mechanisms of inheritance, such as epigenetic regulation of the intrauterine environment (Stöger 2008). While epidemiological studies support the idea that maternal nutrition influences the metabolic state of the child, the mechanistic basis of this association is poorly understood (Ravelli et al. 1976). However, a growing body of evidence suggests that parental influences are associated with both changes in chromatin structure through histone modifications and DNA methylation, and deposition of non-coding RNAs (Burgio et al. 2015). Another factor contributing to obesity that has recently gained interest is the effect of the gut microbiome on host metabolism. While the mechanistic basis of these associations are still poorly understood, the relative compositions of gut microbial species have been linked with different cardiometabolic disease states, and are thought to influence chronic inflammation (Aron-Wisnewsky and Clément 2015; Miele et al. 2015).

The current state of obesity may then be driven by global-scale changes in food production and availability, a shift towards sedentary lifestyles, genetic variation influencing the quantity, quality and distribution of stored fats, and epigenetic forces that program the metabolic profile of the fetus *in utero*. This has led to a wide range of theories on the evolutionary origins of obesity which are not necessarily mutually exclusive and likely not exhaustive (Genné-Bacon 2014). Here we will briefly discuss some of the environmental and genetic factors that are thought to shape obesity as well as the current theories on the evolutionary origins of obesity.

Environmental factors including the increased accessibility of calorie dense foods and a shift towards a sedentary lifestyle are important drivers of the current state of obesity.

Food intake and physical activity are two factors that balance energy homeostasis, affecting the rates of energy input and utilization respectively. Over the past several decades technological advancements have shifted the quantity and quality of global food supplies and reduced the amount of physical labor required for many aspects of life (Hill et al. 2003; Hill 2006; Swinburn et al. 2011; Hallal et al. 2012). These factors have created an environment where total energy consumption exceeds utilization, generating a positive energy balance that is believed to be the primary cause of increased obesity around the world (Hill et al. 2003; Crino et al. 2015). Obesity is generally thought of as a chronic condition in which fat stores gradually accumulate over time. Some analyses have found that a net increase in total daily energy as low as 15 kcal is sufficient to drive yearly increases in body weight of ~1.8-2.0 pounds in 20 to 40 year old adults (Hill et al. 2003). Understanding the factors that shape a positive energy balance along with their global distribution will lead to better predictions of obesity rates around the world and offer insight into intervention strategies.

Dietary changes have largely increased the amount of consumed energy in nearly every part of the world (Vandevijvere et al. 2015). In fact, highly processed, calorie dense foods have become so readily available that health issues related to over-nutrition have become more prevalent than under-nutrition on a global scale (Crino et al. 2015). Wholesale shifts in the world's food supply have been driven by technological advancements that have made nearly every aspect of production more efficient from agricultural innovation to improvements in production, shipping and preservation

(Christian and Rashad 2009; Crino et al. 2015). The industrialization of food production has greatly reduced costs and initiated a transition towards the consumption of ultra-processed foods, which have been shown to contain higher levels of total energy due to increased levels of sugar, saturated fat and sodium (Christian and Rashad 2009; Monteiro et al. 2011; Moubarac et al. 2013; Baker and Friel 2014). Problems associated with processed foods are exacerbated by the increased consumption of sugary beverages, particularly carbonated soft drinks which are one of the most important factors driving the increased global consumption of sugar (Nielsen and Popkin 2004; Moubarac et al. 2013; Baker and Friel 2014). Processed foods also typically lack key macronutrients including protein and fiber (Monteiro et al. 2011; Moubarac et al. 2013), which are important factors in weight maintenance and promoting satiation of appetite (Slavin 2005; Hall et al. 2012; Arciero et al. 2013; Tremblay and Bellisle 2015).

The drastic changes in food quality over the latter half of the 20th century coincided with increased overall abundance. This manifested in large food portions which steadily grew in size from 1977 to 1998 (Nielsen 2003). Portion sizes are highly correlated with increased total energy consumption with many studies reporting a 30% or greater increase in consumption when subjects are offered a larger portion size (reviewed in Steenhuis and Vermeer 2009). These factors among others are responsible for promoting an obesogenic environment, which led to large increases in consumed energy as global daily calorie intake was estimated to have increased from 2250 kcal per person in 1961 to 2750 kcal by 2007 (Crino et al. 2015). In roughly the same time period (1970-2000) individual daily energy consumption in the U.S. also increased by roughly 500 kcal, which coincided with an average adult weight increase of ~19 pounds (Swinburn et al. 2009).

Many studies have demonstrated that the estimated increases in food energy availability are more than sufficient to explain observed increases in body weight in most parts of the world (Swinburn et al. 2009; Scarborough et al. 2011; Vandevijvere et al. 2015). These studies, combined with evidence from a comprehensive survey in the United States that found an extremely small impact of physical activity on the incidence of obesity (Dwyer-Lindgren et al. 2013), have led some to suggest that increased food supply is the primary driver of the global obesity crisis (Crino et al. 2015; Vandevijvere et al. 2015). While there is evidence to support this idea, it is important to note that the measurements in these studies are either relatively crude (i.e. individual dietary consumption was estimated from national food supply data, Swinburn et al. 2009) or subject to potential bias due to self-reporting error (i.e. self reported physical activity rates, Dwyer-Lindgren et al. 2013). The combination of these reports and a general lack of data on global physical activity trends in the late 20th century (Hallal et al. 2012) have convoluted the relative impact of physical inactivity on the current prevalence of obesity. However, it is widely accepted that technological advancements since the industrial revolution have changed the amount of physical activity required for labor, transport and leisure (Hallal et al. 2012; Hill et al. 2012). Some have argued that understanding how these advancements have affected total energy expenditure rates is deserving of further analysis (Bauman et al. 2015). While the data are relatively limited, there is evidence to suggest that physical activity levels in developed nations have remained constant or slightly increased over the past 10-30 years (Westerterp and Speakman 2008; Hallal et al. 2012; Dwyer-Lindgren et al. 2013). Despite this, worldwide levels of physical activity were low in 2012, with approximately 31% of adults reported to have engaged in little to no physical activity on a weekly basis (Hallal et

al. 2012). It is therefore possible that activity levels were low prior to changes in nutrition that developed in the 1970's and set the stage for the current epidemic. There is some data to suggest that decreased activity in the workplace began in the mid-20th century as the fraction of low activity jobs in the U.S. workforce increased from 1950-2000 (Brownson et al. 2005). Regardless of the relative impact of diet or activity on the current state of obesity, low levels of physical activity negatively correlate with BMI across multiple countries (Dyck et al. 2015), suggesting that interventions to increase physical activity may be beneficial. Longitudinal studies using objective measures such as accelerometery-based methods will be critical in tracking trends in physical activity moving forward (Dyck et al. 2015).

While nutrition and exercise are some of the most well characterized factors that influence obesity but there is still no scientific consensus on how exactly they have shaped the current epidemic of obesity and related diseases around the world (Swinburn et al. 2011). Because diet and exercise are effective interventions to reduce body weight (Clark 2015), studies have suggested small behavioral changes such as walking for 15 minutes each day or skipping a snack would be sufficient to counter the predicted 15 kcal positive energy balance that drives weight grain for much of the population (Hill et al. 2003). While small lifestyle changes might be effective in slowing the rise of obesity, further measures would be required to generate the negative energy balance required for weight loss. Because one pound of body fat is estimated to contain 3500 kcal of energy (Hall 2008), the U.S. Department of Health and Human Services (DHHS) recommends reducing weekly caloric intake by 500 for every 1 pound of desired weight loss (DHHS, AIM for a Health Weight). While this model has been widely accepted and used as a target for weight loss

interventions, the physiological processes of weight loss in practice have been show to be highly dynamic as the body adapts the expenditure of energy in response to energy deficit over time (Hall 2008; Hall et al. 2011). For instance, increased exercise may lead to compensatory responses that vary among individuals, ranging from changes in metabolism to behavioral adaptations that stimulate appetite, which ultimately balance energetic homeostasis and slow weight loss (King et al. 2007; Blundell et al. 2015). Our understanding of the interactions between the environment and energy homeostasis is likely to increase in complexity as we learn more about additional forces, including metabolic effects associated with the gut microbiota (Payne et al. 2012; Rosenbaum et al. 2015). While these environmental factors may largely explain the current world-wide increase in obesity, individual and population-level differences in the face of similar environments may be shaped by other factors.

The genetic basis of obesity

Studies on the heritability of body mass index (BMI) in twins (Stunkard, Foch, et al. 1986; Stunkard et al. 1990) and in correlation of adoptee BMI to biological or adoptive parent (Stunkard, Sørensen, et al. 1986) have long suggested a genetic component to obesity. These preliminary reports were later corroborated by numerous studies which found high levels of broad sense heritability (h^2) of BMI between parent/offspring or sibling pairs, with heritable factors estimated to explain between 20-80% of the variance in BMI (reviewed in Maes et al. 1997). In studies of monozygotic twins where genetic material is nearly identical, correlation in BMI is even higher ranging between 50-90% (Maes et al. 1997). While this could be due to a shared early environment h^2 values have been reported

to be as high as ~0.7 even when monozygotic twins are reared apart (Stunkard et al. 1990). Studies have largely supported the idea that genetics is a more likely predictor of BMI than environmental factors, particularly in young subjects, where additive genetic effects explain a much larger portion of the overall variation in BMI than environmental influences (Silventoinen et al. 2010; van Dongen et al. 2013).

In addition to BMI, genetic factors have been found to explain high levels of variance in many traits associated with the metabolic syndrome, including the fasting levels of important lipid metabolites (total cholesterol, low-density lipoprotein, high-density lipoprotein and triglycerides), components of carbohydrate metabolism (glucose and insulin) and blood pressure (systolic and diastolic pressure; van Dongen et al. 2013). Genetic factors have also been shown to contribute to the overall distribution of body fat, with respect to both the localization (i.e. trunk, lower body; Malis et al. 2005) and tissue subtype (i.e. subcutaneous and visceral adipose tissues; Fox et al. 2007).

Because obesity is highly heritable it is possible that population-level differences in global obesity rates (Stevens et al. 2012) are driven by genetic variation, with some individuals or populations more susceptible to increasing body fat in response to similar environmental changes. Conversely, local environments could be shaped by socio-economic or political climates that alter factors such as the population-level food supply (Swinburn et al. 2011). These hypotheses are difficult to discriminate, largely because the genetic basis of obesity remains largely uncharacterized. However, several lines of evidence suggest that genetics may play a role in shaping the global distribution of obesity rates. Firstly, populations around the world have wide-ranging rates of obesity and in some instances, when populations become admixed, BMI levels positively correlate with the

degree of ancestry, even after controlling for several socioeconomic factors (Stevens et al. 2012; Norden-Krichmar et al. 2014; Goonesekera et al. 2015). This evidence suggests that genetic variation within a given ethnicity may be sufficient to affect phenotypic change in BMI. This idea is further supported by genome-wide association studies, which have found evidence for loci associated with BMI that vary across populations and ethnic cohorts (reviewed in Grarup et al. 2014). This may not be entirely surprising as an extensive amount of genetic variation is separated across geographical space, with polymorphisms from 1,092 individuals across 14 international populations demonstrating large-scale regional differentiation (McVean et al. 2012). Still it remains unclear as to what extent this variation is capable of explaining population-level differences in BMI. To address this some studies have begun to track regional distributions of obesity-associated loci (Dorajoo et al. 2012; Raj et al. 2013). While these studies provide some evidence for population-level differences in several obesity-associated loci, they are measured in only a small number of markers and were insufficient to explain intra-population differences in BMI within the Indian subcontinent (Raj et al. 2013). These types of experiments will continue to improve as more obesity-associated loci are discovered and incorporated into the analysis. Indeed, one recent study which included ~12,000 loci, found that genetic variants could explain a small but significant amount of the variation in BMI across 14 European populations (Robinson et al. 2015). While future studies that incorporate additional loci across more diverse populations will offer further insight, the preliminary data suggest that genetics plays a role in shaping population-level differences in obesity rates.

The clearest evidence for a genetic component to obesity comes in the form of inherited Mendelian disorders. Monogenic forms of obesity are quite rare and associate

with a small number of genes, with nearly 200 known mutations that map to 11 different genes (Mutch and Clément 2006; Rankinen et al. 2006). Many of these genes are associated with regulation of nutrient intake and expenditure through feedback mechanisms in the hypothalamus (Farooqi and O'Rahilly 2005; O'Rahilly and Farooqi 2008). Typically these disorders present with severe early-onset obesity which can be debilitating and may lead to early mortality (Farooqi and O'Rahilly 2005). Identification of genetic disorders with mutations in the leptin gene (*LEP*) led to the development of hormone replacement therapies, which have proven to be effective treatment options (O'Rahilly and Farooqi 2008). On the other end of the spectrum are mutations that lead to lipodystrophic disorders, where adipose tissue depots are either partially or completely depleted, primarily occurring through mutations in one of 12 known genes (Vatier et al. 2013). Interestingly, some of the consequences of severe obesity and lipodystrophy are similar. As adipose tissue is either completely saturated or ablated, fats are ectopically stored in peripheral tissues leading to organ dysfunction and systemic complications such as insulin resistance (Vatier et al. 2013).

While monogenic disorders highlight the extreme genetic contributions to fat storage and utilization, common obesity is largely polygenic, representing a continuous distribution of individual predisposition and susceptibility. In order to understand the genetic basis of obesity, some have begun trying to identify variants in the human genome that are commonly associated with obese phenotypes (Walley et al. 2009). While some initial studies allowed for the simultaneous analysis of several hundred thousand polymorphisms on SNP-array chips (Walley et al. 2009), recent advances have increased that number to ~2.5 million (HumanOmni2.5-8 BeadChip, Illumina Inc, San Diego CA.). SNP

chips are cost efficient and cover many common polymorphisms, but are unable to capture the entirety of human variation. For instance, deep-sequencing of over 1000 individuals found ~38 million SNPs with many more variants in the form of insertions and deletions (McVean et al. 2012). Efforts to identify the genetic basis of obesity from these large number of polymorphisms have been successful in uncovering interesting loci (Willer et al. 2009; Fall and Ingelsson 2014; Locke et al. 2015), but still only account for a small fraction of the overall heritability with studies generally reporting <~10% of variance in BMI explained by candidate SNPs (Bogardus 2009; Xia and Grant 2013; Locke et al. 2015). With genetic factors estimated to explain ~20-80% of variability in BMI (Maes et al. 1997), a large gap remains in our understanding of the genetic landscape of obesity. This gap may begin to narrow as we gain understanding into the synergistic effects of epistatic interactions between co-inherited alleles, however it is likely that a large number of variants with low effect sizes remain to be implicated in the phenotype. Despite efforts and meta-analyses to increase sampling sizes to discover more associations, GWAS studies are further limited by their inability to consign causality to candidate loci. Even as strong candidates emerge across multiple studies, such as polymorphisms in the fat mass and obesity-associated (*Fto*) gene (Loos and Yeo 2013; Xia and Grant 2013; Tan et al. 2014), they may alter unpredicted targets. In this case, later studies demonstrated the intronic *Fto* SNP affected a cis-regulatory enhancer for the nearby Iroquois-class homeobox (*Irx3*/5) gene. The reported T-to-C transition was found to promote white adipocyte differentiation by altering the binding affinity for the ARID5B transcription factor (Claussnitzer et al. 2015; Herman and Rosen 2015). The inability of GWAS to determine causality is an inherent limitation of the technique and an issue that will become more complex as the

dynamics of transcriptional regulation and nuclear architecture are unraveled, including long range (40-80kB) cis-regulatory and interchromosomal trans-acting enhancers (Zhang et al. 2013; Tai et al. 2014). Despite these limitations GWAS has uncovered a large amount of genetic variation associated with complex traits over the past 10 years and led to discoveries such as *Irx3/5* may have been overlooked without such study. Understanding the limitations and refining methods to determine causality in model organisms may eventually improve the efficacy of GWAS in understanding the genetic variation that contributes to obesity.

The evolutionary origins of obesity

Natural forces may shape the upper and lower thresholds for body fats (Genné-Bacon 2014). Increased fat storage may be adaptive for its utility in surviving periodic famines, importance in reproduction and ability to regulate temperature through insulation (white adipose tissue) or heat generation (brown adipose tissue) (Genné-Bacon 2014). Conversely, too much fat could be maladaptive by reducing locomotion, increasing the risk of predation or maintaining the high energetic cost of constant foraging (Genné-Bacon 2014). Despite the importance of body fat in maintaining energetic homeostasis, there is no clear understanding of how evolution has shaped the quantity and distribution of body fats across species and between individual organisms. This question became increasingly important as the rates of obesity and diabetes spiked over the later half of the 20th century, sparking many theories which are still contested today.

One of the first theories on the evolutionary origins of obesity was the thrifty gene hypothesis, which suggests that the genetic variants that are capable of efficiently storing

and utilizing body fats are selected for during famine events that have occurred over evolutionary time (Neel 1962). The rising rates of obesity and diabetes in westernized civilization would then simply be a consequence of a mismatch between genetic predisposition to retain energy and an overwhelmingly positive energy environment (Neel 1962). By 1989 this hypothesis was partially rebuked by its own author, James Neel, who stated, "The data on which that (rather soft) hypothesis was based have now largely collapsed…" (Neel 1989). In part, this was due to a lack of evidence for positive selection on the low number of genetic candidates that existed at the time (Neel 1989). Relatively recent advancements in the genomic era have allowed for the discovery of more obesity-associated loci and renewed interest in testing the thrifty gene hypothesis. However, GWAS studies over the past decade have found little support for positive selection on any of the risk loci in human populations (Southam et al. 2009; Ayub et al. 2014). Another criticism of the thrifty gene hypothesis is that it has been unable to predict differences in body fat between different populations (Genné-Bacon 2014). Part of this may be due to a lack of knowledge of the evolutionary history of different populations. For example, obesity rates exceed 50% for many island nations in the Pacific Ocean (Stevens et al. 2012). However because the evolutionary history of these populations is not fully understood, they are used as an example for and against the thrifty gene hypothesis, with some suggesting the tropical climates have a low history of famine, while others suggest the opposite (Genné-Bacon 2014; O'Rourke 2014). Others have argued that if famines have driven selection since the beginning of human history, nearly all thrifty alleles would be fixed and most everyone would be obese (Speakman 2008). Furthermore if famines are a more recent phenomenon in human history due to a shift from a hunter-gathering lifestyle to

dependence on agriculture, the number of famines that actually cause significant mortality are likely too rare to affect evolutionary change (Speakman 2008).

Due to some of these concerns, the thrifty gene hypothesis has become controversial and many others have put forth a variety of compelling alternatives (reviewed in Genné-Bacon 2014). For instance, the thrifty epigenome hypothesis suggests that maternal nutrition preconditions the metabolic profile of the developing fetus *in utero* through epigenetic mechanisms (Stöger 2008). This is supported by the study of offspring from mothers who gestated during a famine in Netherlands during World War II ("The Dutch Hungry Winter" study, reviewed in Genné-Bacon 2014). Male offspring were more prone to develop obesity and diabetes, which was later found to be associated with altered DNA methylation patterns of key metabolic genes (Tobi et al. 2009). Some have suggested that epigenetic adaptations to westernized lifestyles may be driving the plateauing obesity rates that are currently being observed in many developed nations (Genné-Bacon 2014). Another theory, the drifty gene hypothesis, suggests that human innovations over the past 2 million years have decreased the risk of predation and effectively eliminated the selective pressures that maintain the upper limit of fat storage. These freedoms are thought to have lifted selective constraints, allowing genetic drift and mutation to drive individual susceptibility (Speakman 2008).

These theories are not necessarily mutually exclusive. The dynamic nature of evolution likely incorporates pieces of each to drive the wide variation in body fats found both within and among species observed today. While an understanding of how obesity evolves is an interesting question in its own right, it is also an important matter for human health. For example, the thrifty gene hypothesis predicts that the human genome is better

adapted for ancestral environments. This is the basis behind dietary interventions designed to mimic the foods eaten by our hunter-gatherer ancestors, commonly known as the "Paleo" diet. The Paleo diet has been shown to improve the metabolic health of patients with type-II diabetes (Masharani et al. 2015). Conversely, if epigenetic mechanisms are found to primarily control metabolism, efforts may be focused to improve maternal nutrition while increasing research efforts to understand epigenetic mechanisms. While not the explicit goal of the work described here, predictions from these hypothesis may be rigorously tested with experimental evolution in model organisms.

1.4 *Drosophila* are a well suited model organism to study obesity and its associated diseases.

Obesity is a complex disorder that represents a fundamental imbalance in energetic homeostasis. It is a function of all levels of biological organization, ranging from the ecological factors that shape the availability of resources, to the metabolic cellular process that govern storage and utilization. The wide range of factors that contribute to the etiology of obesity and its associated disorders in humans makes it difficult to study. Due to the deep evolutionary conservation of metabolic processes across metazoans, researchers have turned to model organisms to understand the core environmental and genetic factors that influence metabolism.

Recently *Drosophila melanogaster* has emerged as an important platform of discovery in obesity research as many of the genes and organ systems responsible for maintaining energetic homeostasis are functionally conserved. For instance, both the systems of hormonal regulation and the cellular signaling pathways that maintain carbohydrate metabolism are functionally conserved (Das and Dobens 2015). In some instances, the degree of homology is quite remarkable, with mammalian insulin able to activate the *Drosophila* insulin receptor and vice versa (Sajid et al. 2011). In total it is estimated that ~75% of disease-associated genes in humans share a high degree of sequence homology in *Drosophila*, with ~33% predicted to have functional homology (Bier 2005). Because of this, the *Drosophila* scientific community has developed several important resources, which allow for large-scale screens to identify genes that contribute to metabolic defects (Dietzl et al. 2007; Mackay et al. 2012). *Drosophila* are particularly amenable for the genetic analysis of complex traits because in most cases they exhibit

lower levels of redundancy (Bakal 2011; Zhang 2012) and researchers have developed sophisticated tools that enhance tractability (Duffy 2002; Dietzl et al. 2007; Yu et al. 2013). As discussed earlier in this chapter, *Drosophila* posses a wide range of natural variation in total lipid content, which may be controlled by genetic factors and is shaped by ecological forces. These complex gene/environment interactions, which make obesity difficult to study in mammals, can be readily dissected by modeling different components of obesity in the laboratory. To date, researchers have modeled obesity in *Drosophila* through dietary modification, genetic manipulation, alteration of the gut microbiome and adaptation to evolutionary stress (Chippindale et al. 1996; Harshman et al. 1999; Birse et al. 2010; Lee et al. 2010; Sujkowski et al. 2012; Buescher et al. 2013; Na et al. 2013; Reynolds 2013; Newell et al. 2014; Diop et al. 2015). The experimental treatment in some of these models induces characteristics that resemble the metabolic syndrome in mammals, including the progression of insulin resistance and heart disease (Birse et al. 2010; Na et al. 2013). There are several important limitations of the *Drosophila* model in obesity research. For instance, *Drosophila* lack brown adipose tissue, which is important component of thermogenesis in mammals. *Drosophila* also have an open circulatory system, which limits the study of vascular disorders that are commonly associated with obesity. Despite these limitations *Drosophila* have been used to examine the basic physiological and genetic mechanisms that link adiposity to increased cardiometabolic risk. Here we will focus our discussion on the metabolic similarities between *Drosophila* and mammals, as well as highlight recent studies on obesity-associated heart disease.

The fat body plays a central role in maintaining metabolic homeostasis.

One of the primary sites of metabolic regulation in *Drosophila* is the fat body, a heterogeneous tissue which is functionally homologous to mammalian adipose tissue, but is also responsible for immune function and integration of systemic signals (Hoffmann and Reichhart 2002; Arrese and Soulages 2010; Bai et al. 2012; Rajan and Perrimon 2012). Throughout larval development the fat body serves as a nutritional sensor and adjusts cellular metabolism to couple available energy with growth across various tissues (Mirth and Riddiford 2007). Larval acquisition of resources is vital for holometabolous insects to provide the energy required to support growth and maintenance during metamorphosis and young adult life (Aguila et al. 2007). As larvae approach pupariation a series of pulses of the steroid hormone 20-hydroxyecdysone (20E) trigger the onset of metamorphosis, which results in profound changes in the structure and distribution of the fat body (Thummel 1995; Aguila et al. 2007). Specifically, the larval fat body dissociates from tightly packed clusters into individual cells, which may persist into the first several days of adulthood to provide energy resources for the newly eclosed animal (Hoshizaki 2005; Aguila et al. 2007). The adult fat body is thought to be synthesized *de novo* during metamorphosis, giving rise to a diffuse tissue that is predominantly localized to the abdomen but found distributed throughout the entire animal (Haunerland and Shirk 1995; Hoshizaki 2005).

Within fat body cells, highly dynamic lipid droplets serve as the primary site of lipid storage and breakdown (Kuhnlein 2012). Several protein families associate with lipid droplets, including lipases and perilipins, which are evolutionarily conserved and function under control of similar cellular networks that stimulate lipolysis to mobilize energy in

response to low nutrient levels in mammals (Arrese and Soulages 2010). Genetics play a large role in regulating the size and number of lipid droplets, which are important factors in maintaining healthy levels of stored fat (Krahmer et al. 2013). Variants that alter this balance in mammalian adipocytes ultimately influence the individual capacity for fat storage, which generates a wide distribution of susceptibilities to many diseases (Krahmer et al. 2013). Some of these genes and associated pathologies are conserved in *Drosophila*. For example, missense mutations in the human lipid droplet-associated protein, adipose triglyceride lipase (ATGL), lead to neutral lipid storage disease (NLSD), a rare condition marked by high systemic TG levels in various tissues and increased risk for cardiovascular disease (Schweiger et al. 2009). The *Drosophila* homolog of *ATGL*, brummer lipase (*bmm*), can be knocked out through the introduction of loss-of-function alleles which similarly lead to increased TG accumulation and heart dysfunction (Grönke et al. 2005; Diop et al. 2015).

The mechanisms that control the coordination of nutritional status and metabolism are also highly conserved in *Drosophila*. Specialized neurosecretory cells in the brain, including the insulin producing cells (IPCs) and corpora cardiaca (CC), secrete insulin-like peptides (Ilps) and adipokinetic hormone (Akh) respectively, which affect metabolism in peripheral tissues analogously to the pancreatic release of insulin and glucagon in mammals (Arrese and Soulages 2010; Das and Dobens 2015). These molecules activate downstream signaling cascades in the fat body which are highly interconnected, forming a network that shifts between cellular programs that promote either anabolic energy storage in response to Ilp signals or catabolic energy mobilization in response to Akh (Arrese and Soulages 2010; Das and Dobens 2015).

Drosophila have 8 insulin-like peptides (Ilp1-8) which share a degree of functional redundancy, but are differentially expressed in a tissue specific manner (for a full review see Kannan and Fridell 2013). The primary function of the Ilps is to couple cellular metabolism with nutritional status. For instance, Ilp2 and Ilp3 may be secreted from the IPCs in response to high circulating levels of amino acids or sugars respectively (Kim and Neufeld 2015). These neuropeptide hormones bind the *Drosophila* insulin-like receptor (*InR*) in peripheral tissues, which initiates a cascade that activates several conserved members of the core insulin signaling pathway, including Akt and TOR, which promote anabolic gene expression and cell growth (Das and Dobens 2015). In mammals adipose tissue plays an important role in secreting cytokines in response to nutrient levels to balance systemic metabolism (Leal and Mafra 2013). The *Drosophila* fat body is similarly capable of recognizing dietary macronutrients and releasing cytokines, such as Unpaired 2 (Upd2), which activates systemic Ilp release from the IPCs (Géminard et al. 2009; Rajan and Perrimon 2012). Under starved conditions the fat body expresses and hormonally secretes Ilp6, which acts to negatively feedback on Ilp2 expression in the IPCs (Bai et al. 2012) and promote lipid mobilization through hepatic-like cells called oenocytes (Chatterjee et al. 2014). Ilp6 is also expressed in the fat body during metamorphosis in response to 20E and is required to promote growth of the developing tissues (Slaidina et al. 2009).

Akh largely antagonizes Ilp signaling in *Drosophila* by promoting the mobilization of stored lipids and carbohydrates in the fat body under starved conditions (Das and Dobens 2015). Akh signaling in the fat body is activated through binding of the neuropeptide to the adipokinetic hormone receptor (AkhR), which initiates a G-protein associated signaling cascade leading to the activation of central catabolic regulators such as Protein Kinase A

(Pka) (Grönke et al. 2007). Pka promotes lipolytic signals directly by activating lipid droplet protein (Lsd-1) and further promotes the expression of catabolic genes through activation of Creb and foxo transcription factors (Patel et al. 2005; Arrese et al. 2008; Wang et al. 2011; Yang et al. 2013). Cross-talk and feedback mechanisms between components of the Akh and Ilp signaling pathways allow the cell to adjust to acute nutritional changes.

The functional conservation of the Drosophila heart is remarkable given its largely simplified design.

The *Drosophila* heart is a simple tube, comprised of two rows of semicircular shaped cardiomyocytes which interlock to form a contiguous lumen (Lehmacher et al. 2012). Adherens junctions on the dorsal and ventral aspects of the cardiomyocytes anchor actin myofibrils which run circumferentially through the cells to generate a contractile ring (Lehmacher et al. 2012). The heart tube is localized within the abdomen, closely associated with the dorsal cuticle and contracts in response to both myogenic pacemakers and neurogenic signals (Dulcis 2005). Hemolymph, the primary circulating fluid in arthropods, flows into the heart lumen during diastole through small cellular invaginations formed from neighboring cardiomyocytes called ostia, whose valvular lips passively constrict to block inflow during systole. Another set of specialized cardiomyocytes called intracardiac valve cells break the heart into four primary chambers. The most rostral chamber near the anterior abdomen widens, forming the conical chamber, whose increased size provides the extra force required to eject fluids through the non-contractile thoracic aorta. In *Drosophila* contraction patterns are dynamic as the fly may switch between anterograde or retrograde heartbeats to circulate hemolymph through an open circulatory system (Wasserthal 2007;

Slama 2010). Anterograde contractions are more common and necessary to expel hemolymph through the aorta where it is spilled into the posterior head. The primary pacemaker cell is thought to reside in the caudal chamber of the heart, although others have suggested another pacemaker exists near the conical chamber (Wasserthal 2007; Slama 2010). Relaxation of the heart during diastole is assisted by sets of alary muscles whose myofibrils run perpendicular to those of the cardiomyocytes and tether the heart to the dorsal cuticle at several intervals along the abdomen (Klowden 2007; Lehmacher et al. 2012). The alary muscles are not directly bound to the cardiomyocytes, instead they are bridged by extracellular matrix fibers which are hypothesized to increase the elasticity of the connection (Lehmacher et al. 2012). Several long syncytial muscles run ventrally down the length of the tube. The function of these ventral longitudinal fibers remains unclear, however they are thought to be important in support and may assist in contraction (Lehmacher et al. 2012). Several pairs of rounded pericardial cells border the edges the heart and serve as nephrocytes, filtering the hemolymph as it circulates (Weavers et al. 2009).

While the *Drosophila* and mammalian heart have many obvious differences, early studies identified the genes and signaling cascades that drive differentiation and morphogenesis throughout development to be highly conserved, sparking interest in using *Drosophila* as a model to study congenital heart disease (Bodmer 1995; Bier and Bodmer 2004). The subsequent identification of conserved genes associated with other cardiovascular diseases including muscle defects, conduction blocks and hypertension led to expanded efforts to identify novel genetic factors through large-scale screens and to perform genetic manipulations to study the underlying physiological changes (Piazza and

Wessells 2011; Wolf and Rockman 2011). Some studies have generated models of human cardiac disease in *Drosophila*, which has highlighted the remarkable degree of functional conservation (Sujkowski and Wessells 2015). For example, researchers have developed a fly model for long QT syndrome (LQTS), a genetic disorder caused by mutations in a K^+ ion channel subunit (*KCNQ1*). Mutations in *KCNQ1* lead to slow cardiac repolarization, which ultimately induces arrhythmia and increased susceptibility to sudden heart failure (Ocorr et al. 2007). Heart dysfunction in flies with mutated *KCNQ* was shown to mirror LQTS, with early onset of arrhythmia and pacing-induced heart dysfunction (Ocorr et al. 2007). Another group developed a model to study cardiac disorders associated with Duchenne and Becker Musclar Dystrophies, which are genetic diseases marked by mutations in the *dystrophin (Dys)* gene which may manifest in dilated cardiomyopathy, arrhythmia and heart failure (Taghli-Lamallem et al. 2008; Taghli-Lamallem et al. 2014). The dystrophin protein plays important roles in transducing both mechanical force and cellular signals (Taghli-Lamallem et al. 2008). *Drosophila dys* mutants have myofibril disorganization, dilated cardiomyopathy and altered contraction patterns, which could be improved by expressing constructs of human *Dys* in the *Drosophila* heart (Taghli-Lamallem et al. 2008; Taghli-Lamallem et al. 2014). The high levels of genetic similarity observed in these disease models has prompted researchers to study gene by environment interactions on cardiac physiology for many factors including exercise, ageing and nutrition (Piazza and Wessells 2011; Diop and Bodmer 2015; Sujkowski and Wessells 2015). The studies focused on the interaction between diet and genes involved in energy homeostasis have provided insight into obesity-associated heart disease.

Lipotoxicity is a common mechanism linking obesity to the development of heart disease in Drosophila.

There are many ways in which in which obesity may alter cardiovascular health, which vary by individual genetic makeup and environmental factors. In general, obesity may lead to hypertension, increased levels of circulating carbohydrate and lipid molecules, generalized inflammation and atherosclerosis (Hall et al. 2014). Under chronic conditions these factors commonly lead to increased left-ventricular mass, resulting in dilation and low fractional shortening (Alpert et al. 1995). These changes in the left ventricle are associated with hypertrophic remodeling of the cardiomyocytes, fibrosis and increased epicardial and myocardial fat deposits (Poirier 2006; Cavalera et al. 2014; Murdolo et al. 2014). The infiltration of fibrotic and and epicardial fat cells within the myocardium may further lead to conduction defects, which contribute to arrhythmic contraction patterns (Poirier 2006; Cavalera et al. 2014). Poor left ventricle function and arrhythmia are highly associated with heart failure and a pose a major health risk for obese individuals (Eckel 1997; Mathew et al. 2008; Lavie et al. 2013).

The relative distribution of body fats is a major predictor for cardiometabolic risk factors, as hypertension, inflammation and high circulating metabolites are more highly associated with individual levels of visceral adipose tissue (VAT) than subcutaneous adipose tissue (SAT) or overall body fat (Després et al. 1990; Tchernof and Despres 2013). SAT is hypothesized to be a neutral reservoir, which can store excess fats with relatively low risk for the development of cardiometabolic disease (Despres 2012; Bastien et al. 2014). When lipid levels exceed the storage capacity of SAT, fats are improperly stored in VAT or ectopically in peripheral tissues like the heart or pancreas (Unger et al. 2010;

Bastien et al. 2014). The ectopic accumulation of fats within the myocardium disrupts cellular function, leading to a phenomenon known as lipotoxicity. Lipotoxicity is highly associated with heart failure and thought to be a central mechanism of many obesity-associated disorders (Zhang and Ren 2011; Bastien et al. 2014).

The molecular basis of lipotoxicity is poorly characterized, but may be associated with changes in the availability of substrates used to generate cellular energy. The heart primarily derives cellular energy through the metabolism of glucose and fatty acids (Taegtmeyer 1994). While metabolism of both molecules produce acetyl-CoA for entry into the TCA-cycle, the breakdown of glucose additionally supplies oxaloacetate through pyruvate carboxylation, which is a critical component of the TCA-cycle (Taegtmeyer 1994). Obesity induces high circulating levels of both glucose and free fatty acids. However, obesity also induces the onset of insulin resistance, which reduces the heart's ability to fully utilize glucose (Zhang and Ren 2011). Ultimately this results in a heavy reliance on fatty acids, which reduces the efficiency of ATP production and impacts contraction (Lopaschuk et al. 2007). This likely occurs through the buildup of fatty acid intermediates as the metabolic capacity of β-oxidation is overwhelmed (Zhang and Ren 2011). This stress is thought to both damage myocardial mitochondria and lead to changes in gene expression that may increase inflammation and TG accumulation (Guzzardi and Iozzo 2011).

Researchers have developed different models in *Drosophila* to study lipotoxicity on different levels- to both understand how genetic variation may influence the fundamental storage capacity of adipose tissue, and how the problem is exacerbated by chronic over-nutrition (Birse et al. 2010; Lee et al. 2010; Lim et al. 2011; Palanker Musselman et al. 2011; Sujkowski et al. 2012; Na et al. 2013; Diop et al. 2015). When *Drosophila* are reared

on lipogenic diets which are high in fat or sugar, they develop an obese phenotype, resulting in a higher percentage of body fat, insulin resistance and heart anomalies (Birse et al. 2010; Palanker Musselman et al. 2011; Na et al. 2013: 2). Specifically, chronic over-nutrition disrupts Ilp expression in the IPCs, which leads to high levels of circulating sugars, and decreased levels of insulin signaling in peripheral tissues (Birse et al. 2010; Na et al. 2013). This promotes a lipotoxic state, leading to increased cardiac steatosis, associated with conduction defects, arrhythmia and poor contractility due to myofibrillar disorganization (Birse et al. 2010; Na et al. 2013).

Many of the pathophysiological effects of a high calorie diet were found to be the result of hyperactive Tor signaling. Tor was found to respond to a HFD by promoting the expression of genes involved in lipid synthesis such as fatty acid synthase (*FAS*), while repressing the expression of lipocatabolic genes like brummer lipase (*bmm*) (Birse et al. 2010). The deleterious effects of a HFD could be reduced by knocking down many of these components in the Tor pathway specifically in the fat body (Birse et al. 2010). Furthermore, heart-specific knockdown of Tor signaling components reduced cardiac steatosis, which led to improved heart function despite high levels of total body fat (Birse et al. 2010). These findings suggest that obesity-associated heart dysfunction in *Drosophila* is not the result of high body fat *per se*, but a function of cardiac lipid accumulation (Birse et al. 2010).

In the fat body, Tor integrates inputs from changes in nutrition, energy and stress and responds by controlling transcription factors that promote anabolic metabolism and cellular growth. Studies in *Drosophila* have uncovered genetic interactions involved in this signaling pathway, which may contribute new avenues for treatment and explain individual genetic susceptibilities (Lee et al. 2010; Lim et al. 2011; Diop et al. 2015). For example, Tor

hyperactivity leads to increases in reactive oxygen species which are correlated with the increased expression of a stress-responsive gene known as *sestrin* (Lee et al. 2010). Sestrin was found to be an important suppressor of Tor activity, which could reduce body fat and heart disease in hyperactive Tor mutants of *Drosophila* (Lee et al. 2010). Others have studied downstream components of Tor signaling, including sterol regulatory element binding protein (SREBP), PPARγ coactivator-1 (PGC-1), FAS and Bmm. All of these downstream components were found to be important for body fat accumulation, lipotoxicity and heart dysfunction under a HFD (Birse et al. 2010; Teleman 2010; Lim et al. 2011; Diop et al. 2015).

There are also genes which may promote lipotoxic heart dysfunction independently of a high calorie diet and not directly related with Tor signaling. This was observed in *Drosophila* that were heterozygous for a loss-of-function mutation in the fatty acid transport protein (*Fatp*). *Fatp* mutants develop high levels of body fat on a standard diet (Sujkowski et al. 2012). This results in the accumulation of cardiac TGs and poor heart function as measured by low stress resistance to external pacing (Sujkowski et al. 2012).

Genome-wide studies of obesity in Drosophila

Due to the conservation of individual genes and gene networks in regulating metabolism in *Drosophila*, some have performed large-scale genomic screens to find genes involved in metabolism in an unbiased approach. While genome-wide studies of obesity are limited in *Drosophila*, they hold promise in identifying many more genes, which can be further studied and functionally validated. One large-scale screen used genome-wide RNA interference to identify ~500 genes which significantly altered TG storage (Pospisilik et al.

2010). These genes were subsequently knocked down in individual tissues including the fat body, where genes involved in hedgehog signaling were identified as important in suppressing TG accumulation (Pospisilik et al. 2010). The study found these genes had conserved function in mice and were responsible for repression of white adipocyte differentiation (Pospisilik et al. 2010). A similar study performed an RNAi screen of 6796 genes in the gut and fat body of adult flies and found 77 genes that positively or negatively affected lipid storage (Baumbach et al. 2014). Of these 77, 58 were previously unidentified as lipid modifiers and 46 had a directly known human homolog (Baumbach et al. 2014). The group followed up on a set of genes associated with Ca^{2+} signaling and found they were capable of inducing obesity, with one gene, Stromal interaction molecule (*Stim*) involved in controlling food intake (Baumbach et al. 2014).

While not explicitly targeting obesity, other studies have utilized the *Drosophila* Genetic Resource Panel (DGRP), a set of fully sequenced inbred lines, to identify polymorphisms associated with macromolecule storage in response to low or high glucose diet (Unckless et al. 2015) and starvation resistance (Mackay et al. 2012). These studies identified a large amount of genetic variation underlying these metabolic traits and found that the most significant loci for any given trait were found in introns or predicted to code for a non-synonymous substitution (Unckless et al. 2015).

1.5 Starvation selected *Drosophila* as a model to study the physiology, genetics and evolutionary origins of obesity.

The focus of this dissertation will be the analysis of populations of *D. melanogaster* laboratory selected for starvation resistance. The populations of study here were established in 2006 by Allen Gibbs, who was interested in investigating the mechanisms of adaptation to starvation resistance, as well as developing a model to study the *genetic* basis of obesity and its associated diseases. To date, the starvation-selected populations have been selected for over 100 generations. In response they have become obese, storing nearly two times the levels of stored fats as their unselected controls. Previous studies have measured many correlated tradeoffs in these lines, some of which resemble characteristics of the metabolic syndrome in mammals. Here, we investigate the physiological consequences of starvation-selection on heart function, the genetic basis of adaptation and how selection affects gene expression during critical developmental windows.

Evolutionary history of the starvation-selected populations

The starvation-selected populations were derived from a previous experimental evolution experiment selecting for desiccation resistance (described in Gefen et al. 2006). The founding population for the desiccation selection experiment was comprised of ~400 adult female *D. melanogaster* collected from the wild in Terhune New Jersey in 1999. After about a year of acclimation to laboratory conditions, the original population was split into 3 large cohorts, each with 3 replicate populations for a total of 9 populations. Every generation each cohort was subjected to one of three environmental conditions. The desiccation selected cohort (populations D_{A-C}) were housed in plexi-glass cages containing approximately 200 grams of silica gel desiccant to remove the environmental water supply.

Because desiccation also requires the removal of food, the D populations were co-selected for starvation resistance. To control for the effects of starvation in the D populations another cohort of 3 populations, the starved controls (populations SC_{A-C}) were given agar plates, which provided a water supply while offering no nutritional value. A third cohort of 3 populations, the fed controls (populations FC_{A-C}) were essentially unstressed, given *ad libitum* access to food and water. All populations were handled in parallel with the exception of the selective treatment, silica desiccant (D_{A-C}), non-nutritious agar (SC_{A-C}) or standard cornmeal medium (FC_{A-C}), during the selection phase of each generation. Selection began each generation after the flies had reached 4 days of adulthood and persisted until 80-85% mortality was reached in the D populations. At this point survivors for all nine populations were fed fresh cornmeal medium and eggs were collected to propagate the next generation.

In 2006, after generation 70 of the desiccation selection experiment, subpopulations were derived from the starved controls (SC_{A-C}) and the fed controls (FC_{A-C}) to begin the starvation selection experiment studied here. The starvation selection experiment consists of 2 major cohorts, the starvation-selected populations (hereafter "$\mathbf{S_{A-C}}$"), which were derived from SC_{A-C} and the fed controls (hereafter "$\mathbf{F_{A-C}}$"), derived from FC_{A-C}. Each generation, ~10,000 four-day-old adult flies for each S population were housed in an individual plexi-glass cage and given non-nutritious agar plates until 80-90% mortality was achieved. For each of the F populations, ~2,000 four day old adult flies were maintained in parallel and given *ad libitum* access to standard cornmeal medium. After the selection phase of each generation, all 6 populations (S_{A-C} and F_{A-C}) were given fresh cornmeal medium, given 4 days to recover, then eggs were collected to propagate the next

generation. To date, the S populations have been selected for 100 generations, however the experiments here were performed roughly between generations 50-80.

Evolved physiologies and correlated responses to starvation-selection

The S populations evolved many physiologies that were similar to previous starvation-selection experiments (Chippindale et al. 1996; Harshman et al. 1999). For instance after ~45 generations, the S flies could survive starvation ~2-3 times longer than the F controls (Reynolds 2013). This was due to large changes in body fat composition as the average S fly carried ~170 μg of total lipids compared to ~70 μg for the average F fly (Reynolds 2013). These changes in lipid content were not associated with changes in other macromolecules, as glycogen and protein levels were not significantly different between F and S flies (Reynolds 2013). The shift towards lipid storage and starvation resistance created a marked tradeoff in fecundity as the S populations had lower daily fecundity than the Fs throughout the first few weeks of adulthood (Reynolds 2013). Unlike previous studies, the S flies were found to have a lower metabolic rate even after accounting for the excess lipid weight as CO_2 production per hour standardized to lean mass was ~40% lower than the F controls (Reynolds 2013). There was also a trend towards lower activity levels in the S populations, however the data failed to reach significance (Reynolds 2013).

The S populations have also evolved a ~24 hour delay in development (Reynolds 2013). This delay increases the S larval feeding period, during which they acquire excess resources, which results in higher lipid content than the F populations upon eclosion (Reynolds 2013). The delay in development is thought to be due to dysregulation of 20E signaling as the S populations have a ~24 hour delay in expression of 20E target genes

(Reynolds 2013). However it is not clear whether this delay in expression is due to a delay in the neural synthesis and release of 20E or a delay in the cellular response of peripheral tissues to 20E. Feeding 20E to F and S larva at the beginning of 3rd instar only partially decreases the developmental delay in the S populations (Reynolds 2013). This could indicate that the S populations have adapted mechanisms to attenuate 20E-induced expression. This is supported by preliminary data which suggest the S larval fat body is less responsive to 20E, as it fails to completely dissociate during metamorphosis and delays programmed cell death in the adult fly (N.D. Bond, personal communication). More experiments are needed to discriminate between these possibilities.

Another set of experiments demonstrated that S flies may have reduced energy expenditure through adaptations that increase sleep duration and impair flight performance (Brewer 2013; Masek et al. 2014). In addition, these studies found evidence to suggest that behavioral adaptations may reduce foraging in response to selection. For instance, acute starvation in wild-type *Drosophila* will suppress sleep, likely in a behavioral response to find food (Masek et al. 2014). However, the S populations maintain a high constant level of sleep throughout starvation. Furthermore, S adults were found to eat less than the F controls and failed to increase compensatory feeding after starvation (Masek et al. 2014).

Summary

Experimental evolution affords the opportunity to understand the physiological and genetic basis of adaptation. Adaptation to laboratory selection for starvation resistance in *D. melanogaster* leads to metabolic disorder and increased total lipid stores, which are at

the heart of the global obesity crisis. The complex factors that contribute to obesity in humans can be simplified and modeled in *Drosophila*. Here we investigate the physiological and genetic basis of adaptation in starvation-selected *D. melanogaster*. In Chapter 2 we study the physiological consequence of starvation selection on the heart, investigating whether heart function is an evolutionary tradeoff with starvation resistance. We report that the S heart is dilated and less contractile than the F controls. Strikingly, the basis of dysfunction is correlated with enlarged fat body tissue, which severely alters the anatomical placement of the heart. We did not observe cardiac steatosis as observed in other *Drosophila* models. Instead excess lipids were found in large lipid droplets within the S fat body, suggesting that selection greatly increases the capacity to store neutral fats. In Chapter 3 we perform an E&R experiment to understand the genetic basis of adaptation. We find that starvation selection had profound effects on allele frequencies, with many large-scale regions across the genome approaching fixation. Allelic frequencies were variable across S populations, which correlated with differences in starvation resistance. To find alleles that responded to selection we generated a novel algorithm to filter the effects of genetic drift. We found ~120,000 loci whose difference in frequency was consistent with selection. These loci mapped to many genes involved in metabolic homeostasis including many in the insulin and adipokinetic hormone signaling pathways. In Chapter 4 I discuss my role in a larger effort to understand the mechanistic basis of delayed larval development in the S populations. Specifically we focused on how gene expression in the fat body differed between selection treatments in response to the late larval 20E pulse. I identified genes that were differentially regulated in response to selection which will provide the basis for future work.

1.6 Literature cited

Aggarwal DD. 2014. Physiological basis of starvation resistance in Drosophila leontia: analysis of sexual dimorphism. J. Exp. Biol. 217:1849–1859.

Aguila JR, Hoshizaki DK, Gibbs AG. 2013. Contribution of larval nutrition to adult reproduction in Drosophila melanogaster. J. Exp. Biol. 216:399–406.

Aguila JR, Suszko J, Gibbs AG, Hoshizaki DK. 2007. The role of larval fat cells in adult Drosophila melanogaster. J. Exp. Biol. 210:956–963.

Alpert MA, Lambert CR, Panayiotou H, Terry BE, Cohen MV, Massey CV, Hashimi MW, Mukerji V. 1995. Relation of duration of morbid obesity to left ventricular mass, systolic function, and diastolic filling, and effect of weight loss. Am. J. Cardiol. 76:1194–1197.

Archer MA, Phelan JP, Beckman KA, Rose MR. 2003. Breakdown in correlations during laboratory evolution. II. Selection on stress resistance in Drosophila populations. Evolution 57:536.

Arciero PJ, Ormsbee MJ, Gentile CL, Nindl BC, Brestoff JR, Ruby M. 2013. Increased protein intake and meal frequency reduces abdominal fat during energy balance and energy deficit: Meal Frequency, Protein, Obesity, Thermogenesis. Obesity 21:1357–1366.

Arnold M, Leitzmann M, Freisling H, Bray F, Romieu I, Renehan A, Soerjomataram I. 2016. Obesity and cancer: An update of the global impact. Cancer Epidemiol. 41:8–15.

Aron-Wisnewsky J, Clément K. 2015. The gut microbiome, diet, and links to cardiometabolic and chronic disorders. Nat. Rev. Nephrol. 12:169–181.

Arrese EL, Rivera L, Hamada M, Mirza S, Hartson SD, Weintraub S, Soulages JL. 2008. Function and structure of lipid storage droplet protein 1 studied in lipoprotein complexes. Arch. Biochem. Biophys. 473:42–47.

Arrese EL, Soulages JL. 2010. Insect Fat Body: Energy, Metabolism, and Regulation. Annu. Rev. Entomol. 55:207–225.

Ayub Q, Moutsianas L, Chen Y, Panoutsopoulou K, Colonna V, Pagani L, Prokopenko I, Ritchie GRS, Tyler-Smith C, McCarthy MI, et al. 2014. Revisiting the Thrifty Gene Hypothesis via 65 Loci Associated with Susceptibility to Type 2 Diabetes. Am. J. Hum. Genet. 94:176–185.

Bai H, Kang P, Tatar M. 2012. Drosophila insulin-like peptide-6 (*dilp6*) expression from fat body extends lifespan and represses secretion of Drosophila insulin-like peptide-2 from the brain: *dilp6* expression increases *Drosophila* lifespan. Aging Cell 11:978–985.

Bakal C. 2011. Drosophila RNAi screening in a postgenomic world. Brief. Funct. Genomics 10:197–205.

Baker P, Friel S. 2014. Processed foods and the nutrition transition: evidence from Asia: Processed foods and nutrition transition in Asia. Obes. Rev. 15:564–577.

Baldal EA, Brakefield PM, Zwaan BJ. 2006. Multitrait evolution in lines of Drosophila melanogaster selected for increased starvation resistance: the role of metabolic rate and implications for the evolution of longevity. Evol. Int. J. Org. Evol. 60:1435–1444.

Baldwin-Brown JG, Long AD, Thornton KR. 2014. The Power to Detect Quantitative Trait Loci Using Resequenced, Experimentally Evolved Populations of Diploid, Sexual Organisms. Mol. Biol. Evol. 31:1040–1055.

Ballard JWO, Melvin RG, Simpson SJ. 2008. Starvation resistance is positively correlated with body lipid proportion in five wild caught Drosophila simulans populations. J. Insect Physiol. 54:1371–1376.
Bastien M, Poirier P, Lemieux I, Després J-P. 2014. Overview of Epidemiology and Contribution of Obesity to Cardiovascular Disease. Prog. Cardiovasc. Dis. 56:369–381.
Bauman A, McGill B, Powell K, Lee I-M, Heath G, Pratt M, Kohl HW, Hallal P. 2015. Tackling obesity: challenges ahead. The Lancet 386:741–742.
Baumbach J, Hummel P, Bickmeyer I, Kowalczyk KM, Frank M, Knorr K, Hildebrandt A, Riedel D, Jäckle H, Kühnlein RP. 2014. A Drosophila In Vivo Screen Identifies Store-Operated Calcium Entry as a Key Regulator of Adiposity. Cell Metab. 19:331–343.
Beissinger TM, Hirsch CN, Vaillancourt B, Deshpande S, Barry K, Buell CR, Kaeppler SM, Gianola D, de Leon N. 2014. A Genome-Wide Scan for Evidence of Selection in a Maize Population Under Long-Term Artificial Selection for Ear Number. Genetics 196:829–840.
Bennett AF. 2003. Experimental Evolution and the Krogh Principle: Generating Biological Novelty for Functional and Genetic Analyses1. Physiol. Biochem. Zool. 76:1–11.
Bergland AO, Behrman EL, O'Brien KR, Schmidt PS, Petrov DA. 2014. Genomic Evidence of Rapid and Stable Adaptive Oscillations over Seasonal Time Scales in Drosophila.Bolnick D, editor. PLoS Genet. 10:e1004775.
Bier E. 2005. Drosophila, the golden bug, emerges as a tool for human genetics. Nat. Rev. Genet. 6:9–23.
Bier E, Bodmer R. 2004. Drosophila, an emerging model for cardiac disease. Gene 342:1–11.
Birse RT, Choi J, Reardon K, Rodriguez J, Graham S, Diop S, Ocorr K, Bodmer R, Oldham S. 2010. High-Fat-Diet-Induced Obesity and Heart Dysfunction Are Regulated by the TOR Pathway in Drosophila. Cell Metab. 12:533–544.
Blundell JE, Gibbons C, Caudwell P, Finlayson G, Hopkins M. 2015. Appetite control and energy balance: impact of exercise: Appetite control and exercise. Obes. Rev. 16:67–76.
Bodmer R. 1995. Heart development in Drosophila and its relationship to vertebrates. Trends Cardiovasc. Med. 5:21–28.
Bogardus C. 2009. Missing Heritability and GWAS Utility. Obesity 17:209–210.
Brewer ML. 2013. Kinematic analysis of axial rotations and the effects of stress selection on takeoff flight performance. ThesesDissertationsProfessional Pap. [Internet] Paper 1806. Available from: http://digitalscholarship.unlv.edu/thesesdissertations/1806
Brock TD, Freeze H. 1969. Thermus aquaticus gen. n. and sp. n., a Nonsporulating Extreme Thermophile. J. Bacteriol. 98:289–297.
Brownson RC, Boehmer TK, Luke DA. 2005. Declining rates of physical activity in the United States: What are the Contributors? Annu. Rev. Public Health 26:421–443.
Buescher JL, Musselman LP, Wilson CA, Lang T, Keleher M, Baranski TJ, Duncan JG. 2013. Evidence for transgenerational metabolic programming in Drosophila. Dis. Model. Mech. 6:1123–1132.
Burgio E, Lopomo A, Migliore L. 2015. Obesity and diabetes: from genetics to epigenetics. Mol. Biol. Rep. 42:799–818.
Burke MK. 2012. How does adaptation sweep through the genome? Insights from long-term selection experiments. Proc. R. Soc. B Biol. Sci. 279:5029–5038.

Burke MK, Dunham JP, Shahrestani P, Thornton KR, Rose MR, Long AD. 2010. Genome-wide analysis of a long-term evolution experiment with Drosophila. Nature 467:587–590.
Burke MK, Liti G, Long AD. 2014. Standing Genetic Variation Drives Repeatable Experimental Evolution in Outcrossing Populations of Saccharomyces cerevisiae. Mol. Biol. Evol. 31:3228–3239.
Carey HV, Martin SL, Horwitz BA, Yan L, Bailey SM, Podrabsky J, Storz JF, Ortiz RM, Wong RP, Lathrop DA. 2012. Elucidating Nature's Solutions to Heart, Lung, and Blood Diseases and Sleep Disorders. Circ. Res. 110:915–921.
Cavalera M, Wang J, Frangogiannis NG. 2014. Obesity, metabolic dysfunction, and cardiac fibrosis: pathophysiological pathways, molecular mechanisms, and therapeutic opportunities. Transl. Res. 164:323–335.
Chatterjee D, Katewa SD, Qi Y, Jackson SA, Kapahi P, Jasper H. 2014. Control of metabolic adaptation to fasting by dILP6-induced insulin signaling in *Drosophila* oenocytes. Proc. Natl. Acad. Sci. 111:17959–17964.
Chien A, Edgar DB, Trela JM. 1976. Deoxyribonucleic acid polymerase from the extreme thermophile Thermus aquaticus. J. Bacteriol. 127:1550–1557.
Chippindale AK, Chu TJF, Rose MR. 1996. Complex Trade-Offs and the Evolution of Starvation Resistance in Drosophila melanogaster. Evolution 50:753.
Christian T, Rashad I. 2009. Trends in U.S. food prices, 1950–2007. Econ. Hum. Biol. 7:113–120.
Clark JE. 2015. Diet, exercise or diet with exercise: comparing the effectiveness of treatment options for weight-loss and changes in fitness for adults (18–65 years old) who are overfat, or obese; systematic review and meta-analysis. J. Diabetes Metab. Disord. [Internet] 14. Available from: http://www.jdmdonline.com/content/14/1/31
Claussnitzer M, Dankel SN, Kim K-H, Quon G, Meuleman W, Haugen C, Glunk V, Sousa IS, Beaudry JL, Puviindran V, et al. 2015. *FTO* Obesity Variant Circuitry and Adipocyte Browning in Humans. N. Engl. J. Med. 373:895–907.
Crino M, Sacks G, Vandevijvere S, Swinburn B, Neal B. 2015. The Influence on Population Weight Gain and Obesity of the Macronutrient Composition and Energy Density of the Food Supply. Curr. Obes. Rep. 4:1–10.
Das R, Dobens LL. 2015. Conservation of gene and tissue networks regulating insulin signalling in flies and vertebrates. Biochem. Soc. Trans. 43:1057–1062.
Despres J-P. 2012. Body Fat Distribution and Risk of Cardiovascular Disease: An Update. Circulation 126:1301–1313.
Després JP, Moorjani S, Lupien PJ, Tremblay A, Nadeau A, Bouchard C. 1990. Regional distribution of body fat, plasma lipoproteins, and cardiovascular disease. Arterioscler. Dallas Tex 10:497–511.
Dietzl G, Chen D, Schnorrer F, Su K-C, Barinova Y, Fellner M, Gasser B, Kinsey K, Oppel S, Scheiblauer S, et al. 2007. A genome-wide transgenic RNAi library for conditional gene inactivation in Drosophila. Nature 448:151–156.
Diop SB, Bisharat-Kernizan J, Birse RT, Oldham S, Ocorr K, Bodmer R. 2015. PGC-1/Spargel Counteracts High-Fat-Diet-Induced Obesity and Cardiac Lipotoxicity Downstream of TOR and Brummer ATGL Lipase. Cell Rep. 10:1572–1584.
Diop SB, Bodmer R. 2015. Gaining Insights into Diabetic Cardiomyopathy from Drosophila. Trends Endocrinol. Metab. 26:618–627.

Djawdan M, Rose MR, Bradley TJ. 1997. Does Selection for Stress Resistance Lower Metabolic Rate? Ecology 78:828–837.
van Dongen J, Willemsen G, Chen W-M, de Geus EJC, Boomsma DI. 2013. Heritability of metabolic syndrome traits in a large population-based sample. J. Lipid Res. 54:2914–2923.
Dorajoo R, Blakemore AIF, Sim X, Ong RT-H, Ng DPK, Seielstad M, Wong T-Y, Saw S-M, Froguel P, Liu J, et al. 2012. Replication of 13 obesity loci among Singaporean Chinese, Malay and Asian-Indian populations. Int. J. Obes. 36:159–163.
Duffy JB. 2002. GAL4 system indrosophila: A fly geneticist's swiss army knife. genesis 34:1–15.
Dulcis D. 2005. Glutamatergic Innervation of the Heart Initiates Retrograde Contractions in Adult Drosophila melanogaster. J. Neurosci. 25:271–280.
Dwyer-Lindgren L, Freedman G, Engell RE, Fleming TD, Lim SS, Murray CJ, Mokdad AH. 2013. Prevalence of physical activity and obesity in US counties, 2001–2011: a road map for action. Popul. Health Metr. 11:7.
Dyck DV, Cerin E, De Bourdeaudhuij I, Hinckson E, Reis RS, Davey R, Sarmiento OL, Mitas J, Troelsen J, MacFarlane D, et al. 2015. International study of objectively measured physical activity and sedentary time with body mass index and obesity: IPEN adult study. Int. J. Obes. 39:199–207.
Ebert D. 1998. Experimental Evolution of Parasites. Science 282:1432–1436.
Eckel RH. 1997. Obesity and Heart Disease : A Statement for Healthcare Professionals From the Nutrition Committee, American Heart Association. Circulation 96:3248–3250.
Fall T, Ingelsson E. 2014. Genome-wide association studies of obesity and metabolic syndrome. Mol. Cell. Endocrinol. 382:740–757.
Farooqi IS, O'Rahilly S. 2005. Monogenic Obesity in Humans. Annu. Rev. Med. 56:443–458.
Fox CS, Massaro JM, Hoffmann U, Pou KM, Maurovich-Horvat P, Liu C-Y, Vasan RS, Murabito JM, Meigs JB, Cupples LA, et al. 2007. Abdominal visceral and subcutaneous adipose tissue compartments: association with metabolic risk factors in the Framingham Heart Study. Circulation 116:39–48.
Franssen SU, Nolte V, Tobler R, Schlötterer C. 2015. Patterns of Linkage Disequilibrium and Long Range Hitchhiking in Evolving Experimental *Drosophila melanogaster* Populations. Mol. Biol. Evol. 32:495–509.
Garland Jr. T. 2003. Selection experiments: An under-utilized tool in biomechanics and organismal biology. In: Bels VL, Gasc JP, Casinos A, editors. Vertebrate biomechanics and evolution. Oxford, UK: BIOS Scientific Publishers Limited. p. 23–56.
Garland T, Rose MR eds. 2009. Experimental evolution: concepts, methods, and applications of selection experiments. Berkeley: University of California Press
Gefen E, Marlon AJ, Gibbs AG. 2006. Selection for desiccation resistance in adult Drosophila melanogaster affects larval development and metabolite accumulation. J. Exp. Biol. 209:3293–3300.
Géminard C, Rulifson EJ, Léopold P. 2009. Remote Control of Insulin Secretion by Fat Cells in Drosophila. Cell Metab. 10:199–207.
Genné-Bacon EA. 2014. Thinking Evolutionarily About Obesity. Yale J Biol Med 87:99–112.
Gibbs AG, Reynolds LA. 2012. Drosophila as a Model for Starvation: Evolution, Physiology, and Genetics. In: McCue MD, editor. Comparative Physiology of Fasting, Starvation,

and Food Limitation. Berlin, Heidelberg: Springer Berlin Heidelberg. p. 37–51. Available from: http://link.springer.com/10.1007/978-3-642-29056-5_4
Gilchrist GW, Jeffers LM, West B, Folk DG, Suess J, Huey RB. 2008. Clinal patterns of desiccation and starvation resistance in ancestral and invading populations of *Drosophila subobscura*. Evol. Appl. 1:513–523.
Goenaga J, Fanara JJ, Hasson E. 2013. Latitudinal Variation in Starvation Resistance is Explained by Lipid Content in Natural Populations of Drosophila melanogaster. Evol. Biol. 40:601–612.
Goonesekera SD, Fang SC, Piccolo RS, Florez JC, McKinlay JB. 2015. Biogeographic Ancestry Is Associated with Higher Total Body Adiposity among African-American Females: The Boston Area Community Health Survey.Thameem F, editor. PLOS ONE 10:e0122808.
Grarup N, Sandholt CH, Hansen T, Pedersen O. 2014. Genetic susceptibility to type 2 diabetes and obesity: from genome-wide association studies to rare variants and beyond. Diabetologia 57:1528–1541.
Grönke S, Mildner A, Fellert S, Tennagels N, Petry S, Müller G, Jäckle H, Kühnlein RP. 2005. Brummer lipase is an evolutionary conserved fat storage regulator in Drosophila. Cell Metab. 1:323–330.
Grönke S, Müller G, Hirsch J, Fellert S, Andreou A, Haase T, Jäckle H, Kühnlein RP. 2007. Dual Lipolytic Control of Body Fat Storage and Mobilization in Drosophila.O'Rahilly S, editor. PLoS Biol. 5:e137.
Grundy SM. 2015. Metabolic syndrome update. Trends Cardiovasc. Med. [Internet]. Available from: http://linkinghub.elsevier.com/retrieve/pii/S1050173815002492
Guzzardi MA, Iozzo P. 2011. Fatty Heart, Cardiac Damage, and Inflammation. Rev. Diabet. Stud. 8:403–417.
Hallal PC, Andersen LB, Bull FC, Guthold R, Haskell W, Ekelund U. 2012. Global physical activity levels: surveillance progress, pitfalls, and prospects. The Lancet 380:247–257.
Hall KD. 2008. What is the required energy deficit per unit weight loss? Int. J. Obes. 2005 32:573–576.
Hall KD, Heymsfield SB, Kemnitz JW, Klein S, Schoeller DA, Speakman JR. 2012. Energy balance and its components: implications for body weight regulation. Am. J. Clin. Nutr. 95:989–994.
Hall KD, Sacks G, Chandramohan D, Chow CC, Wang YC, Gortmaker SL, Swinburn BA. 2011. Quantification of the effect of energy imbalance on bodyweight. The Lancet 378:826–837.
Hall ME, do Carmo JM, da Silva AA, Juncos LA, Wang Z, Hall JE. 2014. Obesity, hypertension, and chronic kidney disease. Int. J. Nephrol. Renov. Dis. 7:75–88.
Harms M, Seale P. 2013. Brown and beige fat: development, function and therapeutic potential. Nat. Med. 19:1252–1263.
Harshman, Hoffmann, Clark. 1999. Selection for starvation resistance in Drosophila melanogaster : physiological correlates, enzyme activities and multiple stress responses. J. Evol. Biol. 12:370–379.
Harshman LG, Schmid JL. 1998. Evolution of Starvation Resistance in Drosophila melanogaster: Aspects of Metabolism and Counter-Impact Selection. Evolution 52:1679.

Haunerland NH, Shirk PD. 1995. Regional and Functional Differentiation in the Insect Fact Body. Annu. Rev. Entomol. 40:121–145.
Herman MA, Rosen ED. 2015. Making Biological Sense of GWAS Data: Lessons from the FTO Locus. Cell Metab. 22:538–539.
van Herrewege J, David JR. 1997. Starvation and desiccation tolerances in Drosophila: Comparison of species from different climatic origins. Écoscience 4:151–157.
Hill JO. 2006. Understanding and Addressing the Epidemic of Obesity: An Energy Balance Perspective. Endocr. Rev. 27:750–761.
Hill JO, Wyatt HR, Peters JC. 2012. Energy Balance and Obesity. Circulation 126:126–132.
Hill JO, Wyatt HR, Reed GW, Peters JC. 2003. Obesity and the environment: where do we go from here? Science 299:853–855.
Hodgkin AL, Huxley AF. 1952. A quantitative description of membrane current and its application to conduction and excitation in nerve. J. Physiol. 117:500–544.
Hoffmann JA, Reichhart J-M. 2002. Drosophila innate immunity: an evolutionary perspective. Nat. Immunol. 3:121–126.
Hoshizaki DK. 2005. Fat-Cell Development. In: Comprehensive Molecular Insect Science. Elsevier. p. 315–345. Available from: http://linkinghub.elsevier.com/retrieve/pii/B0444519246000259
Hunt P, Martinelli A, Modrzynska K, Borges S, Creasey A, Rodrigues L, Beraldi D, Loewe L, Fawcett R, Kumar S, et al. 2010. Experimental evolution, genetic analysis and genome re-sequencing reveal the mutation conferring artemisinin resistance in an isogenic lineage of malaria parasites. BMC Genomics 11:499.
Jalvingh KM, Chang PL, Nuzhdin SV, Wertheim B. 2014. Genomic changes under rapid evolution: selection for parasitoid resistance. Proc. R. Soc. B Biol. Sci. 281:20132303–20132303.
Johansson AM, Pettersson ME, Siegel PB, Carlborg Ö. 2010. Genome-Wide Effects of Long-Term Divergent Selection.Walsh B, editor. PLoS Genet. 6:e1001188.
Kalra B, Parkash R. 2014. Trade-off of ovarian lipids and total body lipids for fecundity and starvation resistance in tropical populations of *Drosophila melanogaster*. J. Evol. Biol. 27:2371–2385.
Kang L, Aggarwal DD, Rashkovetsky E, Korol AB, Michalak P. 2016. Rapid genomic changes in Drosophila melanogaster adapting to desiccation stress in an experimental evolution system. BMC Genomics [Internet] 17. Available from: http://www.biomedcentral.com/1471-2164/17/233
Kannan K, Fridell Y-WC. 2013. Functional implications of Drosophila insulin-like peptides in metabolism, aging, and dietary restriction. Front. Physiol. [Internet] 4. Available from: http://journal.frontiersin.org/article/10.3389/fphys.2013.00288/abstract
Karan D, Dahiya N, Munjal AK, Gibert P, Moreteau B, Parkash R, David JR. 1998. Desiccation and Starvation Tolerance of Adult Drosophila: Opposite Latitudinal Clines in Natural Populations of Three Different Species. Evolution 52:825.
Kawecki TJ, Lenski RE, Ebert D, Hollis B, Olivieri I, Whitlock MC. 2012. Experimental evolution. Trends Ecol. Evol. 27:547–560.
Kelly JK, Koseva B, Mojica JP. 2013. The Genomic Signal of Partial Sweeps in Mimulus guttatus. Genome Biol. Evol. 5:1457–1469.

Kennington WJ, Gilchrist AS, Goldstein DB, Partridge L. 2001. The genetic bases of divergence in desiccation and starvation resistance among tropical and temperate populations of Drosophila melanogaster. Heredity 87:363–372.
Kessner D, Novembre J. 2015. Power Analysis of Artificial Selection Experiments Using Efficient Whole Genome Simulation of Quantitative Traits. Genetics 199:991–1005.
Kim J, Neufeld TP. 2015. Dietary sugar promotes systemic TOR activation in Drosophila through AKH-dependent selective secretion of Dilp3. Nat. Commun. 6:6846.
King NA, Caudwell P, Hopkins M, Byrne NM, Colley R, Hills AP, Stubbs JR, Blundell JE. 2007. Metabolic and behavioral compensatory responses to exercise interventions: barriers to weight loss. Obes. Silver Spring Md 15:1373–1383.
Klowden MJ. 2007. Physiological systems in insects. 2nd ed. Amsterdam ; Boston: Elsevier/Academic Press
Krahmer N, Farese RV, Walther TC. 2013. Balancing the fat: lipid droplets and human disease: Lipid droplets in disease. EMBO Mol. Med. 5:973–983.
Krebs HA. 1975. The August Krogh principle: “For many problems there is an animal on which it can be most conveniently studied.” J. Exp. Zool. 194:221–226.
Krebs HA, Johnson WA. 1980. The role of citric acid in intermediate metabolism in animal tissues. FEBS Lett. 117:K2–K10.
Kuhnlein RP. 2012. Lipid droplet-based storage fat metabolism in Drosophila: Thematic Review Series: Lipid Droplet Synthesis and Metabolism: from Yeast to Man. J. Lipid Res. 53:1430–1436.
Lavie CJ, Alpert MA, Arena R, Mehra MR, Milani RV, Ventura HO. 2013. Impact of Obesity and the Obesity Paradox on Prevalence and Prognosis in Heart Failure. JACC Heart Fail. 1:93–102.
Leal V de O, Mafra D. 2013. Adipokines in obesity. Clin. Chim. Acta 419:87–94.
Lee JH, Budanov AV, Park EJ, Birse R, Kim TE, Perkins GA, Ocorr K, Ellisman MH, Bodmer R, Bier E, et al. 2010. Sestrin as a Feedback Inhibitor of TOR That Prevents Age-Related Pathologies. Science 327:1223–1228.
Lee KP, Jang T. 2014. Exploring the nutritional basis of starvation resistance in *Drosophila melanogaster*.Davidowitz G, editor. Funct. Ecol. 28:1144–1155.
Lehmacher C, Abeln B, Paululat A. 2012. The ultrastructure of Drosophila heart cells. Arthropod Struct. Dev. 41:459–474.
Lim H-Y, Wang W, Wessells RJ, Ocorr K, Bodmer R. 2011. Phospholipid homeostasis regulates lipid metabolism and cardiac function through SREBP signaling in Drosophila. Genes Dev. 25:189–200.
Locke AE, Kahali B, Berndt SI, Justice AE, Pers TH, Day FR, Powell C, Vedantam S, Buchkovich ML, Yang J, et al. 2015. Genetic studies of body mass index yield new insights for obesity biology. Nature 518:197–206.
Long A, Liti G, Luptak A, Tenaillon O. 2015. Elucidating the molecular architecture of adaptation via evolve and resequence experiments. Nat. Rev. Genet. 16:567–582.
Loos RJF, Yeo GSH. 2013. The bigger picture of FTO—the first GWAS-identified obesity gene. Nat. Rev. Endocrinol. 10:51–61.
Lopaschuk GD, Folmes CDL, Stanley WC. 2007. Cardiac Energy Metabolism in Obesity. Circ. Res. 101:335–347.

Mackay TFC, Richards S, Stone EA, Barbadilla A, Ayroles JF, Zhu D, Casillas S, Han Y, Magwire MM, Cridland JM, et al. 2012. The Drosophila melanogaster Genetic Reference Panel. Nature 482:173–178.
Maes HH, Neale MC, Eaves LJ. 1997. Genetic and environmental factors in relative body weight and human adiposity. Behav. Genet. 27:325–351.
Malik VS, Willett WC, Hu FB. 2012. Global obesity: trends, risk factors and policy implications. Nat. Rev. Endocrinol. 9:13–27.
Malis C, Rasmussen EL, Poulsen P, Petersen I, Christensen K, Beck-Nielsen H, Astrup A, Vaag AA. 2005. Total and regional fat distribution is strongly influenced by genetic factors in young and elderly twins. Obes. Res. 13:2139–2145.
Marron MT, Markow TA, Kain KJ, Gibbs AG. 2003. Effects of starvation and desiccation on energy metabolism in desert and mesic Drosophila. J. Insect Physiol. 49:261–270.
Martins NE, Faria VG, Nolte V, Schlotterer C, Teixeira L, Sucena E, Magalhaes S. 2014. Host adaptation to viruses relies on few genes with different cross-resistance properties. Proc. Natl. Acad. Sci. 111:5938–5943.
Masek P, Reynolds LA, Bollinger WL, Moody C, Mehta A, Murakami K, Yoshizawa M, Gibbs AG, Keene AC. 2014. Altered regulation of sleep and feeding contributes to starvation resistance in Drosophila melanogaster. J. Exp. Biol. 217:3122–3132.
Masharani U, Sherchan P, Schloetter M, Stratford S, Xiao A, Sebastian A, Nolte Kennedy M, Frassetto L. 2015. Metabolic and physiologic effects from consuming a hunter-gatherer (Paleolithic)-type diet in type 2 diabetes. Eur. J. Clin. Nutr. 69:944–948.
Mathew B, Francis L, Kayalar A, Cone J. 2008. Obesity: Effects on Cardiovascular Disease and its Diagnosis. J. Am. Board Fam. Med. 21:562–568.
McVean GA, Altshuler (Co-Chair) DM, Durbin (Co-Chair) RM, Abecasis GR, Bentley DR, Chakravarti A, Clark AG, Donnelly P, Eichler EE, Flicek P, et al. 2012. An integrated map of genetic variation from 1,092 human genomes. Nature 491:56–65.
Miele L, Giorgio V, Alberelli MA, De Candia E, Gasbarrini A, Grieco A. 2015. Impact of Gut Microbiota on Obesity, Diabetes, and Cardiovascular Disease Risk. Curr. Cardiol. Rep. [Internet] 17. Available from: http://link.springer.com/10.1007/s11886-015-0671-z
Mirth CK, Riddiford LM. 2007. Size assessment and growth control: how adult size is determined in insects. BioEssays News Rev. Mol. Cell. Dev. Biol. 29:344–355.
Monteiro CA, Levy RB, Claro RM, de Castro IRR, Cannon G. 2011. Increasing consumption of ultra-processed foods and likely impact on human health: evidence from Brazil. Public Health Nutr. 14:5–13.
Moubarac J-C, Martins APB, Claro RM, Levy RB, Cannon G, Monteiro CA. 2013. Consumption of ultra-processed foods and likely impact on human health. Evidence from Canada. Public Health Nutr. 16:2240–2248.
Murdolo G, Angeli F, Reboldi G, Giacomo L, Aita A, Bartolini C, Vedecchia P. 2014. Left Ventricular Hypertrophy and Obesity: Only a Matter of Fat? High Blood Press. Cardiovasc. Prev. 22:29–41.
Mutch DM, Clément K. 2006. Unraveling the Genetics of Human Obesity. PLoS Genet. 2:e188.
Na J, Musselman LP, Pendse J, Baranski TJ, Bodmer R, Ocorr K, Cagan R. 2013. A Drosophila Model of High Sugar Diet-Induced Cardiomyopathy.Rulifson E, editor. PLoS Genet. 9:e1003175.

Neel JV. 1962. Diabetes Mellitus: A “Thrifty” Genotype Rendered Detrimental by “Progress”? Am J Hum Genet 14:353–362.
Neel JV. 1989. Update to “The Study of Natural Selection in Primitive and Civilized Human Populations.” Hum. Biol. 61:811–823.
Nelson MD, Victor RG, Szczepaniak EW, Simha V, Garg A, Szczepaniak LS. 2013. Cardiac Steatosis and Left Ventricular Hypertrophy in Patients With Generalized Lipodystrophy as Determined by Magnetic Resonance Spectroscopy and Imaging. Am. J. Cardiol. 112:1019–1024.
Newell PD, Chaston JM, Wang Y, Winans NJ, Sannino DR, Wong ACN, Dobson AJ, Kagle J, Douglas AE. 2014. In vivo function and comparative genomic analyses of the Drosophila gut microbiota identify candidate symbiosis factors. Front. Microbiol. [Internet] 5. Available from: http://journal.frontiersin.org/article/10.3389/fmicb.2014.00576/abstract
Ng M, Fleming T, Robinson M, Thomson B, Graetz N, Margono C, Mullany EC, Biryukov S, Abbafati C, Abera SF, et al. 2014. Global, regional, and national prevalence of overweight and obesity in children and adults during 1980–2013: a systematic analysis for the Global Burden of Disease Study 2013. The Lancet 384:766–781.
Nielsen SJ. 2003. Patterns and Trends in Food Portion Sizes, 1977-1998. JAMA 289:450.
Nielsen SJ, Popkin BM. 2004. Changes in beverage intake between 1977 and 2001. Am. J. Prev. Med. 27:205–210.
Nolis T. 2014. Exploring the pathophysiology behind the more common genetic and acquired lipodystrophies. J. Hum. Genet. 59:16–23.
Norden-Krichmar TM, Gizer IR, Libiger O, Wilhelmsen KC, Ehlers CL, Schork NJ. 2014. Correlation analysis of genetic admixture and social identification with body mass index in a Native American Community: Genetic Admixture and Body Mass Index. Am. J. Hum. Biol. 26:347–360.
Ocorr K, Reeves NL, Wessells RJ, Fink M, Chen H-SV, Akasaka T, Yasuda S, Metzger JM, Giles W, Posakony JW, et al. 2007. KCNQ potassium channel mutations cause cardiac arrhythmias in Drosophila that mimic the effects of aging. Proc. Natl. Acad. Sci. 104:3943–3948.
Olds T, Maher C, Zumin S, Péneau S, Lioret S, Castetbon K, Bellisle, de Wilde J, Hohepa M, Maddison R, et al. 2011. Evidence that the prevalence of childhood overweight is plateauing: data from nine countries. Int. J. Pediatr. Obes. 6:342–360.
O’Rahilly S, Farooqi IS. 2008. Human Obesity: A Heritable Neurobehavioral Disorder That Is Highly Sensitive to Environmental Conditions. Diabetes 57:2905–2910.
Orozco-terWengel P, Kapun M, Nolte V, Kofler R, Flatt T, SchlöTterer C. 2012. Adaptation of *Drosophila* to a novel laboratory environment reveals temporally heterogeneous trajectories of selected alleles: Genomic signatures of adaptation to new enviornment. Mol. Ecol. 21:4931–4941.
O’Rourke RW. 2014. Metabolic Thrift and the Genetic Basis of Human Obesity: Ann. Surg. 259:642–648.
Paaby AB, Bergland AO, Behrman EL, Schmidt PS. 2014. A highly pleiotropic amino acid polymorphism in the *Drosophila* insulin receptor contributes to life-history adaptation: ADAPTIVE POLYMORPHISM AT *InR*. Evolution 68:3395–3409.

Paaby AB, Blacket MJ, Hoffmann AA, Schmidt PS. 2010. Identification of a candidate adaptive polymorphism for *Drosophila* life history by parallel independent clines on two continents: ALLELIC VARIATION AT *INR*. Mol. Ecol. 19:760–774.
Palanker Musselman L, Fink JL, Narzinski K, Ramachandran PV, Sukumar Hathiramani S, Cagan RL, Baranski TJ. 2011. A high-sugar diet produces obesity and insulin resistance in wild-type Drosophila. Dis. Model. Mech. 4:842–849.
Parts L, Cubillos FA, Warringer J, Jain K, Salinas F, Bumpstead SJ, Molin M, Zia A, Simpson JT, Quail MA, et al. 2011. Revealing the genetic structure of a trait by sequencing a population under selection. Genome Res. 21:1131–1138.
Patel RT, Soulages JL, Hariharasundaram B, Arrese EL. 2005. Activation of the Lipid Droplet Controls the Rate of Lipolysis of Triglycerides in the Insect Fat Body. J. Biol. Chem. 280:22624–22631.
Payne AN, Chassard C, Lacroix C. 2012. Gut microbial adaptation to dietary consumption of fructose, artificial sweeteners and sugar alcohols: implications for host-microbe interactions contributing to obesity: Fructose impacts on gut microbiota and obesity. Obes. Rev. 13:799–809.
Piazza N, Wessells RJ. 2011. Drosophila Models of Cardiac Disease. In: Progress in Molecular Biology and Translational Science. Vol. 100. Elsevier. p. 155–210. Available from: http://linkinghub.elsevier.com/retrieve/pii/B9780123848789000054
Poirier P. 2006. Obesity and Cardiovascular Disease: Pathophysiology, Evaluation, and Effect of Weight Loss: An Update of the 1997 American Heart Association Scientific Statement on Obesity and Heart Disease From the Obesity Committee of the Council on Nutrition, Physical Activity, and Metabolism. Circulation 113:898–918.
Pospisilik JA, Schramek D, Schnidar H, Cronin SJF, Nehme NT, Zhang X, Knauf C, Cani PD, Aumayr K, Todoric J, et al. 2010. Drosophila Genome-wide Obesity Screen Reveals Hedgehog as a Determinant of Brown versus White Adipose Cell Fate. Cell 140:148–160.
Rajan A, Perrimon N. 2012. Drosophila Cytokine Unpaired 2 Regulates Physiological Homeostasis by Remotely Controlling Insulin Secretion. Cell 151:123–137.
Raj SM, Halebeedu P, Kadandale JS, Mirazon Lahr M, Gallego Romero I, Yadhav JR, Iliescu M, Rai N, Crivellaro F, Chaubey G, et al. 2013. Variation at Diabetes- and Obesity-Associated Loci May Mirror Neutral Patterns of Human Population Diversity and Diabetes Prevalence in India: Variation at Diabetes- and Obesity-Associated Loci in Indians. Ann. Hum. Genet. 77:392–408.
Rankinen T, Zuberi A, Chagnon YC, Weisnagel SJ, Argyropoulos G, Walts B, Pérusse L, Bouchard C. 2006. The human obesity gene map: the 2005 update. Obes. Silver Spring Md 14:529–644.
Ravelli GP, Stein ZA, Susser MW. 1976. Obesity in young men after famine exposure in utero and early infancy. N. Engl. J. Med. 295:349–353.
Remolina SC, Chang PL, Leips J, Nuzhdin SV, Hughes KA. 2012. Genomic basis of aging and life-history evolution in *Drosophila melanogaster*: Genomics of life-history evolution. Evolution 66:3390–3403.
Reynolds LA. 2013. The Effects of Starvation Selection on Drosophila Melanogaster Life History and Development. UNLV ThesesDissertationsProfessional Pap. Paper 1876.

Rion S, Kawecki TJ. 2007. Evolutionary biology of starvation resistance: what we have learned from *Drosophila*: Starvation resistance in *Drosophila*. J. Evol. Biol. 20:1655–1664.
Robinson E, Hunger JM, Daly M. 2015. Perceived weight status and risk of weight gain across life in US and UK adults. Int. J. Obes. 39:1721–1726.
Rose MR. 1984. Laboratory Evolution of Postponed Senescence in Drosophila melanogaster. Evolution 38:1004.
Rose MR, Vu LN, Park SU, Graves JL. 1992. Selection on stress resistance increases longevity in Drosophila melanogaster. Exp. Gerontol. 27:241–250.
Rosenbaum M, Knight R, Leibel RL. 2015. The gut microbiota in human energy homeostasis and obesity. Trends Endocrinol. Metab. 26:493–501.
Rubin C-J, Zody MC, Eriksson J, Meadows JRS, Sherwood E, Webster MT, Jiang L, Ingman M, Sharpe T, Ka S, et al. 2010. Whole-genome resequencing reveals loci under selection during chicken domestication. Nature 464:587–591.
Sajid W, Kulahin N, Schluckebier G, Ribel U, Henderson HR, Tatar M, Hansen BF, Svendsen AM, Kiselyov VV, Norgaard P, et al. 2011. Structural and Biological Properties of the Drosophila Insulin-like Peptide 5 Show Evolutionary Conservation. J. Biol. Chem. 286:661–673.
Scarborough P, Burg MR, Foster C, Swinburn B, Sacks G, Rayner M, Webster P, Allender S. 2011. Increased energy intake entirely accounts for increase in body weight in women but not in men in the UK between 1986 and 2000. Br. J. Nutr. 105:1399–1404.
Schmidt PS, Matzkin L, Ippolito M, Eanes WF. 2005. Geographic variation in diapause incidence, life-history traits, and climatic adaptation in Drosophila melanogaster. Evolution 59:1721.
Schulz TJ, Tseng Y-H. 2013. Brown adipose tissue: development, metabolism and beyond. Biochem. J. 453:167–178.
Schwasinger-Schmidt TE, Kachman SD, Harshman LG. 2012. Evolution of starvation resistance in Drosophila melanogaster: measurement of direct and correlated responses to artificial selection: Evolution of starvation resistance. J. Evol. Biol. 25:378–387.
Schweiger M, Lass A, Zimmermann R, Eichmann TO, Zechner R. 2009. Neutral lipid storage disease: genetic disorders caused by mutations in adipose triglyceride lipase/PNPLA2 or CGI-58/ABHD5. AJP Endocrinol. Metab. 297:E289–E296.
Segula D. 2014. Complications of obesity in adults: A short review of the literature. Malawi Med. J. 26:20–24.
Service PM, Rose MR. 1985. Genetic Covariation Among Life-History Components: The Effect of Novel Environments. Evolution 39:943–945.
Sharmila Bharathi N, Prasad NG, Shakarad M, Joshi A. 2003. Variation in adult life history and stress resistance across five species of Drosophila. J. Genet. 82:191–205.
Shimabukuro M, Kozuka C, Taira S, Yabiku K, Dagvasumberel M, Ishida M, Matsumoto S, Yagi S, Fukuda D, Yamakawa K, et al. 2013. Ectopic fat deposition and global cardiometabolic risk: new paradigm in cardiovascular medicine. J. Med. Investig. JMI 60:1–14.

Silventoinen K, Rokholm B, Kaprio J, Sørensen TIA. 2010. The genetic and environmental influences on childhood obesity: a systematic review of twin and adoption studies. Int. J. Obes. 2005 34:29–40.
Sisodia S, Singh BN. 2010. Resistance to environmental stress in Drosophila ananassae: latitudinal variation and adaptation among populations: Resistance to environmental stress in D. ananassae. J. Evol. Biol. 23:1979–1988.
Slaidina M, Delanoue R, Gronke S, Partridge L, Léopold P. 2009. A Drosophila Insulin-like Peptide Promotes Growth during Nonfeeding States. Dev. Cell 17:874–884.
Slama K. 2010. Physiology of heartbeat reversal in adult Drosophila melanogaster (Diptera: Drosophilidae). Eur. J. Entomol. 107:13–31.
Slavin JL. 2005. Dietary fiber and body weight. Nutrition 21:411–418.
Smith JM, Haigh J. 1974. The hitch-hiking effect of a favourable gene. Genet. Res. 23:23–35.
Southam L, Soranzo N, Montgomery SB, Frayling TM, McCarthy MI, Barroso I, Zeggini E. 2009. Is the thrifty genotype hypothesis supported by evidence based on confirmed type 2 diabetes- and obesity-susceptibility variants? Diabetologia 52:1846–1851.
Speakman JR. 2008. Thrifty genes for obesity, an attractive but flawed idea, and an alternative perspective: the “drifty gene” hypothesis. Int. J. Obes. 32:1611–1617.
Steenhuis IH, Vermeer WM. 2009. Portion size: review and framework for interventions. Int. J. Behav. Nutr. Phys. Act. 6:58.
Stevens GA, Singh GM, Lu Y, Danaei G, Lin JK, Finucane MM, Bahalim AN, McIntire RK, Gutierrez HR, Cowan M, et al. 2012. National, regional, and global trends in adult overweight and obesity prevalences. Popul. Health Metr. 10:22.
Stöger R. 2008. The thrifty epigenotype: An acquired and heritable predisposition for obesity and diabetes? BioEssays 30:156–166.
Stunkard AJ, Foch TT, Hrubec Z. 1986. A twin study of human obesity. JAMA 256:51–54.
Stunkard AJ, Harris JR, Pedersen NL, McClearn GE. 1990. The Body-Mass Index of Twins Who Have Been Reared Apart. N. Engl. J. Med. 322:1483–1487.
Stunkard AJ, Sørensen TI, Hanis C, Teasdale TW, Chakraborty R, Schull WJ, Schulsinger F. 1986. An adoption study of human obesity. N. Engl. J. Med. 314:193–198.
Sujkowski A, Saunders S, Tinkerhess M, Piazza N, Jennens J, Healy L, Zheng L, Wessells R. 2012. dFatp regulates nutrient distribution and long-term physiology in Drosophila. Aging Cell 11:921–932.
Sujkowski A, Wessells R. 2015. Drosophila Models of Cardiac Aging and Disease. In: Vaiserman MA, Moskalev AA, Pasyukova GE, editors. Life Extension: Lessons from Drosophila. Cham: Springer International Publishing. p. 127–150. Available from: http://dx.doi.org/10.1007/978-3-319-18326-8_6
Swinburn BA, Sacks G, Hall KD, McPherson K, Finegood DT, Moodie ML, Gortmaker SL. 2011. The global obesity pandemic: shaped by global drivers and local environments. The Lancet 378:804–814.
Swinburn B, Sacks G, Ravussin E. 2009. Increased food energy supply is more than sufficient to explain the US epidemic of obesity. Am. J. Clin. Nutr. 90:1453–1456.
Taegtmeyer H. 1994. Energy metabolism of the heart: from basic concepts to clinical applications. Curr. Probl. Cardiol. 19:59–113.
Taghli-Lamallem O, Akasaka T, Hogg G, Nudel U, Yaffe D, Chamberlain JS, Ocorr K, Bodmer R. 2008. Dystrophin deficiency in Drosophila reduces lifespan and causes a dilated cardiomyopathy phenotype. Aging Cell 7:237–249.

Taghli-Lamallem O, Jagla K, Chamberlain JS, Bodmer R. 2014. Mechanical and non-mechanical functions of Dystrophin can prevent cardiac abnormalities in Drosophila. Exp. Gerontol. 49:26–34.
Tai PWL, Zaidi SK, Wu H, Grandy RA, Montecino M, van Wijnen AJ, Lian JB, Stein GS, Stein JL. 2014. The Dynamic Architectural and Epigenetic Nuclear Landscape: Developing the Genomic Almanac of Biology and Disease: EPIGENETICS OF NUCLEAR ORGANIZATION. J. Cell. Physiol. 229:711–727.
Tan L-J, Zhu H, He H, Wu K-H, Li J, Chen X-D, Zhang J-G, Shen H, Tian Q, Krousel-Wood M, et al. 2014. Replication of 6 Obesity Genes in a Meta-Analysis of Genome-Wide Association Studies from Diverse Ancestries.Palmer ND, editor. PLoS ONE 9:e96149.
Tchernof A, Despres J-P. 2013. Pathophysiology of Human Visceral Obesity: An Update. Physiol. Rev. 93:359–404.
Teleman AA. 2010. Molecular mechanisms of metabolic regulation by insulin in *Drosophila*. Biochem. J. 425:13–26.
Teotónio H, Chelo IM, Bradić M, Rose MR, Long AD. 2009. Experimental evolution reveals natural selection on standing genetic variation. Nat. Genet. 41:251–257.
Thummel CS. 1995. From embryogenesis to metamorphosis: The regulation and function of drosophila nuclear receptor superfamily members. Cell 83:871–877.
Tobi EW, Lumey LH, Talens RP, Kremer D, Putter H, Stein AD, Slagboom PE, Heijmans BT. 2009. DNA methylation differences after exposure to prenatal famine are common and timing- and sex-specific. Hum. Mol. Genet. 18:4046–4053.
Tremblay A, Bellisle F. 2015. Nutrients, satiety, and control of energy intake [1]. Appl. Physiol. Nutr. Metab. 40:971–979.
Tsai AG, Williamson DF, Glick HA. 2011. Direct medical cost of overweight and obesity in the USA: a quantitative systematic review: USA obesity direct medical cost. Obes. Rev. 12:50–61.
Turner TL, Miller PM. 2012. Investigating Natural Variation in Drosophila Courtship Song by the Evolve and Resequence Approach. Genetics 191:633–642.
Turner TL, Stewart AD, Fields AT, Rice WR, Tarone AM. 2011. Population-Based Resequencing of Experimentally Evolved Populations Reveals the Genetic Basis of Body Size Variation in Drosophila melanogaster.Gibson G, editor. PLoS Genet. 7:e1001336.
Unckless RL, Rottschaefer SM, Lazzaro BP. 2015. A Genome-Wide Association Study for Nutritional Indices in Drosophila. G3amp58 GenesGenomesGenetics 5:417–425.
Unger RH, Clark GO, Scherer PE, Orci L. 2010. Lipid homeostasis, lipotoxicity and the metabolic syndrome. Biochim. Biophys. Acta BBA - Mol. Cell Biol. Lipids 1801:209–214.
Vandevijvere S, Chow CC, Hall KD, Umali E, Swinburn BA. 2015. Increased food energy supply as a major driver of the obesity epidemic: a global analysis. Bull. World Health Organ. 93:446–456.
Vatier C, Bidault G, Briand N, Guénantin A-C, Teyssières L, Lascols O, Capeau J, Vigouroux C. 2013. What the Genetics of Lipodystrophy Can Teach Us About Insulin Resistance and Diabetes. Curr. Diab. Rep. 13:757–767.
Walley AJ, Asher JE, Froguel P. 2009. The genetic contribution to non-syndromic human obesity. Nat. Rev. Genet. 10:431–442.

Wang B, Moya N, Niessen S, Hoover H, Mihaylova MM, Shaw RJ, Yates JR, Fischer WH, Thomas JB, Montminy M. 2011. A Hormone-Dependent Module Regulating Energy Balance. Cell 145:596–606.
Wasserthal LT. 2007. Drosophila flies combine periodic heartbeat reversal with a circulation in the anterior body mediated by a newly discovered anterior pair of ostial valves and `venous' channels. J. Exp. Biol. 210:3707–3719.
Wayne ML, Soundararajan U, Harshman LG. 2006. Environmental stress and reproduction in Drosophila melanogaster : starvation resistance, ovariole numbers and early age egg production. BMC Evol. Biol. 6:1–10.
Weavers H, Prieto-Sánchez S, Grawe F, Garcia-López A, Artero R, Wilsch-Bräuninger M, Ruiz-Gómez M, Skaer H, Denholm B. 2009. The insect nephrocyte is a podocyte-like cell with a filtration slit diaphragm. Nature 457:322–326.
Westerterp KR, Speakman JR. 2008. Physical activity energy expenditure has not declined since the 1980s and matches energy expenditures of wild mammals. Int. J. Obes. 32:1256–1263.
Willer CJ, Speliotes EK, Loos RJF, Li S, Lindgren CM, Heid IM, Berndt SI, Elliott AL, Jackson AU, Lamina C, et al. 2009. Six new loci associated with body mass index highlight a neuronal influence on body weight regulation. Nat. Genet. 41:25–34.
Williams AE, Rose MR, Bradley TJ. 2004. The respiratory pattern in Drosophila melanogaster selected for desiccation resistance is not associated with the observed evolution of decreased locomotory activity. Physiol. Biochem. Zool. PBZ 77:10–17.
Wolf MJ, Rockman HA. 2011. Drosophila, Genetic Screens, and Cardiac Function. Circ. Res. 109:794–806.
Xia Q, Grant SFA. 2013. The genetics of human obesity: Genetics of human obesity. Ann. N. Y. Acad. Sci. 1281:178–190.
Yang H, He X, Yang J, Deng X, Liao Y, Zhang Z, Zhu C, Shi Y, Zhou N. 2013. Activation of cAMP-response element-binding protein is positively regulated by PKA and calcium-sensitive calcineurin and negatively by PKC in insect. Insect Biochem. Mol. Biol. 43:1028–1036.
Yu Z, Ren M, Wang Z, Zhang B, Rong YS, Jiao R, Gao G. 2013. Highly Efficient Genome Modifications Mediated by CRISPR/Cas9 in Drosophila. Genetics 195:289–291.
Zhang J. 2012. Genetic Redundancies and Their Evolutionary Maintenance. In: Soyer OS, editor. Evolutionary Systems Biology, Advances in Experimental Medicine and Biology. Springer Science+Business Media, LLC. p. 279–300.
Zhang Y, Ren J. 2011. Role of Cardiac Steatosis and Lipotoxicity in Obesity Cardiomyopathy. Hypertension 57:148–150.
Zhang Y, Wong C-H, Birnbaum RY, Li G, Favaro R, Ngan CY, Lim J, Tai E, Poh HM, Wong E, et al. 2013. Chromatin connectivity maps reveal dynamic promoter–enhancer long-range associations. Nature 504:306–310.
Zhou D, Udpa N, Gersten M, Visk DW, Bashir A, Xue J, Frazer KA, Posakony JW, Subramaniam S, Bafna V, et al. 2011. Experimental selection of hypoxia-tolerant Drosophila melanogaster. Proc. Natl. Acad. Sci. 108:2349–2354.

CHAPTER 2

OBESITY-ASSOCIATED CARDIAC DYSFUNCTION IN STARVATION-SELECTED *DROSOPHILA MELANOGASTER*

Previously published as:
Hardy, C.M., Birse, R.T., Wolf, M.J., Yu, L., Bodmer, R. & Gibbs, A.G., 2015. Obesity-associated cardiac dysfunction in starvation-selected *Drosophila melanogaster*. Am. J. Physiol. - Regul. Integr. Comp. Physiol. 309, R658–R667. doi:10.1152/ajpregu.00160.2015

Christopher M. Hardy[1], Ryan T. Birse[2], Matthew J. Wolf[3], Lin Yu[4], Rolf Bodmer[2] and Allen G. Gibbs[1]

[1]School of Life Sciences, University of Nevada Las Vegas, Las Vegas, NV.

[2]Development, Aging and Regeneration Program, Sanford Burnham Medical Research Institute, La Jolla, CA.

[3]Department of Medicine, Robert M. Berne Cardiovascular Research Center, University of Virginia School of Medicine, Charlottesville, VA.

[4]School of Medicine- Cardiology, Duke University, Durham, NC.

Author Contributions: C.M.H. and A.G.G. planned experiments with assistance from R.T.B. C.M.H. and A.G.G. performed statistical analyses and wrote the paper. C.M.H and R.T.B. performed semi-automated heart beat analysis (SOHA) and heart structure staining with assistance from R.B. Optical coherence tomography (OCT) was performed by M.J.W. and

histology performed by L.Y. All other experiments were performed by C.M.H. Each author contributed to editing the final manuscript.

2.1 Abstract

There is a clear link between obesity and cardiovascular disease, but the complexity of this interaction in mammals makes it difficult to study. Among the animal models used to investigate obesity-associated diseases, *Drosophila melanogaster* has emerged as an important platform of discovery. In the laboratory, *Drosophila* can be made obese through lipogenic diets, genetic manipulations and adaptation to evolutionary stress. While dietary and genetic changes that cause obesity in flies have been demonstrated to induce heart dysfunction, there have been no reports investigating how obesity affects the heart in laboratory-evolved populations. Here, we studied replicated populations of *Drosophila* that had been selected for starvation resistance for over 65 generations. These populations evolved characteristics that closely resemble hallmarks of metabolic syndrome in mammals. We demonstrate that starvation-selected *Drosophila* have dilated hearts with impaired contractility. This phenotype appears to be correlated with large fat deposits along the dorsal cuticle, which alter the anatomical position of the heart. We demonstrate a strong relationship between fat storage and heart dysfunction, as dilation and reduced contractility can be rescued through prolonged fasting. Unlike other *Drosophila* obesity models, the starvation-selected lines do not exhibit excessive intracellular lipid deposition within the myocardium and rather store excess triglycerides in large lipid droplets within the fat body. Our findings provide a new model to investigate obesity-associated heart dysfunction.

2.2 Introduction

Obesity is a leading risk factor for many diseases, including type-II diabetes, cardiovascular disease and certain types of cancer (De Pergola and Silvestris 2013; Bastien et al. 2014). With worldwide obesity rates at an all-time high, attention has focused on understanding the etiology of obesity-associated diseases. Recently, *Drosophila melanogaster* has emerged as an excellent model to investigate the genetic causes and physiological consequences of obesity. In the laboratory, *Drosophila* can be made obese through dietary changes, genetic manipulation and adaptation to evolutionary stress (Chippindale et al. 1996; Harshman et al. 1999; Birse et al. 2010; Lee et al. 2010; Birse and Bodmer 2011; Lim et al. 2011; Diop and Bodmer 2012; Na et al. 2013; Diop et al. 2015). These models recapitulate many aspects of obesity, and some have provided the tools to investigate how increased lipids affect the heart. For instance, *Drosophila* fed lipogenic diets high in fat or sugar, store higher levels of triglycerides (TG) and exhibit a range of associated cardiomyopathies (Birse et al. 2010; Na et al. 2013). Genetic mutations that alter lipid homeostasis can also induce heart dysfunction. For example, hyperactivation of TOR signaling through reduction of sestrin function or mutation of downstream components of TOR, such as PGC-1 and ATGL lipase, lead to increased total TG and heart dysfunction-including arrhythmia, reduced cardiac contractility and defects in structural integrity (Lee et al. 2010; Diop et al. 2015). Additionally, genetic dysregulation of phospholipid metabolism results in increased expression of *Drosophila* sterol regulatory element-binding protein (*dSREBP*), leading to higher levels of stored fat and alterations to the structure and function of the heart (Lim et al. 2011). Another study found that the loss of

one copy of the gene coding for the *Drosophila* fatty acid transport protein (*dFatp*) results in obese flies, which exhibit low cardiac stress resistance (Sujkowski et al. 2012).

Common among many of these models is the increase in intracellular accumulation of lipids within the myocardium, hypothesized to cause structural and functional damage to the heart (Birse et al. 2010; Lim et al. 2011; Sujkowski et al. 2012; Na et al. 2013; Diop et al. 2015). This lipotoxic effect is well documented in mammals and occurs when TG levels surpass the storage capacity for lipids within adipose tissue (Bastien et al. 2014). In *Drosophila*, the functional equivalent of adipose tissue is the fat body, a heterogeneous tissue responsible for nutrient storage and utilization amidst many other functions (Arrese and Soulages 2010). Within the fat body, highly conserved intracellular lipid droplets act as the primary site of TG synthesis, storage and breakdown (Kuhnlein 2012). In lipotoxic conditions, lipid droplets within the adipose tissue become oversaturated which leads to ectopic fat deposition in non-adipose tissues. In mammals, excess accumulation of lipids in non-adipose tissues is strongly correlated with organ degeneration, leading to disrupted structure and function (Unger et al. 2010). In *Drosophila* this may result in reduced lifespan (Na et al. 2013), altered carbohydrate homeostasis (Birse et al. 2010; Na et al. 2013) and heart dysfunction (Birse et al. 2010; Lim et al. 2011; Sujkowski et al. 2012; Na et al. 2013; Diop et al. 2015).

While obesity has many pathophysiological effects, the ability to store excess lipids may have an ecological advantage in the context of starvation resistance. In nature, lipids stored within the fat body may be used as a vital resource to survive periods of low nutrient availability (Parkash et al. 2012; Aggarwal 2014). Indeed, natural variation for starvation-resistance in *Drosophila simulans* positively correlates with stored fats (Ballard

et al. 2008). In the laboratory, selection for starvation-resistance in *Drosophila melanogaster* leads to correlated increases in stored lipids (Chippindale et al. 1996; Harshman et al. 1999). However adaptation to starvation-resistance incurs evolutionary costs, including reductions in metabolic rate, locomotion and longevity (Rion and Kawecki 2007). While these phenotypes are similar to the increased lipids, impaired activity levels (via geotaxic response) and decreased longevity reported in other obesity models (Birse et al. 2010; Na et al. 2013), to our knowledge there have been no investigations into the physiological consequences of starvation selection on the heart.

We selected replicated populations of *Drosophila melanogaster* for starvation resistance for over 65 generations. In response to selection, the Starvation-selected (hereafter "S") populations evolved an obese condition, storing nearly twice the level of total lipids as compared to their ostensibly unselected Fed controls (hereafter "F" populations) (Reynolds 2013). The stored lipids are metabolized upon exposure to starvation, and utilized by the S populations to survive nearly 14 days without food. The excess lipids in the S lines accumulate during an extended larval feeding period (Reynolds 2013). However S flies remain obese in adulthood despite consuming fewer calories than their unselected controls when fed *ad libitum* (Masek et al. 2014). There are many evolutionary tradeoffs associated with increased adiposity in the S lines including decreases in developmental rate, fecundity, metabolic rate, activity levels, flight performance and disrupted sleeping patterns (Brewer 2013; Reynolds 2013; Masek et al. 2014). Because many of these phenotypes are suggestive of metabolic disorder, we questioned whether starvation-selected *Drosophila* also exhibited heart dysfunction.

Here, we demonstrate using multiple approaches that starvation-selected *Drosophila melanogaster* have dilated, less-contractile hearts than their unselected controls. Our data and observations suggest that this dysfunction is in part related to expanded fat body tissue which physically interferes with the anatomical position of the heart. We also demonstrate that heart dysfunction in the S populations is associated with increased fat storage, as cardiac enlargement and contractile impairment can be rescued through prolonged fasting. Unlike most obesity models in *Drosophila*, our data suggest S flies do not ectopically store lipids within the myocardium. Instead S flies have adapted by increasing the storage capacity of lipids within the fat body by increasing lipid droplet volume. These findings shed light into the evolutionary origins of obesity and provide a unique model to study the genetics and physiology of obesity associated cardiac disease.

2.3 Methods

Laboratory natural selection for starvation resistance

The starvation-selected ("S") populations were derived from wild caught *D. melanogaster* collected in Terhune New Jersey in 1998 as previously described (Gefen and Gibbs 2009). In 2007, subpopulations were derived from these lines and subjected to selection for starvation resistance. Each generation, 4 day-old post-eclosion adults were given non-caloric agar and maintained until 80-90% had died. The survivors were fed and used as founders for the next generation. Fed control ("F") populations were given unrestricted access to food but otherwise handled in parallel with the starvation-selected lines. Each cohort (starvation-selected and fed control) is composed of 3 independent replicates. Experiments conducted here were from generations 65-80. For all experiments the S populations were removed from selection for one generation, maintained and treated in parallel to the controls to remove potential parental effects. All experiments were performed on females.

Semi-automated Optical Heartbeat Analysis (SOHA)

To analyze cardiac contractions we used previously described video microscopy techniques (Karen Ocorr et al. 2007; K. Ocorr et al. 2007a; Fink et al. 2009). For this method it is necessary to surgically expose the fly's heart in order to make it accessible for high-resolution filming (Vogler and Ocorr 2009). In brief, dissections to expose the fly's heart within the abdomen were kept in oxygenated saline and high-speed digital movies were taken and analyzed using custom software (sohasoftware.com) for end-diastolic (EDD), end-systolic (ESD) diameter, heart period intervals and arrhythmia (Karen Ocorr et

al. 2007; K. Ocorr et al. 2007a; K. Ocorr et al. 2007b; Fink et al. 2009). Fractional shortening (FS) was calculated as [EDD-ESD]/EDD x 100.

Optical Coherence Tomography (OCT)

Cardiac function was also measured using a custom built OCT microscopy system (Bioptigen, Inc. Durham, NC) as previously described (Wolf et al. 2006; Yu et al. 2013). Flies were briefly anesthetized using CO_2, immobilized, and allowed to awaken prior to performing OCT. M-mode images, resulting from a method that measures heart wall movement during the cardiac cycle were acquired, processed, and analyzed to calculate EDD and ESD, determined from 3 consecutive heart beats. Heart rates were calculated from m-mode images and expressed as the period in seconds per heart beat.

Rescue Experiments

We performed two sets of experiments to reduce TG content in S flies in an attempt to rescue heart function. For adult rescue experiments, both F and S flies were aged 4-5 days then placed on media containing either non-caloric 1% agar or standard cornmeal. S lines were evenly split between these two conditions while F flies were transferred only to fresh standard cornmeal medium, with care taken to maintain similar densities between S and F cohorts. Flies on all treatments were aged for 7 days then subjected to TG measurements, SOHA or OCT.

The larval rescue protocol has been previously described (Masek et al. 2014). In short, F and S larvae were reared in parallel. When F larvae began to wander, 3rd instar S larvae were picked from their media and placed in either fresh standard cornmeal medium

or 1% agar. Eclosing flies were placed on standard cornmeal medium and aged 4-5 days then subjected to TG measurements and SOHA.

Triglyceride and Protein Measurements

Individual flies were homogenized using a motorized pestle in 120µL of western lysis buffer (previously described, (Aguila et al. 2013)) on ice. Homogenates were incubated at 70°C for 5 minutes to heat-kill lipases. Samples were centrifuged and the supernatant was used to measure either total TG or total protein levels. For TG, a 1:10 dilution of supernatant to Infinity™ Triglycerides Reagent (Thermo Scientific, Middletown, CA.) was mixed in a 96-well plate. The plate was covered with parafilm to prevent evaporation and incubated for 30 minutes at 37°C, then was measured using a µQuant™ Microplate Spectrophotometer (BioTek® Instruments Inc., Winooski, VT.) at 540nm. For total protein, a 1:5 solution of supernatant to dye (dye: 1 part 4% $CuSO_4$ to 49 parts bicinchonicic acid) was mixed in a 96-well plate, covered and incubated at 25°C for 12 hours and assayed for absorbance at 562nm. Final concentrations for all samples were calculated compared to a standard curve of either Triglyceride Standard (Pointe Scientific, Ann Arbor, MI) or bovine serum albumin for protein standards. The number and age of flies assayed varied depending on experiment and are labeled in the figure legends.

For heart-specific assays, 15-30 individual hearts were exposed in 1xPBS. Excess fat and associated cells were removed from the sides of the heart using a finely pulled glass micro-pipette attached to a vacuum. Samples were washed 3 times with 1xPBS then dissected into 15-30µL of western lysis buffer. Samples were homogenized with a motorized pestle, briefly sonicated then incubated for 5 minutes at 70°C. Solutions were

treated as stated above to determine the final concentrations of heart-specific TG or protein. 9 such samples were analyzed per selection treatment.

Histology

Histological sections were obtained as previously described (Yu et al. 2013). Briefly, adult female flies (4-5 days post eclosion) were collected and placed in Telly's fixation buffer (60% ethanol, 3.33% formalin, 4% glacial acetic acid) for at least one week at 4°C prior to paraffin embedding. Serial 8-micron sections were stained with hemotoxin and eosin (H&E) then analyzed using a Leica DM2500 microscope equipped with a Leica DFC310FX digital camera. For each selection treatment, 3-5 serial sections from 13 animals were scored for the presence and degree of fat body accumulation between the heart and the dorsal cuticle. Data were analyzed using the Freeman-Halton extension of the Fisher's Exact Test with the R software package (R Core Team 2015). Images were cropped and annotated to demonstrate anatomical displacement.

Heart Structure

Hearts were dissected, stained and imaged as previously described (Alayari et al. 2009). Briefly, flies were dissected in oxygenated artificial hemolymph then the exposed hearts were chemically relaxed, fixed and stained with a 1:1000 dilution of GFP-conjugated phalloidin (Alexa Fluor®488 phalloidin, Grand Island, NY). Images were taken with a Zeiss Apotome in conjunction with the Axiovision software package. Image stacks were processed using the Fiji software package (Schindelin et al. 2012) to visualize the circumferential fibers of the cardiomyocytes. Images were randomly labeled and blindly

scored for structural defects. 25-32 hearts were scored per selection treatment and data were analyzed with Fisher's Exact Test using the R software package (R Core Team 2015).

Lipid Droplet Size

Adult flies, ~4-5 days old, were embedded in Tissue-Tek® O.C.T. Compound (Sakura® Finetek, Torrance, CA.), frozen, then cut longitudinally into 30µm sections using a Vibratome UltraPro™ 5000 Cryostat (The Vibratome Co. St Louis, MO.). When the cryostat approached the midline of the animal, sections were transferred to a glass slide and mounted in a medium containing 10µL Nile Red Stock Solution (0.1% w/v, Nile Red/acetone), 10µL Triton X-100, 5mL glycerol and 5mL 1xPBS. Samples were immediately imaged (<2 hours) using a Nikon A1R Confocal (Nikon Instruments Inc, Melville, NY) at 40x with a 1.5x digital zoom. Z-stacks were taken and used to generate maximum intensity projections. Lipid droplet size was quantified based off of previously described techniques (Wang et al. 2012). Briefly, the 5 largest droplets per section were measured for 2D area using the Fiji software package (Schindelin et al. 2012), for a total of 19 animals per selection treatment.

Statistical Analysis

All analyses were performed using either Statistica 7.1 software package (StatSoft Inc, Tulsa, OK.) or the R software package (R Core Team 2015). Fisher's Exact Test was used to quantify qualitative analyses and variations of a nested ANOVA were used where appropriate. Our standard model to compare the S and F populations is a nested ANOVA with selection regime and replicate population as independent variables with replicate

population nested within selection regime. Because the individual replicate populations are independent, they are treated as a random effect. In the case of the rescue experiments, the replicate populations were not independent as one replicate was split into either a control or rescued group. In this situation replicate was treated as a fixed effect. Statistics for the rescue experiments were generated by pairwise variations of the nested ANOVA's between the 3 groups (F, S, SR) with replicate population treated as a fixed or random effect where appropriate (Fig. 2.4B-H, Fig. 2.5B-E). Fisher's Exact Tests were performed in R. The standard test was used for the 2x2 contingency table generated when looking at heart structure (Fig. 2.6D), however the 2x3 contingency tables generated by the histological analysis required the Freeman-Halton Extension of Fisher's Exact Test (Fig. 2.3B).

2.4 Results

Selection for starvation resistance leads to a dilated heart phenotype.

To test whether selection for starvation resistance leads to cardiac dysfunction in *Drosophila melanogaster*, we employed two methods. First, we surgically exposed the hearts of adult flies in oxygenated artificial hemolymph in a denervated, purely myogenic state and recorded cardiac contractions using high-speed video microscopy (SOHA) (Karen Ocorr et al. 2007; K. Ocorr et al. 2007a; K. Ocorr et al. 2007b; Fink et al. 2009; Cammarato et al. 2015). End systolic and diastolic diameters of the heart wall were measured from these recordings at a defined point in the 2nd heart chamber in the A3 abdominal segment and used to calculate fractional shortening. Custom software (Fink et al 2009, sohasoftware.com) was used to analyze high-speed movies for the quantification of heart period (duration of each cardiac cycle), contraction intervals, arrhythmia and fractional shortening. We found no significant differences between the F and S populations for heart beat length (heart period, Fig. 2.1A), arrhythmia or contraction intervals (Fig. 2.2A-C). We observed an overall reduction in fractional shortening ($p<0.03$), a measure of relative heart contractility, that was the result of a significant increase in the systolic diameter suggesting systolic dysfunction (Fig. 2.1A). The diastolic diameters also tended to be larger than the controls, although this increase did not reach statistical significance. Representative M-modes, which display heart wall movements over time, from the starvation-selected lines also demonstrated a dilated, less contractile heart with preserved systolic as well as diastolic intervals (Fig. 2.1C, bottom panel; Fig. 2.2B,C).

The *Drosophila* heart runs along the cuticle of the dorsal abdomen, tethered to the cuticle by sets of alary muscles. Many times upon dissection, we observed that the hearts in

the S lines were loosely bound to the dorsal cuticle and appeared distended due to large fat body deposits. These hearts would often detach from the cuticle during preparation and could not be used in the video analysis. Because this phenomenon was not observed in the F lines, we hypothesized that the abnormal heart parameters in the S lines represented the lower limits of heart dysfunction, since cardiac function in a subset of S flies could not be measured.

To validate our results with a complementary method, we performed optical coherence tomography (OCT), which measures heart function in intact flies, which includes innervation. OCT is a non-invasive, non-destructive imaging modality that produces image information similar to the M-modes obtained with SOHA (Fig. 2.1C,D), or to echocardiography in mammals, including humans (Wolf et al. 2006; Wolf and Rockman 2011). Although resolution is lower in OCT than in SOHA, OCT captured a more inclusive range of variation within the S populations, as it was not affected by the surgical limitations found in the S flies. Both end systolic and diastolic diameters, measured in this case at a defined point in the first heart chamber (conical chamber), were increased ($p<3.3x10^{-3}$, $p<5.1x10^{-3}$ respectively) (Fig. 2.1B), again resulting in an overall reduction in fractional shortening ($p<6.8x10^{4}$). Similar to the findings of surgically prepared specimens, we found no significant changes in heart period (Fig. 2.1B). Transversely oriented M-modes provided a visual representation of the differences in end diastolic and systolic diameters (Fig. 2.1D).

Increased fat body mass physically interferes with the heart.

Alary muscles are responsible for anchoring the heart to the cuticle and assisting in relaxation during diastole (Klowden 2007). In the starvation-selected lines the alary muscles appeared to be compromised, presenting as a loose attachment of the heart to the dorsal cuticle upon dissection. This appeared to be caused by large deposits of fat body morphologically altering the position of the heart towards the ventral abdomen. To investigate this possibility, we performed histology and evaluated serial longitudinal sections of adult flies. Many S flies had gross anatomical displacement of the heart towards the ventral abdomen with large deposits of adipose tissue between the heart and the dorsal cuticle (Fig. 2.3A, right panel). Fat body deposits between the dorsal cuticle and heart were observed in ~85% of S flies compared to ~31% of F flies ($p<0.02$) (Fig. 2.3B). Of the S flies with fat between the dorsal cuticle and the heart, ~27% had a severe phenotype where the heart was drastically distended towards the ventral abdomen (Fig. 2.3A, right panel). The severe phenotype was not observed in the F populations (Fig. 2.3B).

Heart dysfunction in the starvation-selected lines is dependent on increased fat storage.

Many phenotypic differences between the S and F lines are likely genetic, caused by alterations in allelic frequencies in response to selection for starvation resistance over many generations. These genetic differences may directly lead to heart dysfunction or may affect the heart as a secondary consequence of increased fat storage. To address this question, we performed experiments to decouple fat accumulation and heart dysfunction. In the first experiment, we transferred 4-day-old adults to non-caloric 1% agar for 7 days (Fig. 2.4A). After a week of starvation the "rescued" S lines (hereafter "SR") had reduced TG levels compared to their age-matched S controls ($p<1.2x10^{-10}$) (Fig. 2.4B). TG levels in the

SR lines were not significantly different from the age-matched F controls suggesting that starvation for 7 days was sufficient to rescue the S lines from obesity. To investigate the relationship between fat storage and cardiac dysfunction, we measured heart parameters on the SR lines using SOHA and OCT. SOHA demonstrated that lean SR flies had lower diastolic and systolic diameters than their age-matched S controls ($p<0.04$ and $p<1.6x10^{-4}$ respectively) (Fig. 2.4C and Fig. 2.4D) as well as increased contractility as measured through fractional shortening ($p<1.4x10^{-4}$)(Fig. 2.4E). While the end diastolic and systolic diameters failed to fully recover to F levels, fractional shortening levels in the SR lines were rescued, as they did not differ from the F controls ($p>0.39$) (Fig. 2.4E). The OCT data largely supported the results obtained by SOHA. After a 7-day diet, SR flies had lower end diastolic and systolic diameters ($p<1.5x10^{-11}$ and $p<3.3x10^{-4}$ respectively) (Fig. 2.4F,G) as well as greater fractional shortening ($p<2.1x10^{-3}$) (Fig. 2.4H). Average diastolic diameter was higher in the S lines as compared to the age-matched F controls, but the data failed to reach significance ($p>0.12$) (Fig. 2.4F). Differences in the absolute values between Figures 1 and 4 are likely a function of age and generations of selection.

Larval development time in the S populations is ~24 hours longer than in the F populations, during which they accumulate lipids available for adult starvation resistance (Reynolds 2013). In additional rescue experiments, we transferred S larvae to non-caloric 1% agar when the F larvae began to wander, to standardize larval feeding time (Fig. 2.5A). Adults were aged 4 to 5 days with food and assayed for heart dysfunction by SOHA. Rescued SR adults had lower TG content compared to the S controls ($p<2.0x10^{-7}$) and were not significantly different from the F flies (Fig. 2.5B). We found this improved the contractility of the heart to F levels as SR fractional shortening was significantly increased

compared to the S controls ($p<1.1x10^{-4}$) (Fig. 2.5E). This improvement in fractional shortening was a function of lower systolic diameter in the SR lines ($p<0.04$)(Fig. 2.5D) as diastolic diameter was not different from the S controls ($p>0.87$)(Fig. 2.5C).

Starvation-selected lines do not ectopically store lipids in the heart but instead increase storage capacity of lipids within the fat body.

Drosophila challenged with lipogenic diets store TG ectopically in non-adipose tissues such as the heart (Birse et al. 2010; Na et al. 2013). Intracellular lipid accumulation in the cardiomyocytes appears to disrupt myofibrillar architecture, and can lead to severe cardiac defects including partial conduction blocks, dysfunctional ostia and decreases in fractional shortening (Birse et al. 2010). To test the hypothesis that heart dysfunction in the S lines is caused by intracellular fat accumulation, we dissected hearts and measured their TG contents in F and S flies. Despite higher whole-body levels of TG in the S flies ($p<0.03$) (Fig. 2.6A), we found no significant changes in heart-specific TG levels (standardized to total heart protein, $p>0.84$), indicating no difference in cardiac lipids between the S and F lines (Fig. 2.6B). Intramyocardial lipid deposition is further hypothesized to lead to structural changes in the myofibrillar architecture of the cardiomyocytes (Birse et al. 2010; Lim et al. 2011). To address this possibility we examined hearts for gross structural changes. Adult hearts were surgically exposed and stained with GFP-conjugated phalloidin to visualize the actin fibers of the cardiomyocytes. We found low levels of myofibrillar disruption in the cardiomyocytes of both the F and S flies, but quantitatively the frequency of disruption was not significantly different (Fig. 2.6D) ($p>0.21$).

The S populations harbored higher whole body TG ($p<0.02$) (Fig. 2.7A), but total protein levels were not significantly different from the F controls ($p>0.54$) (Fig. 2.7B). Despite comparable protein levels, S flies have visibly large, distended abdomens (Masek et al. 2014) and during dissection we observed extensive fat body tissue in the S abdomen. Adipose tissue has a limited storage capacity for fats and the fat-mediated lipotoxic effects on the heart have been attributed to conditions when lipids are in excess of storage capacity. We hypothesized that the S lines had adapted to starvation selection by increasing TG storage capacity within the fat body. We examined lipid droplets within the fat body using Nile Red staining. In the S lines, longitudinal sections of the fat body near the dorsal cuticle had large lipid droplets (Fig. 2.6E, bottom panel). The area of the largest droplets was approximately 65% larger than the area of the largest lipid droplets from the F populations ($p<0.04$) (Fig. 2.6F). This corresponded to an approximate 117% increase in lipid droplet volume.

2.5 Discussion

Obesity associated heart dysfunction in starvation-selected Drosophila.

Many recent studies have demonstrated the merits of using *Drosophila* as a model to study the genetics and physiology of obesity-induced heart dysfunction (Birse et al. 2010; Lee et al. 2010; Lim et al. 2011; Sujkowski et al. 2012; Na et al. 2013; Diop et al. 2015). Here we present the first study to investigate the effects of obesity on the heart in laboratory-evolved populations. We found that long-term laboratory selection for starvation resistance leads to obese flies with a correlated tradeoff in heart function. Using independent methods we demonstrated that starvation-selected hearts are dilated and less contractile than their unselected controls.

While the data from SOHA and OCT largely agree, there are some important technical differences that affect their individual interpretation. The surgical preparation required for SOHA severs the ventral thorax and head from the abdomen, eliminating the effects of neurogenic innervation on the heart from the central nervous system, leaving a purely myogenic heart that will beat for hours in oxygenated artificial hemolymph. Therefore these data are useful in understanding the myogenic properties of the heart. On the other hand, OCT is an *in vivo* assay that measures the heart parameters of adult flies which have their entire nervous system intact. These differences are observed in the data as heart rate in OCT is nearly 4 times larger than with SOHA (Fig. 2.1) which may be expected in a neurologically innervated versus completely myogenic heart (Brooks and Lange 1977) and has been documented in *Drosophila* (K. Ocorr et al. 2007a). Because of the unique physiology of the S populations, we lost many S hearts during dissection for SOHA which may have limited our ability to statistically resolve the increased diastolic

diameter observed in the OCT data. Furthermore, the surgical preparation for SOHA requires the partial removal of fat body to better visualize the heart. By removing this tissue, this procedure may provide a slight, acute improvement in contractility, leading to reduced differentiation between the F and S populations. Despite their inherent differences, both methods consistently agreed on the relative differences in diameter and contractility between the F and S populations.

The genetic basis of heart dysfunction in starvation-selected Drosophila is correlated with disrupted lipid homeostasis.

The genetic basis of heart dysfunction in the S lines could be due to pleiotropic effects of starvation-selected alleles, which directly affect the development or structure of the heart. Many genetic mechanisms could explain maladaptive heart phenotypes in the context of selection for starvation-resistance. For example, linkage disequilibrium (LD) between positively selected starvation-resistance genes and heart-specific loci could have caused increased frequency of particular alleles with direct negative effects on the heart. Alternatively, rearing flies in small cages with plentiful food and lack of predation, may have lifted selective restraints on the heart, allowing genetic drift towards dysfunction. In addition, selected alleles may have tissue-specific effects with alleles favoring starvation-resistance in one tissue causing off-target effects in other cell types like the heart, which may not be crucial to starvation survival. Conversely, starvation-selected alleles may affect the heart as a secondary consequence of disrupted lipid homeostasis. Our data support the latter, as we demonstrated that heart function could be improved by reducing total TG through a 7-day starvation period. We interpret these findings to suggest that heart

dysfunction is not caused by alleles which directly disrupt the development or function of the heart, but by a fat-dependent mechanism.

One of the most important factors leading to obesity-associated heart dysfunction in *Drosophila* is cardiac steatosis (Birse et al. 2010; Lim et al. 2011; Sujkowski et al. 2012; Na et al. 2013; Diop et al. 2015). Our data suggest this is not the case in starvation-selected *Drosophila*, as these flies do not ectopically store TG in the heart. Instead we believe starvation-selected *Drosophila* have adapted to the extreme context of their ecology by increasing the storage capacity of lipids within their fat body. Histological analysis confirmed the presence of expansive fat body tissue in the S lines, and further examination revealed this tissue contained large lipid droplets. The expanded tissue morphologically altered the proper anatomical placement of the heart along the dorsal cuticle. Our data suggest that this physical interference contributes to heart dysfunction in the S lines.

An alternative mechanism for obesity-induced heart disease is the chronic inflammation of adipose tissue leading to changes in cytokine production and cellular signaling in responding tissues (Wang and Nakayama 2010; Sun et al. 2012). Cross talk between the fat body and other organs has been well documented in *Drosophila* (Agaisse and Perrimon 2004; Bai et al. 2012; Rajan and Perrimon 2012; Andersen et al. 2013). Our data do not exclude the possibility that the fat body is inflamed in the S populations, leading to changes in fat body-heart signaling. This intriguing possibility requires further investigation that is beyond the scope of the current study.

Perspectives and Significance

Many theories have been proposed to explain the evolutionary origins of obesity in

humans (Genné-Bacon 2014). Of many interesting ideas, our data are consistent with the thrifty genotype hypothesis, which argues that genetic variants which promote the efficient utilization and storage of nutrients are selected for during periods of famine and starvation (Neel 1962). While this theory has faced criticism (Speakman 2008; Stöger 2008; Hales and Barker 2013) it is important to note its plausibility in the context of extreme selection pressures across repeated generations in our starvation selected populations, which are unmatched in the anthropological record. Other theories argue that epigenetic factors may play a role in driving obesity, as gene/environment interactions in the womb may lead to changes in chromatin structure (Stöger 2008). This has recently been supported in *Drosophila* as both maternal and paternal high-sugar diets have been shown to cause transgenerational effects on metabolism and macronutrient homeostasis (Buescher et al. 2013; Öst et al. 2014). However, our preliminary tests have revealed no such parental effects on lipid storage, fecundity or starvation-resistance in our populations (data unpublished, Gibbs A.G.). In addition our flies are removed from selection for one generation and reared with identical environmental conditions as the F populations prior to each experiment. This suggests that genetics plays the primary role in the evolved characteristics of the S populations.

In mammals it is hypothesized that a larger capacity to store fats in subcutaneous adipose tissue (SAT) limits the harmful effects of ectopic fat deposition in other tissues (Bastien et al. 2014). This helps explain why low SAT levels in individuals with lipodystrophic disorders leads to high levels of ectopic fat accumulation and metabolic disorders (Nelson et al. 2013; Nolis 2014). Selection on genetic variants that increase the storage capacity of adipose tissue may then be an adaptive response to provide the

organism with a larger reservoir to store neutral fats. Evidence for the protective role of adipose tissue has been demonstrated in *Drosophila,* where the fat body has been shown to protect against hyperglycemia in response to a high-sugar diet by switching to a lipogenic expression profile (Musselman et al. 2013). In nature the ability to store excess lipids in adipose tissue may provide a protective buffer against periods of famine while also avoiding metabolic disorders caused when fats are stored ectopically. Counter-selective forces (eg. predation, decreased mobility) that result in decreased dispersal ability or increased predation, would likely balance allelic frequencies to an adaptive state. In our experiments some of these counter forces are removed, reducing selective restraint against increased adipose storage capacity. This resulted in S flies that store so much fat that the tissue appears to physically interfere with the normal function of the heart. This unique mechanism of adaptation may provide S flies with increased energy reserves vital to survive starvation while dampening the lipotoxic heart phenotype traditionally associated with obesity. It will be interesting to further examine this hypothesis and test whether the S populations are resistant to other lipotoxic phenotypes traditionally associated with obesity - including insulin resistance and reduced longevity - in future studies.

2.6 Literature Cited

Agaisse H, Perrimon N. 2004. The roles of JAK/STAT signaling in Drosophila immune responses. Immunol. Rev. 198:72–82.

Aggarwal DD. 2014. Physiological basis of starvation resistance in Drosophila leontia: analysis of sexual dimorphism. J. Exp. Biol. 217:1849–1859.

Aguila JR, Hoshizaki DK, Gibbs AG. 2013. Contribution of larval nutrition to adult reproduction in Drosophila melanogaster. J. Exp. Biol. 216:399–406.

Alayari NN, Vogler G, Taghli-Lamallem O, Ocorr K, Bodmer R, Cammarato A. 2009. Fluorescent Labeling of Drosophila Heart Structures. J. Vis. Exp. [Internet]. Available from: http://www.jove.com/index/Details.stp?ID=1423

Andersen DS, Colombani J, Léopold P. 2013. Coordination of organ growth: principles and outstanding questions from the world of insects. Trends Cell Biol. 23:336–344.

Arrese EL, Soulages JL. 2010. Insect Fat Body: Energy, Metabolism, and Regulation. Annu. Rev. Entomol. 55:207–225.

Bai H, Kang P, Tatar M. 2012. Drosophila insulin-like peptide-6 (*dilp6*) expression from fat body extends lifespan and represses secretion of Drosophila insulin-like peptide-2 from the brain: *dilp6* expression increases *Drosophila* lifespan. Aging Cell 11:978–985.

Ballard JWO, Melvin RG, Simpson SJ. 2008. Starvation resistance is positively correlated with body lipid proportion in five wild caught Drosophila simulans populations. J. Insect Physiol. 54:1371–1376.

Bastien M, Poirier P, Lemieux I, Després J-P. 2014. Overview of Epidemiology and Contribution of Obesity to Cardiovascular Disease. Prog. Cardiovasc. Dis. 56:369–381.

Birse RT, Bodmer R. 2011. Lipotoxicity and cardiac dysfunction in mammals and *Drosophila*. Crit. Rev. Biochem. Mol. Biol. 46:376–385.

Birse RT, Choi J, Reardon K, Rodriguez J, Graham S, Diop S, Ocorr K, Bodmer R, Oldham S. 2010. High-Fat-Diet-Induced Obesity and Heart Dysfunction Are Regulated by the TOR Pathway in Drosophila. Cell Metab. 12:533–544.

Brewer ML. 2013. Kinematic analysis of axial rotations and the effects of stress selection on takeoff flight performance. ThesesDissertationsProfessional Pap. [Internet] Paper 1806. Available from: http://digitalscholarship.unlv.edu/thesesdissertations/1806

Brooks CM, Lange G. 1977. Interaction of myogenic and neurogenic mechanisms that control heart rate. Proc. Natl. Acad. Sci. U. S. A. 74:1761–1762.

Buescher JL, Musselman LP, Wilson CA, Lang T, Keleher M, Baranski TJ, Duncan JG. 2013. Evidence for transgenerational metabolic programming in Drosophila. Dis. Model. Mech. 6:1123–1132.

Cammarato A, Ocorr S, Ocorr K. 2015. Enhanced assessment of contractile dynamics in Drosophila hearts. BioTechniques 58:77–80.

Chippindale AK, Chu TJF, Rose MR. 1996. Complex Trade-Offs and the Evolution of Starvation Resistance in Drosophila melanogaster. Evolution 50:753.

De Pergola G, Silvestris F. 2013. Obesity as a Major Risk Factor for Cancer. J. Obes. 2013:1–11.

Diop SB, Bisharat-Kernizan J, Birse RT, Oldham S, Ocorr K, Bodmer R. 2015. PGC-1/Spargel Counteracts High-Fat-Diet-Induced Obesity and Cardiac Lipotoxicity Downstream of TOR and Brummer ATGL Lipase. Cell Rep. 10:1572–1584.
Diop SB, Bodmer R. 2012. Drosophila as a model to study the genetic mechanisms of obesity-associated heart dysfunction. J. Cell. Mol. Med. 16:966–971.
Fink M, Callol-Massot C, Chu A, Ruiz-Lozano P, Belmonte J, Giles W, Bodmer R, Ocorr K. 2009. A new method for detection and quantification of heartbeat parameters in Drosophila, zebrafish, and embryonic mouse hearts. BioTechniques 46:101–113.
Gefen E, Gibbs AG. 2009. Interactions between enviornmental stress and male mating success may enhance evolutionary divergence of stress-resistant *Drosophila* populations. Evolution 63:1653–1659.
Genné-Bacon EA. 2014. Thinking Evolutionarily About Obesity. Yale J Biol Med 87:99–112.
Hales C, Barker D. 2013. Type 2 (non-insulin-dependent) diabetes mellitus: the thrifty phenotype hypothesis. Int. J. Epidemiol. 42:1215–1222.
Harshman, Hoffmann, Clark. 1999. Selection for starvation resistance in Drosophila melanogaster : physiological correlates, enzyme activities and multiple stress responses. J. Evol. Biol. 12:370–379.
Klowden MJ. 2007. Physiological systems in insects. 2nd ed. Amsterdam ; Boston: Elsevier/Academic Press
Kuhnlein RP. 2012. Lipid droplet-based storage fat metabolism in Drosophila: Thematic Review Series: Lipid Droplet Synthesis and Metabolism: from Yeast to Man. J. Lipid Res. 53:1430–1436.
Lee JH, Budanov AV, Park EJ, Birse R, Kim TE, Perkins GA, Ocorr K, Ellisman MH, Bodmer R, Bier E, et al. 2010. Sestrin as a Feedback Inhibitor of TOR That Prevents Age-Related Pathologies. Science 327:1223–1228.
Lim H-Y, Wang W, Wessells RJ, Ocorr K, Bodmer R. 2011. Phospholipid homeostasis regulates lipid metabolism and cardiac function through SREBP signaling in Drosophila. Genes Dev. 25:189–200.
Masek P, Reynolds LA, Bollinger WL, Moody C, Mehta A, Murakami K, Yoshizawa M, Gibbs AG, Keene AC. 2014. Altered regulation of sleep and feeding contributes to starvation resistance in Drosophila melanogaster. J. Exp. Biol. 217:3122–3132.
Musselman LP, Fink JL, Ramachandran PV, Patterson BW, Okunade AL, Maier E, Brent MR, Turk J, Baranski TJ. 2013. Role of Fat Body Lipogenesis in Protection against the Effects of Caloric Overload in Drosophila. J. Biol. Chem. 288:8028–8042.
Na J, Musselman LP, Pendse J, Baranski TJ, Bodmer R, Ocorr K, Cagan R. 2013. A Drosophila Model of High Sugar Diet-Induced Cardiomyopathy.Rulifson E, editor. PLoS Genet. 9:e1003175.
Neel JV. 1962. Diabetes Mellitus: A “Thrifty” Genotype Rendered Detrimental by “Progress”? Am J Hum Genet 14:353–362.
Nelson MD, Victor RG, Szczepaniak EW, Simha V, Garg A, Szczepaniak LS. 2013. Cardiac Steatosis and Left Ventricular Hypertrophy in Patients With Generalized Lipodystrophy as Determined by Magnetic Resonance Spectroscopy and Imaging. Am. J. Cardiol. 112:1019–1024.
Nolis T. 2014. Exploring the pathophysiology behind the more common genetic and acquired lipodystrophies. J. Hum. Genet. 59:16–23.

Ocorr K, Akasaka T, Bodmer R. 2007. Age-related cardiac disease model of Drosophila. Mech. Ageing Dev. 128:112–116.
Ocorr K, Reeves NL, Wessells RJ, Fink M, Chen H-SV, Akasaka T, Yasuda S, Metzger JM, Giles W, Posakony JW, et al. 2007a. KCNQ potassium channel mutations cause cardiac arrhythmias in Drosophila that mimic the effects of aging. Proc. Natl. Acad. Sci. 104:3943–3948.
Ocorr K, Reeves NL, Wessells RJ, Fink M, Chen H-SV, Akasaka T, Yasuda S, Metzger JM, Giles W, Posakony JW, et al. 2007b. KCNQ potassium channel mutations cause cardiac arrhythmias in Drosophila that mimic the effects of aging. Proc. Natl. Acad. Sci. 104:3943–3948.
Öst A, Lempradl A, Casas E, Weigert M, Tiko T, Deniz M, Pantano L, Boenisch U, Itskov PM, Stoeckius M, et al. 2014. Paternal Diet Defines Offspring Chromatin State and Intergenerational Obesity. Cell 159:1352–1364.
Parkash R, Aggarwal D, Kalra B. 2012. Coadapted changes in energy metabolites and body color phenotypes for resistance to starvation and desiccation in latitudinal populations of D. melanogaster. Evol. Ecol. 26:149–169.
Rajan A, Perrimon N. 2012. Drosophila Cytokine Unpaired 2 Regulates Physiological Homeostasis by Remotely Controlling Insulin Secretion. Cell 151:123–137.
R Core Team. 2015. R: A Language and Enviornment for Statistical Computing. Vienna, Austria: R Foundation for Statistical Computing Available from: http://www.R-project.org/
Reynolds LA. 2013. The Effects of Starvation Selection on Drosophila Melanogaster Life History and Development. UNLV ThesesDissertationsProfessional Pap. Paper 1876.
Rion S, Kawecki TJ. 2007. Evolutionary biology of starvation resistance: what we have learned from *Drosophila*: Starvation resistance in *Drosophila*. J. Evol. Biol. 20:1655–1664.
Schindelin J, Arganda-Carreras I, Frise E, Kaynig V, Longair M, Pietzsch T, Preibisch S, Rueden C, Saalfeld S, Schmid B, et al. 2012. Fiji: an open-source platform for biological-image analysis. Nat. Methods 9:676–682.
Speakman JR. 2008. Thrifty genes for obesity, an attractive but flawed idea, and an alternative perspective: the “drifty gene” hypothesis. Int. J. Obes. 32:1611–1617.
Stöger R. 2008. The thrifty epigenotype: An acquired and heritable predisposition for obesity and diabetes? BioEssays 30:156–166.
Sujkowski A, Saunders S, Tinkerhess M, Piazza N, Jennens J, Healy L, Zheng L, Wessells R. 2012. dFatp regulates nutrient distribution and long-term physiology in Drosophila. Aging Cell 11:921–932.
Sun S, Ji Y, Kersten S, Qi L. 2012. Mechanisms of Inflammatory Responses in Obese Adipose Tissue. Annu. Rev. Nutr. 32:261–286.
Unger RH, Clark GO, Scherer PE, Orci L. 2010. Lipid homeostasis, lipotoxicity and the metabolic syndrome. Biochim. Biophys. Acta BBA - Mol. Cell Biol. Lipids 1801:209–214.
Vogler G, Ocorr K. 2009. Visualizing the Beating Heart in Drosophila J. Vis. Exp. [Internet]. Available from: http://www.jove.com/index/Details.stp?ID=1425
Wang C, Liu Z, Huang X. 2012. Rab32 Is Important for Autophagy and Lipid Storage in Drosophila.Lobaccaro J-MA, editor. PLoS ONE 7:e32086.

Wang Z, Nakayama T. 2010. Inflammation, a Link between Obesity and Cardiovascular Disease. Mediators Inflamm. 2010:1–17.
Wolf MJ, Amrein H, Izatt JA, Choma MA, Reedy MC, Rockman HA. 2006. From The Cover: Drosophila as a model for the identification of genes causing adult human heart disease. Proc. Natl. Acad. Sci. 103:1394–1399.
Wolf MJ, Rockman HA. 2011. Drosophila, Genetic Screens, and Cardiac Function. Circ. Res. 109:794–806.
Yu L, Daniels JP, Wolf MJ. 2013. Vascular and Cardiac Studies in *Drosophila*. In: Ardehali H, Bolli R, Losordo DW, editors. Manual of Research Techniques in Cardiovascular Medicine. Oxford, UK: John Wiley & Sons, Ltd. p. 432–439. Available from: http://doi.wiley.com/10.1002/9781118495148.ch50

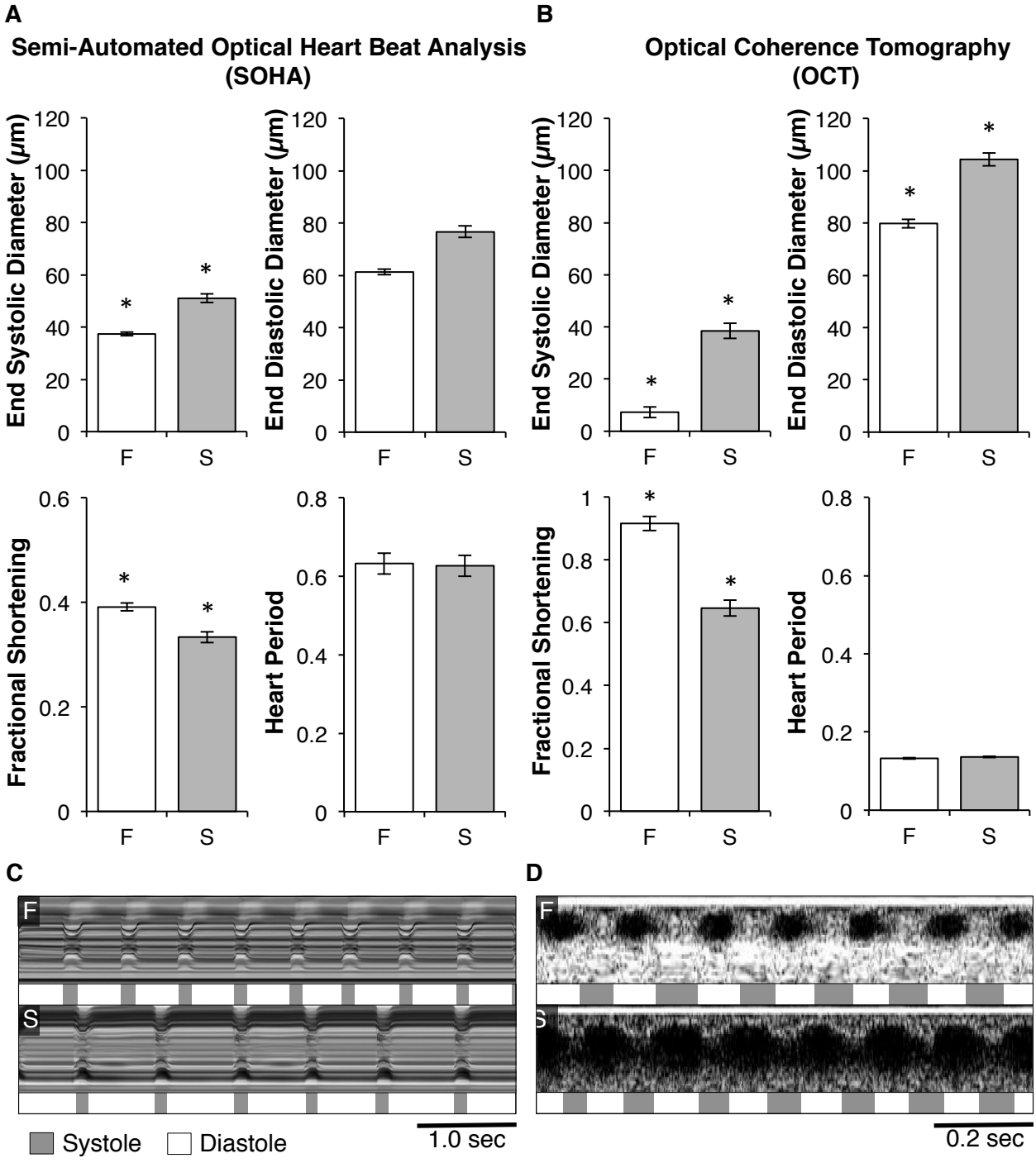

Figure 2.1. Starvation-selected hearts are dilated and less contractile than their unselected controls. (A) Heart parameters measured by semi-automated optical heartbeat analysis (SOHA), showed that the S populations have higher systolic diameter ($p<0.05$), trending but not statistically significantly higher diastolic diameter ($p>0.06$), lower fractional shortening ($p<0.03$) and no difference in heart period ($p>0.86$) compared to the F populations. Nested ANOVA, N=57-74 (B) Heart parameters measured from optical coherence tomography (OCT) largely agreed with SOHA as S populations showed higher systolic diameter ($p<3.3x10^{-3}$), higher diastolic diameter ($p<5.1x10^{-3}$), lower fractional shortening ($p<6.8x10^{-4}$) and no difference in heart period ($p>0.14$). Nested ANOVA, N=42-68. Representative M-modes where the Y-axis is a 1 pixel width slice of the original video viewed over time (x-axis) in either (C) SOHA or (D) OCT demonstrate a S heart which is dilated and less contractile than the F controls.

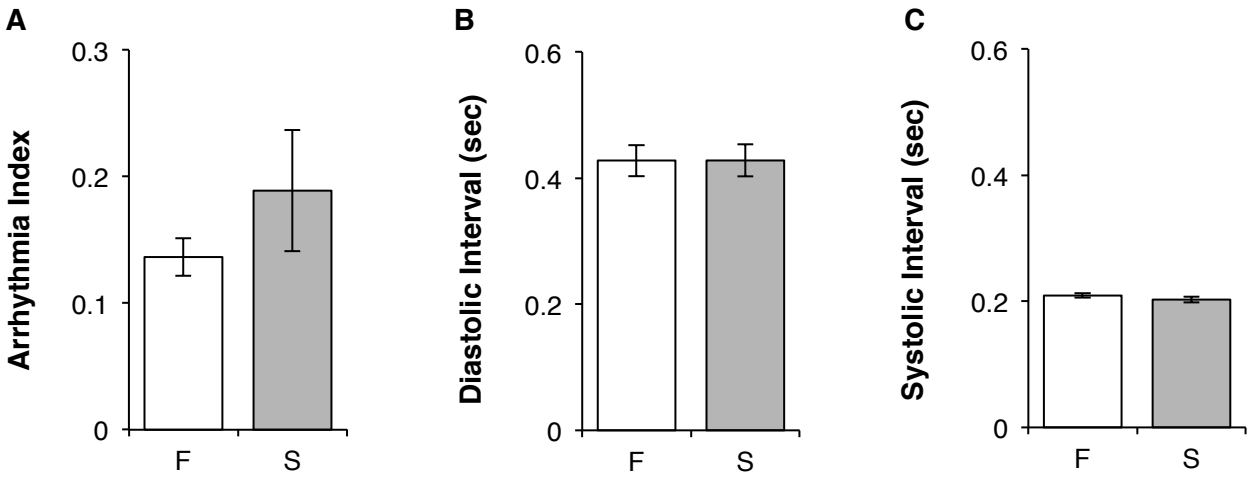

Figure 2.2. Starvation-selected *Drosophila* show no difference in contraction intervals or arrhythmia index. The S populations showed no difference in (A) Arrhythmia Index ($p>0.21$) (B) Diastolic Interval ($p>0.92$) or (C) Systolic Interval ($p>0.49$) compared to their unselected controls. Nested-ANOVA, N=57-74.

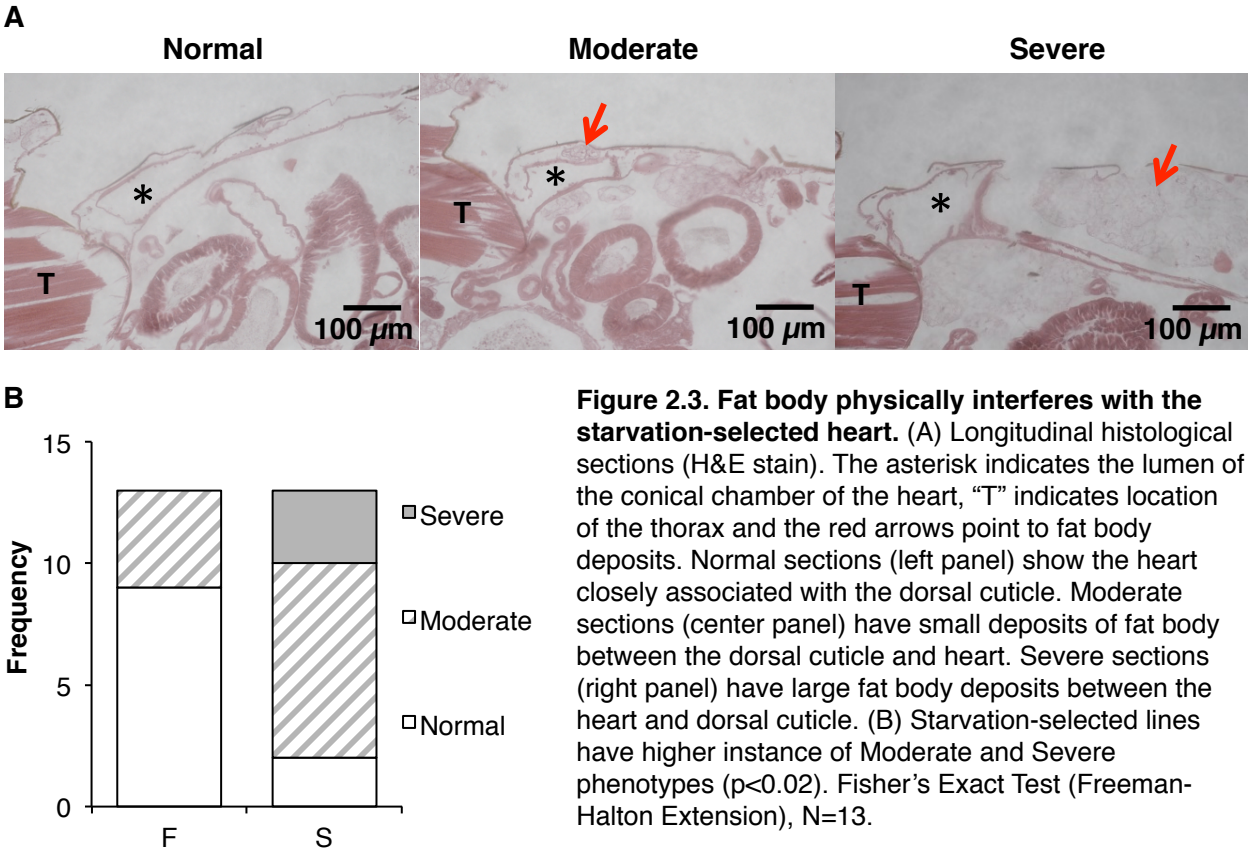

Figure 2.3. Fat body physically interferes with the starvation-selected heart. (A) Longitudinal histological sections (H&E stain). The asterisk indicates the lumen of the conical chamber of the heart, "T" indicates location of the thorax and the red arrows point to fat body deposits. Normal sections (left panel) show the heart closely associated with the dorsal cuticle. Moderate sections (center panel) have small deposits of fat body between the dorsal cuticle and heart. Severe sections (right panel) have large fat body deposits between the heart and dorsal cuticle. (B) Starvation-selected lines have higher instance of Moderate and Severe phenotypes ($p<0.02$). Fisher's Exact Test (Freeman-Halton Extension), N=13.

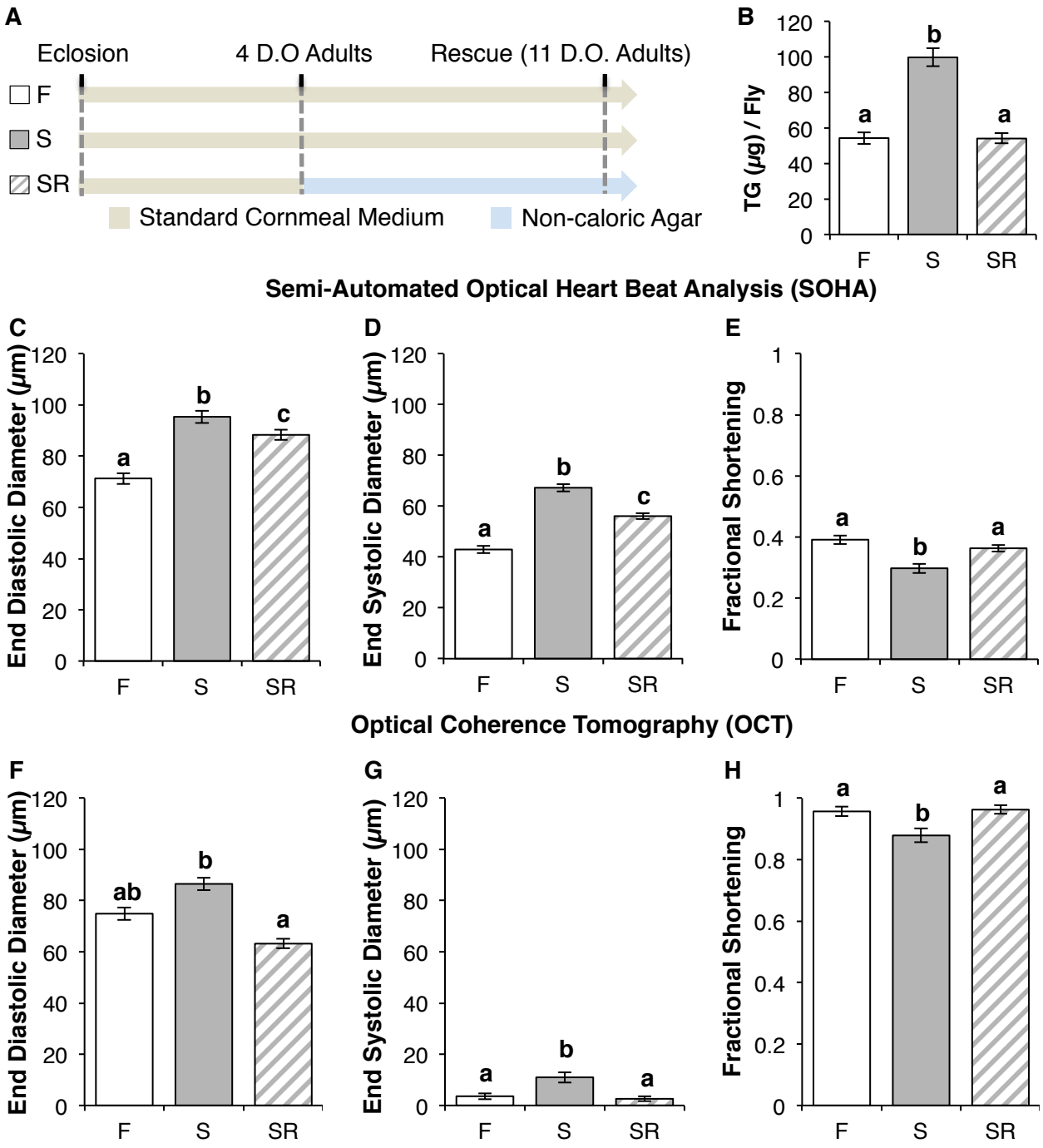

Figure 2.4. The heart phenotype can be partially rescued through a week-long diet (A) Experimental design: A cohort of the starvation-selected lines were made lean ("SR" Group) by a week-long diet of 1% non-caloric agar. (B) The diet significantly reduced total TG's compared to the age-matched S control lines ($p<1.2x10^{-10}$, N=24) and were non-significantly different from the F lines. Results from SOHA showed SR populations had correlated improvements in (C) systolic and (D) diastolic diameters as well as (E) improved fractional shortening as compared to the S populations. ($p<1.6x10^{-4}$, $p<0.04$ and $p<1.4x10^{-4}$, respectively, N=45-46). OCT measurements showed SR populations had correlated improvements in (F) systolic and (G) diastolic diameters as well as (H) improved fractional shortening as compared to the S populations. ($p<3.3x10^{-4}$, $p<1.5x10^{-11}$ and $p<2.1x10^{-3}$, respectively, N=44-45). Differing letters 'a', 'b' and 'c' denote significant differences between groups ($p<0.05$). Pairwise nested ANOVAs (F vs S, F vs SR, S vs SR) were used for these assays (see methods for details).

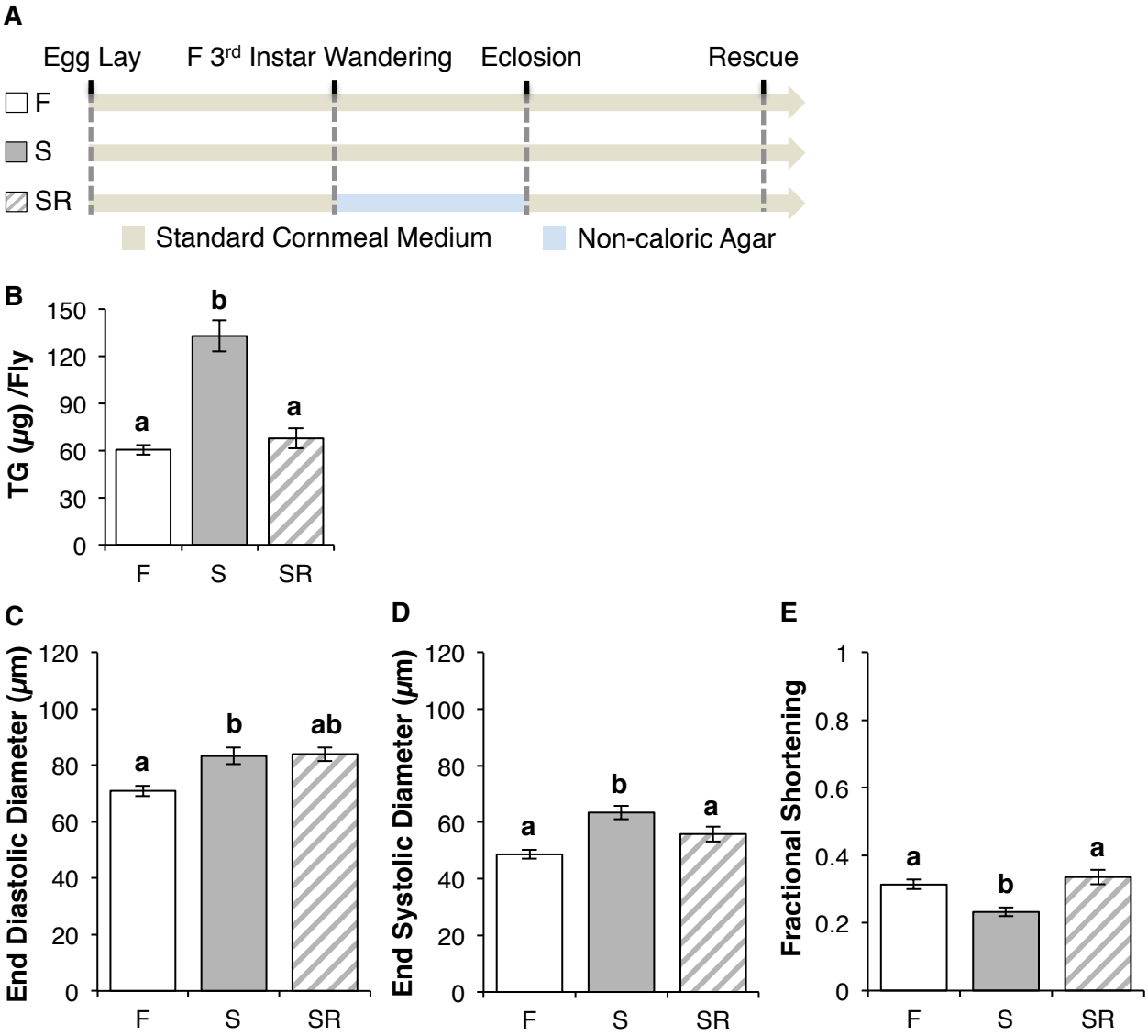

Figure 2.5. The heart phenotype can be partially rescued by removing nutrient sources during extended larval development in the S lines. (A) Experimental design: S flies are deprived of nutrients during their extended larval feeding period. This standardizes their nutrient availability to that of the F lines leading to (B) reduced total TG/fly in the rescued S (SR) populations ($p<2.0x10^{-7}$). Nested ANOVA, N=18. (C) The treatment did not affect diastolic diameter ($p>0.87$), however (D) systolic diameter was significantly reduced in the S populations ($p<0.04$) leading to (E) an overall improvement in contractility as measured through fractional shortening ($p<1.1x10^{-4}$). Pairwise nested ANOVA, N=53-58. Differing letters 'a', 'b' and 'c' denote significant differences between groups ($p<0.05$).

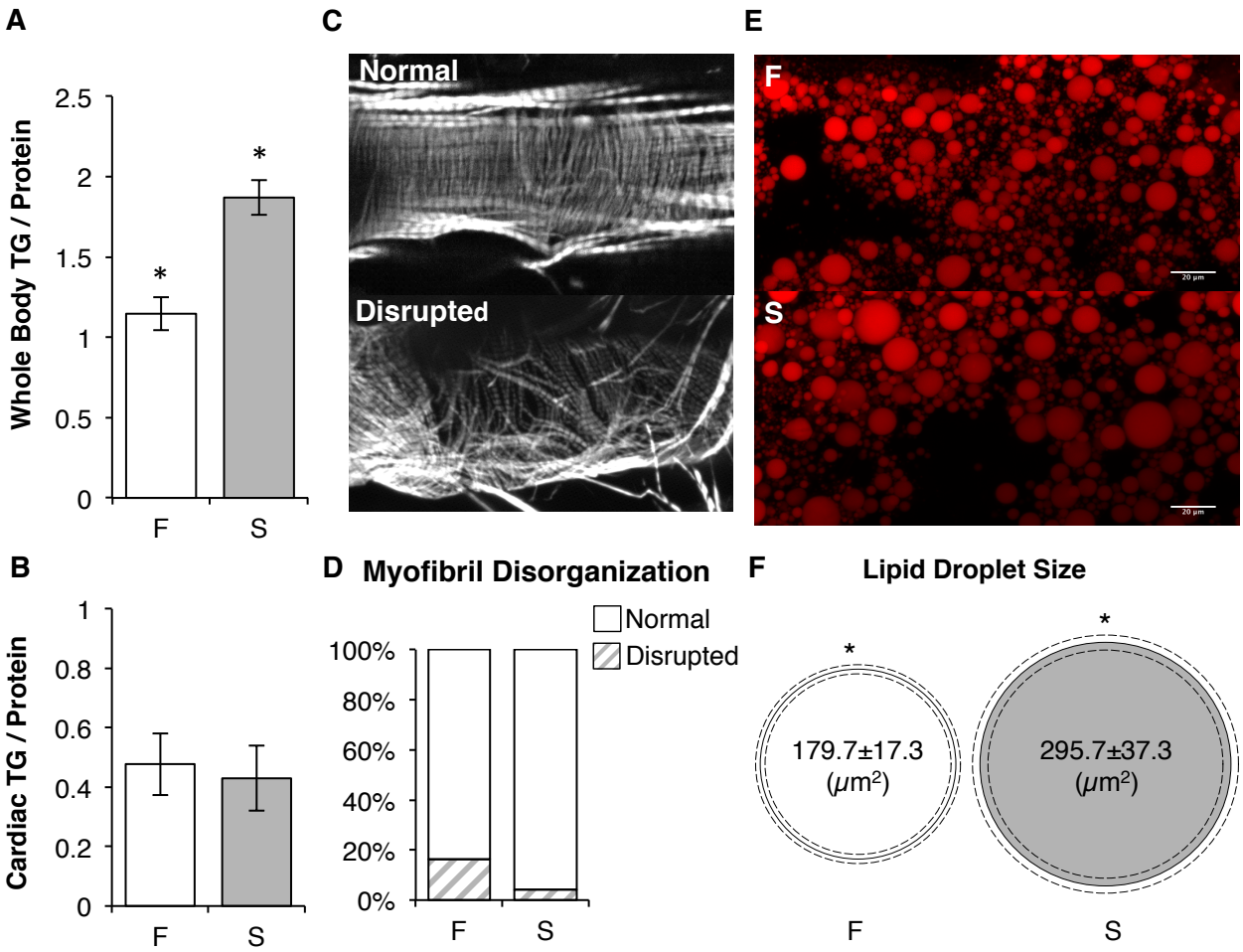

Figure 2.6. Starvation Selected Lines resist ectopic lipid storage in the heart. (A) The S populations store higher whole body levels of TGs than the F populations ($p<0.03$, standardized to total protein). Nested ANOVA, N=24. (B) The excess lipids in the S populations are not ectopically stored within the heart ($p>0.84$, standardized to total heart protein). Nested ANOVA, N=9). (C) We then screened for disrupted myofibrils in our populations. Normal circumferential fibers (Top Panel) are oriented vertically, perpendicular to the heart tube. Disrupted fibers (Lower Panel) have gaps between these fibers. (D) We found low levels of disruption in both F and S populations, however no difference between selection treatments ($p>0.21$). Fisher's Exact Test, N=25-32. (E) We stained the lipid droplets of the adult fat body in the F and S populations with Nile Red. (F) The 2-dimensional area per lipid droplet was on average much larger in the S populations ($p<0.04$). Nested ANOVA, N=19.

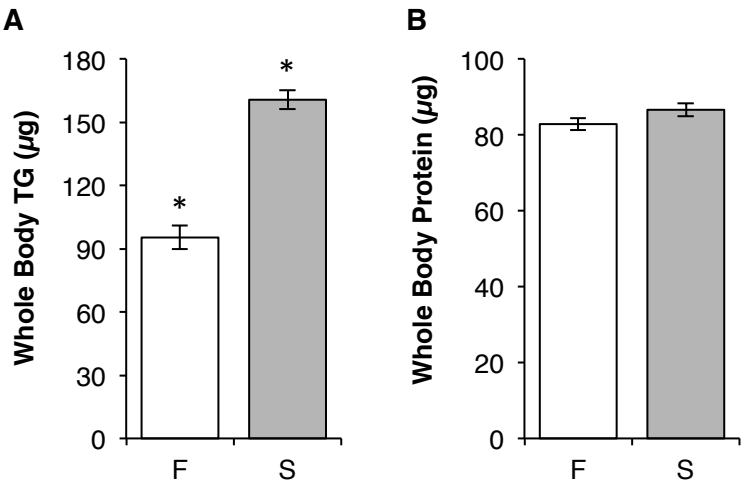

Figure 2.7. Whole Body TG and Total Protein Levels. (A) The S populations have higher levels of whole body TG than F populations ($p<0.02$). (B) There were no differences in whole body protein levels between the S and F populations ($p>0.54$). Nested ANOVA, N=24.

CHAPTER 3

GENOME-WIDE ANALYSIS OF STARVATION-SELECTED *DROSOPHILA MELANOGASTER*: A GENETIC MODEL OF OBESITY

Christopher M. Hardy[1,4], Molly K. Burke[2], Mira V. Han[1,4], Logan J. Everett[3], Kathryn M. Lantz[1,4] and Allen G. Gibbs[1,4]

[1]School of Life Sciences, University of Nevada Las Vegas, Las Vegas, NV.

[2]Department of Integrative Biology, Oregon State University, Corvallis, OR.

[3]Department of Biological Sciences, North Carolina State University, Raleigh, NC.

[4]Nevada Institute of Personalized Medicine, University of Nevada Las Vegas, Las Vegas, NV.

Author Contributions: C.M.H. and A.G.G planned experiments and wrote the paper with assistance from all other authors. K.M.L. and C.M.H. prepared genomic DNA, oversaw library prep and maintained data storage. M.H. and C.M.H. designed and executed alignment pipeline. M.B. and C.M.H. performed intra-replicate genetic correlations, designed code to measure genome-wide heterozygosity and graphing. L.E. and C.M.H. designed drift filter and statistical analysis. K.M.L. and C.M.H. designed molecular pathway diagram. All other experiments were performed by C.M.H. Each author contributed to editing the final manuscript.

3.1 Abstract

Experimental evolution affords the opportunity to investigate adaptation to stressful environments. Studies combining experimental evolution with whole-genome resequencing have provided insight into the dynamics of adaptation and a new tool to uncover genes associated with polygenic traits. Here, we selected for starvation resistance in populations of *Drosophila melanogaster* for over 80 generations. In response, the starvation-selected lines developed an obese condition, storing nearly twice the level of total lipids than their unselected controls. While these fats provide a ~3-fold increase in starvation resistance, the imbalance in lipid homeostasis incurs evolutionary cost. Some of these tradeoffs resemble obesity-associated pathologies in mammals including metabolic depression, low activity levels, dilated cardiomyopathy and disrupted sleeping patterns. To determine the genetic basis of these traits we resequenced genomic DNA from the selected lines and their controls. We found 1,046,373 polymorphic sites, many of which diverged between selection treatments. Additionally, we found a wide range of genetic heterogeneity between the replicates of the selected lines, suggesting multiple mechanisms of adaptation. Genome-wide heterozygosity was low in the selected populations, with many large blocks of SNPs nearing fixation. We found loci under selection by generating an algorithm to control for the effects of genetic drift. These loci were mapped to a set of 1,453 genes, which were associated with morphogenesis, development, tissue differentiation and regulation of metabolism. The results of our study speak to the evolutionary origins of obesity and provide new targets to understand the polygenic nature of obesity in a unique model system.

3.2 Introduction

Natural selection drives organisms to adapt to a wide variety of stressors which are dynamic across evolutionary time. Investigating the mechanistic basis of these adaptations has fundamentally transformed modern science and medicine (Hodgkin and Huxley 1952; Chien et al. 1976; Krebs and Johnson 1980). A complimentary approach to studying uniquely adapted organisms in nature is to simulate evolution in the laboratory, where investigators mimic selective pressures an organism may face in the wild with highly controlled, replicated designs (Bennett 2003). Traditionally, experimental evolution has been a powerful tool in testing theories of evolution and understanding the physiological basis of adaptation to novel environments (Garland and Rose 2009; Kawecki et al. 2012).

Recently, experimental evolution has been elevated by the increased accessibility of next-generation sequencing, which has provided insight into the genetic basis of adaptation on a genome-wide level. The "Evolve and Resequence" (E&R, Turner et al. 2011) strategy has been frequently implemented in work with Drosophila, where researchers have analyzed whole-genome datasets for a variety of selected traits including hypoxia tolerance (Zhou et al. 2011), longevity (Remolina et al. 2012), courtship song (via interpulse interval; Turner and Miller 2012), body size (Turner et al. 2011), desiccation resistance (Kang et al. 2016), development time (Burke et al. 2010), temperature tolerance (Orozco-terWengel et al. 2012) and resistance to both the parasitoid *Asobara tabida* (Jalvingh et al. 2014) and the Drosophila C virus (Martins et al. 2014). While future improvements in experimental design promise to increase the power to detect adaptive loci (Baldwin-Brown et al. 2014; Kofler and Schlotterer 2014; Kessner and Novembre 2015), studies of existing selected Drosophila populations have done a great deal to describe the genomic topography of

laboratory-selected phenotypes. They provide evidence that adaptation is driven by standing genetic variation (Burke et al. 2010), and they also find evidence for multiple temporal trajectories for alleles under selection (Orozco-terWengel et al. 2012; but see Burke and Long 2012). Regions of the genome that change in frequency following laboratory selection may harbor adaptive polymorphisms; genes at or near these candidate alleles have been associated with selected traits (Burke et al. 2010; Turner et al. 2011; Zhou et al. 2011; Orozco-terWengel et al. 2012; Remolina et al. 2012; Turner and Miller 2012; Jalvingh et al. 2014; Martins et al. 2014; Kang et al. 2016). Consigning causality to candidate loci remains challenging as linkage disequilibrium may increase in experimentally evolved populations of Drosophila (Teotónio et al. 2009; Franssen et al. 2015). While this may inflate the number of loci detected under selection, techniques to discriminate causal variants are available in Drosophila. There have been many E&R studies in other species (reviewed in: Kawecki et al. 2012; Long et al. 2015), however Drosophila is particularly well suited for evolution experiments due to its reasonably short generation times, low maintenance costs and genetic tractability. In addition, the relative genetic similarity between flies and mammals provides promise for translational impact (Reiter et al. 2001).

Here, we performed an E&R study on populations of *Drosophila melanogaster* that were selected for starvation resistance for 83 generations. In response to this selection regime, the starvation-selected lines have evolved an obese condition, storing nearly 2 times the levels of total lipids as compared to their unselected controls (Reynolds 2013; Figure 1A). They metabolize these fats when starved, allowing them to live ~11-14 days without food which is 3-4 times longer than the unselected controls. Obesity in these

populations is largely driven by a developmental delay during the 3rd larval instar (Reynolds 2013). This delay provides time for the selected lines to acquire excess nutrients, which are synthesized into lipids as nutrient deprivation during this window has been shown to reduce whole body triglycerides to control levels in adult flies (Masek et al. 2014; Hardy et al. 2015). The selected populations are also adapted to maintain high fat stores as adults, presenting with high whole body triglyceride levels at 4 and 11 days post-eclosion despite consuming fewer overall calories (Masek et al. 2014; Hardy et al. 2015). The starvation-selected populations are genetically programmed to store and retain fat, which comes with many evolutionary costs. The tradeoffs associated with disrupted lipid homeostasis range from depressed metabolic rate accompanied by low activity levels and poor flight performance to low fecundity, dilated cardiomyopathy and excess sleep (Brewer 2013; Reynolds 2013; Masek et al. 2014; Hardy et al. 2015). Many of these phenotypes are reminiscent of other Drosophila models of obesity (Birse et al. 2010; Na et al. 2013) and are also characteristic of metabolic disorder in mammals.

To understand the genetic basis for these complex phenotypes we sequenced pooled genomic DNA from replicate populations of both the starvation-selected and unselected lines. We found many polymorphisms at dissimilar frequencies between the replicate populations of selected lines, which correlated with phenotypic differences in starvation resistance. Genome-wide levels of heterozygosity showed strong signatures of selection, with many large regions of the genome approaching fixation, which were fairly inconsistent across selected replicates. Despite heterogeneity among replicate populations, the differences in allelic frequencies between selective treatments were much higher. To look for conserved mechanisms of adaptation in response to selection, we developed an

algorithm to filter polymorphisms that may be divergent due to genetic drift. After filtering for drift, we mapped the remaining loci to a set of 1,453 genes which were conserved across replicate populations. We found enrichment for genes involved in many pathways including regulation of metabolism, with a high number of genes associated with the insulin and adipokinetic hormone signaling network. The human orthologs for these genes were involved in a host of mammalian diseases including myopathy, cardiomyopathy and type-2 diabetes.

From an evolutionary perspective, our study is consistent with the thrifty gene hypothesis, an evolutionary theory of obesity in which alleles that increase nutrient storage and dampen utilization are selected for during periods of famine (Neel 1962). Here we provide a list of such candidate genes, which can be functionally validated and used as targets for future research.

3.3 Results

Genetic heterogeneity between the replicates of the starvation-selected populations correlates with differences in starvation resistance.

After the 83rd generation of starvation selection we resequenced genomic DNA from pools of 100 females for each of the 3 starvation-selected populations (hereafter "S" populations "A-C") and their 3 unselected fed controls (hereafter "F" populations "A-C"; see Methods for detailed evolutionary history; outlined in Figure 3.1B). The raw sequence reads were mapped and filtered for quality control, resulting in a set of 1,046,373 polymorphisms across all 6 populations (F_{A-C}, S_{A-C}; Methods). We performed a principal component analysis (PCA) to visualize the relationships between populations with respect to reference allele frequency. The analysis resulted in 6 principal components, with the first 3 explaining a combined 88.0% of the variation in allele frequency between populations (Appendix A Table S3.1). The F populations clustered tightly together, separated from the S populations, suggesting an overall effect of selection on allele frequency (Figure 3.2A-C). However the S populations appeared more variable, with the SA replicate clustering independently from the SB and SC populations. We quantified the observed PCA trends by calculating the Pearson product-moment correlation coefficient (r) with respect to reference allele frequency between all 6 populations in a pairwise manner (Figure 3.2D, Appendix A Figure S3.2C-D). Correlations in allele frequencies between the F and S populations were relatively low (r = 0.45-0.54, lower left quadrant, Figure 3.2D) compared to correlations within F replicate populations (r = 0.71-0.82, upper left quadrant, Figure 3.2D), consistent with a strong effect from the selection treatment. We also found relatively low correlation of allele frequencies between the selected replicate populations (r = 0.45-

0.71, lower right quadrant, Figure 3.2D), compared to intra-population correlations in the F populations (r = 0.71-0.82). This was largely due to poor correlation of the SA population with the other S populations (SAxSB, r = 0.45; SAxSC, r =0.45) while SB and SC maintained higher relative correlation (r = 0.71). All correlations were statistically significant with Bonferroni adjusted p-values less than $2.0x10^{-16}$ (Appendix A Figure S3.1D).

Next we wanted to test if genetic variation between the S populations correlated with differences at the organismal level. To do this we measured starvation resistance in the S populations. On average, SA females survived starvation for 344.6±4.7 hours, a 25.8–29.4% increase in duration over SB and SC females (SB: 266.3±4.2 hours, $p<2.0x10^{-16}$; SC: 274.0±4.7 hours, $p<2.0x10^{-16}$, Figure 3.3A). Similarly, SA males survived an average of 283.7±3.9 hours of starvation, 20.5-31.6% longer than their sex matched SB and SC controls (SB: 215.5±3.5 hours, $p<2.0x10^{-16}$; SC: 235.4±4.2 hours, $p<2.0x10^{-16}$, Figure 3.3B). We found the SB and SC populations were more similar in starvation survival with no significant difference between SB and SC females ($p>0.46$, Figure 3.3A) and a relatively small 9.3% increase in starvation survival in SC over SB males ($p<1.2x10^{-3}$, Figure 3.3B).

Genome-wide heterozygosity levels provide evidence for strong selective sweeps.

During natural selection, advantageous loci and regions within linkage disequilibrium increase in frequency leading to localized reduction in variance marked by low levels of heterozygosity (Burke 2012). To study the regional effects of selection in the S populations, we calculated average heterozygosity for blocks of SNPs within a 100 kb sliding window with a step size of 2000 bases across the genome. The F populations demonstrated fairly consistent genome-wide levels of heterozygosity (black lines, Figure

3.4A-C), as average block heterozygosity was equal to 0.30-0.32 (Figure 3.4D) with low variance, ranging from $1.3x10^{-3}$ to $1.6x10^{-3}$ between populations (Figure 3.4E). The S populations however displayed many regional declines in heterozygosity (red lines, Figure 3.4A-C), which presented in lower average block heterozygosity (0.21-0.23, $p<2e-16$, Figure 3.4D) and a 4.4-4.9 fold increase in variance over the F populations ($p<2.2e-16$, Figure 3.4E).

In some instances we found regions of the genome approaching fixation, as we discovered 1,983-3,184 100 kb blocks in the S populations with less than 0.05 average heterozygosity and no more than 4 in any F population (Appendix A Figure S3.2A). Many times these 100 kb blocks overlapped and clustered together into contiguous sequences. For each population (S_{A-C}) we found 17-30 contiguous blocks of low heterozygosity (Figure 3.5A) which averaged 321±38 kb (S.E.M.) in length and ranged from 104 to 2,120 kb (Figure 3.5B). We looked for overlapping regions of these contiguous blocks across replicates to look for any repeatable signatures of selection (Figure 3.5C). While many of the blocks were associated with a specific population, we did find 4 regions across chromosomes X, 3L and 3R which had low heterozygosity (<0.05) across all replicates which ranged from 72-176 kb (bottom row, Figure 3.5C). We found a set of 12 previously characterized genes within these windows and 36 in total (Appendix A Table S3.2). These genes did not cluster into any significant gene ontology categories.

Finding polymorphisms that are consistent with selection

Troughs in heterozygosity are indicative of selection favoring a variant and "sweeping", or reducing, neutral variation linked to the selected locus. However, alleles

associated with complex traits in sexual species may respond to selection through incomplete sweeps and/or dynamic trajectories that do not involve fixation (Burke 2012). Such loci may be difficult to distinguish from those which have changed in frequency due to genetic drift. In order to find loci that were consistent with selection we developed an algorithm to filter SNPs whose difference in allele frequency between selection treatments could be explained by genetic drift. The algorithm models the work of Motoo Kimura, using a diffusion model (Eq. 3.1) to describe genetic drift (Supplemental Code, Kimura 1955). While Kimura's diffusion approximation has been used to model drift elsewhere (Stemshorn et al. 2011), to our knowledge it has not been adapted for use in E&R studies.

Equation 3.1

$$\phi(p,x;t) = \sum_{i=1}^{\infty} p(1-p)i(i+1)(2i+1)F(1-i,i+2,2,p)F(1-i,i+2,2,x)e^{-\frac{i(i+1)t}{4Ne}}$$

Given the number of generations (t), effective population size (Ne) and initial allele frequency (p), the algorithm generates a posterior probability distribution of allele frequency due to drift. Kimura's equation requires the Gauss hypergeometric function 2F1, which was calculated using the hyp2f1 function from SciPy (Release 0.14.0). We found that 50 summations, $\sum_{i=1}^{50}$, and x=1000 was sufficient sampling to generate an appropriate distribution with adequate speed.

Next we needed to define the parameters (t, Ne, p) for the starvation-selection experiment. Here, we used t = 154 generations as replicates were split for 70 generations prior to the 83 generations of selection for starvation resistance plus the generation removed from selection (See detailed phylogeny in Figure 3.1B). Effective population size

was then estimated by measuring the variance in allele frequency between the unselected ($F_{A\text{-}C}$) populations, using the 1,046,373 quality control filtered SNPs and the theoretical equation for variance in allele frequency after t generations (Eq. 3.2; Templeton 2006).

Equation 3.2

$$Var(p_t) = p(1-p)\left[1 - \frac{1}{2Ne}^{t}\right]$$

We grouped SNPs whose average minor allele frequency across populations $F_{A\text{-}C}$ was equal when rounded to the nearest hundredth and calculated the variance of each bin. We then calculated *Ne* for each bin, using the bin's associated allele frequency p = {0.0, 0.01, 0.02 … 0.50} and t = 154 generations. Variation calculated from low allele frequency bins (p<0.07) was much lower than from higher frequencies, which led to suspiciously high *Ne* values (Figure 3.6A). However, the bias quickly resolved towards a stable estimate at allele frequencies greater than 0.07. Because of this bias we took the median *Ne* from all 51 bins. From the data we calculated effective population sizes of 972 for autosomes and 748 for the X chromosome. We believe these estimates are reasonable given the census population size of ~2000 individuals (Methods). Furthermore, the X to Autosome N_e ratio of ~0.77 is consistent with the theoretical 0.75 ratio, given no evidence of a sex bias in our populations.

We used Kimura's equation described above using parameters t = 154 and *Ne* = {972|748} for each starting allele frequency p = {0.01, 0.02, 0.03 … 0.50}. For each value of p we obtained a probability distribution of allele frequencies, which described the

likelihood of posterior allele frequencies due to genetic drift from 0 to 1 (Figure 3.6B). We randomly sampled from these probability distributions to perform simulations of genetic drift. Specifically, for each value of *p* we simulated 2 populations under drift by generating a set of 3.0×10^7 values for each population by randomly sampling from its associated probability distribution. We then calculated the absolute difference between the indices of both sets, creating a distribution of absolute difference in allele frequency between two populations under drift (Figure 3.6C). We calculated the 99.999% quantile of each distribution to observe extreme absolute changes in allele frequency (Figure 3.6C). The 99.999% value became the 'Drift Threshold', which was calculated for each value of *p*, to generate a curve which described the relationship between starting allele frequency and the maximum allele frequency difference expected between 2 populations by drift (Figure 3.6D). To corroborate our approach, we adjusted the number of simulations in our algorithm to match the first 13,000 runs of a forward simulation of genetic drift (Appendix A Figure S3.3A). We found a high degree of similarity between our algorithm and the forward simulation (Appendix A Figure S3.3B-C, autosomes: $r^2 = 0.96$, $p < 5.9 \times 10^{-36}$; X: $r^2 = 0.93$, $p < 4.5 \times 10^{-29}$).

Starting allele frequency for each SNP was estimated as the average minor allele frequency across F replicates. This value was rounded to the nearest hundredth and used as the starting allele frequency to find the Drift Threshold for that SNP. If the absolute difference in allele frequency between the independent replicates (ie. $|MAF_{FA}-MAF_{SA}|$) was less than the Drift Threshold, the SNP was discarded. We were therefore 99.999% confident that the remaining SNPs were not different between the F and S populations due to drift.

Selection converges on biological processes despite low SNP-level repeatability.

After filtering for drift we were left with 37,062, 45,506 and 61,370 high-quality SNPs for replicates A, B and C whose differences between selection treatments were consistent with selection. We plotted the absolute difference in minor allele frequency between the F and S populations for all SNPs across the genome and found many peaks across all 3 replicates (red points, Figure 3.7A-C). We mapped SNPs from each population ($S_{A\text{-}C}$) to genomic features, including total gene region, introns, exons, promoter regions (1kb up or down stream) and intergenic regions. We found a nearly identical distribution of SNPs by genomic feature across populations (Figure 3.8A). In total we found 120,764 SNPs represented by 1 or more populations. Out of this set, only 1,796 SNPs (1.5%) were conserved across all populations, with 99,386 (82.3%) associating within a single population (Figure 3.8B). The remaining 19,582 SNPs associated with pairs of populations, the bulk of which (15,285) were shared between the SB and SC population. The SA population had fewer SNPs in common with the SB and SC populations, sharing just 1,501 and 2,796 SNPs respectively, consistent with our previous measurements of low allelic correlation (Figure 3.2).

We then wanted to test if SNPs at different loci across populations were found in similar genes and potentially performing similar functions. To do this we compiled non-redundant lists of genes for each population. If within a given population, more than 1 SNP was associated with a gene, that gene was counted once. We found 4,232, 4,826 and 5,815 genes for each respective population ($S_{A\text{-}C}$) for a total of 8,891 genes across populations. In total 1,453 genes (16.3%) were found to have at least one SNP in all 3 replicate populations. Again we found more genetic similarity between the SB and SC populations as

they shared 1,657 genes compared to 555 or 864 between SA and the SB or SC populations, respectively (Figure 3.8C).

We interpreted the higher fraction of conserved genes (16.3%) to SNPs (1.5%) to indicate selection may be acting on similar genetic networks, despite acting on dissimilar loci. To further explore this hypothesis, we analyzed gene ontology enrichments for the population-level gene sets. In total we found 261, 290 and 202 GO terms within each population for a total of 341 unique terms. 163 (47.8%) of these terms were conserved across $S_{A\text{-}C}$, with ~73% found in at least 2 replicates, suggesting that selection may have acted on more similar mechanisms of adaptation than may have been predicted from the low level of SNP conservation (Figure 3.8D).

The central mechanisms of adaptation are related to a wide variety of cellular processes including morphogenesis, development, tissue differentiation and regulation of metabolism.

We focused on characterizing the set of 1,453 genes that were conserved across $S_{A\text{-}C}$ (Figure 3.8C), to understand how they may contribute to adaptation. We performed gene ontology enrichment and found 668 GO terms with a Benjamini-Hochberg corrected p-value < 0.05. We controlled for false positives within our list using GO-Module (Yang et al. 2011), and re-adjusted our significance threshold to 5×10^{-3}, leaving us with a set of 370 enriched terms (Appendix C Supplementary Gene Ontology Table). The set of 1,453 genes was enriched for a broad range biological processes, with the top categories largely involving morphogenesis, development and differentiation (Table 3.1). In addition to these major groupings we found enrichment for genes associated with processes which have been previously identified in the S populations (Table 3.1). For instance, the S populations

have low metabolic rates and increased lipid stores which correlate with gene enrichments for several categories related to metabolism, including regulation of both metabolic process and macromolecule biosynthetic process (Table 3.1, Appendix C Supplementary Gene Ontology Table). Furthermore, enrichment for genes involved in locomotion, behavior, sleep, oogenesis, female gamete generation and heart development correlate with the low activity levels, poor flight performance, disrupted sleep patterns, altered foraging behaviors, poor fecundity and heart dysfunction previously reported in the S populations (Table 2, Brewer 2013; Reynolds 2013; Masek et al. 2014; Hardy et al. 2015).

Because Drosophila and humans share a high degree of genetic similarity (Reiter et al. 2001), we wanted to examine the predicted function of the starvation-selected gene orthologs in humans. To do this we converted the set of 1,453 genes to their corresponding human orthologs and looked for disease enrichments. We found that 1,041 of the 1,453 starvation-selected genes were conserved in humans, which mapped to a set of 2,846 human orthologs due to the increased levels of genetic redundancy in higher metazoans. For instance, the Drosophila gene *Sprouty-related protein with EVH-1 domain* (*sprd*) has 3 human orthologs (*SPRD1, SPRD2* and *SPRD3*). Genes from the ortholog set were enriched in several human disease categories including myopathy, cardiomyopathy, type-II diabetes, leukemia, dilated & hypertrophic cardiomyopathy and osteoporosis (Table 3.2).

3.4 Discussion

Here we report the first E&R study to look at the genome-wide effects of experimental selection for starvation resistance in *D. melanogaster*. We found 1,046,373 polymorphic sites across populations F_{A-C} and S_{A-C} with 120,764 unique loci whose frequency diverged greater than expected by drift between selection treatments. Allelic frequencies at these loci varied between S_{A-C}, although genetic dissimilarity on the SNP level converged on higher order processes, as SNPs across populations S_{A-C} clustered into similar genes within conserved ontology categories. Here we discuss the evolutionary forces driving genetic adaptation to starvation resistance, highlight the allelic response to genes involved in metabolic homeostasis and consider how these data speak to the evolutionary origins of obesity.

Evolutionary dynamics of adaptation to starvation selection

Laboratory adaptation in Drosophila generally occurs through selection on standing genetic variation, typically resulting in apparent convergent evolution across experimental replicates (Burke 2012; Long et al. 2015; but see Kang et al. 2016). In asexual species, adaptation occurs via a different mechanism, sometimes called "hard" selective sweeps, where beneficial *de-novo* mutations arise then are driven toward fixation (Burke 2012). Hard sweeps in asexual E&R studies tend to be heterogeneous across replicate populations and implicate candidate alleles private to a single replicate (e.g. Tenaillon et al. 2012; reviewed in Long et al. 2015). Here we observe heterogeneous sweep patterns among our evolutionary replicates (S_{A-C}) with large (100-2000 kb) footprints of low heterozygosity that approach fixation. While this may be consistent with a hard sweep model, it is

extremely unlikely that *de-novo* mutations are driving adaptation due to the small population sizes (~10^3) and relatively low number of generations in our experiment. While near-fixation of large portions of the genome may also be caused by genetic drift, there was little evidence of large-scale fixation in any of the F populations which were under drift for the same number of generations with roughly equal population sizes. Instead we suspect that differences in experimental design explain many of the differences from other E&R experiments in Drosophila. For instance the starvation-selection regime imposes extreme selection pressures (~85% mortality/generation) which are lethal, analogous to experimental culling or domestication (Rose et al. 1990; Bennett 2003). While a few artificial selection studies in Drosophila have also reported fixation, the degree of fixation in these studies is not as pervasive as reported here and generally localized to small numbers of ~10-50kb windows, which is consistent with complete soft sweeps (Turner et al. 2011; Zhou et al. 2011). One study on desiccation-selected *Drosophila* also found evidence for hard selective sweeps, but at a lower frequency than reported here (Kang et al. 2016). A more appropriate comparison may then be made with studies on domestication, such as genomic data from domesticated rabbits which similarly demonstrate large troughs in heterozygosity that are inconsistent across populations/strains (Carneiro et al. 2014). The large sweeps (~300kb) in our dataset are consistent with high selection pressure, as studies in domesticated rice have used the size of selective sweeps to estimate the strength of selection- with large selective sweeps associated with high selection strength (Olsen et al. 2006).

Selection can affect rapid allelic change especially as selection coefficients approach 1, and rapid fixation would allow less time for recombination events to break apart linked

loci, leading to larger sweep sizes. While we do not have genetic data to track allele frequencies over the course of selection, experimental selection for starvation resistance in the S populations and in similar studies have revealed rapid adaptation with evolved responses within as few as 5 generations despite differences in selective strengths ranging from ~85% mortality/generation in the S populations (data unpublished) to ~50% mortality/generation elsewhere (Harshman and Schmid 1998). In nature, Drosophila must adapt rapidly to seasonal changes in climate and polymorphisms with large effects on starvation resistance phenotypes have been shown to vary in their frequency by nearly 20% per season (Bergland et al. 2014; Paaby et al. 2014). It is therefore possible that starvation selection in Drosophila is unique in that it selects on loci with an evolutionary history of rapid adaptation. Because selection pressures in the laboratory are likely much higher than experienced in the wild, these alleles may be pulled toward fixation rapidly. Rapid adaptation is also consistent with epigenetic inheritance as parental nutritional status may alter chromatin structure in both humans and Drosophila (Stöger 2008; Buescher et al. 2013; Öst et al. 2014). However, we have found no evidence for parental effects on starvation resistance or lipid storage in our lines, suggesting a largely genetic response (data not published). The high strength of starvation selection was also observed in studies where reverse evolution of starvation-selected Drosophila failed to fully recover ancestral states, suggesting the possibility of fixation and loss of genetic variation during forward evolution (Teotonio and Rose 2000).

The inconsistency in sweeps across $S_{A\text{-}C}$ is also different from most E&R experiments in Drosophila and may be a consequence of selection acting on multiple adaptive solutions to the same evolutionary problem. This has been observed in experimental selection for

high levels of physical activity in mice, where half of the replicate selected populations have evolved a "mini-muscle" phenotype that confers an increase in oxidative capacity (Garland Jr. et al. 2002; Garland Jr. 2003). Differential selection may be influenced by founder effects as subtle variations in allele frequency in the starting population may promote disparate evolutionary trajectories (Garland Jr. 2003). Here, small allelic differences in the founding populations may have further differentiated during the 70-generation "lead in" to starvation selection when the S populations served as controls for a desiccation selection experiment with mild selection pressures (~20% mortality/generation, Figure 3.1B, Methods). Adaptation by drift or selection during this period may have amplified ancestral allelic differences in the S populations, leading to divergent evolution when severe starvation selection was imposed.

The physiological mechanisms to survive starvation are diverse and may offer many independent targets for selection. For instance, Drosophila may adapt to starvation selection by increasing energy reserves, reducing energy consumption rates or increasing the tolerance of organ systems to starvation stress (Rion and Kawecki 2007; Gibbs and Reynolds 2012; Schwasinger-Schmidt et al. 2012). These physiological mechanisms are likely built upon complex genetic networks that may be convergent, but may also function independently. This is supported by studies in iso-female populations of Drosophila where these genetic networks may be isolated. Such studies have found that genes underlying energy storage and utilization are independent, as metabolic rate and stored TG correlate poorly across strains (Jumbo-Lucioni et al. 2010). However, the interaction between these networks is important for starvation survival as neither metabolic rate nor stored TG correlated well with starvation resistance in iso-female lines (Hoffmann et al. 2001; Jumbo-

Lucioni et al. 2010). In natural populations and in large outbred evolution experiments, these traits are highly correlative with starvation resistance, suggesting the ability to properly utilize energy stores during starvation is dependent on genetic background and epistasis (Ballard et al. 2008; Schwasinger-Schmidt et al. 2012; Reynolds 2013). The genes controlling the broad physiological mechanisms such as reduction of energy expenditure may also be diverse as multiple adaptations such as lower metabolic rate, reduced physical activity and disrupted sleep cycles have been reported in starvation-selected Drosophila (Schwasinger-Schmidt et al. 2012; Reynolds 2013; Masek et al. 2014). This potentially offers more selective targets as some of these phenotypes may be genetically independent (e.g. an allele that disrupts flight muscle may reduce physical activity but have no effect on sleep duration). While increased lipid stores and decreased energy expenditure are consistent adaptations in the S populations (Reynolds 2013; Masek et al. 2014), the genetic basis of these phenotypes may be driven by different mechanisms, which could help explain the variation in allele frequency among S populations.

While highly unlikely, our data are consistent with hard selective sweeps and could suggest beneficial *de-novo* mutations within the dataset. This hypothesis is difficult to address because we lack sequence information from the founding populations. Even when founding populations are sequenced, it is hard to determine if a low frequency variant existed in the starting population due to sampling or sequencing error. The likelihood of a *de-novo* mutation could be higher if any part of the starvation-selection regime inadvertently increased mutagenesis/genomic re-arrangements such as starvation-induced mutagenesis in prokaryotes and yeast (Coyle and Kroll 2008) or diet-induced genomic rearrangements in Drosophila (Aldrich and Maggert 2015). The only way to test these

hypotheses is to restart evolution with the intended purpose of resequencing, using recently developed guidelines for increased replication and time-series sampling (Baldwin-Brown et al. 2014; Kofler and Schlotterer 2014).

Experimental selection for starvation resistance alters the frequency of alleles associated with metabolic homeostasis.

Analysis of the candidate genes revealed the potential for many adaptive mechanisms which will require further study. For instance, changes in locomotion and behavior could be affected by candidates such as *foraging* and *couch potato*, which are well-known regulators of these phenotypes (Schmidt et al. 2008; Kent et al. 2009). Furthermore, the S flies are developmentally delayed and have disrupted 20-hydroxyecdysone signaling (Reynolds 2013), which could be due to allelic differences in candidates associated with steroid hormone signaling including *Smter*, *Ecdysone-induced protein 75B*, *Nitric oxide synthase*, *ultraspiracle* and *βFTZ-F1* (Hall and Thummel 1998; Tsai et al. 1999; Fortier et al. 2003; Hong and Park 2010; Caceres et al. 2011; Koyama et al. 2014). However, we decided to focus on candidates involved in metabolism because shifts in metabolic homeostasis are a consistent response to starvation selection (Chippindale et al. 1996; Harshman et al. 1999; Gibbs and Reynolds 2012; Schwasinger-Schmidt et al. 2012; Reynolds 2013) and these physiological changes correlated with selection on genetic variants involved in regulating metabolism ($p < 4.1 \times 10^{-8}$, Table 3.1). Furthermore, we found enrichment for signaling pathways controlled by receptor tyrosine kinase (RTK) and G-protein coupled receptors (GPCR) ($p < 1.5 \times 10^{-5}$, $p < 1.2 \times 10^{-3}$, Appendix C Supplementary Gene Ontology Table). In Drosophila, insulin-like peptides (Ilp) and adipokinetic hormone (Akh) signal

through receptors of the RTK and GPCR families respectively, to regulate metabolism by coordinating cellular responses to balance systemic nutrient levels. The downstream components of these pathways are interconnected, creating a network that shifts between pro-growth, anabolic processes in response to Ilp secretion or catabolic metabolism and stress-resistance in response to Akh (Figure 3.9). These pathways are remarkably conserved among metazoans and function analogously to insulin and glucagon signaling in mammals (Geminard et al. 2006; Piñero González et al. 2009). Of the many processes implicated in this study we limited our focus to genes associated with these pathways because they were strongly targeted by selection, have well-characterized roles in controlling starvation resistant phenotypes and are highly conserved in mammals- with implications in obesity and its associated diseases.

Alleles of receptors and upstream components of important metabolic pathways are favored targets of starvation selection.

In the S populations the receptors for both insulin and adipokinetic hormone signaling were targeted by selection (candidates hereafter displayed in **boldface**, **InR** and **AkhR,** Figure 3.9). Disruptive mutations in either receptor have profound metabolic consequences, with pleiotropic effects in varying tissues, as ecological factors such as nutrition and stress are decoupled from the intracellular metabolic machinery (Brogiolo et al. 2001; Tatar 2001; Grönke et al. 2007; Bharucha et al. 2008; Kayashima et al. 2013). Despite high levels of conservation across Drosophila species, receptors have evolved under relatively low levels of selective constraint compared to other protein families in Drosophila (Clark et al. 2007). Relaxed constraints may have allowed intra-species

variation to persist despite evidence of positive selection driving adaptive changes in receptor sequences across species (Schmidt et al. 2000; Guirao-Rico and Aguade 2009). Experimental evidence has shown this may be the case for at least the **InR**, as polymorphisms in natural populations of *D. melanogaster* show clinal patterns of positive selection and associate with variation in fecundity, development time, lipid weight and starvation resistance (Paaby et al. 2010; Paaby et al. 2014). In the S populations we found 71 and 20 loci within **InR** and **AkhR** respectively, which were consistent with selection. Many of these SNPs were found in non-coding regions which have the potential to alter regulation of the receptors themselves, but could also affect remote targets. For **InR** we also found predicted amino acid substitutions His1150Tyr and Asp1192Gly which reside in the second fibronectin type-III domain, an extracellular region which has been associated with Ilp ligand binding (Garza-Garcia et al. 2007; Sajid et al. 2011). We also found a predicted non-synonymous Thr389Asn substitution in the cytoplasmic domain of **AkhR** near the C-terminus. Threonine residues in similar regions of AkhR in *Bombyx mori* are crucial sites for proper AkhR trafficking, with disruption altering receptor internalization and desensitization in response to Akh signals (Huang et al. 2011).

Comparative studies of the insulin pathway across Drosophila species have found lower levels of selective constraint and higher sequence diversity in upstream components of the pathway compared to downstream effectors (Alvarez-Ponce et al. 2008). This pattern may help explain why selection in the S populations favored alleles of upstream kinases/phosphatases, phosphodiesterases, G-proteins, phospholipases, perilipins, transcriptional co-activators, adenylyl cyclases and calcium channels (Figure 3.9), while major downstream transcription factors were conserved (*foxo, Creb, SREBP*, ect.).

Furthermore, proteins with high degrees of known connectivity such as Akt and Tor, were not targeted by selection in the S populations. These proteins may be constrained by selection acting antagonistically on different pathways or could be a function of low diversity due to an evolutionary history of positive selection on highly interconnected nodes (Alvarez-Ponce et al. 2008).

Ligands of the Insulin and Adipokinetic Hormone signaling pathways are largely conserved with the exception of Ilp6.

Ligands of the neuropeptide hormone family including Ilps and Akh are highly evolutionarily conserved due to strong stabilizing selection across the Drosophila phylogeny (Wegener and Gorbashov 2008; Guirao-Rico and Aguade 2011). Consistent with these findings, we did not find evidence for selection in any ligand of these pathways, with the notable exception of **Ilp6**, the homolog of insulin-like growth factor and the only one of 8 Ilps primarily expressed in the fat body (Kannan and Fridell 2013). **Ilp6** is released from the fat body and acts hormonally to coordinate the mobilization of energy stores when nutrients are low during starvation or developmental periods such as metamorphosis (Okamoto et al. 2009; Slaidina et al. 2009). In the S populations loci across **Ilp6** were found in synonymous or non-coding regions, which could alter regulatory mechanisms of **Ilp6** but may impact remote targets. In Drosophila, **Ilp6** is known to be under transcriptional control of Foxo, which is activated in response to Akh signaling in low nutrient conditions (Okamoto et al. 2009). If selected loci were to disrupt such a regulatory pathway it could be an adaptive response to block lipid mobilization during starvation, as **Ilp6** is known to promote lipolysis through the oenocytes and inhibit systemic insulin signaling in the IPCs

(Chatterjee et al. 2014). Alleles that lower **Ilp6** expression would then promote an anabolic state even under starvation conditions. The tradeoff between lipid storage and reproduction in the S populations is also consistent with **Ilp6** misexpression, as **Ilp6** mutants have small ovaries due to an inability to mobilize energy stores from the fat body during metamorphosis (Okamoto et al. 2009; Reynolds 2013).

Selection on alleles associated with lipolysis may alter the mobilization of lipids in response to fasting signals.

Lipid mobilization in insects is stimulated by Akh and octopamine signals which are homologous to glucagon and noradrenaline-stimulated lipolysis in mammalian adipocytes (Arrese and Soulages 2010). These hormones are released in response to starvation and increase intracellular levels of secondary messengers cAMP and Ca^{2+} in peripheral tissues through G-protein mediated cascades. High levels of intracellular cAMP and Ca^{2+} are critical in activating lipases associated with lipid droplets and promoting catabolic gene expression through **Crtc**/Creb and Foxo (Chino et al. 1989; Lum and Chino 1990; Patel et al. 2005; Arrese et al. 2008; Arrese and Soulages 2010; Wang et al. 2011; Yang et al. 2013). Many members of the lipolytic pathway were associated with adaptation within the S populations including receptors (**AkhR**, **Oamb**, **Octβ2R** and **Octβ3R**), the G-protein α subunit (**Gαq**), adenylyl cyclases (**Ac76E**, **Ac13E**, **rut** and **CG43373**), phosphodiesterases (**Pde1c**,**6**,**8**,**9**,**11** and **dnc**), protein kinase A-catalytic subunit (**Pka-C3**), lipid storage droplet 1 (**Lsd-1**), phospholipase C (**Plc21c**) and plasma membrane Ca^{2+} channel (**Olf186-F;** Figure 3.9).

Because the S populations have evolved physiologies to store and resist mobilization of lipids, it is tempting to view the large number of candidates in these pathways as part of an adaptive response to attenuate lipolysis in response to starvation-

induced signals. While this remains to be tested, one particular area of interest is in the genes maintaining cAMP levels as they were over-represented in the S populations ($p < 3.6 \times 10^{-4}$, Appendix C Supplemental Gene Ontology Table) and cAMP production rates are correlated with the rate of lipolysis and influence adipocyte size in mammals (Arner et al. 1979; Mowers et al. 2013). Intracellular cAMP is synthesized from ATP through adenylyl cyclases (ACs) and converted to AMP through phosphodiesterases (PDEs). In the S populations, selection targeted alleles across 4 AC and 6 PDE genes which are distributed across the genome and thus likely independent targets of selection and not linkage artifacts of gene clusters. Natural polymorphisms and mutations in many of these enzymes are associated with major metabolic consequences in Drosophila and mammals (Tong et al. 2007; Mattila et al. 2009; Wang et al. 2009; Jumbo-Lucioni et al. 2010; Basile et al. 2014; Maurice et al. 2014; Knigge et al. 2015; Locke et al. 2015).

While the effects of PDEs on lipolysis in Drosophila are poorly characterized, it has long been known that chemical inhibition of PDEs increases lipid mobilization in insects (Spencer and Candy 1976). Furthermore, recent studies in Drosophila have found that PDEs may affect metabolism by influencing food preference, which is altered in the S populations (Masek et al. 2014; Zhang et al. 2015). While allelic variants of the PDEs in the S populations were largely found in non-coding regions, post-translational regulation of PDEs can be heavily influenced by splice variants in mammals, and different isoforms exist in Drosophila PDEs (Sonnenburg et al. 1995; Day et al. 2005; Lu and Sewer 2015). Variants that promote dysregulation of PDEs could impact lipolysis in the S populations and help explain how lipid droplets within the fat body are ~115% larger in volume in a fed state (Hardy et al. 2015). Furthermore, in mammals PDE deregulation during the onset of type-II

diabetes may promote the lipolytic release of free fatty acids into the blood stream, leading to lipotoxicity in peripheral tissues (Choi et al. 2006; Morigny et al. 2015). Despite higher total body fat, the S flies resist ectopic lipid storage in the heart, which could also be a result of decreased lipolysis of TG stores in the fat body (Hardy et al. 2015). These findings now correlate with selection on several PDEs and genes involved in cAMP metabolism which warrants further investigation of their role in lipolysis in the fat body.

Selection on genes which relay environmental signals to Tor may decouple metabolism from nutrient availability.

Target of Rapacmyocin (Tor) is responsible for integrating nutritional and stress signals in the cell and coordinating a metabolic response to promote cell growth in high energy, low-stress cellular environments (Pan et al. 2004). It does this by activating many downstream targets, including proteins involved in translation, transcription factors with anabolic gene targets and by negatively regulating autophagy (Pan et al. 2004; Jin et al. 2015). In the S populations many of the pathways that relay signals from the cellular environment to Tor were targeted by selection, including candidates involved in sensing dietary amino acids (**happyhour**) and sugars (**InR**, **chico**) as well as cellular energy (**AMPK-γ subunit**) and generalized stress signals (**sestrin**; Bryk et al., 2010; Edgar, 2006; Hardie et al., 2012; Johnson et al., 2010; Kim and Neufeld, 2015; Kim and Lee, 2015; Lee et al., 2013, 2012, 2010; Figure 9). Interestingly, many of Tor's downstream effectors including S6K, 4E-BP, TIF-1A, SREBP and Myc were not targeted by selection with the exception of candidate **Atg1** which is repressed by Tor and critical in initiating starvation-induced autophagy (Scott et al. 2004; Figure 9).

Allelic changes to genes in pathways responsible for relaying nutritional and stress signals may be an adaptive response to allow S flies to maintain anabolic activity in the face of stressful, starvation conditions. For example, low cellular energy (by a low ATP/AMP ratio) activates AMPK through its regulatory subunit (candidate **SNF4Aγ**) to inhibit Tor activity (Gwinn et al. 2008; Kim and Lee 2015; Figure 9). AMPK can also be activated by candidate **sestrin**, a protein that accumulates in response to cellular stress and is under transcriptional control of Foxo through the Akh pathway (Lee et al. 2010; Bednářová et al. 2015). Starvation may then activate AMPK through the Akh pathway to block Tor by increasing **sestrin** expression through Foxo and stimulating **AMPK-γ** by altering ATP/AMP levels by activating AC and PDE. If allelic differences in stress response genes such as **sestrin** and **AMPK-γ** are less efficient in repressing the activity of metabolic regulators such as Tor, they could shift metabolic homeostasis in favor of anabolic processes despite nutrient deprivation and high stress. In the S populations this could contribute to a genetic predisposition towards obesity and help explain how they maintain high adult body fat remains high despite consuming fewer calories than the F controls when fed *ad libitum* (Masek et al. 2014; Hardy et al. 2015).

Evolutionary Implications

Theories on the evolutionary origins of obesity began with the proposition of the 'Thrifty Gene Hypothesis' (TGH), which postulates that genes that are efficient in storing and retaining energy are selected for during periods of famine (Neel 1962). Critics have argued that famines severe enough to drive evolution are relatively rare events in human history and cite the lack of candidate obesity genes under selection as weaknesses of the theory (Speakman 2008; Stöger 2008; Genné-Bacon 2014). Clearly our experimental

design supports the TGH as a generalized model given the extensive evolutionary history of severe famine which has led to adaptive 'thrifty' physiologies (i.e. low metabolism, higher energy storage) in the S populations. Here we provide further support for the TGH as we report a wide range of genetic loci with widely divergent allelic frequencies due to the selective treatment. Whether the TGH contributes to the current obesity epidemic in humans is still up for debate, but its effects here are pervasive and may speak more generally to the evolutionary forces controlling obesity.

3.5 Methods

Evolutionary history of the starvation-selected lines

The starvation-selected lines were derived from the controls of a desiccation-selection experiment which began in 1999 as previously described (Gefen and Gibbs 2009) and diagramed in Figure 3.1B. Briefly, the founders for the desiccation-selection experiment were derived from ~400 adult female *Drosophila melanogaster* that were collected from the wild in Terhune New Jersey in 1998. These animals were acclimated to lab conditions for one year, then split into three large cohorts ("D", "SC" and "FC"), each with 3 replicates ("A", "B" and "C") for a total of 9 populations (Figure 3.1B, grey phylogeny). D_{A-C} were selected for desiccation tolerance, with 4-day-old adults from each generation being deprived of food and water and stressed with artificial desiccant until 80-90% of the population had died. Survivors were re-fed, bred and used as founders for the next generation. Because the desiccation treatment also removes food, D_{A-C} were moderately selected for starvation resistance. To control for the effects of starvation, SC_{A-C} were starved during the selection phase of each generation, given non-caloric agar to provide water, but otherwise handled in parallel with D_{A-C}. FC_{A-C} was ostensibly unselected, a handling control given *ad libitum* food and water each generation.

The starvation-selection experiment studied here started in 2006, 70 generations after the start of the desiccation-selection experiment. The starvation-selected populations (hereafter "S_{A-C}") were derived from SC_{A-C} as previously described (Reynolds 2013; Masek et al. 2014; Hardy et al. 2015). Each generation ~10,000 S adults were raised for 4 days, then food was replaced with non-caloric agar until 80-90% of the population had died. Survivors were allowed to breed and served as founders for the next generation. At the

same time, subpopulations were derived from FC_{A-C} of the desiccation-selection experiment and maintained in parallel with S_{A-C}. These lines were ostensibly unselected, with ~2,000 flies given unrestricted access to food and water each generation (Fed-controls, hereafter "F"; Figure 3.1B, black phylogeny).

Sample Preparation

Flies were removed from selection for one generation following the 83rd generation of starvation selection to control for parental effects. Pooled samples of 100, 4-day-old adult females were then collected from all 6 populations (F_{A-C}, S_{A-C}). Pooled samples were homogenized using glass tissue homogenizers in a proprietary buffer (ATL) in accordance with the DNeasy® Blood and Tissue DNA Extraction Kit (Qiagen, Valencia CA). We followed the manufacturer's protocol for purification of total DNA from animal tissues including the optional RNase step. DNA purity and concentration were calculated using a NanoDrop® ND-1000 spectrophotometer (NanoDrop Technologies, Wilmington, DE.).

Library Preparation and Sequencing

Purified samples were shipped to the University of Utah Health Science Center Genomics Core Facility to generate paired-end libraries with 350-bp mean inserts using the TruSeq® DNA PCR-Free Preparation Kit (Illumina®, San Diego CA.). Multiplexed samples were sequenced using an Illumina HiSeq™ sequencer with 125-cycle paired-end sequencing using version-4 chemistry.

Mapping and Variant Discovery

Raw reads were aligned to the *Drosophila melanogaster* genome (Flybase, r6.06) using the Burrows-Wheeler Aligner program (BWA, version 0.7.12) with default settings. Unmapped, low quality (<20) and singleton reads were removed from the Binary Alignment Map (BAM) file, which was then sorted by genomic coordinate using SAMtools (version 1.1). Duplicate reads were removed and the resulting de-duplicated BAM files were merged using Picard (version 1.123). Reads were locally realigned around putative indels using tools in the Genome Analysis Toolkit (GATK, version 3.3) from the Broad Institute. Variants were identified using the Unified Genotyper tool from GATK and annotated with SnpEff (version 4.1) using a custom database built through SnpEff, based on the latest Gene Transfer Format (GTF, r6.06) release from FlyBase (Attrill et al. 2016).

Filtering for Quality Control and Sampling Error

A series of quality control measures were performed using the VariantFiltration tool from GATK. To start, SNPs within 5 nucleotides of a putative insertion or deletion (indel) were discarded to control for mapping errors that occur frequently near indels. In addition we filtered closely clustered SNPs (3 SNPs within a window of 10 nucleotides), SNPs with poor phred-based quality scores (QUAL < 30), high strand bias (FS > 60) or greater than four mapping quality scores of zero across all samples (MQ > 4). Variant Call Format (VCF) files were converted into a customized SNP table with reference and alternate allele counts for each population and ordered by genomic position for chromosomes X, 2L, 2R, 3L and 3R using command line text editors. During this step SNPs with less than 30x coverage across all 6 populations or with more than 1 alternate allele were discarded. Using custom R

scripts (R Core Team 2015), SNPs with a minor allele frequency of less than 0.05 across all 6 populations were filtered as well.

After quality control filters were applied, the SNP table contained 1,046,373 SNPs with 72.6±5.9 (S.E.M.) fold coverage across all 6 populations. To support that our SNPs were largely natural polymorphisms and not due to misalignments, we compared them to those available in the Drosophila Genetic Resource Panel (DGRP Mackay et al. 2012). To do this we downloaded the Variant Call Format (VCF) file for the DGRP Freeze 2.0 calls from dgrp2.gnets.ncsu.edu/data.html. Genomic location was extracted from the dgrp2.vcf file using custom command line text editors to generate a file with the chromosome and position of each SNP. The genomic positions of the DGRP calls and our set of SNPs were based on different FlyBase genome assemblies, resulting in discordant genomic coordinates. To match our coordinates we used the Drosophila Sequence Coordinates Converter from FlyBase (Attrill et al. 2016) to switch our SNPs from the version 6 assembly to the version 5 assembly. The converted positions were uploaded into R and compared to the DGRP SNP locations. In total we found 94.6% overlap between our SNPs and naturally occurring polymorphisms in the DGRP lines (data not shown).

In order to filter SNPs that could be explained by sampling error we used a scaled Chi-Squared test (Huang et al. 2012), which was applied independently to each replicate pair (ie. FA compared to SA; Appendix B Supplementary Code). To correct for multiple comparisons we used a Bonferonni correction with a 0.01 adjusted p-value threshold. This step filtered ~88% of the SNPs with 120,825, 115,000 and 168,100 SNPs remaining for replicates A, B and C respectively.

Principal Component Analysis and Pearson Product-Moment Correlation

We used the Principal Component Analysis (prcomp) function of the *stats* package (version 3.1.3) in R to visualize differences in reference allele frequency across populations. In R, we plotted the pairwise coordinates of the first 3 components which explained 88% of the variation (Appendix A Table S3.1). Also using the *stats* package in R we performed the Test for Association/Correlation Between Paired Samples (cor.test) to calculate the Pearson Product-Moment Correlation Coefficient (r) for pairwise associations of reference allele frequencies between populations. P-values for all correlations were $< 2.0 \times 10^{-16}$ (data not shown).

Starvation Resistance

Flies were removed from selection for one generation to control for parental effects. The progeny were aged to 4 days post-eclosion, briefly anesthetized with CO_2, then separated into vials containing non-caloric 1% agar. Each vial contained either 5 males or females from the 3 selected populations (SA, SB or SC), with a total of 10 vials per sex, resulting in a total of 100 flies (50 males, 50 females) per population. All vials were maintained on a 24-hour light cycle at 25°C and scored for mortality every 8 hours until the completion of the experiment. Every 3 days flies were manually transferred (without anesthetic) to fresh vials to replenish water resources. Data were split for each sex and processed in R, using a one-way ANOVA with population as the categorical factor for each sex followed by a Tukey *post-hoc* test.

Heterozygosity

Heterozygosity for each SNP was calculated as *2pq* with the alternate alleles divided by total coverage for that SNP, per population. Custom functions in R were used to calculate the average heterozygosity of SNPs within 100kb windows with a step size of 2kb across the genome. Mean block heterozygosity was calculated from the total number of 100kb windows for each population, with a one-way ANOVA and Tukey's *post-hoc* test used to find statistical differences. We calculated the variance in the mean heterozygosity for all 100kB blocks within each population and used the "F Test to Compare Two Variances" (var.test) function in the *stats* package in R to test for pairwise differences between populations. We found contiguous blocks of low heterozygosity by locating overlapping 100kb blocks whose mean heterozygosity was less than 0.05 using the Intervals (version 0.15.0) package in R. Contiguous blocks were analyzed for count, size and genomic location. Overlapping regions of contiguous blocks from populations SA, SB and SC were found and the coordinates of these overlaps were used to find genes using a custom gene database, built from the r6.06 FlyBase release.

Human Orthologs

We uploaded our list of 1,453 candidate genes into FlyMine v41.0 to search for gene ontology enrichments, pathway enrichments, expression patterns and orthologs. Using the 'Orthologs Widget' we found 1,041 of our genes had an ortholog in *Homo sapiens*. In total we found 2,846 human orthologs due to genetic redundancy in higher metazoans. This set of genes was uploaded to Enrichr, an online mammalian gene-list enrichment

analysis tool (Chen et al. 2013). We analyzed our gene-set for enriched mammalian disease terms against Enrichr's Online Mendelian Inheritance in Man (OMIM) Disease gene-set.

3.6 Literature Cited

Aldrich JC, Maggert KA. 2015. Transgenerational Inheritance of Diet-Induced Genome Rearrangements in Drosophila.Cavalli G, editor. PLOS Genet. 11:e1005148.

Alvarez-Ponce D, Aguade M, Rozas J. 2008. Network-level molecular evolutionary analysis of the insulin/TOR signal transduction pathway across 12 Drosophila genomes. Genome Res. 19:234–242.

Arner P, Engfeldt P, Ostman J. 1979. Relationship between lipolysis, cyclic AMP, and fat-cell size in human adipose tissue during fasting and in diabetes mellitus. Metabolism. 28:198–209.

Arrese EL, Rivera L, Hamada M, Mirza S, Hartson SD, Weintraub S, Soulages JL. 2008. Function and structure of lipid storage droplet protein 1 studied in lipoprotein complexes. Arch. Biochem. Biophys. 473:42–47.

Arrese EL, Soulages JL. 2010. Insect Fat Body: Energy, Metabolism, and Regulation. Annu. Rev. Entomol. 55:207–225.

Attrill H, Falls K, Goodman JL, Millburn GH, Antonazzo G, Rey AJ, Marygold SJ, the FlyBase consortium. 2016. FlyBase: establishing a Gene Group resource for *Drosophila melanogaster*. Nucleic Acids Res. 44:D786–D792.

Baldwin-Brown JG, Long AD, Thornton KR. 2014. The Power to Detect Quantitative Trait Loci Using Resequenced, Experimentally Evolved Populations of Diploid, Sexual Organisms. Mol. Biol. Evol. 31:1040–1055.

Ballard JWO, Melvin RG, Simpson SJ. 2008. Starvation resistance is positively correlated with body lipid proportion in five wild caught Drosophila simulans populations. J. Insect Physiol. 54:1371–1376.

Basile KJ, Johnson ME, Xia Q, Grant SFA. 2014. Genetic Susceptibility to Type 2 Diabetes and Obesity: Follow-Up of Findings from Genome-Wide Association Studies. Int. J. Endocrinol. 2014:1–13.

Bednářová A, Kodrík D, Krishnan N. 2015. Knockdown of adipokinetic hormone synthesis increases susceptibility to oxidative stress in Drosophila — A role for dFoxO? Comp. Biochem. Physiol. Part C Toxicol. Pharmacol. 171:8–14.

Bennett AF. 2003. Experimental Evolution and the Krogh Principle: Generating Biological Novelty for Functional and Genetic Analyses1. Physiol. Biochem. Zool. 76:1–11.

Bergland AO, Behrman EL, O'Brien KR, Schmidt PS, Petrov DA. 2014. Genomic Evidence of Rapid and Stable Adaptive Oscillations over Seasonal Time Scales in Drosophila.Bolnick D, editor. PLoS Genet. 10:e1004775.

Bharucha KN, Tarr P, Zipursky SL. 2008. A glucagon-like endocrine pathway in Drosophila modulates both lipid and carbohydrate homeostasis. J. Exp. Biol. 211:3103–3110.

Birse RT, Choi J, Reardon K, Rodriguez J, Graham S, Diop S, Ocorr K, Bodmer R, Oldham S. 2010. High-Fat-Diet-Induced Obesity and Heart Dysfunction Are Regulated by the TOR Pathway in Drosophila. Cell Metab. 12:533–544.

Brewer ML. 2013. Kinematic analysis of axial rotations and the effects of stress selection on takeoff flight performance. ThesesDissertationsProfessional Pap. [Internet] Paper 1806. Available from: http://digitalscholarship.unlv.edu/thesesdissertations/1806

Brogiolo W, Stocker H, Ikeya T, Rintelen F, Fernandez R, Hafen E. 2001. An evolutionarily conserved function of the Drosophila insulin receptor and insulin-like peptides in growth control. Curr. Biol. 11:213–221.

Bryk B, Hahn K, Cohen SM, Teleman AA. 2010. MAP4K3 regulates body size and metabolism in Drosophila. Dev. Biol. 344:150–157.
Buescher JL, Musselman LP, Wilson CA, Lang T, Keleher M, Baranski TJ, Duncan JG. 2013. Evidence for transgenerational metabolic programming in Drosophila. Dis. Model. Mech. 6:1123–1132.
Burke MK. 2012. How does adaptation sweep through the genome? Insights from long-term selection experiments. Proc. R. Soc. B Biol. Sci. 279:5029–5038.
Burke MK, Dunham JP, Shahrestani P, Thornton KR, Rose MR, Long AD. 2010. Genome-wide analysis of a long-term evolution experiment with Drosophila. Nature 467:587–590.
Burke MK, Long AD. 2012. What paths do advantageous alleles take during short-term evolutionary change? Mol. Ecol. 21:4913–4916.
Caceres L, Necakov AS, Schwartz C, Kimber S, Roberts IJH, Krause HM. 2011. Nitric oxide coordinates metabolism, growth, and development via the nuclear receptor E75. Genes Dev. 25:1476–1485.
Carneiro M, Rubin C-J, Di Palma F, Albert FW, Alfoldi J, Barrio AM, Pielberg G, Rafati N, Sayyab S, Turner-Maier J, et al. 2014. Rabbit genome analysis reveals a polygenic basis for phenotypic change during domestication. Science 345:1074–1079.
Chatterjee D, Katewa SD, Qi Y, Jackson SA, Kapahi P, Jasper H. 2014. Control of metabolic adaptation to fasting by dILP6-induced insulin signaling in *Drosophila* oenocytes. Proc. Natl. Acad. Sci. 111:17959–17964.
Chen EY, Tan CM, Kou Y, Duan Q, Wang Z, Meirelles G, Clark NR, Ma'ayan A. 2013. Enrichr: interactive and collaborative HTML5 gene list enrichment analysis tool. BMC Bioinformatics 14:128.
Chien A, Edgar DB, Trela JM. 1976. Deoxyribonucleic acid polymerase from the extreme thermophile Thermus aquaticus. J. Bacteriol. 127:1550–1557.
Chino H, Kiyomoto Y, Takahashi K. 1989. In vitro study of the action of adipokinetic hormone in locusts. J. Lipid Res. 30:571–578.
Chippindale AK, Chu TJF, Rose MR. 1996. Complex Trade-Offs and the Evolution of Starvation Resistance in Drosophila melanogaster. Evolution 50:753.
Choi YH, Park S, Hockman S, Zmuda-Trzebiatowska E, Svennelid F, Haluzik M, Gavrilova O, Ahmad F, Pepin L, Napolitano M, et al. 2006. Alterations in regulation of energy homeostasis in cyclic nucleotide phosphodiesterase 3B–null mice. J. Clin. Invest. 116:3240–3251.
Clark AG, Eisen MB, Smith DR, Bergman CM, Oliver B, Markow TA, Kaufman TC, Kellis M, Gelbart W, Iyer VN, et al. 2007. Evolution of genes and genomes on the Drosophila phylogeny. Nature 450:203–218.
Coyle S, Kroll E. 2008. Starvation Induces Genomic Rearrangements and Starvation-Resilient Phenotypes in Yeast. Mol. Biol. Evol. 25:310–318.
Day JP, Dow JAT, Houslay MD, Davies S-A. 2005. Cyclic nucleotide phosphodiesterases in *Drosophila melanogaster*. Biochem. J. 388:333–342.
Edgar BA. 2006. How flies get their size: genetics meets physiology. Nat. Rev. Genet. 7:907–916.
Fortier TM, Vasa PP, Woodard CT. 2003. Orphan nuclear receptor βFTZ-F1 is required for muscle-driven morphogenetic events at the prepupal–pupal transition in Drosophila melanogaster. Dev. Biol. 257:153–165.

Franssen SU, Nolte V, Tobler R, Schlötterer C. 2015. Patterns of Linkage Disequilibrium and Long Range Hitchhiking in Evolving Experimental *Drosophila melanogaster* Populations. Mol. Biol. Evol. 32:495–509.
Garland Jr. T. 2003. Selection experiments: An under-utilized tool in biomechanics and organismal biology. In: Bels VL, Gasc JP, Casinos A, editors. Vertebrate biomechanics and evolution. Oxford, UK: BIOS Scientific Publishers Limited. p. 23–56.
Garland Jr. T, Morgan MT, Swallow JG, Rhodes JS, Girard I, Belter JG, Carter PA. 2002. Evolution of a small-muscle polymorphism in lines of house mice selected for high activity levels. Evolution 56:1267.
Garland T, Rose MR eds. 2009. Experimental evolution: concepts, methods, and applications of selection experiments. Berkeley: University of California Press
Garza-Garcia A, Patel DS, Gems D, Driscoll PC. 2007. RILM: a web-based resource to aid comparative and functional analysis of the insulin and IGF-1 receptor family. Hum. Mutat. 28:660–668.
Gefen E, Gibbs AG. 2009. Interactions between enviornmental stress and male mating success may enhance evolutionary divergence of stress-resistant *Drosophila* populations. Evolution 63:1653–1659.
Geminard C, Arquier N, Layalle S, Bourouis M, Slaidina M, Delanoue R, Bjordal M, Ohanna M, Ma M, Colombani J, et al. 2006. Control of Metabolism and Growth Through Insulin-Like Peptides in Drosophila. Diabetes 55:S5–S8.
Genné-Bacon EA. 2014. Thinking Evolutionarily About Obesity. Yale J Biol Med 87:99–112.
Gibbs AG, Reynolds LA. 2012. Drosophila as a Model for Starvation: Evolution, Physiology, and Genetics. In: McCue MD, editor. Comparative Physiology of Fasting, Starvation, and Food Limitation. Berlin, Heidelberg: Springer Berlin Heidelberg. p. 37–51. Available from: http://link.springer.com/10.1007/978-3-642-29056-5_4
Grönke S, Müller G, Hirsch J, Fellert S, Andreou A, Haase T, Jäckle H, Kühnlein RP. 2007. Dual Lipolytic Control of Body Fat Storage and Mobilization in Drosophila.O'Rahilly S, editor. PLoS Biol. 5:e137.
Guirao-Rico S, Aguade M. 2009. Positive Selection Has Driven the Evolution of the Drosophila Insulin-Like Receptor (InR) at Different Timescales. Mol. Biol. Evol. 26:1723–1732.
Guirao-Rico S, Aguade M. 2011. Molecular Evolution of the Ligands of the Insulin-Signaling Pathway: dilp Genes in the Genus Drosophila. Mol. Biol. Evol. 28:1557–1560.
Gwinn DM, Shackelford DB, Egan DF, Mihaylova MM, Mery A, Vasquez DS, Turk BE, Shaw RJ. 2008. AMPK Phosphorylation of Raptor Mediates a Metabolic Checkpoint. Mol. Cell 30:214–226.
Hall BL, Thummel CS. 1998. The RXR homolog ultraspiracle is an essential component of the Drosophila ecdysone receptor. Development 125:4709–4717.
Hardie DG, Ross FA, Hawley SA. 2012. AMPK: a nutrient and energy sensor that maintains energy homeostasis. Nat. Rev. Mol. Cell Biol. 13:251–262.
Hardy CM, Birse RT, Wolf MJ, Yu L, Bodmer R, Gibbs AG. 2015. Obesity-associated cardiac dysfunction in starvation-selected *Drosophila melanogaster*. Am. J. Physiol. - Regul. Integr. Comp. Physiol. 309:R658–R667.
Harshman, Hoffmann, Clark. 1999. Selection for starvation resistance in Drosophila melanogaster : physiological correlates, enzyme activities and multiple stress responses. J. Evol. Biol. 12:370–379.

Harshman LG, Schmid JL. 1998. Evolution of Starvation Resistance in Drosophila melanogaster: Aspects of Metabolism and Counter-Impact Selection. Evolution 52:1679.
Hodgkin AL, Huxley AF. 1952. A quantitative description of membrane current and its application to conduction and excitation in nerve. J. Physiol. 117:500–544.
Hoffmann AA, Hallas R, Sinclair C, Mitrovski P. 2001. Levels of variation in stress resistance in drosophila among strains, local populations, and geographic regions: patterns for desiccation, starvation, cold resistance, and associated traits. Evol. Int. J. Org. Evol. 55:1621–1630.
Hong J-W, Park KW. 2010. Further understanding of fat biology: Lessons from a fat fly. Exp. Mol. Med. 42:12.
Huang H, Deng X, He X, Yang W, Li G, Shi Y, Shi L, Mei L, Gao J, Zhou N. 2011. Identification of distinct c-terminal domains of the Bombyx adipokinetic hormone receptor that are essential for receptor export, phosphorylation and internalization. Cell. Signal. 23:1455–1465.
Huang W, Richards S, Carbone MA, Zhu D, Anholt RRH, Ayroles JF, Duncan L, Jordan KW, Lawrence F, Magwire MM, et al. 2012. Epistasis dominates the genetic architecture of Drosophila quantitative traits. Proc. Natl. Acad. Sci. 109:15553–15559.
Jalvingh KM, Chang PL, Nuzhdin SV, Wertheim B. 2014. Genomic changes under rapid evolution: selection for parasitoid resistance. Proc. R. Soc. B Biol. Sci. 281:20132303–20132303.
Jin A, Neufeld TP, Choe J. 2015. Kibra and aPKC regulate starvation-induced autophagy in Drosophila. Biochem. Biophys. Res. Commun. 468:1–7.
Johnson EC, Kazgan N, Bretz CA, Forsberg LJ, Hector CE, Worthen RJ, Onyenwoke R, Brenman JE. 2010. Altered Metabolism and Persistent Starvation Behaviors Caused by Reduced AMPK Function in Drosophila.Hassan BA, editor. PLoS ONE 5:e12799.
Jumbo-Lucioni P, Ayroles JF, Chambers M, Jordan KW, Leips J, Mackay TF, De Luca M. 2010. Systems genetics analysis of body weight and energy metabolism traits in Drosophila melanogaster. BMC Genomics 11:297.
Kang L, Aggarwal DD, Rashkovetsky E, Korol AB, Michalak P. 2016. Rapid genomic changes in Drosophila melanogaster adapting to desiccation stress in an experimental evolution system. BMC Genomics [Internet] 17. Available from: http://www.biomedcentral.com/1471-2164/17/233
Kannan K, Fridell Y-WC. 2013. Functional implications of Drosophila insulin-like peptides in metabolism, aging, and dietary restriction. Front. Physiol. [Internet] 4. Available from: http://journal.frontiersin.org/article/10.3389/fphys.2013.00288/abstract
Kawecki TJ, Lenski RE, Ebert D, Hollis B, Olivieri I, Whitlock MC. 2012. Experimental evolution. Trends Ecol. Evol. 27:547–560.
Kayashima Y, Sato A, Kumazawa S, Yamakawa-Kobayashi K. 2013. A heteroallelic Drosophila insulin-like receptor mutant and its use in validating physiological activities of food constituents. Biochem. Biophys. Res. Commun. 434:258–262.
Kent CF, Daskalchuk T, Cook L, Sokolowski MB, Greenspan RJ. 2009. The Drosophila foraging Gene Mediates Adult Plasticity and Gene–Environment Interactions in Behaviour, Metabolites, and Gene Expression in Response to Food Deprivation.Gibson G, editor. PLoS Genet. 5:e1000609.

Kessner D, Novembre J. 2015. Power Analysis of Artificial Selection Experiments Using Efficient Whole Genome Simulation of Quantitative Traits. Genetics 199:991–1005.
Kim J, Neufeld TP. 2015. Dietary sugar promotes systemic TOR activation in Drosophila through AKH-dependent selective secretion of Dilp3. Nat. Commun. 6:6846.
Kim M, Lee J. 2015. Identification of an AMPK Phosphorylation Site in Drosophila TSC2 (gigas) that Regulate Cell Growth. Int. J. Mol. Sci. 16:7015–7026.
Kimura M. 1955. Solution of a process of random genetic drift with a continuous model. Proc. Natl. Acad. Sci. U. S. A. 41:144–150.
Knigge A, Klöting N, Schön MR, Dietrich A, Fasshauer M, Gärtner D, Lohmann T, Dreßler M, Stumvoll M, Kovacs P, et al. 2015. ADCY5 Gene Expression in Adipose Tissue Is Related to Obesity in Men and Mice.Eckel J, editor. PLOS ONE 10:e0120742.
Kofler R, Schlotterer C. 2014. A Guide for the Design of Evolve and Resequencing Studies. Mol. Biol. Evol. 31:474–483.
Koyama T, Rodrigues MA, Athanasiadis A, Shingleton AW, Mirth CK. 2014. Nutritional control of body size through FoxO-Ultraspiracle mediated ecdysone biosynthesis. eLife [Internet] 3. Available from: http://elifesciences.org/lookup/doi/10.7554/eLife.03091
Krebs HA, Johnson WA. 1980. The role of citric acid in intermediate metabolism in animal tissues. FEBS Lett. 117:K2–K10.
Lee JH, Budanov AV, Karin M. 2013. Sestrins Orchestrate Cellular Metabolism to Attenuate Aging. Cell Metab. 18:792–801.
Lee JH, Budanov AV, Park EJ, Birse R, Kim TE, Perkins GA, Ocorr K, Ellisman MH, Bodmer R, Bier E, et al. 2010. Sestrin as a Feedback Inhibitor of TOR That Prevents Age-Related Pathologies. Science 327:1223–1228.
Lee JH, Budanov AV, Talukdar S, Park EJ, Park HL, Park H-W, Bandyopadhyay G, Li N, Aghajan M, Jang I, et al. 2012. Maintenance of Metabolic Homeostasis by Sestrin2 and Sestrin3. Cell Metab. 16:311–321.
Locke AE, Kahali B, Berndt SI, Justice AE, Pers TH, Day FR, Powell C, Vedantam S, Buchkovich ML, Yang J, et al. 2015. Genetic studies of body mass index yield new insights for obesity biology. Nature 518:197–206.
Long A, Liti G, Luptak A, Tenaillon O. 2015. Elucidating the molecular architecture of adaptation via evolve and resequence experiments. Nat. Rev. Genet. 16:567–582.
Lu JY, Sewer MB. 2015. p54 ^{nrb} /NONO Regulates Cyclic AMP-Dependent Glucocorticoid Production by Modulating Phosphodiesterase mRNA Splicing and Degradation. Mol. Cell. Biol. 35:1223–1237.
Lum PY, Chino H. 1990. Primary role of adipokinetic hormone in the formation of low density lipophorin in locusts. J. Lipid Res. 31:2039–2044.
Mackay TFC, Richards S, Stone EA, Barbadilla A, Ayroles JF, Zhu D, Casillas S, Han Y, Magwire MM, Cridland JM, et al. 2012. The Drosophila melanogaster Genetic Reference Panel. Nature 482:173–178.
Martins NE, Faria VG, Nolte V, Schlotterer C, Teixeira L, Sucena E, Magalhaes S. 2014. Host adaptation to viruses relies on few genes with different cross-resistance properties. Proc. Natl. Acad. Sci. 111:5938–5943.
Masek P, Reynolds LA, Bollinger WL, Moody C, Mehta A, Murakami K, Yoshizawa M, Gibbs AG, Keene AC. 2014. Altered regulation of sleep and feeding contributes to starvation resistance in Drosophila melanogaster. J. Exp. Biol. 217:3122–3132.

Mattila J, Bremer A, Ahonen L, Kostiainen R, Puig O. 2009. Drosophila FoxO Regulates Organism Size and Stress Resistance through an Adenylate Cyclase. Mol. Cell. Biol. 29:5357–5365.
Maurice DH, Ke H, Ahmad F, Wang Y, Chung J, Manganiello VC. 2014. Advances in targeting cyclic nucleotide phosphodiesterases. Nat. Rev. Drug Discov. 13:290–314.
Morigny P, Houssier M, Mouisel E, Langin D. 2015. Adipocyte lipolysis and insulin resistance. Biochimie [Internet]. Available from: http://linkinghub.elsevier.com/retrieve/pii/S0300908415003442
Mowers J, Uhm M, Reilly SM, Simon J, Leto D, Chiang S-H, Chang L, Saltiel AR. 2013. Inflammation produces catecholamine resistance in obesity via activation of PDE3B by the protein kinases IKKε and TBK1. eLife [Internet] 2. Available from: http://elifesciences.org/lookup/doi/10.7554/eLife.01119
Na J, Musselman LP, Pendse J, Baranski TJ, Bodmer R, Ocorr K, Cagan R. 2013. A Drosophila Model of High Sugar Diet-Induced Cardiomyopathy.Rulifson E, editor. PLoS Genet. 9:e1003175.
Neel JV. 1962. Diabetes Mellitus: A "Thrifty" Genotype Rendered Detrimental by "Progress"? Am J Hum Genet 14:353–362.
Okamoto N, Yamanaka N, Yagi Y, Nishida Y, Kataoka H, O'Connor MB, Mizoguchi A. 2009. A Fat Body-Derived IGF-like Peptide Regulates Postfeeding Growth in Drosophila. Dev. Cell 17:885–891.
Olsen KM, Caicedo AL, Polato N, McClung A, McCouch S, Purugganan MD. 2006. Selection Under Domestication: Evidence for a Sweep in the Rice Waxy Genomic Region. Genetics 173:975–983.
Orozco-terWengel P, Kapun M, Nolte V, Kofler R, Flatt T, SchlöTterer C. 2012. Adaptation of *Drosophila* to a novel laboratory environment reveals temporally heterogeneous trajectories of selected alleles: Genomic signatures of adaptation to new enviornment. Mol. Ecol. 21:4931–4941.
Öst A, Lempradl A, Casas E, Weigert M, Tiko T, Deniz M, Pantano L, Boenisch U, Itskov PM, Stoeckius M, et al. 2014. Paternal Diet Defines Offspring Chromatin State and Intergenerational Obesity. Cell 159:1352–1364.
Paaby AB, Bergland AO, Behrman EL, Schmidt PS. 2014. A highly pleiotropic amino acid polymorphism in the *Drosophila* insulin receptor contributes to life-history adaptation: ADAPTIVE POLYMORPHISM AT *InR*. Evolution 68:3395–3409.
Paaby AB, Blacket MJ, Hoffmann AA, Schmidt PS. 2010. Identification of a candidate adaptive polymorphism for *Drosophila* life history by parallel independent clines on two continents: ALLELIC VARIATION AT *INR*. Mol. Ecol. 19:760–774.
Pan D, Dong J, Zhang Y, Gao X. 2004. Tuberous sclerosis complex: from Drosophila to human disease. Trends Cell Biol. 14:78–85.
Patel RT, Soulages JL, Hariharasundaram B, Arrese EL. 2005. Activation of the Lipid Droplet Controls the Rate of Lipolysis of Triglycerides in the Insect Fat Body. J. Biol. Chem. 280:22624–22631.
Piñero González J, Carrillo Farnés O, Vasconcelos ATR, González Pérez A. 2009. Conservation of key members in the course of the evolution of the insulin signaling pathway. Biosystems 95:7–16.

R Core Team. 2015. R: A Language and Enviornment for Statistical Computing. Vienna, Austria: R Foundation for Statistical Computing Available from: http://www.R-project.org/
Reiter LT, Potocki L, Chien S, Gribskov M, Bier E. 2001. A Systematic Analysis of Human Disease-Associated Gene Sequences In Drosophila melanogaster. Genome Res. 11:1114–1125.
Remolina SC, Chang PL, Leips J, Nuzhdin SV, Hughes KA. 2012. Genomic basis of aging and life-history evolution in *Drosophila melanogaster*: Genomics of life-history evolution. Evolution 66:3390–3403.
Reynolds LA. 2013. The Effects of Starvation Selection on Drosophila Melanogaster Life History and Development. UNLV ThesesDissertationsProfessional Pap. Paper 1876.
Rion S, Kawecki TJ. 2007. Evolutionary biology of starvation resistance: what we have learned from *Drosophila*: Starvation resistance in *Drosophila*. J. Evol. Biol. 20:1655–1664.
Rose MR, Graves JL, Hutchinson EW. 1990. The Use of Selection to Probe Patterns of Pleiotropy in Fitness Characters. In: Gilbert F, editor. Insect Life Cycles: Genetics, Evolution and Co-ordination. London: Springer London. p. 29–42. Available from: http://dx.doi.org/10.1007/978-1-4471-3464-0_3
Sajid W, Kulahin N, Schluckebier G, Ribel U, Henderson HR, Tatar M, Hansen BF, Svendsen AM, Kiselyov VV, Norgaard P, et al. 2011. Structural and Biological Properties of the Drosophila Insulin-like Peptide 5 Show Evolutionary Conservation. J. Biol. Chem. 286:661–673.
Schmidt PS, Duvernell DD, Eanes WF. 2000. Adaptive evolution of a candidate gene for aging in Drosophila. Proc. Natl. Acad. Sci. 97:10861–10865.
Schmidt PS, Zhu C-T, Das J, Batavia M, Yang L, Eanes WF. 2008. An amino acid polymorphism in the couch potato gene forms the basis for climatic adaptation in Drosophila melanogaster. Proc. Natl. Acad. Sci. 105:16207–16211.
Schwasinger-Schmidt TE, Kachman SD, Harshman LG. 2012. Evolution of starvation resistance in Drosophila melanogaster: measurement of direct and correlated responses to artificial selection: Evolution of starvation resistance. J. Evol. Biol. 25:378–387.
Scott RC, Schuldiner O, Neufeld TP. 2004. Role and Regulation of Starvation-Induced Autophagy in the Drosophila Fat Body. Dev. Cell 7:167–178.
Slaidina M, Delanoue R, Gronke S, Partridge L, Léopold P. 2009. A Drosophila Insulin-like Peptide Promotes Growth during Nonfeeding States. Dev. Cell 17:874–884.
Sonnenburg WK, Seger D, Kwak KS, Huang J, Charbonneau H, Beavo JA. 1995. Identification of inhibitory and calmodulin-binding domains of the PDE1A1 and PDE1A2 calmodulin-stimulated cyclic nucleotide phosphodiesterases. J. Biol. Chem. 270:30989–31000.
Speakman JR. 2008. Thrifty genes for obesity, an attractive but flawed idea, and an alternative perspective: the “drifty gene” hypothesis. Int. J. Obes. 32:1611–1617.
Spencer IM, Candy DJ. 1976. Hormonal control of diacyl glycerol mobilization from fat body of the desert locust, Schistocerca gregaria. Insect Biochem. 6:289–296.
Stöger R. 2008. The thrifty epigenotype: An acquired and heritable predisposition for obesity and diabetes? BioEssays 30:156–166.

Tatar M. 2001. A Mutant Drosophila Insulin Receptor Homolog That Extends Life-Span and Impairs Neuroendocrine Function. Science 292:107–110.
Templeton AR. 2006. Population genetics and microevolutionary theory. Hoboken, N.J: Wiley-Liss
Tenaillon O, Rodriguez-Verdugo A, Gaut RL, McDonald P, Bennett AF, Long AD, Gaut BS. 2012. The Molecular Diversity of Adaptive Convergence. Science 335:457–461.
Teotónio H, Chelo IM, Bradić M, Rose MR, Long AD. 2009. Experimental evolution reveals natural selection on standing genetic variation. Nat. Genet. 41:251–257.
Teotonio H, Rose MR. 2000. Variation in the reversibility of evolution. Nature 408:463–466.
Tong JJ, Schriner SE, McCleary D, Day BJ, Wallace DC. 2007. Life extension through neurofibromin mitochondrial regulation and antioxidant therapy for neurofibromatosis-1 in Drosophila melanogaster. Nat. Genet. 39:476–485.
Tsai C-C, Kao H-Y, Yao T-P, McKeown M, Evans RM. 1999. SMRTER, a Drosophila Nuclear Receptor Coregulator, Reveals that EcR-Mediated Repression Is Critical for Development. Mol. Cell 4:175–186.
Turner TL, Miller PM. 2012. Investigating Natural Variation in Drosophila Courtship Song by the Evolve and Resequence Approach. Genetics 191:633–642.
Turner TL, Stewart AD, Fields AT, Rice WR, Tarone AM. 2011. Population-Based Resequencing of Experimentally Evolved Populations Reveals the Genetic Basis of Body Size Variation in Drosophila melanogaster.Gibson G, editor. PLoS Genet. 7:e1001336.
Wang B, Moya N, Niessen S, Hoover H, Mihaylova MM, Shaw RJ, Yates JR, Fischer WH, Thomas JB, Montminy M. 2011. A Hormone-Dependent Module Regulating Energy Balance. Cell 145:596–606.
Wang Z, Li V, Chan GCK, Phan T, Nudelman AS, Xia Z, Storm DR. 2009. Adult Type 3 Adenylyl Cyclase–Deficient Mice Are Obese.Tsien JZ, editor. PLoS ONE 4:e6979.
Wegener C, Gorbashov A. 2008. Molecular evolution of neuropeptides in the genus Drosophila. Genome Biol. 9:R131.
Yang H, He X, Yang J, Deng X, Liao Y, Zhang Z, Zhu C, Shi Y, Zhou N. 2013. Activation of cAMP-response element-binding protein is positively regulated by PKA and calcium-sensitive calcineurin and negatively by PKC in insect. Insect Biochem. Mol. Biol. 43:1028–1036.
Zhang Y, Liu G, Yan J, Zhang Y, Li B, Cai D. 2015. Metabolic learning and memory formation by the brain influence systemic metabolic homeostasis. Nat. Commun. 6:6704.
Zhou D, Udpa N, Gersten M, Visk DW, Bashir A, Xue J, Frazer KA, Posakony JW, Subramaniam S, Bafna V, et al. 2011. Experimental selection of hypoxia-tolerant Drosophila melanogaster. Proc. Natl. Acad. Sci. 108:2349–2354.

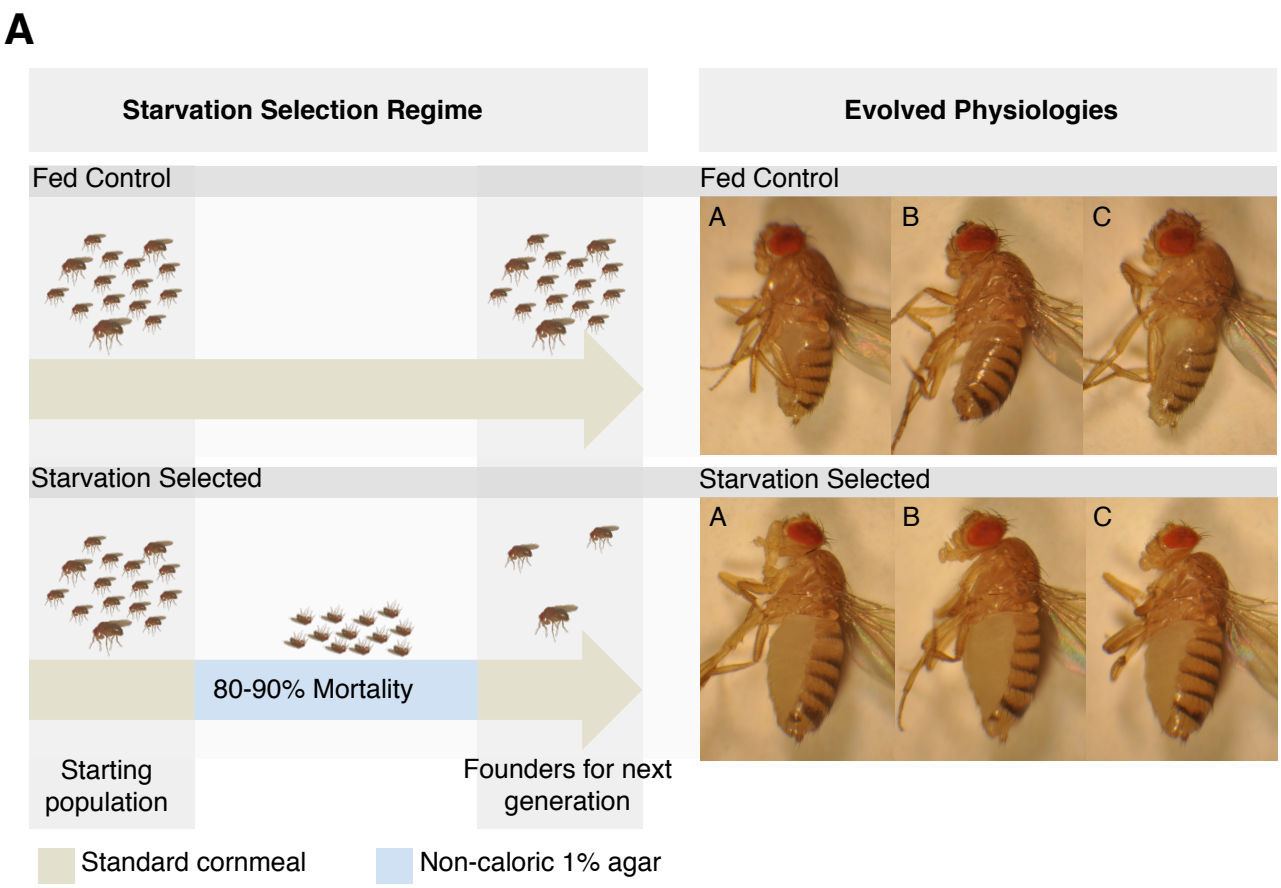

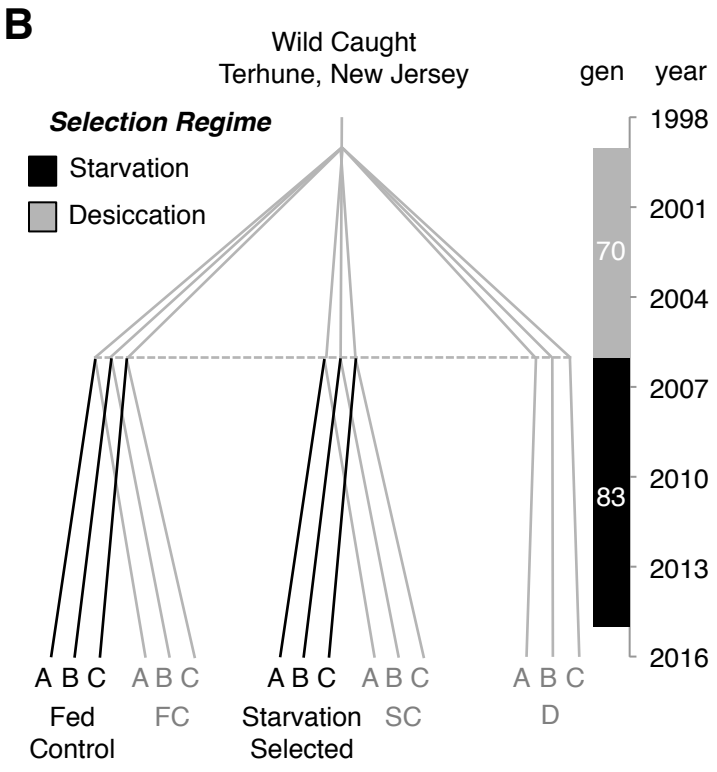

Figure 3.1 Selection regime, phylogeny and evolutionary history of the selected populations. (A) Each generation the starvation-selected populations S_{A-C} were starved until 80-90% had died. The survivors were used as founders for the subsequent generation. At the same time the fed control populations F_{A-C} were handled in parallel and fed *ad libitum.* The visible differences between F_{A-C} and S_{A-C} as 4-5 day old adults demonstrate some of the evolved characteristics. (B) Detailed phylogeny and evolutionary history of the starvation-selected lines. Axis to the right displays the number of generations and year. Black lines represent the starvation-selection experiment studied here. To date, the starvation-selection experiment has been running for over 100 generations, however sequence data was collected at generation 83.

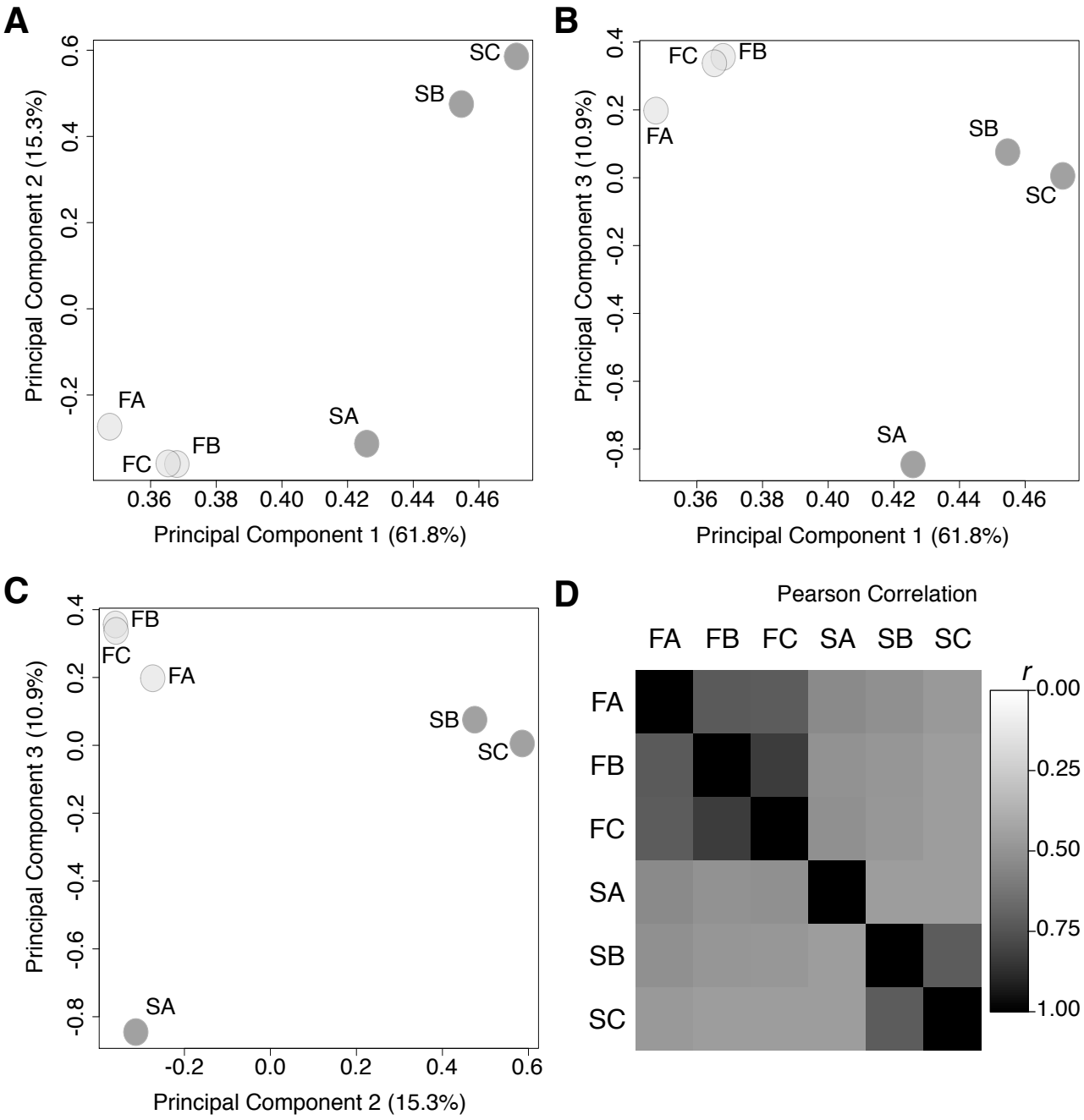

Figure 3.2 Genetic heterogeneity in the starvation-selected replicates. (A-C) Principal Component Analysis (PCA) plots of the first 3 components, which explain ~88% of the variation in reference allele frequency between the populations. Dark grey circles represent populations S_{A-C} while the light grey circles represent F_{A-C}. F_{A-C} cluster together and are separated from the S populations. The S_A population appears to cluster independently from S_{B-C}. (D) Pairwise Pearson Product Moment Correlation Analysis of all 6 populations. Darker squares represent a higher degree of correlation in reference allele frequency.

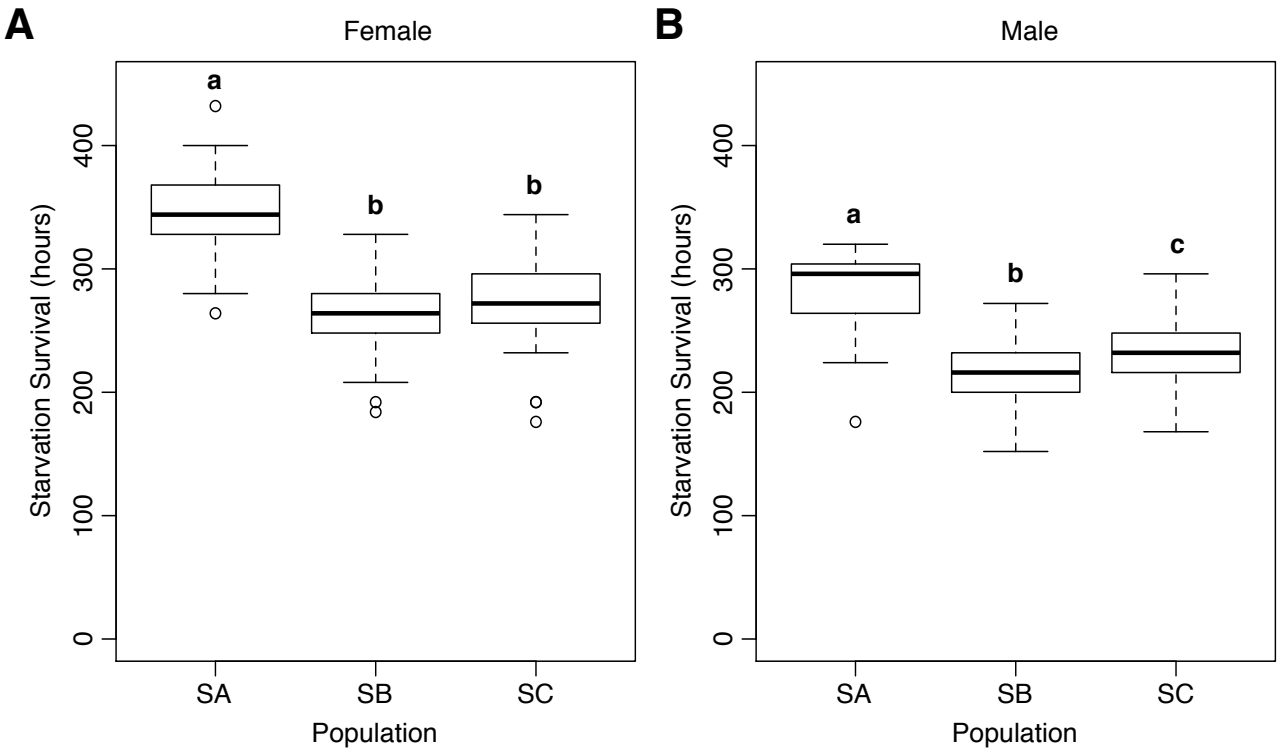

Figure 3.3 Differences in starvation resistance between the starvation-selected populations match patterns of genetic heterogeneity. The S_A population is significantly better at surviving starvation than the S_B and S_C populations for both (A) Females and (B) Males. Different letters signify statistically different groups where $p<0.05$; Tukey Posthoc; ANOVA; N=47-50.

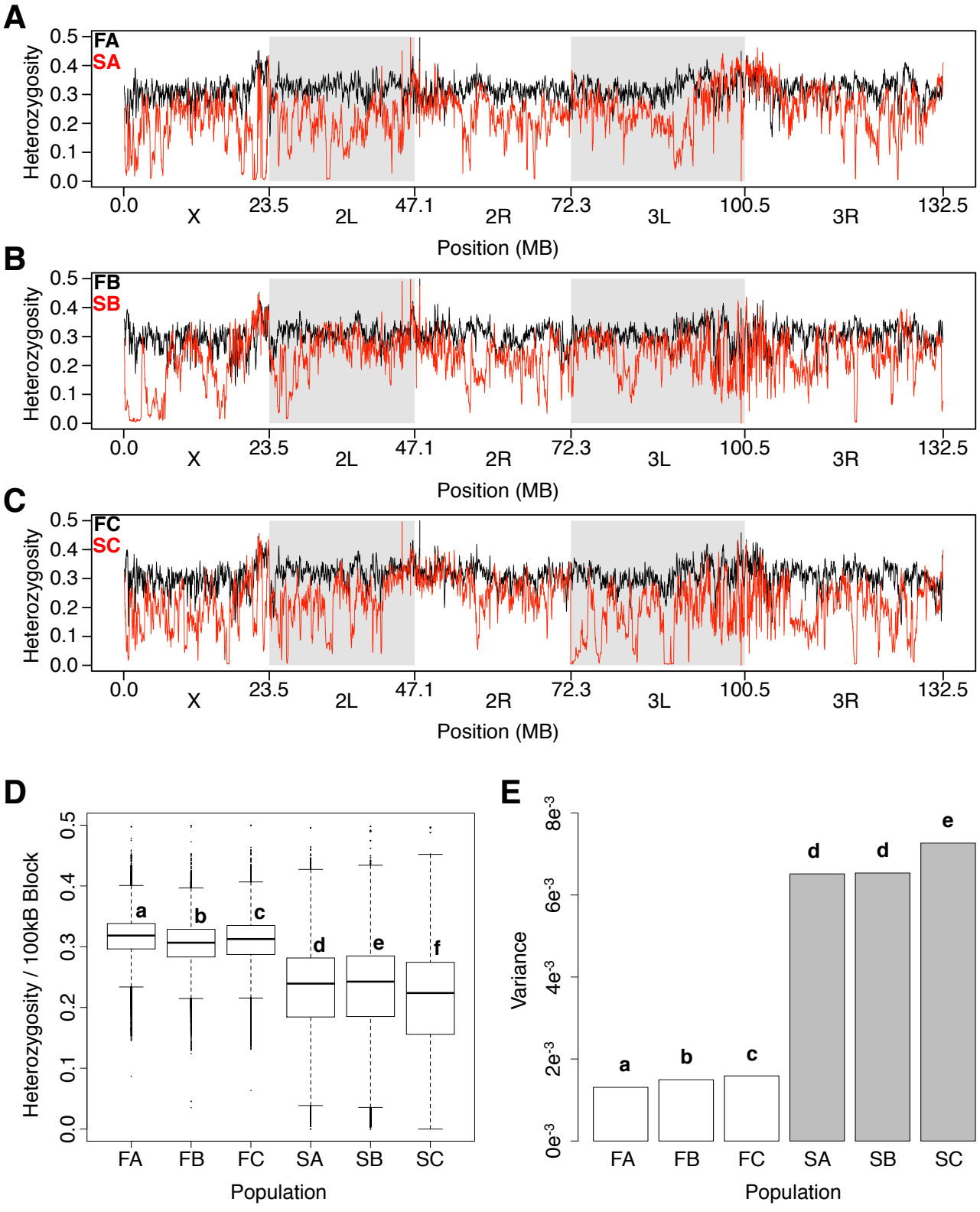

Figure 3.4 Genome-wide heterozygosity. (A-C) Genome-wide sliding window heterozygosity plots (100kb window, with 2kb steps). $S_{A\text{-}C}$ (red) display many regional declines in heterozygosity, while $F_{A\text{-}C}$ (black) heterozygosity remains stable. This results in (D) lower mean heterozygosity per 100kb block and (E) increased levels of variance in the selected lines. Different letters signify statistically different groups where $p<0.05$. See methods for statistical tests.

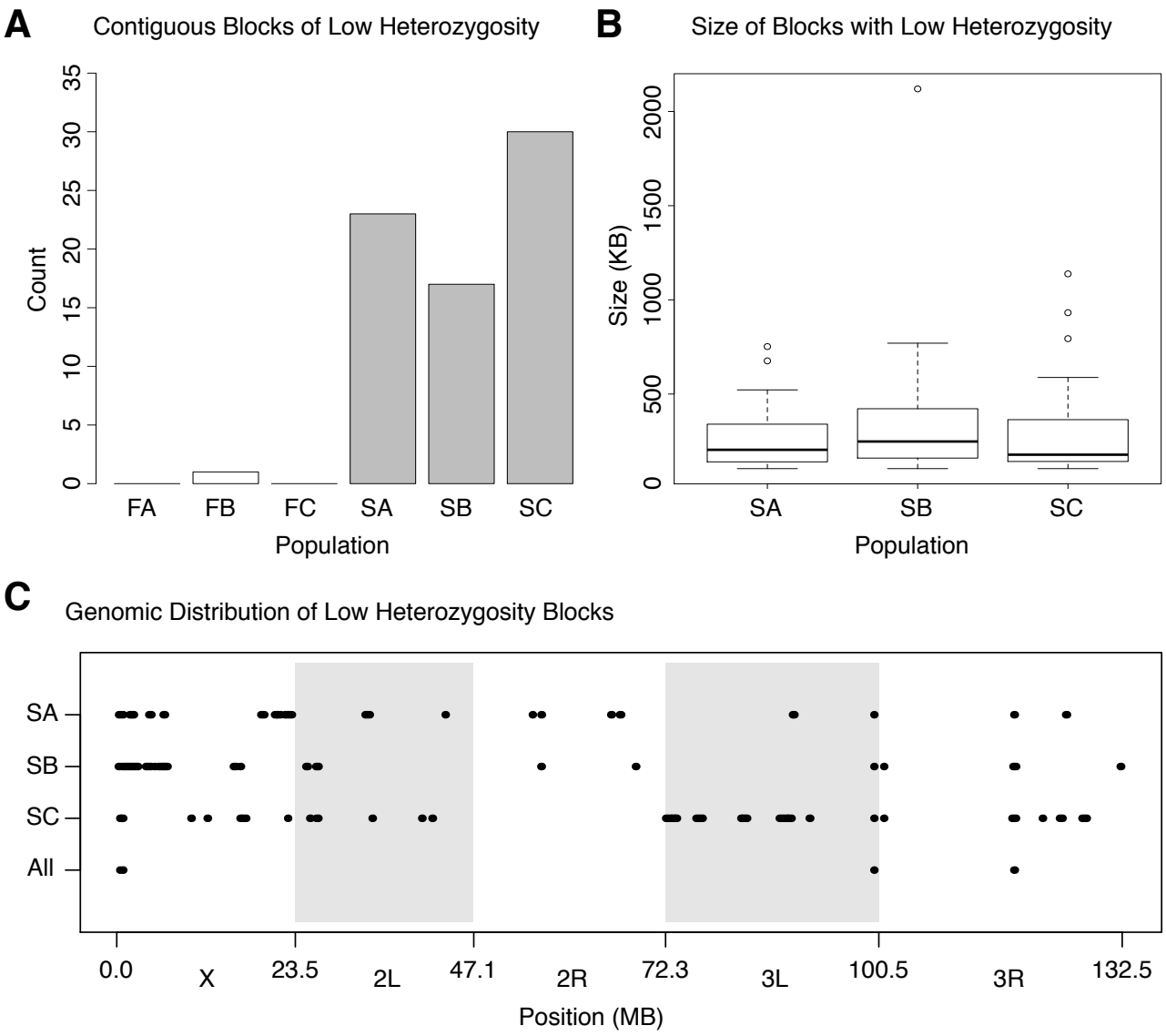

Figure 3.5 Selective sweeps are large and inconsistent in the starvation-selected populations
(A) $S_{A\text{-}C}$ have many extended regions of low heterozygosity approaching fixation (*2pq*<0.05), (B) which average ~300kb in size but range from ~100 to 2000kb. (C) The large contiguous blocks of heterozygosity are inconsistent across replicates. On the "All" horizontal axis are the 4 regions of overlap across the S populations. The regions of low heterozygosity are not to scale; they were made large to visualize the approximate region.

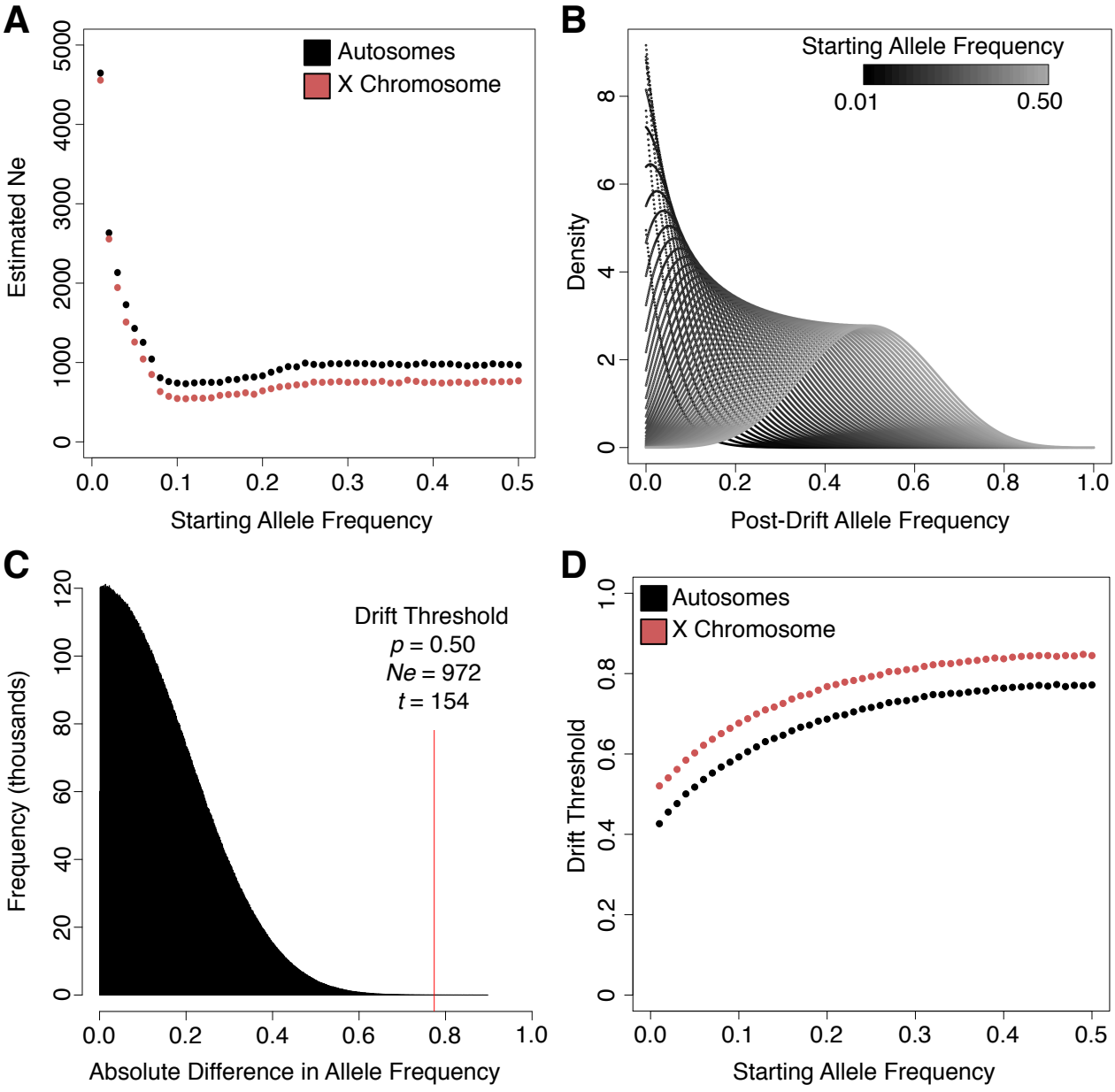

Figure 3.6 Filtering for genetic drift. (A) Effective population size was estimated from the data using Equation 2, plotted here as a function of the starting allele frequency. (B) Posterior density distribution of post-drift allele frequency for each starting allele frequency in {0.01, 0.02 … 0.50}. These distribution were obtained using Kimura's diffusion equation. (C) Histogram, showing the 1.0 x 10^7 values of absolute difference in allele frequency obtained from simulating 2 populations under drift. The 99.999% quantile of each distribution became the Drift Threshold. (D) Relationship between the starting allele frequency and the Drift Threshold for autosomes (black) and the X chromosome (red).

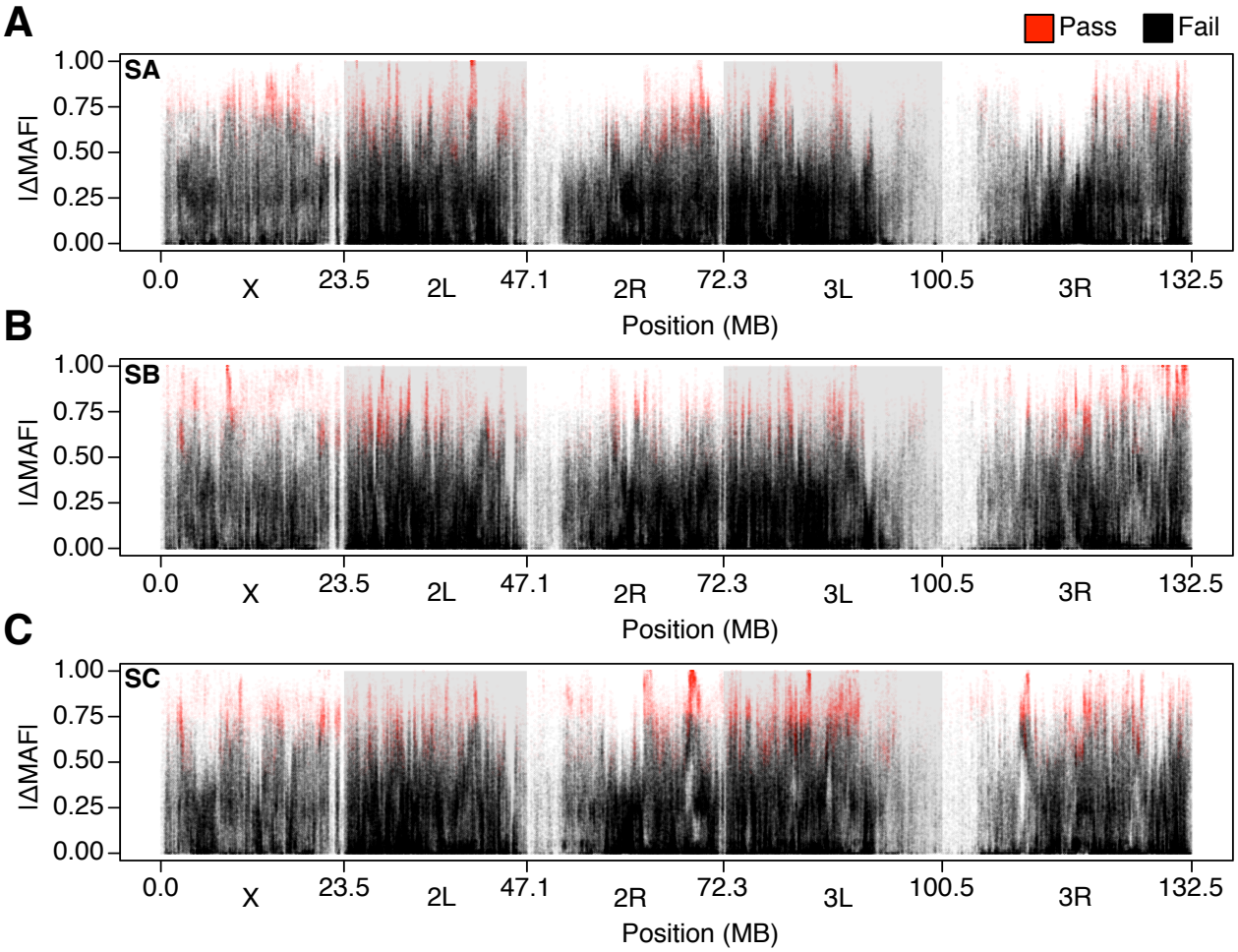

Figure 3.7 Candidate loci (A-C) Absolute difference in allele frequency between the replicate F-S pairs. Red points indicate SNPs whose absolute difference in allele frequency is greater than the Drift Threshold, making them consistent with selection. The loci in black could not be distinguished from drift.

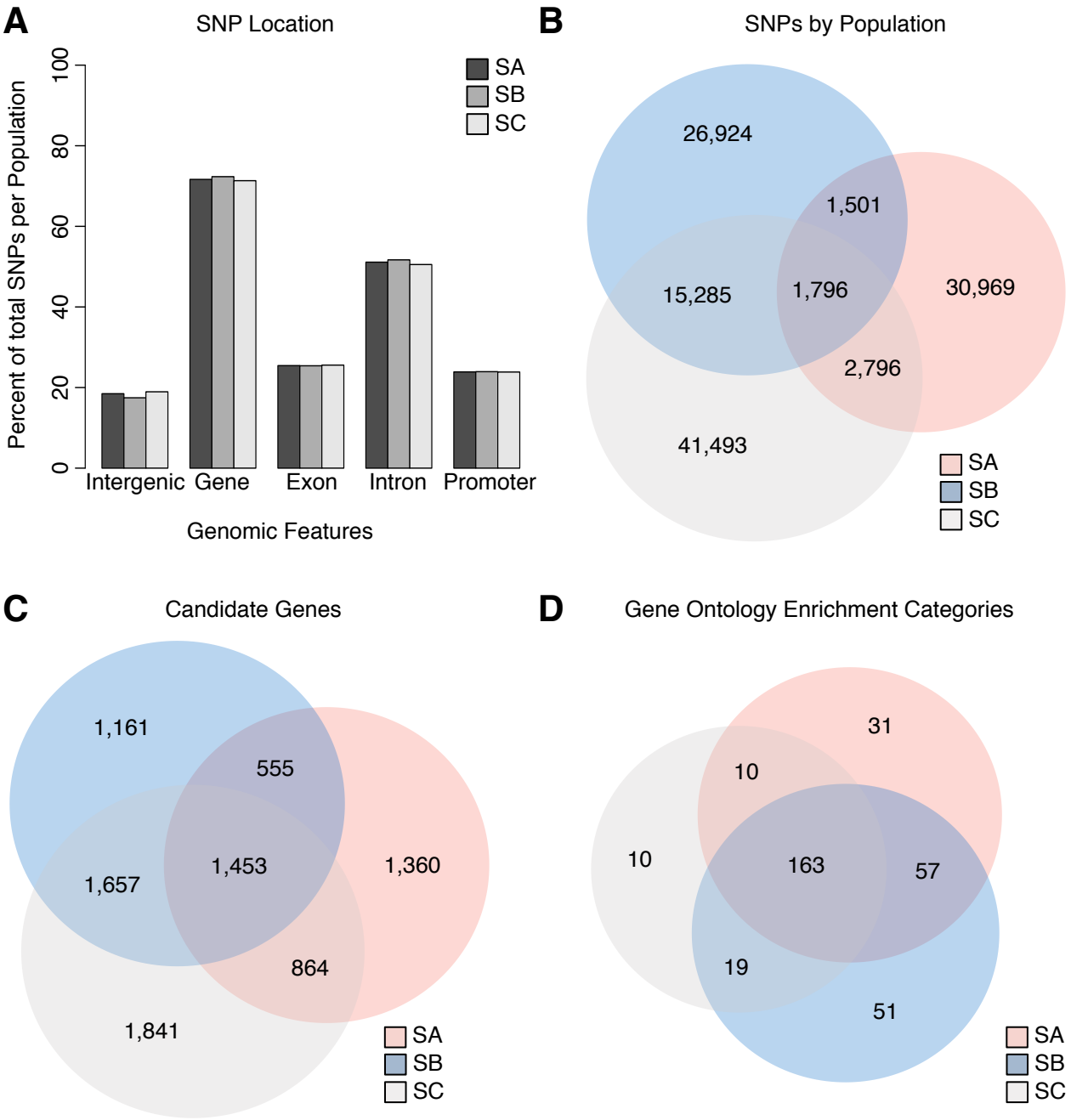

Figure 3.8 Mapping candidate loci to genetic features and biological processes. (A) The S populations had nearly identical distribution of SNPs in different genomic elements. (B) Selection targeted dissimilar loci across S replicates, but converged on more similar (C) genes and even more similar (D) biological processes.

Table 3.1 Gene Ontology Enrichments

GO Terms	GO Accession	p
Top 10 Categories		
anatomical structure morphogenesis	GO:0009653	1.5E-36
organ development	GO:0048513	4.8E-34
organ morphogenesis	GO:0009887	1.1E-30
single-multicellular organism process	GO:0044707	5.4E-29
system development	GO:0048731	8.7E-29
post-embryonic organ development	GO:0048569	4.1E-27
multicellular organismal development	GO:0007275	7.1E-27
neuron differentiation	GO:0030182	7.2E-27
biological regulation	GO:0065007	1.2E-26
cell development	GO:0048468	1.6E-26
Categories associated with starvation-selected phenotypes		
locomotion	GO:0040011	1.4E-24
behavior	GO:0007610	4.8E-17
oogenesis	GO:0048477	2.7E-11
female gamete generation	GO:0007292	3.2E-11
regulation of metabolic process	GO:0019222	4.1E-08
heart development	GO:0007507	1.8E-06
ovarian follicle cell migration	GO:0007297	4.1E-05
regulation of circadian sleep/wake cycle	GO:0042749	1.7E-03
sleep	GO:0030431	3.8E-03
positive regulation of macromolecule biosynthetic process	GO:0010557	3.9E-03

Table 3.2 Human Disease Enrichment for Ortholos of Starvation-selected Genes

OMIM Disease Category	p
myopathy	2.0E-03
cardiomyopathy	3.7E-03
diabetes mellitus, type 2	4.7E-03
leukemia	1.3E-02
cardiomyopathy, dilated	1.5E-02
cardiomyopathy, hypertrophic	1.7E-02
osteoporosis	4.7E-02

Figure 3.8 Mapping candidate loci to genetic features and biological processes.

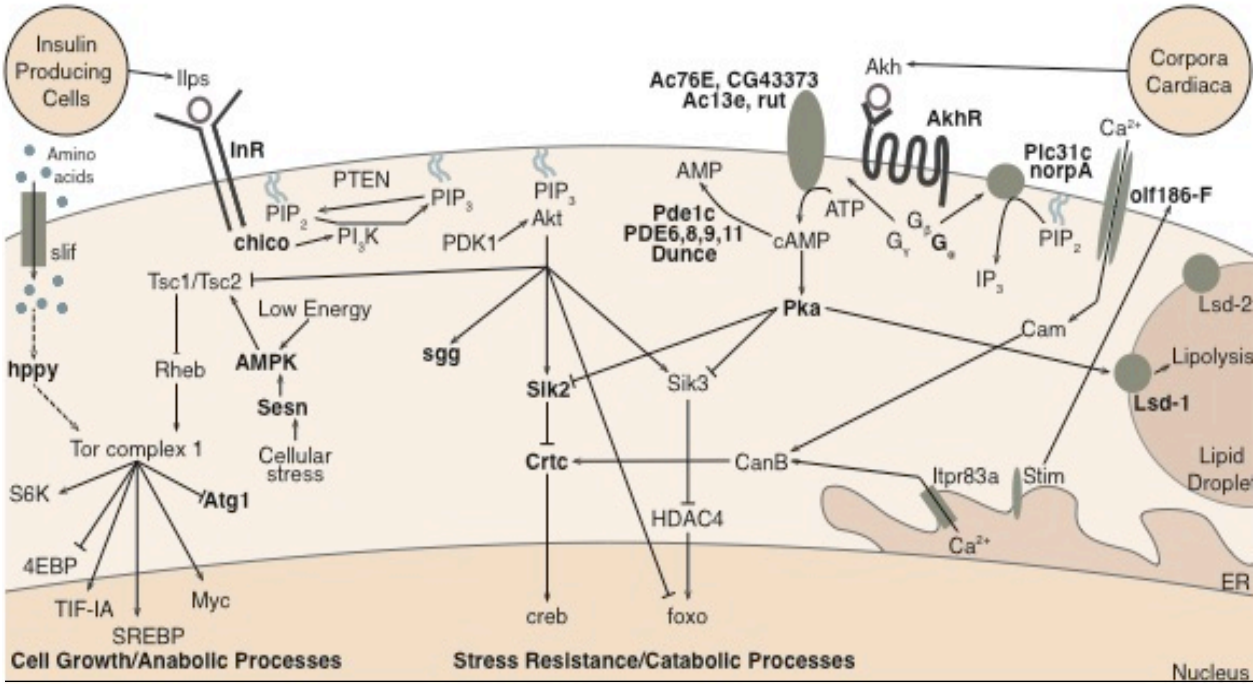

Gene	Symbol	Class	Accession
Insulin Receptor	*InR*	Receptor	FBgn0283499
chico	*chico*	Signal Transduction	FBgn0024248
shaggy	*sgg*	Kinase	FBgn0003371
happyhour	*hppy*	Kinase	FBgn0263395
AMPK-γ subunit	*SNF4Aγ*	Kinase	FBgn0264357
Sestrin	*Sesn*	Stress Response	FBgn0034897
Salt-inducible kinase 2	*Sik2*	Kinase	FBgn0025625
CREB-regulated transcription coactivator	*Crtc*	Transcriptional co-activator	FBgn0036746
G protein a q subunit	*Gaq*	G-protein	FBgn0004435
Phospholipase C at 21C	*Plc21C*	Phopholipase C	FBgn0004611
no receptor potential A	*norpA*	Phopholipase C	FBgn0262738
Adipokinetic Hormore Receptor	*AkhR*	Receptor	FBgn0025595
Adenylyl cyclase 76E	*Ac76E*	Adenylyl Cyclase	FBgn0004852
rutabaga	*rut*	Adenylyl Cyclase	FBgn0003301
Adenylyl cyclase 13E	*Ac13E*	Adenylyl Cyclase	FBgn0022710
CG43373	*CG43373*	Adenylyl Cyclase	FBgn0263131
olf186-F	*olf186-F*	Ca^{2+} channel protein	FBgn0041585
Lipid storage droplet-1	*Lsd-1*	Perilipin	FBgn0039114
Protein Phosphatase 2C	*Pp2C1*	Phoshpatase	FBgn0022768
Pde1c	*Pde1c*	cAMP Phosphodiesterase	FBgn0264815
Phosphodiesterase 6	*Pde6*	cNMP Phosphodiesterase	FBgn0038237
Phosphodiesterase 8	*Pde8*	cAMP Phosphodiesterase	FBgn0266377
Phosphodiesterase 9	*Pde9*	cGMP Phosphodiesterase	FBgn0259171
Phosphodiesterase 11	*Pde11*	cAMP Phosphodiesterase	FBgn0085370
dunce	*dnc*	cAMP Phosphodiesterase	FBgn0000479
Insulin-like peptide 6	*Ilp6*	Peptide hormone	FBgn0044047

CHAPTER 4

FUNCTIONAL GENOMIC ANALYSIS OF DIFFERENTIAL GENE EXPRESSION IN THE FAT BODY DURING PUPARIATION IN STARVATION-SELECTED DROSOPHILA MELANOGASTER.

4.1 Abstract

During development, holometabolous insects do not feed for an extended period, beginning near the end of the final larval instar and persisting through the beginning of adulthood. In preparation, larvae feed continuously and amass large amounts of lipids and storage proteins, which are stored in the fat body. During pupariation the larval fat body is remodeled in response to the steroid hormone 20-hydroxyecdysone (20E). This results in the dissociation of the larval fat body into individual cells. Lipids within these cells are catabolized to provide energy for the other developing tissues throughout metamorphosis. In *Drosophila melanogaster* some larval fat cells persist into the first couple days of adult life. These cells provide an important source of energy to the adult fly, which may be allocated towards reproduction or used for processes such as starvation resistance. Laboratory selection for starvation resistance in *D. melanogaster* causes the selected larva to be developmentally delayed. This delay increases their larval feeding period and allows for the accumulation of excess lipids. These larval-derived lipids are carried by the larval fat body into adulthood where they play a critical role in adult starvation resistance. Despite the importance of these events in driving starvation resistance, there have been few studies on the mechanistic basis of the delay or the physiology of the larval fat body

during development. We studied populations of *D. melanogaster* that had been laboratory selected for starvation resistance for over 70 generations. Selection has led to a ~24 hour delay in larval development. We previously demonstrated that this delay correlates with a ~24 hour delay in the expression of a 20E-inducible gene, *E74A*. This led us to hypothesize that selection altered the timing of 20E signaling. If this hypothesis is correct, we predicted that the expression profiles of 20-inducible genes during and after the onset of pupariation would be similar between the selected populations and their unselected controls. To test this, we sequenced genomic RNA from the fat bodies of F and S larvae, sampled during and after the initiation of pupariation. In support of our hypothesis, a majority of differentially expressed genes were altered in response to the developmental timepoint. However, we also found many genes which were differentially expressed in response to selection. This set was enriched for upregulation of genes associated with the proteasome, spliceosome and mitochondrial translation, as well as the downregulation of many catabolic genes. These results suggest that 20E signaling is altered in the fat body in response to starvation selection.

4.2 Introduction

The life cycle of holometabolous insects can be broadly divided into the egg, larval, pupal and adult stages. Each stage is separated by dynamic developmental transitions that profoundly alter the morphological and physiological status of the animal. Throughout the entire life cycle, energy must be acquired and utilized to drive development, growth and ultimately fuel reproduction. This is particularly challenging for holometabolous insects because their ability to feed changes during each developmental stage. For example, they are unable to feed during a long period of development, which spans portions of the larval, pupal and adult stages. In *Drosophila melanogaster*, this window begins before the onset of pupariation, near the end of the 3rd larval instar, and persists until several hours after metamorphosis, a period spanning ~4-5 days (Tyler 2000; Aguila et al. 2007).

Insects are able to meet the high energetic demand during the non-feeding window by accumulating energetic reserves during the larval stages. The energy derived from larval feeding is critical in fueling the complete reorganization of the animal during metamorphosis and also constitutes a significant portion of the adult energy reserve (Aguila et al. 2007; Aguila et al. 2013). In *D. melanogaster*, much of the larval-derived energy is stored in the form of lipids in the larval fat body. During metamorphosis, lipids accumulated during larval development are catabolized, fueling greater than 80% of total metabolism (Merkey et al. 2011). Larval-derived lipids are additionally carried into the adult fly, where they play an important role in adult starvation resistance and fecundity (Aguila et al. 2013).

The physiology of the larval fat body changes drastically throughout the non-feeding developmental window. This begins at the onset of pupariation, when hormonal cues

initiate a transcriptional cascade that ultimately drives the animal to cease feeding and find a suitable site for metamorphosis. Commitment to this developmental transition is largely driven by the synthesis and release of the steroid hormone ecdysone from the prothoracic gland (PG) in the ring gland (Andersen et al. 2013). Once secreted, ecdysone enters peripheral tissues where it is converted into its more biologically active form, 20-hydroxyecdysone (20E). This is accomplished through the enzymatic products of cytochrome P450 genes such as *shade* (Petryk et al. 2003). This leads to a late-larval pulse of 20E that initiates pupariation. 20E elicits tissue-specific responses which can vary between differentiation and growth, remodeling or programmed cell death (Yin and Thummel 2005; Yamanaka et al. 2013).

The larval fat body is remodeled in response to the late-larval pulse of 20E, leading it to dissociate into individual cells. This is controlled in part through the 20E-induced expression of genes involved in the digestion of the extracellular matrix (Bond et al. 2011). Throughout metamorphosis the number of larval fat cells declines at a slow rate, but some larval fat cells persist into the first few days of adult life (Butterworth et al. 1988). These cells eventually undergo programmed cell death and provide energy for the young adult fly (Aguila et al. 2007). This source of energy is critical for the young adult fly, which continues to develop, despite not feeding for ~8 hours after eclosion (Aguila et al. 2007; references therein). If nutrients are scarce during this period, the energy derived from the larval fat body can be used for adult starvation resistance (Aguila et al. 2007). Otherwise the lipid resources are heavily allocated towards reproduction (Aguila et al. 2013).

When populations of *D. melanogaster* are experimentally evolved to be starvation resistant, they commonly adapt by delaying larval development (Chippindale et al. 1996;

Harshman et al. 1999; Reynolds 2013). This delay provides a longer larval feeding period, during which starvation-selected larvae amass high levels of lipids within the larval fat body. These lipids are carried into adulthood and invested into adult starvation resistance (Chippindale et al. 1996; Harshman et al. 1999; Reynolds 2013). Despite its importance in driving adult starvation resistance, the mechanistic basis of the developmental delay and the physiology of the larval fat body are poorly studied in starvation-selected populations of *D. melanogaster*.

The work described here is part of a broader project to understand (1) if and how 20E signaling is altered in response to starvation-selection, and (2) how this impacts the physiology of the larval fat body. We study these questions in populations of *D. melanogaster* that have been selected for starvation resistance for over 70 generations. In response to selection, the starvation-selected populations (hereafter "S" populations) have evolved many unique physiologies, including a significant ~24 hour delay in larval development compared to their unselected fed controls (hereafter "F" populations; Reynolds 2013). Our preliminary experiments have found that the delay in larval development correlates with a ~24 hour delay in the expression of a key 20E target gene, *E74A* (Reynolds, 2013). *E74A* is upregulated in response to 20E approximately 6-10 hours prior to pupariation in both the F populations and wild-type laboratory strains of *D. melanogastger*, (*w1118*; Beckstead et al. 2005; F populations; Reynolds 2013). Despite having delayed expression, *E74A* is still induced ~6-10 hours prior to pupariation in the S populations (Reynolds, 2013). These data suggest that selection has altered the timing of the late-larval 20E pulse, which we hypothesize gives the animal sufficient time to feed and accumulate lipids. If this is the case, then I predict that the major patterns of 20E-induced

gene expression will be similar in both the F and S populations during the late-larval 20E pulse.

We tested this hypothesis by staging animals both at pupariation and mid-way through their exposure to the late-larval 20E pulse. From these time points we isolated and resequenced RNA from the larval fat bodies to observe genome-wide changes in gene expression. As predicted, we found that a majority of 20E-induced genes (~1,788) had similar patterns of expression between the F and S populations. However, we also found a subset of 645 genes whose expression pattern during this developmental window was altered in response to selection. Further analysis found that selection led to the upregulation of genes associated with the proteasome, spliceosome and mitochondrial translation, along with the downregulation of genes associated with catabolism. These data suggest that starvation selection altered the tissue-specific response of the larval fat body to 20E signaling.

4.3 Methods

Sample Preparation

For a detailed description of the evolutionary history of the F and S populations please see the methods section in Chapter 3. To begin preparation for RNA collection, flies were removed from selection for 1 generation to control for parental effects. Then approximately 100-200 F1 adult flies from each population were housed in cages and given molasses egg caps with yeast paste. Every 12 hours egg caps were removed from the cages and 100 1st instar larvae were transferred into vials containing standard media with the addition of 0.05% bromophenol blue. The addition of the dye turns the media blue, which is part of a well-established protocol to approximate the timing of pupariation (Andres and Thummel 1994). Briefly, as larvae feed throughout the 3rd instar, the dye in the food can be visualized through the gut. As the animals stop feeding (~10-20 hours prior to pupariation), the gut gradually clears such that animals with a clear gut are 1-6 hours from pupariation (Andres and Thummel 1994). This physiological stage is routinely used to select animals that have been exposed to the late-larval 20E pulse for ~4 hours. Several hours later there is a brief developmental window just after puparium formation has begun called the white prepupa stage.

To study how gene expression differed between $F_{A\text{-}C}$ and $S_{A\text{-}C}$ in response to the late-larval ecdysone pulse, we collected 2 samples of 3rd instar larvae with clear guts and 2 samples of white prepupae from each population for a total of 24 samples (Figure 4.1). Each sample consisted of 15-25 dissected fat bodies in DPBS, which were pooled into 150µL of TRIzol® Reagent (Invitrogen Corp, Carslbad, CA). Extreme care was taken to remove the tightly associated testes and imaginal discs from the preparation. To isolate

RNA, we used the Direct-zol™ RNA Mini Prep Protocol (Zymo Research Corporation, Irvine, CA) under the manufacturers guidelines**.** RNA quantity and quality were assessed using the Experion™ Automated Electrophoresis System (Bio-Rad Laboratories, Inc, Hercules, CA), with samples prepared using the Experion™ RNA StdSens Analysis Kit (Bio-Rad Laboratories, Inc, Hercules, CA). Each sample was diluted in nuclease free water to 25 ng/μL and sent to the Genomics Center in the Huntsman Cancer Institute at the University of Utah for library preparation and sequencing.

Library Preparation and Sequencing

After quality control, libraries were prepared for each sample using the TruSeq® Stranded Total RNA Sample Prep with Ribo-Zero rRNA Removal (Illumina Inc, San Diego, CA). The protocol did not require a strict size selection, however after adjusting fragmentation time, mean fragments were ~300bp in length. Our experimental design included 2 replicates for each population ($F_{A\text{-}C}$ and $S_{A\text{-}C}$) at each developmental timepoint (3IN and WPP) for a total of 24 unique libraries. These replicates were split into 2 groups, which were independently multiplexed and spread onto 2 separate lanes on the flowcell. We then performed a 101-cycle paired-end run with an Illumina HiSeq™ Sequencing System using version 4 chemistry, obtaining nearly 3.50×10^8 reads with an average of 1.46×10^7 reads per library.

Alignment, Feature Counting and Differential Expression

Genome sequences, annotations and indices were downloaded from the *Drosophila melanogaster* dm6 build from UCSC as part of the Illumina iGenomes collection. Raw reads

were aligned to the genome using tools from the Tuxedo Suite (TopHat v2.1.0, Bowtie2 v2.2.6). To align reads to the *Drosophila melanogaster* reference genome, we used TopHat with gene annotations provided from the iGenomes collection using options to filter reads with multiple alignments (max-multihits = 1) or without a successfully aligned paired read (no-mixed). Because our average insert size was ~300bp and we sequenced 100bp from each end we set the average distance between paired end reads to 100bp (mate-inner-dist = 100). Finally, because we used a stranded Illumina TruSeq Kit for library preparation we also implemented the fr-firststrand option.

For each library TopHat generates an alignment file of accepted hits. Reads in these files were sorted by name using SAMtools (version 1.1) to order paired reads together. Sorted alignment files were run through HTSeq (version 0.6.1p2) using the htseq-count function to map reads to genomic features. Specifically, we mapped reads with an alignment quality >20 (minaqual = 20) to exons from the annotation file (genes.gtf) provided in the iGenomes collection. We used the intersection-nonempty mode as a slightly less conservative approach to aligning features and set strandedness to reverse based on our library preparation. Htseq-count assigns each successfully mapped read to a parent gene id, providing a finalized list with read counts per gene for each individual sample.

We developed custom Unix-based command line scripts to concatenate these read count files into a single 16,727 x 24 matrix (X_{ij}). Each index of the matrix contained an integer, representing the read count for each gene (i), corresponding to 1 of our 24 total samples (j). This data table was loaded into R and formatted for integration with DESeq2 for differential expression analysis.

Differential Expression Analysis

For differential expression analysis, we used DESeq2 in R (Love et al. 2014; R Core Team 2015). We implemented a multi-factor design, with selection and developmental stage as the main effects, along with a selection-by-developmental stage interaction term. Levels of selection were "F" for the Fed control populations of "S" for the Starvation selected lines. Levels of the developmental stage term were either "3IN" for RNA samples collected form 3rd instar larva or "WPP" for those collected at the white prepupa timepoint. The model was run through DESeq2 and results were parsed into 3 tables containing genes that were significant for the main effect of selection, development or the interaction term respectively. To perform a *post-hoc* analysis on genes with a significant interaction term, we re-ran DESeq with 1 effect, "Group" with levels of "F3IN", "FWPP", "S3IN" and "SWPP". We filtered the resulting output table for only genes which had a significant interaction effect from the original model. These tables were written out of R into plain text files for enrichment analysis.

Enrichment Analysis

Enrichment analysis for each gene list was performed using FlyMine (Lyne et al. 2007). Gene lists were uploaded and submitted to FlyMine which returns "widgets" with information on enrichment for gene ontology terms, pathways and protein domain categories within the gene list. Gene ontology categories were further optimized to reduce hierarchical clustering using GO-module (Yang et al. 2011). In a few instances, the widget for physical interaction network demonstrated a large degree of physical interactions

within the gene list. These networks were opened in esyN (www.esyn.org), which was used to determine network parameters and export the network image.

Principal Component Analysis and Pearson Product Moment Correlation

The raw count table was imported into R and read counts were normalized by library size. The Principal Component Analysis (PCA) was performed using the *prcomp* function in the stats package in R. The first 2 principal components explained ~96% of the variation in gene expression between samples and were plotted using customized scripts in R. The Pearson Product Moment Correlation Coefficient was calculated using the *pr.comp* function in the stats package in R. Custom scripts were written to perform pairwise correlations. The mean correlation for each major group was calculated in R and differences in the mean were determined with an ANOVA and Tukey *post hoc* test in R.

4.4 Results

Starvation-selection alters genome-wide patterns of gene expression within the fat body in response to pupariation.

The overarching goal of this study is to understand if and how starvation selection alters gene expression throughout pupariation. Therefore we sampled genomic RNA from the F and S populations at two developmental timepoints- during and after the onset of pupariation. This generated 4 major "groups", the Fed Control 3rd Instar (hereafter "F 3IN"), the Starvation-selected 3rd Instar (hereafter "S 3IN"), the Fed Control White Prepupa ("F WPP") and the Starvation-selected White Prepupa (hereafter "S WPP"). Each group was defined by 4 factors; the selection treatment (F | S), developmental timepoint (3IN | WPP), the evolutionary replicate population of origin (A | B | C) and the biological replicate (1 | 2)(see Figure 4.1 for an overview of the experimental design). In total this design led to 24 independent RNA libraries- or hereafter "samples"- with 6 samples in each of the 4 major groups.

Before performing differential expression analysis to look for gene-level differences between groups, we performed a Principal Component Analysis (PCA) to visualize the relationships in genome-wide expression patterns between all 24 samples. We plotted the first two principal components, which explained a combined ~96% of the variation in gene expression across samples (Figure 4.2). We first examined the patterns of gene expression across the 3IN groups. We observed that the expression patterns between F 3IN and S 3IN were fairly similar, but slightly separated by selection treatment (Figure 4.2; F 3IN: light gray; S 3IN: light red). The subtle differences between these groups were largely overshadowed by the high degree of separation between the 3IN and WPP groups (Figure

4.2; F WPP: Dark gray; S WPP: Dark red). Interestingly, samples in the S WPP group were highly variable, especially compared to the tight clustering of samples within F WPP (Figure 4.2). Most of the variation within the S WPP group was due to differences between the replicate populations, as the two S_A WPP biological replicates were more closely associated with samples from the F WPP group than they were to the S_{B-C} WPP populations (Figure 4.2). These data suggest that the F and S populations may share a higher degree of similarity in overall patterns of gene expression early in pupariation. The dense clustering of samples within the F WPP group demonstrated the tight control of gene regulation in the fat body during this important developmental transition. However, changes in gene expression were less consistent in the S white prepupal stage.

We then quantified the trends that we observed in PCA by calculating the pair-wise Pearson product-moment correlation coefficient (r) between all 24 samples with respect to genome-wide expression profiles (Figure 4.3A). From these values we calculated the average correlation coefficient ($\overline{r}$) of samples within and across each major group (Figure 4.3B). Gene expression patterns within groups were highly correlated, with $\overline{r}$ exceeding 0.90 in the F 3IN, F WPP and S 3IN groups (Figure 4.3B). However, the samples within the S WPP group were more variable, which resulted in a significantly lower $\overline{r}$ of 0.74±0.06 compared to the other within group correlations ($p<0.05$, Figure 4.3B). One reason for the high degree of variability in the S WPP group, which was not observed in the PCA, was the poor correlation of one of the S_C biological replicates to all other samples experiment-wide (Figure 4.2, bottom row). This even included a relatively low level of correlation with the other S_C WPP biological replicate ($r = 0.76$; Figure 4.2). The poor correlation observed

between the S_C WPP replicate pair was uncommon, as *r* exceeded 0.92 between all other biological replicate pairs and averaged 0.96±0.02 overall (Figure 4.3B).

Next, we wanted to understand how similar the gene expression patterns were between each major group. To do this we calculated the average correlation of samples across groups. Groups at different developmental timepoints had low correlation coefficients, with $\bar{r}$ across samples of F 3IN and F WPP equal to 0.79±0.02 and $\bar{r}$ across samples of S 3IN and S WPP equal to 0.73±0.3 (Figure 4.3B). These correlations were significantly lower than within group $\bar{r}$ for either F 3IN or S 3IN respectively ($\bar{r}$ within samples of F 3IN vs. $\bar{r}$ across samples of F 3IN and F WPP: $p<0.03$; $\bar{r}$ within samples of S 3IN vs. $\bar{r}$ across samples of S 3IN and S WPP $p<1.1x10^{-3}$; Figure 4.3B). These comparisons suggest that pupariation is sufficient to significantly alter patterns of gene expression in both the F and S populations.

We then looked for differences across the F and S populations during and after the onset of pupariation. Samples in the F 3IN group tended to be less correlated to those in the S 3IN group than they were to themselves, however the data failed to reach significance ($\bar{r}$ within F 3IN= 0.94±0.01; $\bar{r}$ across F 3IN and S 3IN = 0.89±0.01; Figure 4.3B). This further suggested that overall gene expression early in pupariation is relatively similar between the F and S populations. We also found that the samples in the F WPP group were significantly less correlated with those in the S WPP group than they were to themselves ($\bar{r}$ within F WPP = 0.99±0.001; $\bar{r}$ across F WPP and S WPP = 0.80±0.04; Figure 4.3B). These findings suggest that selection has a significant effect on the patterns of gene expression following the onset pupariation. Furthermore, the high degree of within-group variance in

the S WPP further suggests that fat body-specific gene expression may differ across the S replicate populations at the onset of metamorphosis.

The onset of pupariation results in the differential expression of many genes within the fat body.

Next we analyzed the dataset for differential gene expression, using a multi-factor design with development (3IN | WPP) and selection (F | S) as the main effects, along with a development by selection interaction term (Methods). We first screened for genes with a significant development term to analyze the overall effects of pupariation on gene expression. In total, we found 1,880 genes whose expression significantly differed between 3IN and WPP ($p<0.05$, Benjamini-Hochberg (BH) adjusted for multiple comparisons). Out of this set of 1,880 genes, 92 also had a significant development-by-selection interaction term. These genes were removed from the list for later analysis. This resulted in a set of 1,788 genes for analysis. We found that a majority of these genes were downregulated, with 1,136 genes displaying lower expression at the WPP developmental timepoint compared to the 3IN. The degree of downregulation varied with $\log_2$-fold changes ranging from -0.33 to -8.25, resulting in an average $\log_2$-fold difference of -2.00±0.04. The remaining 652 genes were upregulated in response to pupariation with an average $\log_2$-fold change of 1.77±0.05, which ranged from 0.29 to 9.67.

We first examined the 10 most highly up- and downregulated genes. The 10 most upregulated included several ecdysone-inducible genes, which are known to be associated with metamorphosis but may also be involved in immune responses to bacteria and autophagic cell death (*Eig71Ei*, *Eig71Eh* and *Eig71Ef*; Table 4.1). The other 7 genes have not

been previously characterized in *Drosophila*, however two are predicted to be involved in proteolysis (CG18179 and CG31954), while CG42717 is predicted to function as a serine-type endopeptidase inhibitor (Table 4.1). We observed that several of the top 10 genes encoded a conserved protein domain which is not functionally classified in *Drosophila*, but is predicted to generate a signaling peptide that is likely excreted (CG43082, *Eig71Ei*, *Eig71Eh* and *Eig71Ef,* Insect protein of unknown function; Interpro: IPR003475). This domain was also overrepresented when considering all 652 upregulated genes, and included several other ecdysone-inducible genes (Eig71Ea, *Eig71Eb*, *Eig71Ec*, *Eig71Ed* and *Eig71Eg*; Table 4.2). We also found enrichment for upregulation of genes involved in defense response, response to bacterium and proteolysis (Table 4.3). Next we looked for over-represented pathways and found enrichment for genes associated with the proteasome (Table 4.4). This included a core set of proteasomal genes coding for the α and β proteasomal subunits (*Prosβ2*, *Prosβ4*, *Prosα2* and *Prosα6*) as well as several regulatory particles (*Rpn1*, *Rpn9*, *Rpn10*, *Rpt1*, *Rpt3*, *Rpt4*, *Rpt5*). The core proteasomal set of genes combined with other upregulated genes, including *PI31*, *Cul1*, *IKKβ*, CG1440 and *Pomp*, to generate enrichment for pathways involved in a variety of cell signaling pathways (described in Table 4.4).

Next we examined the ten most downregulated genes in response to pupariation. Downregulated genes were associated with lipid and cholesterol homeostasis (*mag*), sterol binding and transport (*Npc2c*), proteolysis (*Jon74E*) and puparial adhesion (*Sgs1*, *Sgs3* and *Sgs4*; Table 4.1). The 4 other most downregulated genes are uncharacterized and have no predicted functions (CG31698, CG13460, CG15404 and CG14850). We then analyzed the entire set of 1,136 downregulated genes and found enrichment for single-organism

transport, system development, neurogenesis, ribosome biogenesis, hemolymph coagulation, response to starvation, protein targeting to membrane, rRNA metabolic process, protein localization to the endoplasmic reticulum and cellular response to external stimuli (Table 4.3). Some of these categories such as single-organism transport, neurogenesis and system development were fairly broad and relatively non-informative. However, genes within these categories associated with a variety of processes including sugar or ABC transport activity, phagosome formation, vesicle transport and cellular differentiation pathways (data not shown). We also found several pathways which were over-represented in the downregulated gene set. These included protein processing in the endoplasmic reticulum, ribosome biogenesis and protein export (Table 4.3). The downregulated genes were also enriched for sequences coding for several protein domains, including cytochrome P450, peptidase M13 and Immunoglobulin E-set (Table 4.2).

Starvation-selection alters the expression of genes within the fat body during pupariation.

Next, we wanted to examine differences in gene expression between the F and S populations. To do this we screened for genes with a significant selection term within our multi-factor model. In total we found 188 genes with significant differences in gene expression in response to selection ($p<0.05$, BH adjusted). Within this set of 188 genes, we found 20 which also had a significant selection by development interaction term. These genes were filtered for later analysis. This resulted in a set of 168 genes, which were up- or downregulated in the S populations with respect to F gene expression levels. We found 77 upregulated genes with an average $\log_2$-fold expression increase of 2.3±0.2 (range= 0.5 to

6.4). The other 91 genes were downregulated with an average $\log_2$-fold expression decrease of -1.8±0.1 (range= -0.6 to -4.7).

We analyzed the up- and downregulated gene lists to look for over-represented gene ontology terms, pathways and protein domains, but failed to find significant enrichment. For further analysis, we decided to divide the set of 168 genes into groups based on developmental patterns of gene expression. Specifically we wanted to examine the effects of selection on gene expression for genes whose expression increased, decreased or stayed constant during pupariation. First we considered genes which did not differ in their expression between 3IN and WPP, but were significantly different between the F and S populations (see Figure 4.4 for example). There were 109 genes which met these criteria, 52 of which were upregulated in the S populations, while 57 were downregulated. Again, we failed to find significant enrichment for any gene ontology, pathway or protein domain categories. We examined the 10 most upregulated genes and found they were associated with carnitine synthesis (CG10814), cAMP-dependent protein kinase regulation (CG14692), long non-coding RNA's (CR45194, CR44077 and CR45469), phototransduction and G-protein coupled receptor signaling (*inaD*), degradation of glycans within the lysosome (*LManVI*), sensory perception of chemical stimuli (*dpr4*), glutathione S-transferase activity (*GstD2*) and proteolysis (CG31326; Table 4.5). We then examined the 10 most downregulated genes and found they were associated with stress/bacterial response induced by the humoral factor Turandot (*Victoria*, *TotC*), chitin binding (CG10725, CG10405), ecdysteroid metabolism (CG9509), ligand-gated ion channel activity (*Ir76a*), long non-coding RNA (CR43166) and uncharacterized genes with no predicted function (CG14357, CG34034; Table 4.5).

Next we returned to the list of 168 genes with a significant selection term and filtered for genes whose expression was also significantly altered by development. First we focused on genes which were significantly downregulated during pupariation, but at different levels between the F and S populations (see Figure 4.5 for example). We found 40 genes that met these criteria, with 19 upregulated and 21 downregulated in the S populations. We examined the ten most upregulated genes and found they were associated with several cytochrome P450 enzymes (*Cyp4e3*, *Cyp4ad1*, *Cyp9b1* and *Cyp28a5*), a glutathione transferase (*GstE3*), carnitine biosynthesis (CG4335), dorsal/ventral axis polarity specification and regulation of protein secretion (*sel*), synaptic vesicle exocytosis (*cpx*), proteolysis (CG10073) and an uncharacterized gene with no predicted function (CG15879; Table 4.6). We then examined the 10 most downregulated genes and found they were associated with chitin metabolism (*Muc96D*), negative regulation of pre-miRNA processing (*lin-28*), serine-type endopeptidase and hemolmyph coagulation (CG11313), long non-coding RNA (CR44510), glutathione metabolism (*GstE7*), G-protein couple receptor/stress response (*mthl15*), GABA transporter (*Gat*), protein O-linked glycosylation (CG30463), ionotropic glutamate receptor (*clumsy*) and an uncharacterized gene with no predicted function (CG34291; Table 4.6).

Lastly, we examined the remaining 19 genes from the set of 168 that were differentially expressed in response to selection. Genes in this set also had a significant development term and were upregulated in response to pupariation (see Figure 4.6 for example). Within this list we found 6 genes that were upregulated in the S populations and 13 which were downregulated. The 6 upregulated genes were associated with proteolysis (CG8299), trypsin inhibition (CG31777), a tetraspanin membrane protein (*Tsp42Ed*),

glutathione peroxidase (*PHGPx*), oxidoreductase activity (CG11257) and an uncharacterized gene with no predicted function (CG42711; Table 4.7). The 10 most downregulated genes were associated with lipase activity (CG11406), peptidoglycan catabolism/stress response (*PGRP-SB1*), proteolysis (CG12133, CG30287, CG30088), small GTPase mediated signal transduction (*Rgk1*), hemolymph coagulation (CG42817), mesoderm development (*Swip-1*), proteasomal ubiquitin-dependent protein catabolism (*Ppa*) and an uncharacterized gene with no predicted function (CG42876; Table 4.7).

Many genes have complex patterns of expression that are dependent on both selection and development.

Finally we examined genes whose expression resulted in a significant selection by development interaction. In other words, the effect of selection on gene expression changed depending on the developmental timepoint. In total there were 477 genes with a significant interaction term ($p<0.05$, adjusted for multiple comparisons). We performed a *post-hoc* analysis to investigate differential gene expression across 4 different contrasts, which included F 3IN vs. F WPP, S 3IN vs. S WPP, F 3IN vs. S 3IN and F WPP vs. S WPP. Comparing F 3IN vs. S 3IN and F WPP vs. S WPP allowed us to address the effects of selection on gene expression during and after the onset of pupariation, while comparing F 3IN vs. F WPP and S 3IN vs. S WPP helped describe how gene expression changed in response to pupariation for both the F and S populations. Ultimately this analysis allowed us to make statements such as: Expression of gene X is equal in the F and S populations prior to pupariation (F 3IN = S 3IN), during pupariation expression increases in the S populations (S 3IN < S WPP) but remains the same in the F populations (F3IN = F WPP),

resulting in higher expression of gene X in the S populations at the end of pupariation (F WPP < S WPP). Analysis of the 477 genes found that they clustered into 23 different patterns, which can be determined from the data in Appendix F. The complexity of these interactions is interesting, but difficult to parse into meaningful patterns. Instead, we decided to simplify the analysis of genes with a significant interaction term, by examining gene lists across each of the 4 contrasts.

First we analyzed gene expression differences between the F and S populations during the 3IN developmental timepoint (F 3IN vs. S 3IN). In total there were 25 genes which were differentially expressed, with 4 upregulated and 21 downregulated in the S populations in comparison to the Fs. We did not find enrichment for any gene ontology terms, pathways or protein domains within these sets. We examined the genes with the highest expression and found that they were associated with proteolysis (CG5715), acetyl-CoA biosynthesis/citrate metabolism (*ATPCL*), lipid/triglyceride homeostasis and regulation of response to oxidative stress (*iPLA2-VIA*) and an uncharacterized gene with no predicted function (CG14961; Table 4.8). We then assessed the 10 most downregulated genes. The top 5 were uncharacterized proteins with no predicted function (CG5084, CG5767, CG9682, CG31516 and CG5770). The others were associated with carbohydrate metabolism (*Cda9*), chitin metabolism (CG10140 and *obst-J*), transmembrane transport (*hoe2*) and ecdysis-triggering hormone signaling (*ETHR*; Table 4.8).

Next we examined differential expression between the F 3IN and F WPP groups. In total we found that 108 of the 477 genes with a significant interaction term were differentially expressed in the F populations during and after the onset of pupariation. Out of 108 genes, 21 were upregulated in the F WPP group compared to the F 3IN group, while

97 genes were downregulated. We assessed the top 10 most highly upregulated genes and found that the gene with the largest increase in expression was uncharacterized with no predicted function (CG43133). The others were associated with transmembrane transport (CG12194), G-protein coupled acetylcholine receptor signaling (*mAchR-B*), 3-hydroxyacyl-CoA dehydrogenase activity (CG9914), protein membrane targeting (*Mctp*), MAATS domain involved in spermatogenesis (CG15145), iron ion homeostasis (*Mco1*), protein lipidation (*PIG-C*), acyl-CoA oxidase/fatty acid β-oxidation (*Acox57D-p*) and phosphatidylinositol transporter activity (*rdgBβ*; Table 4.9). We then examined the 10 most downregulated genes and found that they associated with puparial adhesion (*Sgs7*, *Sgs8*), transmembrane transport (*MFS9* and *hoe2*), larval chitin-based cuticle development (*Lcp3*), ecdysis triggering hormone signaling (*ETHR*), protease inhibitor activity (CG5767), immune response (CG15068) and uncharacterized genes with no predicted function (CG5084 and CG5767; Table 4.9). Several components of the proteasome were also upregulated, which resulted in many over-represented pathways within the gene set (*Prosβ6*, *Rpn2*, *Rpn5* and *Rpn6*; Table 4.10).

We next looked at genes with differential expression in the S populations between the 3IN and WPP developmental timepoints. 354 genes were differentially expressed, with 319 upregulated and 35 downregulated in the S WPP group compared to the S 3IN. Interestingly, 68 of the upregulated genes were found to form a network of physical interactions (Figure 4.7). In total the 68 nodes formed 18 sub-networks ranging in size from 2-12 nodes. Genes within this network were enriched for gene ontology terms associated with mitotic spindle organization, cytoskeleton organization, protein folding, microtubule-based process and single-organism organelle organization (Table 4.11). Next,

we expanded the analysis to include all 319 upregulated genes and found enrichment for pathways involved in mitochondrial translation as well as mRNA splicing and RNA degradation (Table 4.12). These pathway enrichments were largely due to the presence of 31 nuclear and mitochondrial ribosomal subunits as well as 12 genes that associated with the spliceosome. The ten most upregulated genes were associated with phosphatase activity (CG9452), a secretory protein (*Ag5r*), fatty acid metabolism (CG10131), non-coding RNAs (*MRE16* and CR43957), short chain dehydrogenase/oxoreductase activity (CG14946), actin filament organization (*Arpc3B*), serine-type endopeptidase activity (*l(2)34Fc*) and uncharacterized genes with no predicted function (CG9689 and CG44250; Table 4.13). We then focused on the 35 genes which were downregulated in the S WPP with respect to the S 3IN. We failed to find enrichment for any gene ontology terms, protein domains or pathways within this set. The ten most downregulated genes were associated with sodium-neurotransmitter symport activity (CG13795), alcohol dehydrogenase (*Adh*), cytochrome P450 oxidation-reduction process (*Cyp28d1*), acetyl-CoA biosynthesis and citrate metabolism (*ATPCL*), DNA methylation (*Ipod*), AMP deaminase (*AMPdeam*), body morphogenesis (*TwdlG*), heat shock protein (*Hsc70-3*) and uncharacterized genes with no predicted function (CG5773 and CG14961; Table 4.13).

Finally we analyzed genes whose expression differed between the F and S populations at the WPP developmental timepoint. This amounted to 399 genes, 357 of which were upregulated in the S relative to F populations, while 42 were found to be downregulated. Of the 357 upregulated genes, 293 were also upregulated in the previous S WPP vs. S 3IN comparison. This led to a similar protein interaction network, which included 74 nodes with network sizes ranging from 2 to 19 (Figure 4.8). These 74 genes

were enriched for similar gene ontology terms such as mitotic spindle organization, mRNA metabolic process, gene expression, microtubule-based process, organelle organization, cellular nitrogen compound metabolic process and protein folding (Table 4.14). We also found enrichment for pathways associated with mitochondrial translation elongation and termination as well as mRNA splicing (Table 4.15). The ten most upregulated genes were associated with metallopeptidase activity (CG5715), fatty acid metabolism (CG10131), phosphatase activity (CG9452), ATP hydrolysis coupled proton transport (CG31030), non-coding RNA (*MRE16*), a pseudogene (CR32207), ecdysteroid metabolic process (CG9521), sterol O-acetyltransferase activity (CG5397), odorant binding protein (*Obp99a*) and an uncharacterized gene with no predicted function (CG1552; Table 4.16). Next, we examined the 42 genes which were downregulated in the S populations with respect to the Fs at the WPP stage. This set was enriched for genes involved in catabolism (GO:9999056, 13 genes, $p<4.5 \times 10^{-3}$). These catabolic genes were associated with the proteasome (*Rpn2*, *Rpn5*, *Rpn6*, *Prosβ6*), alcohol dehydrogenase activity (*Adh*), lipid metabolism and TG mobilization (*bmm*), ubiquitin dependent proteolysis (*Usp14*), glycolytic processes (*Ald*), glycoside catabolic process and bacterial defense (*Fuca*), transcriptional regulator of lipid biosynthesis (*SREBP*), cellular response to oxidative stress and catabolism of misfolded proteins (*Lon*), glycerol-4-phosphate metabolism (*Gdph*) and fatty acid β-oxidation (*Acox57D-p*; Table 4.17). We then examined the 10 most downregulated genes. They were associated with alcohol dehydrogenase activity (*Adh*), body morphogenesis (*TwdlG*), G-protein coupled acetylcholine receptor signaling (*mAchR-B*), transcriptional regulation of defense response to fungus (*Lmpt*), 3-hydroxyacyl-CoA dehydrogenase (CG9914), ABC-

transport like protein (CG31793), DNA methylation (*Ipod*), transmembrane transport (CG12194 and *Mctp*) and iron ion homeostasis (*Mco1*; Table 4.16).

4.5 Discussion

When populations of *D. melanogaster* are laboratory selected for starvation resistance, they adapt by delaying development to extend larval feeding time (Reynolds 2013). The extra feeding allows for greater accumulation of lipids in the larval fat body. Lipids stored within the larval fat body are carried into the adult fly where they play an important role in adult starvation resistance (Aguila et al. 2007). We are interested in understanding the mechanistic basis of the developmental delay as well as the physiology of the larval fat body in response to selection. Our preliminary data led us to hypothesize that the timing of 20E signaling was delayed in our starvation-selected populations (Reynolds 2013). If the 20E signal is simply delayed by ~24 hours in the S populations, we predicted that the transcriptomic profiles of the F and S populations should be similar during and after the late-larval 20E pulse.

To test this hypothesis we analyzed genome-wide RNA expression patterns between the F and S populations, during and after the onset of pupariation. This developmental window is known to be regulated by a late-larval pulse of the steroid hormone ecdysone which promotes differential gene expression in responding tissues. We found large-scale changes in gene expression between samples collected at the 3IN and WPP, with a total of 1,788 differentially expressed genes. This large set of genes with similar expression between the F and S populations supports our prediction and suggests that the developmental delay is due to a delay in 20E signaling. However, we also found 168 genes that were differentially expressed in response to selection and 477 with a significant selection by development interaction term. These sets of genes suggest that the S larval fat body has adapted mechanisms to alter its response to 20E signaling.

The 1,788 genes with altered expression by development were much higher than the 168 identified by selection or the 477 by the interaction between selection and development. This could suggest that development had a higher impact on gene expression than selection. However, it is important to note that the increased variability between the replicate S populations likely reduced the total number of candidates reaching significance by selection. While here we limited the analysis to the most conserved changes in gene expression across replicates, future studies can probe for differences between the replicate populations.

Many of the genes whose expression was altered by development were associated with protein metabolism. This included the upregulation for many genes involved in proteasome structure and function, as well as the downregulation of genes involved in ribosome biogenesis, protein processing and export. Results from other studies support the idea that these processes may be regulated by 20E. For example, proteasomal gene expression is 20E-inducible in other larval tissues in *Drosophila* (Li and White 2003). Furthermore, proteasome activity during metamorphosis has been associated with programmed cell death of larval tissues in *Bombyx mori* (Jia et al. 2007). Genes associated with ribosome biogenesis may also be 20E-induced, as 20E has been shown to downregulate *Myc*; a transcription factor important in ribosome biogenesis (Delanoue et al. 2010). *Myc* expression was also found to be downregulated here in response to development ($\log_2$-fold change of -1.45, $p<3.9 \times 10^{-7}$, Appendix D).

We also found enrichment for genes associated with immune response and starvation within the developmentally regulated gene set. These findings are similar to other studies of whole-body gene expression during pupariation in *Drosophila* (Barnett et

al. 1990; Beckstead et al. 2005). The up-regulation of immune-defense genes in response to 20E is hypothesized to increase protection for the pupa as it enters a compromised state during metamorphosis (Regan et al. 2013). Genes associated with starvation were downregulated in the WPP samples and primarily associated with ribosome biogenesis. However, several of these genes are also regulated by Tor signaling and associated with cell growth and division (*l(2)k09022*, CG11920, CG12301, *l(1)G0020*, *Nop60B*, *NHP2*, data not shown).

Surprisingly, development led to reduced expression of several *Sgs* genes which are typically expressed in the salivary glands (Li and White 2003). Due to their high expression and secretion from the salivary gland during pupariation, it is possible that these are artifacts derived from sample preparation. However, several *Sgs* genes have been previously identified in a screen for genes that are positively regulated by the insulin signaling pathway in the *Drosophila* fat body (L.P. Musselman, personal communication). Furthermore, 9 of the genes we identified as differentially expressed in response to selection were also identified in this insulin pathway screen (CG30463, *P58IPK*, *aralar1*, CG10814, *Cyp9b1*, *TotC*, CG15879, CG4335, *Victoria*; L.P. Musselman, personal communication). Interestingly, all of these genes except for *P58IPK* and *aralar1*, were included in the top 10 most up- or dowregulated lists, and many of them do not have previously characterized function.

Overall, there were fewer genes that were differentially regulated in response to selection compared to developmental stage. This gene set was also not enriched for any pathways or Gene Ontology categories. However, by breaking the set of 168 genes into groups based on the pattern of expression during development, we were able to provide

context for how these genes may respond to 20E. For example, we found a subset of genes that were differentially expressed in response to selection, but did not change in response to development. These genes are likely not 20E-induced, and may represent the activity of other pathways that alter the physiology of the S larval fat body. Genes within this group were associated with many processes such as chitin binding, immune defense and ecdysteroid metabolism (Table 4.5). Chitin is an integral component of the extracellular matrix, and it must be properly regulated during tissue remodeling throughout development (Dong et al. 2014). 20E induces the expression of enzymes which degrade the extracellular matrix of the larval fat body (Bond et al. 2011). This process leads to the dissociation of the larval fat body into individual cells. Our preliminary observations of the S larval fat body have found that it is not fully dissociated in the adult fly upon eclosion (Personal communication, N.D. Bond). This unique physiology could be indicative of incomplete or delayed response to 20E in the S larval fat body, and is now correlated with genes involved in extracellular matrix composition. Selection was also found to decrease the expression of some genes involved in immune defense. These genes have the potential to generate niche environments for different bacterial species. This is important, because certain bacterial species have been shown to control development and metabolism in *Drosophila* (Shin et al. 2011). These genes also correlate with our preliminary studies that have found differences in the microbiome of the S populations (J. Chaston, personal communication). Finally, the differential expression of genes involved in ecdysteroid metabolism could directly affect the levels of 20E within the fat body. The gene in question, CG9509, is predicted to function as an ecdysone oxidase, which metabolizes 20E into an inactive form (Takeuchi et al. 2005). If the S larval fat body is less responsive to 20E we

might predict CG9509 would be upregulated to reduce 20E levels, however we find that it is downregulated in the S larval fat body. Interestingly, we found several cytochrome P450 genes that were downregulated during development but upregulated in the S populations (Table 4.6). While cytochrome P450 genes may have diverse functions, some are known to be involved in ecdysone metabolism (Chung et al. 2009). Understanding if and how these genes influence ecdysone or 20E metabolism in the S larval fat body, may provide further insight into its physiology during development.

The *post-hoc* analysis of genes with a significant interaction term, demonstrated some important differences between the F and S populations at the WPP stage. Specifically we found that the S populations downregulated many genes involved in catabolism, including those involved with the proteasome and upregulated many genes involved with mitochondrial translation and the spliceosome. These were particularly interesting because we had previously observed that genes associated with the proteasome and ribosome biogenesis were downregulated in response to development (Table 4.3). The downregulation of genes involved in catabolic metabolism could explain how the S larval fat body retains lipids throughout metamorphosis. This set included genes like *brummer lipase* (*bmm*), which is associated with the lipid droplet and critical for TG mobilization (Grönke et al. 2005). In *Bombyx mori*, *bmm* is upregulated in the fat body during pupariation and associated with increased lipolysis (Wang et al. 2010). If catabolic genes such as *bmm* are downregulated during pupariation in the S populations, it could allow for higher retention of macromoleucles in the larval fat body.

Finding the upregulation of genes associated with the spliceosome in the S populations suggests the possibility of alternative splicing. It is possible that alternative

splicing could be driving different phenotypes in the S larval fat body as lipid metabolism in the fat body has been shown to be influenced by alternative splice variants of key regulatory genes (Gingras et al. 2014). Future analysis of differentially expressed, alternatively spliced transcripts should offer more insight into these possibilities.

The examples described above are not meant to provide explanations for how the S larval fat body differs from the Fs, but demonstrate how these results may drive hypotheses to be further explored. Overall, these data suggest that gene expression in the larval fat body is differentially regulated during pupariation in response to starvation-selection. Future studies may confirm and characterize the importance of the differentially expressed genes identified here as well as look into differences between the S populations and identify alternatively spliced transcripts.

4.6 Literature Cited

Aguila JR, Hoshizaki DK, Gibbs AG. 2013. Contribution of larval nutrition to adult reproduction in Drosophila melanogaster. J. Exp. Biol. 216:399–406.

Aguila JR, Suszko J, Gibbs AG, Hoshizaki DK. 2007. The role of larval fat cells in adult Drosophila melanogaster. J. Exp. Biol. 210:956–963.

Andersen DS, Colombani J, Léopold P. 2013. Coordination of organ growth: principles and outstanding questions from the world of insects. Trends Cell Biol. 23:336–344.

Andres AJ, Thummel CS. 1994. Methods for quantitative analysis of transcription in larvae and prepupae. In: Goldstein LSB, Fyrberg EA, editors. Drosophila melanogaster: Practical Uses in Cell and Molecular Biology. New York: Academic Press.

Barnett SW, Flynn K, Webster MK, Beckendorf SK. 1990. Noncoordinate expression of Drosophila glue genes: Sgs-4 is expressed at many stages and in two different tissues. Dev. Biol. 140:362–373.

Beckstead RB, Lam G, Thummel CS. 2005. The genomic response to 20-hydroxyecdysone at the onset of Drosophila metamorphosis. Genome Biol. 6:1–13.

Bond ND, Nelliot A, Bernardo MK, Ayerh MA, Gorski KA, Hoshizaki DK, Woodard CT. 2011. ßFTZ-F1 and Matrix metalloproteinase 2 are required for fat-body remodeling in Drosophila. Dev. Biol. 360:286–296.

Butterworth FM, Emerson L, Rasch EM. 1988. Maturation and degeneration of the fat body in the Drosophila larva and pupa as revealed by morphometric analysis. Tissue Cell 20:255–268.

Chippindale AK, Chu TJF, Rose MR. 1996. Complex Trade-Offs and the Evolution of Starvation Resistance in Drosophila melanogaster. Evolution 50:753.

Chung H, Sztal T, Pasricha S, Sridhar M, Batterham P, Daborn PJ. 2009. Characterization of Drosophila melanogaster cytochrome P450 genes. Proc. Natl. Acad. Sci. 106:5731–5736.

Delanoue R, Slaidina M, Léopold P. 2010. The Steroid Hormone Ecdysone Controls Systemic Growth by Repressing dMyc Function in Drosophila Fat Cells. Dev. Cell 18:1012–1021.

Dong B, Miao G, Hayashi S. 2014. A fat body-derived apical extracellular matrix enzyme is transported to the tracheal lumen and is required for tube morphogenesis in Drosophila. Development 141:4104–4109.

Gingras RM, Warren ME, Nagengast AA, DiAngelo JR. 2014. The control of lipid metabolism by mRNA splicing in Drosophila. Biochem. Biophys. Res. Commun. 443:672–676.

Grönke S, Mildner A, Fellert S, Tennagels N, Petry S, Müller G, Jäckle H, Kühnlein RP. 2005. Brummer lipase is an evolutionary conserved fat storage regulator in Drosophila. Cell Metab. 1:323–330.

Harshman, Hoffmann, Clark. 1999. Selection for starvation resistance in Drosophila melanogaster : physiological correlates, enzyme activities and multiple stress responses. J. Evol. Biol. 12:370–379.

Jia S, Li M, Zhou B, Liu W, Zhang Y, Miao X, Zeng R, Huang Y. 2007. Proteomic Analysis of Silk Gland Programmed Cell Death during Metamorphosis of the Silkworm *Bombyx mori*. J. Proteome Res. 6:3003–3010.

Li T-R, White KP. 2003. Tissue-Specific Gene Expression and Ecdysone-Regulated Genomic Networks in Drosophila. Dev. Cell 5:59–72.

Love MI, Huber W, Anders S. 2014. Moderated estimation of fold change and dispersion for RNA-seq data with DESeq2. Genome Biol. [Internet] 15. Available from: http://genomebiology.com/2014/15/12/550

Lyne R, Smith R, Rutherford K, Wakeling M, Varley A, Guillier F, Janssens H, Ji W, Mclaren P, North P, et al. 2007. FlyMine: an integrated database for Drosophila and Anopheles genomics. Genome Biol. 8:R129.

Merkey AB, Wong CK, Hoshizaki DK, Gibbs AG. 2011. Energetics of metamorphosis in Drosophila melanogaster. J. Insect Physiol. 57:1437–1445.

Petryk A, Warren JT, Marqués G, Jarcho MP, Gilbert LI, Kahler J, Parvy J-P, Li Y, Dauphin-Villemant C, O'Connor MB. 2003. Shade is the Drosophila P450 enzyme that mediates the hydroxylation of ecdysone to the steroid insect molting hormone 20-hydroxyecdysone. Proc. Natl. Acad. Sci. U. S. A. 100:13773–13778.

R Core Team. 2015. R: A Language and Enviornment for Statistical Computing. Vienna, Austria: R Foundation for Statistical Computing Available from: http://www.R-project.org/

Regan JC, BrandÃ£o AS, LeitÃ£o AB, Mantas Dias ÃR, Sucena Ã, Jacinto A, Zaidman-RÃ©my A. 2013. Steroid Hormone Signaling Is Essential to Regulate Innate Immune Cells and Fight Bacterial Infection in Drosophila.Schneider DS, editor. PLoS Pathog. 9:e1003720.

Reynolds LA. 2013. The Effects of Starvation Selection on Drosophila Melanogaster Life History and Development. UNLV ThesesDissertationsProfessional Pap. Paper 1876.

Shin SC, Kim S-H, You H, Kim B, Kim AC, Lee K-A, Yoon J-H, Ryu J-H, Lee W-J. 2011. Drosophila Microbiome Modulates Host Developmental and Metabolic Homeostasis via Insulin Signaling. Science 334:670–674.

Takeuchi H, Rigden DJ, Ebrahimi B, Turner PC, Rees HH. 2005. Regulation of ecdysteroid signalling during *Drosophila* development: identification, characterization and modelling of ecdysone oxidase, an enzyme involved in control of ligand concentration. Biochem. J. 389:637–645.

Tyler MS. 2000. Developmental biology: a guide for experimental study. 2nd ed. Sunderland, Mass: Sinauer Associates

Wang S, Liu S, Liu H, Wang J, Zhou S, Jiang RJ, Bendena WG, Li S. 2010. 20-hydroxyecdysone Reduces Insect Food Consumption Resulting in Fat Body Lipolysis During Molting and Pupation. J. Mol. Cell Biol. 2:128–138.

Yamanaka N, Rewitz KF, O'Connor MB. 2013. Ecdysone Control of Developmental Transitions: Lessons from *Drosophila* Research. Annu. Rev. Entomol. 58:497–516.

Yang X, Li J, Lee Y, Lussier YA. 2011. GO-Module: functional synthesis and improved interpretation of Gene Ontology patterns. Bioinformatics 27:1444–1446.

Yin VP, Thummel CS. 2005. Mechanisms of steroid-triggered programmed cell death in Drosophila. Semin. Cell Dev. Biol. 16:237–243.

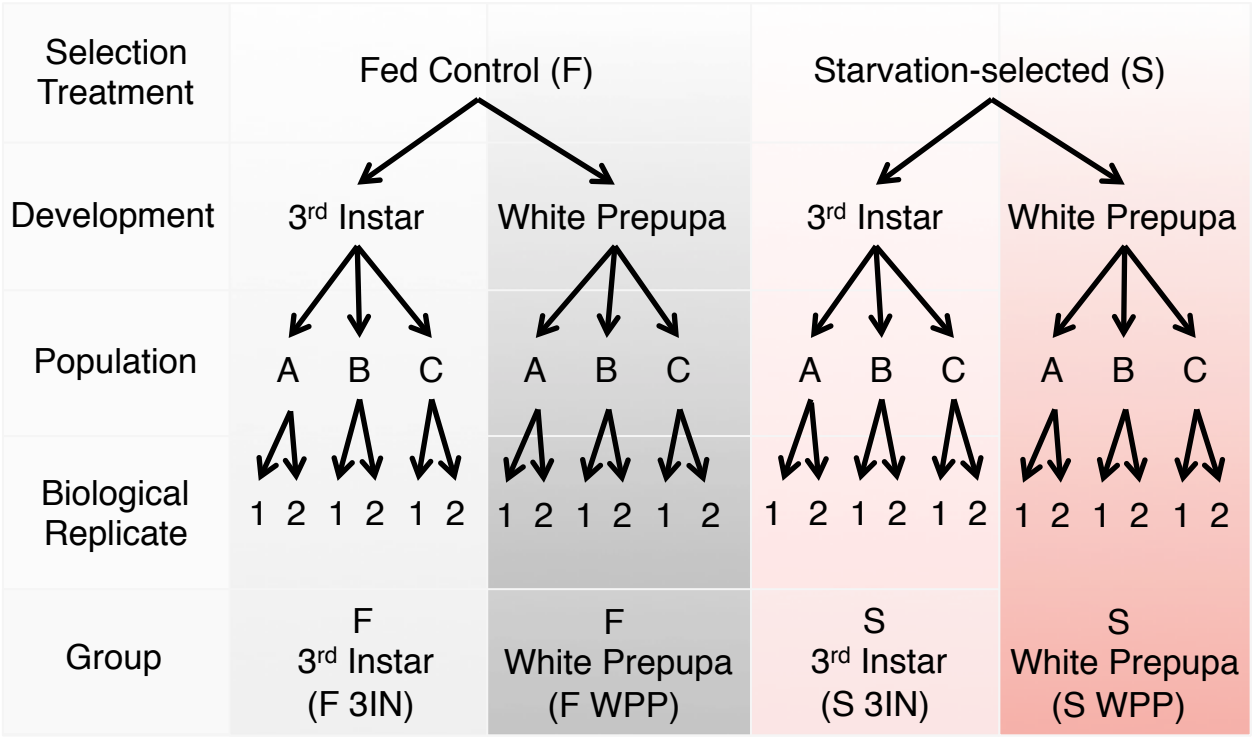

Figure 4.1. Experimental design. This diagram is an overview of the experimental design implemented in this study. Briefly, there were two laboratory selection treatments, the Fed Controls (F) and Starvation-selected (S). Each was sampled at two developmental timepoints, near the end of 3rd instar (3IN) or as a white prepupa (WPP). Each selection treatment has 3 evolutionary replicate populations (A, B and C). From each population, we sampled 2 pools of 15-25 dissected fat bodies. Each pool serves as a biological replicate. RNA was extracted from these samples and sequenced for analysis.

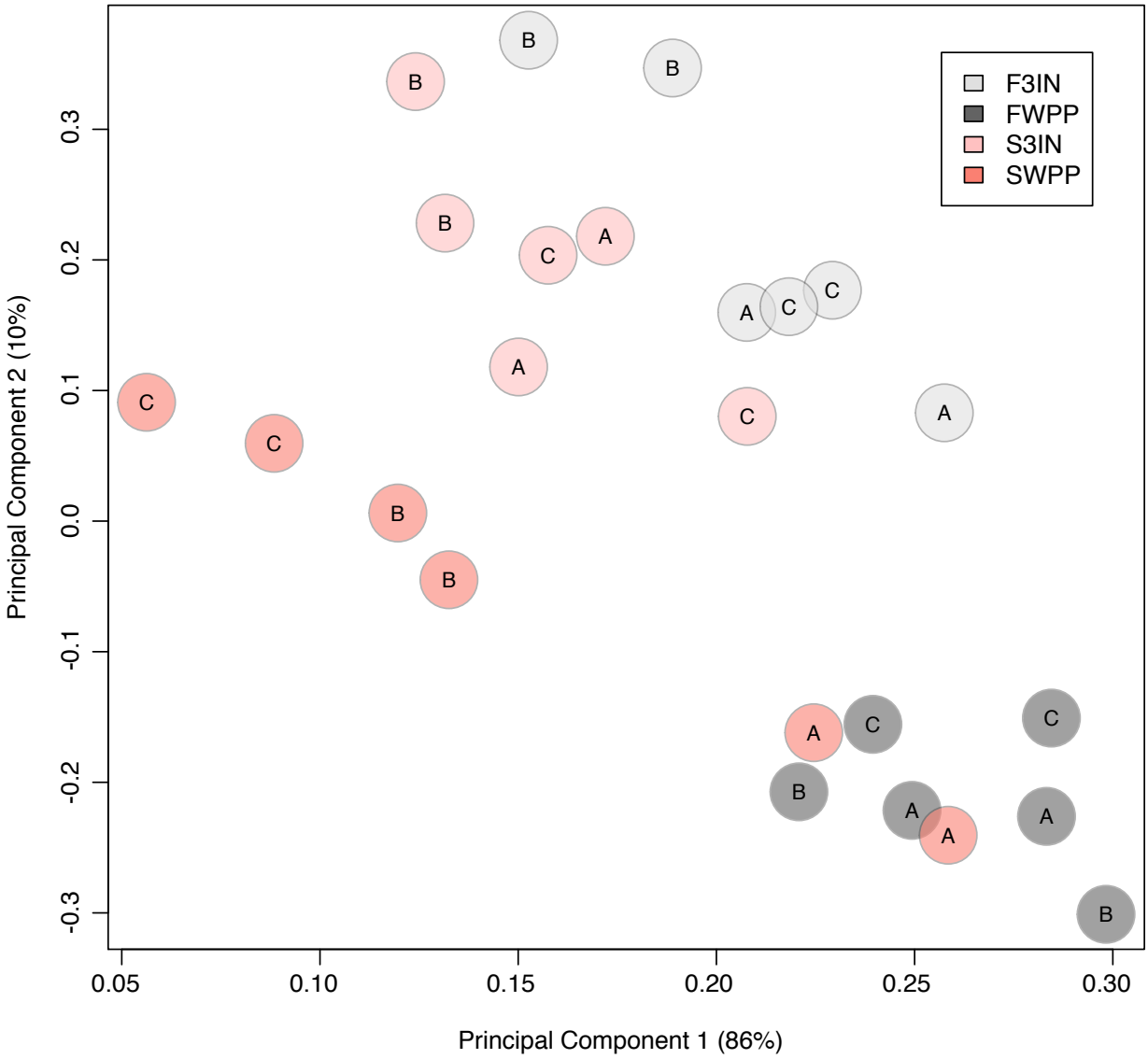

Figure 4.2. Principal Component Analysis of gene expression across all 24 populations. We plotted the first 2 principal components, which explain a combined ~96% of the variation in gene expression between populations. The colors represent the different selective treatments (Fed Control, F or Starvation-selected, S) at the different developmental timepoints (3IN, 3rd Instar or WPP, White prepua). The letters "A","B" and "C" signify the different replicate populations from the original selection experiment. Each group has 2 biological replicates from each population, which are both simply marked "A", "B" or "C" depending on their population of origin.

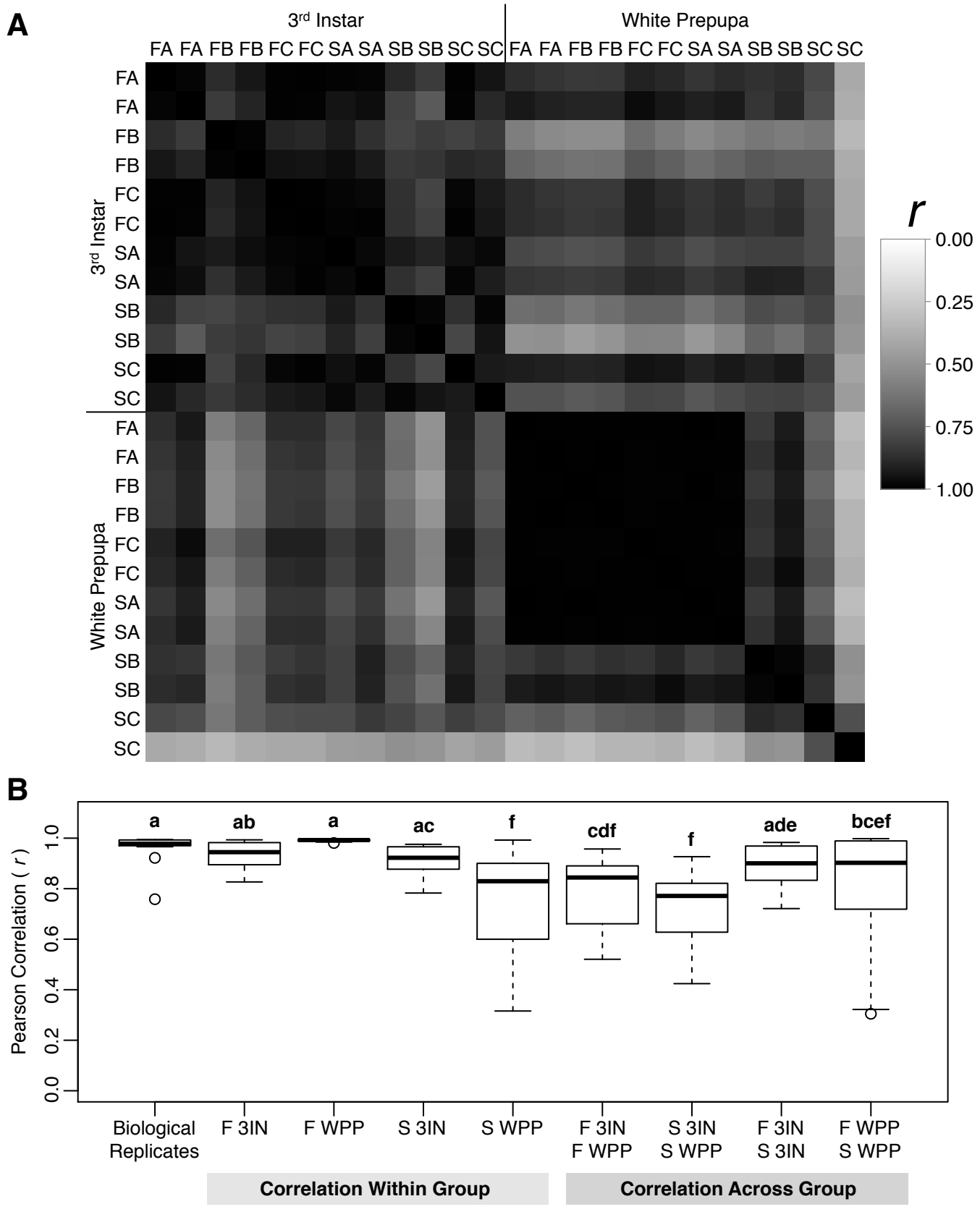

Figure 4.3. Pearson Product Moment Correlation in gene expression between groups. (A) Pairwise correlation diagram, where darker boxes signify a higher degree of correlation in gene expression between groups. (B) Average correlation of samples within and across major groups. Different letters signify significant differences between groups, $p<0.05$, ANOVA.

Table 4.1. Top 10 Up- and Downregulated Genes With a Significant Development Effect

Upregulated			
Gene	*FlyBase Accession*	*Log2 Fold Change*	*Adjusted p-value*
Eig71Eh	FBgn0014848	9.67	6.12E-07
CG8329	FBgn0036022	8.31	2.20E-04
Eig71Ei	FBgn0014849	8.18	2.42E-07
CG33998	FBgn0053998	7.76	2.63E-13
Eig71Ef	FBgn0004593	7.65	8.36E-12
CG18179	FBgn0036023	6.98	7.14E-07
CG43082	FBgn0262528	6.67	1.01E-06
CG42717	FBgn0261634	6.60	4.06E-11
CG45081	FBgn0266456	6.48	3.05E-11
CG31954	FBgn0051954	6.35	1.47E-04
Downregulated			
Gene	*FlyBase Accession*	*Log2 Fold Change*	*Adjusted p-value*
Sgs3	FBgn0003373	-8.25	1.07E-16
mag	FBgn0036996	-7.91	1.10E-05
Sgs1	FBgn0003372	-7.74	1.43E-11
CG14850	FBgn0038239	-7.74	4.09E-03
Jon74E	FBgn0023197	-7.49	2.77E-07
Sgs4	FBgn0003374	-7.45	1.03E-12
Npc2c	FBgn0037783	-7.31	2.59E-03
CG31698	FBgn0051698	-7.17	7.49E-08
CG13460	FBgn0036471	-7.08	5.75E-06
CG15404	FBgn0031512	-7.08	1.71E-09

Table 4.2. Protein Domain Enrichment for Genes With a Significant Development Effect

Upregulated			
Domain	*adj p*	*# of Genes*	*Accession*
Insect protein of unknown function	3.27E-07	9	IPR003475
Downregulated			
Domain	*adj p*	*# of Genes*	*Accession*
Cytochrome P450, conserved site	1.88E-06	27	IPR017972
Cytochrome P450	2.07E-05	27	IPR001128
Cytochrome P450, E-class, group I	5.32E-04	23	IPR002401
Peptidase M13	9.63E-03	12	IPR000718
Immunoglobulin E-set	2.18E-02	19	IPR014756

Table 4.3. Gene Ontology Enrichment for Genes With a Significant Development Effect

Upregulated			
GO Category	*Adjusted p-value*	*# of Genes*	*Accession*
defense response	1.50E-04	42	GO:0006952
response to bacterium	4.44E-04	30	GO:0009617
proteolysis	1.10E-02	65	GO:0006508
Downregulated			
GO Category	*Adjusted p-value*		*Accession*
protein targeting to membrane	2.05E-06	15	GO:0006612
single-organism transport	2.57E-05	190	GO:0044765
system development	4.86E-05	269	GO:0048731
ribosome biogenesis	1.34E-04	25	GO:0042254
hemolymph coagulation	2.94E-04	9	GO:0042381
neurogenesis	3.28E-04	179	GO:0022008
protein localization to endoplasmic reticulum	1.94E-03	11	GO:0070972
cellular response to external stimulus	2.45E-03	27	GO:0071496
response to starvation	2.60E-02	32	GO:0042594
rRNA metabolic process	4.68E-02	15	GO:0016072

Table 4.4. Pathway Enrichment for Genes with a Significant Development Effect

Upregulated		
Pathway	*adj p*	*# of Genes*
Proteasome	1.40E-04	13
Dectin-1 mediated noncanonical NF-kB signaling	5.76E-04	14
NIK-->noncanonical NF-kB signaling	5.76E-04	14
Cross-presentation of soluble exogenous antigens (endosomes)	1.10E-03	12
AUF1 (hnRNP D0) binds and destabilizes mRNA	1.38E-03	12
Regulation of ornithine decarboxylase (ODC)	2.15E-03	12
Degradation of GLI1 by the proteasome	2.15E-03	12
SCF-beta-TrCP mediated degradation of Emi1	2.97E-03	13
Antigen processing: Ubiquitination & Proteasome degradation	2.97E-03	13
CDK-mediated phosphorylation and removal of Cdc6	3.25E-03	12
Regulation of RAS by GAPs	3.97E-03	12
Ubiquitin-dependent degradation of Cyclin D1	3.97E-03	12
Activation of NF-kappaB in B cells	4.25E-03	13
FCERI mediated NF-kB activation	5.06E-03	13
Degradation of AXIN	5.84E-03	12
Ubiquitin Mediated Degradation of Phosphorylated Cdc25A	5.84E-03	12
CLEC7A (Dectin-1) signaling	6.00E-03	13
Asymmetric localization of PCP proteins	7.02E-03	12
Degradation of DVL	7.02E-03	12
Downstream TCR signaling	7.08E-03	13
Hedgehog ligand biogenesis	1.01E-02	12
GLI3 is processed to GLI3R by the proteasome	1.15E-02	13
Degradation of beta-catenin by the destruction complex	2.12E-02	13
APC/C:Cdc20 mediated degradation of Securin	4.31E-02	12
Autodegradation of Cdh1 by Cdh1:APC/C	4.98E-02	12
Separation of Sister Chromatids	4.98E-02	12
Downregulated		
Domain	*adj p*	*# of Genes*
Protein processing in endoplasmic reticulum	3.40E-06	35
Ribosome biogenesis in eukaryotes	1.25E-03	24
Protein export	1.74E-02	10

Table 4.5. Top 10 Up- and Downregulated Genes With a Significant Selection Effect and Non-significant Development Effect

Top 10 Upregulated Genes

Gene	*FlyBase Accession*	*Log2 Fold Change*	*Adjusted p-value*
CG10814	FBgn0033830	6.41	4.58E-16
CG14692	FBgn0037836	6.25	4.55E-08
CR45194	FBgn0266704	5.13	3.25E-17
inaD	FBgn0001263	5.04	1.10E-02
LManVI	FBgn0032069	5.03	1.84E-07
dpr4	FBgn0053512	4.79	4.29E-06
GstD2	FBgn0010038	4.35	1.43E-05
CG31326	FBgn0051326	4.28	1.18E-03
CR44077	FBgn0264886	4.22	2.12E-02
CR45469	FBgn0267025	3.91	2.41E-02

Top 10 Downregulated Genes

Gene	*FlyBase Accession*	*Log2 Fold Change*	*Adjusted p-value*
Victoria	FBgn0053117	-4.73	2.83E-05
CG10725	FBgn0036362	-3.75	2.41E-03
CG14357	FBgn0038204	-3.63	3.67E-02
CG7567	FBgn0039670	-3.48	3.03E-03
CG10405	FBgn0038431	-2.77	3.36E-03
TotC	FBgn0044812	-2.32	3.61E-02
CG9509	FBgn0030594	-2.31	3.92E-04
CG34034	FBgn0054034	-2.20	3.09E-02
Ir76a	FBgn0260874	-2.19	1.42E-05
CR43166	FBgn0262722	-2.14	6.80E-03

Figure 4.4. Example Expression Profiles for Genes With a Significant Selection Effect and Non-Significant Development Effect

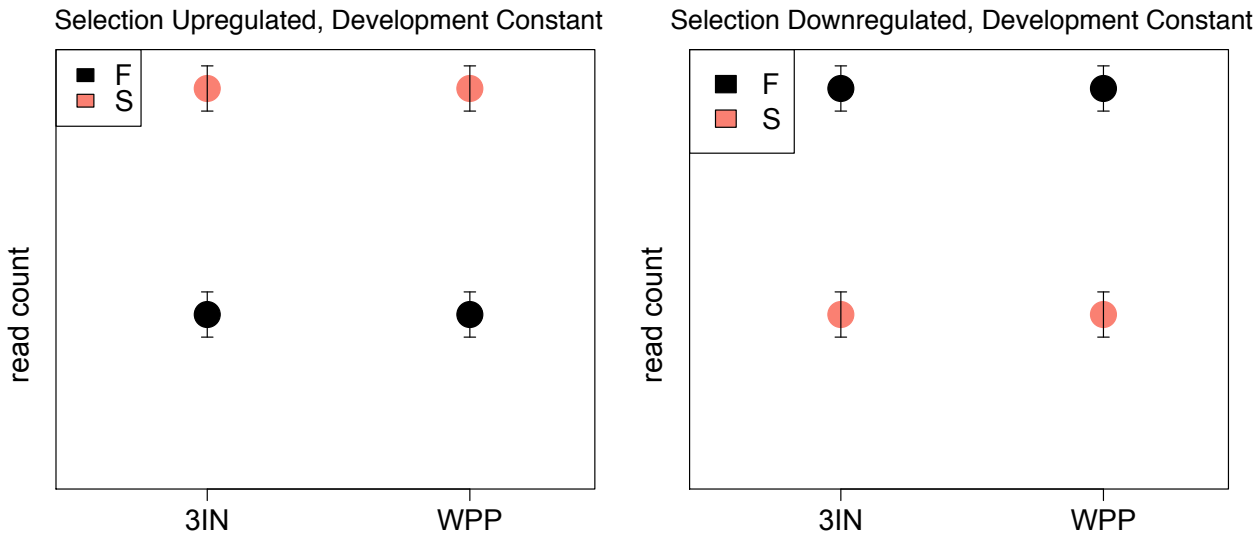

Table 4.6. Top 10 Up- and Downregulated Genes With a Significant Selection Effect and Downregulated Gene Expression in Response to Development

Top 10 Upregulated Genes			
Gene	*FlyBase Accession*	*Log2 Fold Change*	*Adjusted p-value*
Cyp4e3	FBgn0015035	3.95	3.97E-03
CG10073	FBgn0034440	2.14	6.90E-03
Cyp4ad1	FBgn0033292	2.12	2.16E-09
Cyp9b1	FBgn0015038	2.04	2.31E-04
cpx	FBgn0041605	1.97	1.10E-02
CG15879	FBgn0035309	1.80	9.83E-04
GstE3	FBgn0063497	1.69	2.54E-02
CG4335	FBgn0038795	1.46	3.20E-02
sel	FBgn0263260	1.44	1.83E-05
Cyp28a5	FBgn0028940	1.42	2.38E-02
Top 10 Downregulated Genes			
Gene	*FlyBase Accession*	*Log2 Fold Change*	*Adjusted p-value*
Muc96D	FBgn0051439	-3.91	1.78E-02
lin-28	FBgn0035626	-3.57	6.45E-04
CG11313	FBgn0039798	-3.33	1.41E-08
CR44510	FBgn0265703	-3.10	4.55E-08
GstE7	FBgn0063493	-2.58	4.26E-04
mthl15	FBgn0051720	-2.10	7.12E-03
Gat	FBgn0039915	-2.05	1.91E-07
CG34291	FBgn0085320	-1.84	2.37E-02
CG30463	FBgn0050463	-1.81	6.98E-03
clumsy	FBgn0026255	-1.74	4.20E-02

Figure 4.5. Example Expression Profiles for Genes With a Significant Selection Effect and Significant Development Effect

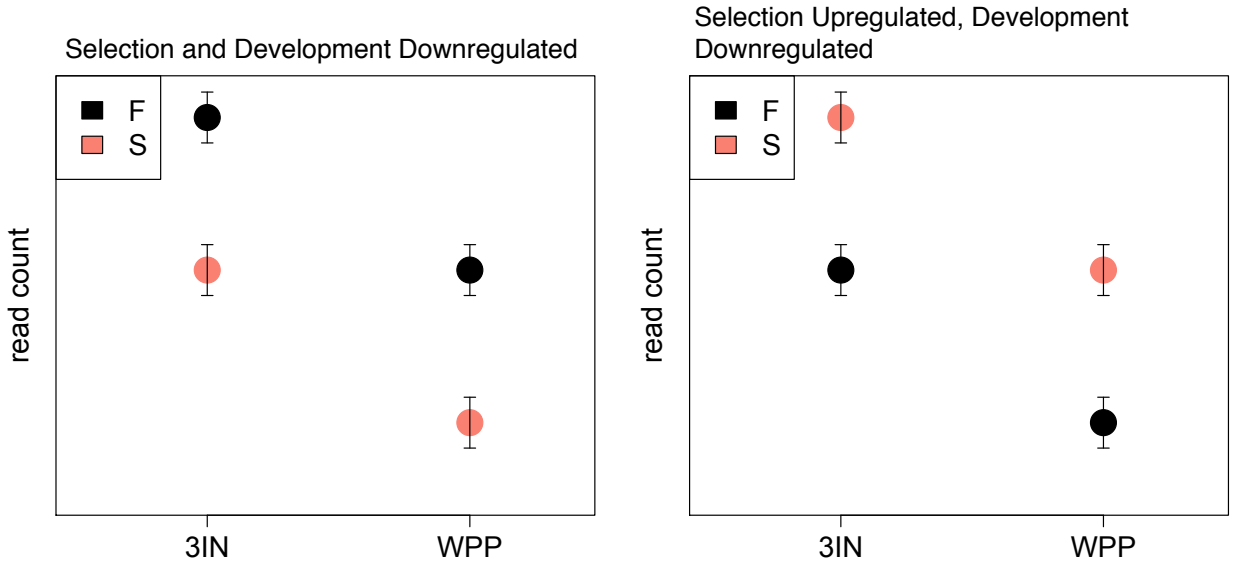

Table 4.7. Top 10 Up- and Downregulated Genes With a Significant Selection Effect and Upregulated Gene Expression in Response to Development

Top 10 Upregulated Genes			
Gene	*FlyBase Accession*	*Log2 Fold Change*	*Adjusted p-value*
CG8299	FBgn0034052	4.39	6.09E-06
CG42711	FBgn0261628	2.42	2.29E-02
CG31777	FBgn0051777	2.13	3.97E-02
Tsp42Ed	FBgn0029507	1.00	1.99E-02
PHGPx	FBgn0035438	0.88	9.11E-03
CG11257	FBgn0034442	0.73	2.41E-02
Top 10 Downregulated Genes			
Gene	*FlyBase Accession*	*Log2 Fold Change*	*Adjusted p-value*
CG11406	FBgn0034990	-4.07	3.60E-02
PGRP-SB1	FBgn0043578	-3.84	4.86E-10
CG12133	FBgn0033469	-3.72	2.47E-03
CG30287	FBgn0050287	-2.85	1.94E-06
CG42876	FBgn0262150	-1.85	3.23E-02
CG30088	FBgn0050088	-1.66	3.14E-02
Rgk1	FBgn0264753	-1.48	2.17E-02
CG42817	FBgn0261999	-1.40	1.10E-02
Swip-1	FBgn0032731	-1.39	1.10E-02
Ppa	FBgn0020257	-0.95	3.56E-02

Figure 4.6. Example Expression Profiles for Genes With a Significant Selection Effect and Significant Development Effect

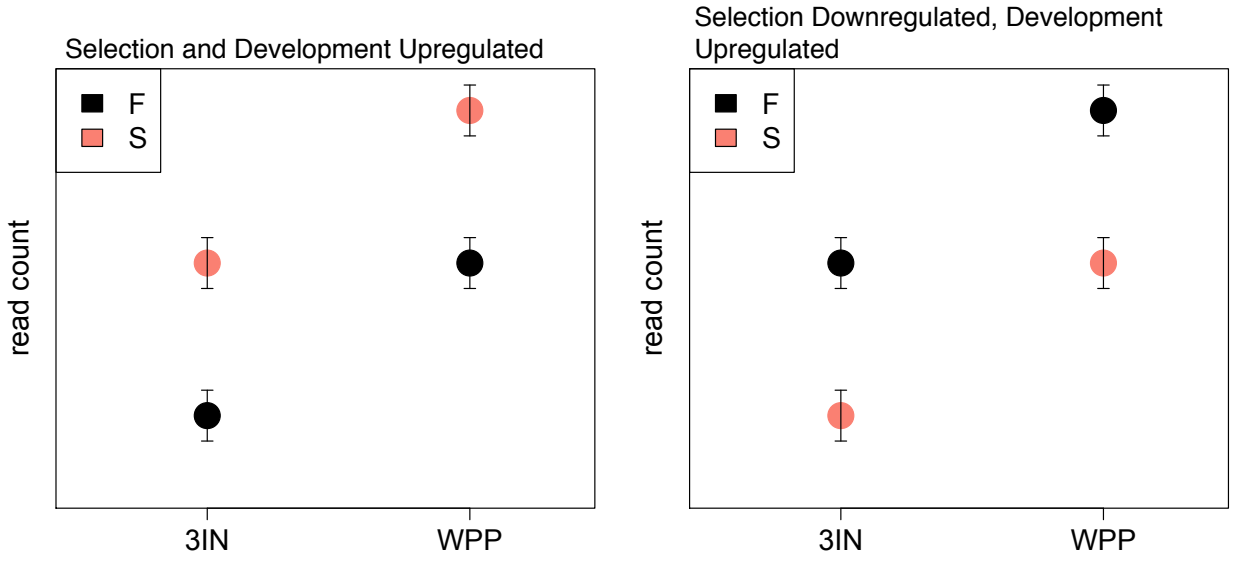

Table 4.8. Top 10 Up- and Downregulated Genes in S 3IN Compared to F 3IN

Upregulated			
Gene	*FlyBase Accession*	*Log2 Fold Change*	*Adjusted p-value*
CG5715	FBgn0039180	7.57	8.96E-20
CG14961	FBgn0035439	1.90	5.60E-04
ATPCL	FBgn0020236	1.65	1.87E-11
iPLA2-VIA	FBgn0036053	1.36	1.31E-06
Downregulated			
Gene	*FlyBase Accession*	*Log2 Fold Change*	*Adjusted p-value*
CG5084	FBgn0034288	-4.32	3.15E-04
CG5767	FBgn0034292	-3.88	3.03E-03
CG9682	FBgn0039760	-3.67	9.67E-04
CG31516	FBgn0051516	-3.50	1.01E-02
CG5770	FBgn0034291	-3.37	1.11E-02
Cda9	FBgn0034197	-3.12	2.70E-02
CG10140	FBgn0036363	-3.09	2.49E-03
obst-J	FBgn0036940	-3.03	2.84E-02
hoe2	FBgn0031649	-2.85	4.05E-03
ETHR	FBgn0038874	-2.73	2.93E-03

Table 4.9. Top 10 Up- and Downregulated Genes in F WPP Compared to F 3IN

Upregulated			
Gene	*FlyBase Accession*	*Log2 Fold Change*	*Adjusted p-value*
CG43133	FBgn0262607	2.53	8.74E-09
CG12194	FBgn0031636	2.08	4.81E-08
mAChR-B	FBgn0037546	1.98	5.02E-03
CG9914	FBgn0030737	1.96	7.88E-07
Mctp	FBgn0034389	1.92	1.99E-05
CG15145	FBgn0032649	1.87	1.71E-02
Mco1	FBgn0032116	1.72	1.54E-03
PIG-C	FBgn0035435	1.26	1.25E-05
Acox57D-p	FBgn0034628	1.20	2.22E-03
rdgBbeta	FBgn0027872	0.91	2.02E-02
Downregulated			
Gene	*FlyBase Accession*	*Log2 Fold Change*	*Adjusted p-value*
Sgs7	FBgn0003377	-4.86	5.04E-07
MFS9	FBgn0038799	-4.70	6.38E-09
CG5084	FBgn0034288	-4.54	9.42E-06
hoe2	FBgn0031649	-4.42	7.54E-09
Lcp3	FBgn0002534	-4.32	4.69E-06
ETHR	FBgn0038874	-4.25	9.46E-09
CG34279	FBgn0085308	-4.24	8.17E-06
CG5767	FBgn0034292	-3.89	2.96E-04
Sgs8	FBgn0003378	-3.78	2.90E-04
CG15068	FBgn0040733	-3.65	3.67E-05

Table 4.10. Pathway Enrichment for Differentially Expressed Genes in F WPP Compared to F 3IN

Upregulated Pathways	*adj p*	*Genes*
Proteasome	6.15E-03	4
Cross-presentation of soluble exogenous antigens (endosomes)	6.15E-03	4
AUF1 (hnRNP D0) binds and destabilizes mRNA	6.65E-03	4
Regulation of ornithine decarboxylase (ODC)	7.76E-03	4
Degradation of GLI1 by the proteasome	7.76E-03	4
CDK-mediated phosphorylation and removal of Cdc6	8.99E-03	4
Regulation of RAS by GAPs	9.66E-03	4
Ubiquitin-dependent degradation of Cyclin D1	9.66E-03	4
Degradation of AXIN	1.11E-02	4
Ubiquitin Mediated Degradation of Phosphorylated Cdc25A	1.11E-02	4
Asymmetric localization of PCP proteins	1.19E-02	4
Degradation of DVL	1.19E-02	4
Hedgehog ligand biogenesis	1.35E-02	4
SCF-beta-TrCP mediated degradation of Emi1	1.64E-02	4
Antigen processing: Ubiquitination & Proteasome degradation	1.64E-02	4
Dectin-1 mediated noncanonical NF-kB signaling	1.74E-02	4
NIK-->noncanonical NF-kB signaling	1.74E-02	4
Activation of NF-kappaB in B cells	1.85E-02	4
FCERI mediated NF-kB activation	1.96E-02	4
CLEC7A (Dectin-1) signaling	2.08E-02	4
Downstream TCR signaling	2.20E-02	4
APC/C:Cdc20 mediated degradation of Securin	2.33E-02	4
Autodegradation of Cdh1 by Cdh1:APC/C	2.46E-02	4
Separation of Sister Chromatids	2.46E-02	4
GLI3 is processed to GLI3R by the proteasome	2.59E-02	4
Orc1 removal from chromatin	2.89E-02	4
APC/C:Cdh1 mediated degradation of Cdc20 and other APC/C:Cdh1 targeted proteins in late mitosis/early G1	3.04E-02	4
Cdc20:Phospho-APC/C mediated degradation of Cyclin A	3.20E-02	4
Degradation of beta-catenin by the destruction complex	3.20E-02	4

Figure 4.7. Physical Interaction Network of Genes Unregulated in S WPP compared to S 3IN

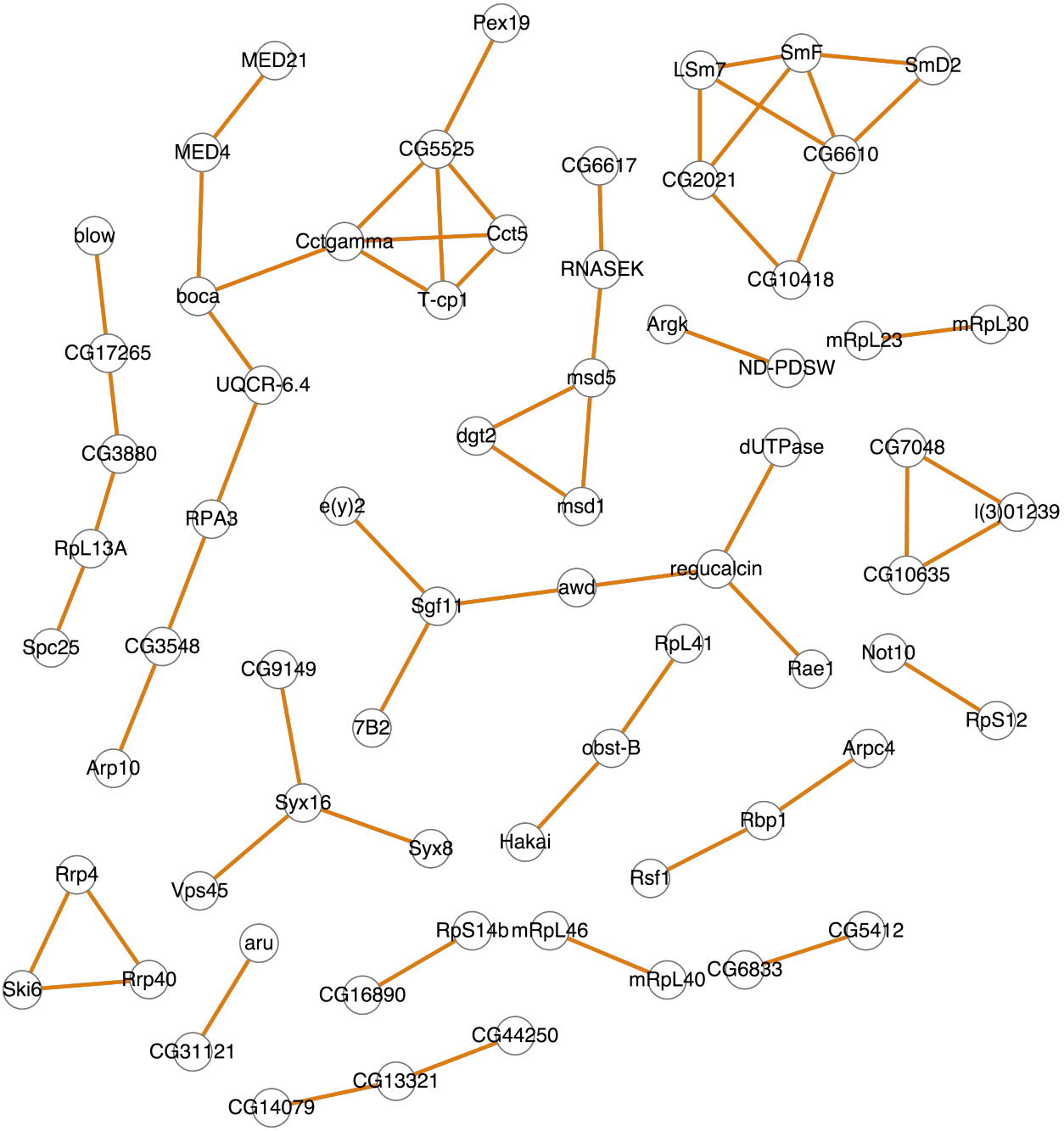

Table 4.11. Gene Ontology Enrichment for Genes in Physical Interaction Network (Figure 7)

Upregulated			
GO Category	*adj p*	*# of Genes*	*GO Accession*
mitotic spindle organization	6.26E-03	10	GO:0007052
cytoskeleton organization	1.38E-02	16	GO:0007010
protein folding	2.15E-02	7	GO:0006457
microtubule-based process	2.83E-02	14	GO:0007017
single-organism organelle organization	4.78E-02	21	GO:1902589

Table 4.12. Pathway Enrichment for Differentially Expressed Genes in S WPP compared to S 3IN

Upregulated

Pathways	*Adjusted p-value*	*# of Genes*
Mitochondrial translation elongation	6.15E-03	15
Mitochondrial translation termination	6.15E-03	15
mRNA Splicing - Minor Pathway	6.65E-03	10
RNA degradation	7.76E-03	9

Table 4.13. Top 10 Up- and Downregulated Genes in S WPP compared to S 3IN

Upregulated

Gene	*FlyBase Accession*	*Log2 Fold Change*	*Adjusted p-value*
CG9452	FBgn0036877	5.18	1.84E-09
Ag5r	FBgn0015010	4.67	1.06E-09
CG10131	FBgn0033949	4.37	1.53E-07
MRE16	FBgn0267910	4.26	1.06E-08
CG14946	FBgn0032405	4.16	1.51E-11
CG9689	FBgn0030159	3.96	4.11E-08
CG44250	FBgn0265185	3.89	1.85E-07
CR43957	FBgn0264617	3.85	1.58E-08
Arpc3B	FBgn0065032	3.82	4.10E-10
l(2)34Fc	FBgn0261534	3.71	1.31E-06

Downregulated

Gene	*FlyBase Accession*	*Log2 Fold Change*	*Adjusted p-value*
CG13795	FBgn0031937	-3.38	3.70E-26
CG5773	FBgn0034290	-2.99	2.44E-15
Adh	FBgn0000055	-2.94	5.16E-07
Cyp28d1	FBgn0031689	-2.81	4.84E-17
ATPCL	FBgn0020236	-2.58	1.02E-30
Ipod	FBgn0030187	-2.40	7.55E-04
AMPdeam	FBgn0052626	-2.13	5.09E-19
TwdlG	FBgn0037225	-2.12	2.97E-02
CG14961	FBgn0035439	-1.89	4.35E-05
Hsc70-3	FBgn0001218	-1.79	1.88E-05

Figure 4.8. Physical Interaction Network of Genes Unregulated in S WPP compared to F WPP

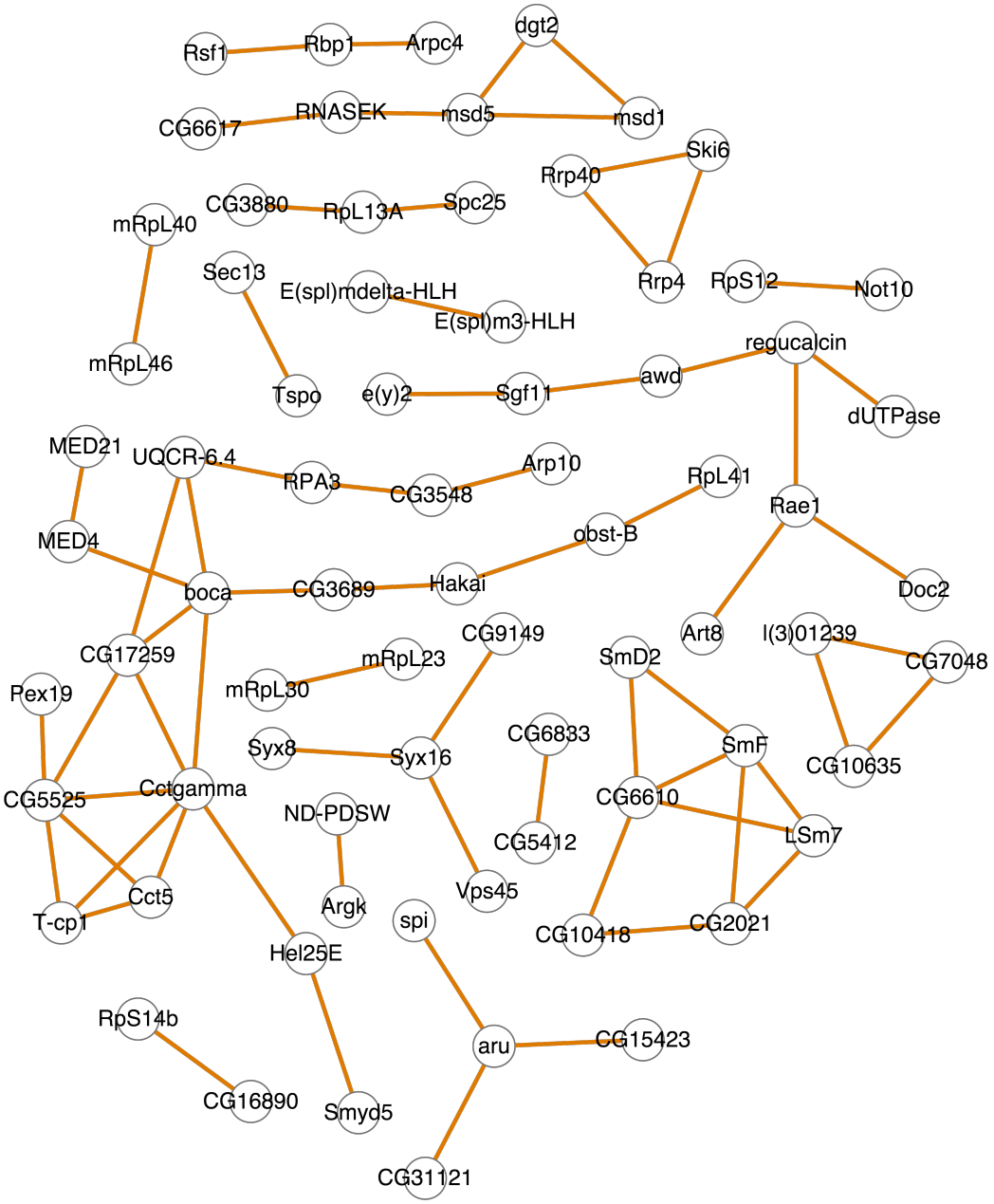

Table 4.14. Gene Ontology Enrichment for Genes in Physical Interaction Network (Figure 8)

Upregulated

GO Category	*Adj. p-value*	*# of Genes*	*GO Accession*
mitotic spindle organization	1.77E-03	11	GO:0007052
mRNA metabolic process	8.24E-03	12	GO:0016071
gene expression	1.21E-02	33	GO:0010467
microtubule-based process	1.84E-02	15	GO:0007017
single-organism organelle organization	1.93E-02	23	GO:1902589
cellular nitrogen compound metabolic process	3.25E-02	37	GO:0034641
protein folding	4.10E-02	7	GO:0006457

Table 4.15. Pathway Enrichment for Differentially Expressed Genes in S WPP compared to F WPP

Upregulated		
Pathways	*Adjusted p-value*	*# of Genes*
Mitochondrial translation elongation	4.34E-05	15
Mitochondrial translation termination	6.61E-05	15
mRNA Splicing - Minor Pathway	4.62E-03	10

Table 4.16. Top 10 Up- and Downregulated Genes in S WPP Compared to F WPP

Upregulated			
Gene	*FlyBase Accession*	*Log2 Fold Change*	*Adjusted p-value*
CG5715	FBgn0039180	4.68	2.07E-07
CG10131	FBgn0033949	4.65	2.07E-07
CG9452	FBgn0036877	4.24	1.16E-05
CG31030	FBgn0051030	3.99	9.64E-06
MRE16	FBgn0267910	3.96	1.14E-06
CR32207	FBgn0052207	3.83	2.26E-07
CG9521	FBgn0030588	3.65	2.65E-04
CG5397	FBgn0031327	3.55	7.61E-07
CG1552	FBgn0030258	3.55	9.41E-04
Obp99a	FBgn0039678	3.49	9.03E-05
Downregulated			
Gene	*FlyBase Accession*	*Log2 Fold Change*	*Adjusted p-value*
Adh	FBgn0000055	-3.01	1.98E-06
TwdlG	FBgn0037225	-2.98	2.25E-03
mAChR-B	FBgn0037546	-2.79	2.08E-04
Lmpt	FBgn0261565	-2.63	8.86E-29
CG9914	FBgn0030737	-2.19	2.17E-07
CG31793	FBgn0051793	-2.03	2.45E-07
Ipod	FBgn0030187	-1.77	2.98E-02
CG12194	FBgn0031636	-1.63	1.00E-04
Mctp	FBgn0034389	-1.61	8.17E-04
Mco1	FBgn0032116	-1.61	3.71E-03

Table 4.17. Catabolic Genes that are Downregulated in S WPP compared to F WPP

Downregulated	
Gene	*FlyBase Accession*
Rpn6	FBgn0028689
Rpn5	FBgn0028690
Rpn2	FBgn0028692
Adh	FBgn0000055
Prosbeta6	FBgn0002284
bmm	FBgn0036449
Usp14	FBgn0032216
Ald	FBgn0000064
Fuca	FBgn0036169
SREBP	FBgn0261283
Lon	FBgn0036892
Gpdh	FBgn0001128
Acox57D-p	FBgn0034628

CHAPTER 5

SUMMARY AND FUTURE DIRECTIONS

5.1 Overview of results and key findings

Here, I investigated the physiological and genetic basis of adaptation in populations of *Drosophila melanogaster* that were laboratory selected for starvation resistance. Previous work had found that the selected populations were obese and had reduced metabolism, poor locomotion as well as sleep and reproductive issues (Brewer, 2013; Masek et al., 2014; Reynolds, 2013). Many of these phenotypes are characteristic of metabolic disorder in mammals, which often correlates with heart disease (Poirier, 2006). I therefore hypothesized that heart function would be an evolutionary tradeoff with starvation resistance. We tested this hypothesis with the top techniques in the field. The first required a semi-intact surgical preparation followed by high-speed video microscopy and semi-optical heartbeat analysis (SOHA), and the other was an *in-vivo* imaging technique known as optical coherence tomography (OCT). Both studies found that the hearts of starvation-selected *Drosophila* were dilated and less contractile than the unselected controls, a condition known as dilated cardiomyopathy. We tested 3 competing hypotheses to investigate the mechanism of dysfunction: (1) Experimental evolution selected on alleles which directly impaired heart function; (2) selection had acted on alleles which increase lipid accumulation to levels where the excess adipose tissue physically impaired heart function; or (3) an imbalance in lipid homeostasis promoted ectopic lipid storage in the heart, leading to lipotoxicity and dysfunction. To test the first hypothesis I

performed rescue experiments where I fasted the selected populations either during larval development or as adults in order to reduce their total lipid levels to match the unselected controls. We predicted that if heart dysfunction were due to selection on alleles which directly impair the heart, then the rescue would have no effect on heart function. Alternatively if heart function improved in response to the rescue, this would suggest that there was nothing inherently wrong with the heart and dysfunction would be due to genetic factors associated with lipid homeostasis. We measured several heart parameters using SOHA and OCT and found that heart function was significantly improved in the rescued selected populations compared to their age-matched selected controls. In most cases heart function was not significantly different from the unselected controls, suggesting that there was nothing inherently wrong with the heart and that dysfunction was due to a fat-dependent mechanism. However, in some instances heart dysfunction was only partially rescued which could suggest that heart-specific alleles contribute to dysfunction. We tested the second hypothesis by performing histology and scoring for the presence of adipose tissue between the dorsal cuticle and the heart. I found that in many selected adults, the anatomical position of the heart was drastically altered and displaced away from the cuticle of the animal. The placement of the excess adipose tissue between the heart and the dorsal cuticle occurred at the attachment site of the heart tube to the dorsal cuticle through sets of alary muscles. Our observations suggest that these muscles were severely compromised, which contributed to dysfunction. Finally I explored the third hypothesis by measuring lipid content in surgically removed hearts. I found no evidence for increased lipids within the heart and further found no evidence for disrupted actin architecture which is highly correlated with ectopic lipid storage. We then hypothesized that the

selected populations had adapted by increasing the storage capacity of lipids within the fat body. I measured lipid droplets in the fat body and found that they were larger in the selected populations compared to the unselected controls. This increase was sufficient to account for the total lipid increase in the starvation-selected populations. In total these results strongly suggested that heart function is an evolutionary tradeoff to starvation resistance in the selected populations. We further found that dysfunction was highly correlated with physical interference of excess adipose tissue, although we could not completely rule out a heart-specific genetic defect contributing to the phenotype.

I next resequenced pools of genomic DNA from the selected populations and their unselected controls to explore the genetic basis of adaptation. Selection led to many genetic differences between the populations. We also found evidence for genetic heterogeneity between the selected populations, which provided the first example of non-parallel evolution in laboratory selected *D. melanogaster*. We found that the genetic differences between the replicate selected populations correlated with differences in starvation resistance. We analyzed genome-wide heterozygosity and found many signatures of selection that differed between populations and were consistent with a "hard" sweep model. These findings were also unprecedented in experimentally evolved populations of *Drosophila* and unique for selection in sexual species. Despite these interesting differences, we decided to look for consistent signals of selection across replicates. In order to discriminate between the effects of selection and genetic drift, we generated a novel algorithm to generate a distribution of allele frequencies that would be expected from genetic drift based on our experimental parameters. We applied this algorithm and found ~120,000 loci with differences in allele frequency that were consistent with selection.

These loci were mapped to a set of 1,453 genes that were involved in many processes associated with development, differentiation, growth and metabolism. We also found genes associated with many of the phenotypes that were previously measured in the selected populations. In total these findings present a unique model of adaptation and implicate many genes that may contribute to starvation resistance and its associated phenotypes.

Finally, we performed an RNA sequencing experiment on the larval fat body of the starvation-selected populations and their unselected controls during pupariation. Lipids stored in the larval fat body are an important source of fuel for adult starvation resistance in starvation-selected *Drosophila*. The larval fat body is typically remodeled during pupariation in response to the steroid hormone 20-hydroxyecdsyone (20E). Initial observations suggested that 20E signaling is delayed in the selected populations. We characterized the transcriptome of the larval fat body in late 3rd instar larvae and in white prepupae in both the selected populations and the unselected controls. A large number of genes has similar patterns of expression between the selected and unselected populations. However, we found many genes with differential expression in response to selection. These findings suggest that 20E signaling in the larval fat body is altered by selection. We also found differences in gene expression patterns among the replicate selected populations. We looked for the most consistent patterns across replicates and found that the selected populations upregulated genes associated with mitochondrial translation and the spliceosome, while downregulating many catabolic genes, including those associated with the proteasome in response to pupariation. These findings provide insight into the mechanistic basis of the developmental delay in the selected populations.

5.2 Future directions

Obesity-associated heart dysfunction

The results presented here provide a detailed characterization of heart function in starvation-selected *Drosophila melanogaster.* We explored some potential mechanisms of dysfunction, but there are many follow-up experiments and improvements in techniques, which can lead to a deeper understanding of the tradeoff. For example, the rescue experiments suggested that dysfunction was largely due to fat-dependent mechanisms, however they were not able to fully falsify the hypothesis that selection acted on alleles which directly disrupt the development or function of the heart. The possibility for selection on mal-adaptive heart alleles was further supported by the genome-wide analysis, which found alleles under selection associated with 32 genes that are known to impact heart development (Appendix C, $p < 1.8 \times 10^{-6}$). Because these genes are heavily associated with developmental signaling pathways, it would be interesting to test when heart dysfunction begins in the selected populations, then explore the role of the candidate genes in dysfunction at that timepoint. Because lipid levels in the selected lines do not surpass the levels in the unselected controls until the 3rd larval instar, heart function could be tested in 1st or 2nd instar larva, 3rd instar larva and again in young adult flies. These results could help identify if the heart is disrupted during embryogenesis, when the cardiac mesoderm is specified and heart tube is formed or in response to the increased lipid levels experienced during the 3rd larval instar, or during cardiac remodeling experienced throughout metamorphosis. The results of these experiments could lead to more informed hypotheses to probe the genetic basis of dysfunction.

While we found that the increased fat body tissue between the dorsal cuticle and the heart was correlated with dysfunction, there are further experiments which could help support this hypothesis. For instance, we could perform histology in the selected populations that were rescued through fasting to see if the heart returns to its normal placement on the dorsal cuticle after total lipids are returned to control levels. Furthermore, using OCT we could measure heart function, then immediately perform histology on the same animal to see if the level of dysfunction correlates with the level of fat between the heart and dorsal cuticle. We also believe based on our observations that the alary muscles are disrupted in response to the increased fat tissue, however we have not directly tested that hypothesis here. This hypothesis could be better explored by developing techniques to either directly measure the tension provided by these muscles, or characterize the cellular architecture in these cells to see if they are compromised.

I also spent a great deal of time attempting to measure lipid levels within the heart using Coherent Anti-stoke Raman Spectroscopy (CARS). CARS is a non-labeling imaging method which has been used to measure lipid levels in several intact tissues (Chien et al., 2010). We believe this would be a much more sensitive method to measure lipotoxicity in individual fly hearts, instead of measuring lipid levels in pools of dissected hearts as performed here. Further development of this method may provide a better way to test for lipotoxicity in general and also allow to explore individual variability of lipotoxicity within the population. Our preliminary tests were limited by the permeability of the dorsal cuticle, then economical factors led to the shut down of the facility before alternate preparations could be tested.

Genome-wide analysis

The first pass through the genome-wide dataset identified several unique characteristics of adaptation for starvation selection. Finding large sweeps which were inconsistent across replicates was very different from other published studies of laboratory adaptation in *Drosophila*. We were also able to identify many genes which were closely associated with loci under selection. Despite these interesting findings, there are many follow-up experiments that would expand the scope of these findings and help better characterize the genomic basis of adaptation.

Firstly, we can explore structural variation, including insertions and deletions as well as copy number variants between populations. Natural polymorphisms of small insertions or deletions have been identified in influencing starvation resistance phenotypes (Paaby et al., 2014). Identifying these in our populations may lead to the discovery of more genes that are associated with selection. It will also help us gain a better understanding of how selection may actually be altering the function of a given gene. Copy number variants of ribosomal RNA genes have been shown to be influenced by parental diet in *Drosophila* (Aldrich and Maggert, 2015). It is possible that the starvation-selection regime could impact copy number variation, which can be explored in future analyses.

We can also examine mitochondrial polymorphisms. Several mitochondrial SNPs have been shown to influence organismal-level phenotypes, including lipid content and starvation resistance (Aw et al., 2011). In my preliminary analyses I have already identified several mitochondrial SNPs at different frequencies between the starvation-selected lines and their unselected controls. Future studies will explore the potential of these SNPs in influencing starvation-resistant phenotypes in the selected populations.

In addition to these discovery-based experiments, we can also do work to expand on the genes that were associated with selection. 542 of the 1,453 candidate genes were not previously characterized in *Drosophila.* While all of the candidates are interesting in their own right, it would be interesting to functionally investigate these genes to explore their role in starvation-selected phenotypes. Because lipid content is a relatively simple assay to perform, the candidates could be knocked down in tissues known to be important in lipid metabolism and screened for lipid content. Genes which pass the preliminary screens can be further characterized with the purpose of finding novel genes in the regulation of lipid metabolism.

Further analysis is also warranted on the genetic differences between the replicate populations. It is interesting to note that the S_A population appears to share more genetic similarity with the unselected populations in both the genome-wide analysis and the transcriptome of the larval fat body. Despite appearing more genetically similar, the S_A population was found to be the most resistant to starvation. It will be interesting to explore the genetic basis of the population-level differences and understand what genetic networks are the most efficient in conferring starvation resistance, and which are associated with functional tradeoffs.

It is also important to follow up on the drift filter and develop it into a tool that can be easily accessible for others performing E&R studies. Future work can be done to assess how the assumptions of the input parameters affect the final results. It will be important to determine how different estimates for the population size and number of generations affect the final gene lists. It would also be interesting to test our algorithm against current statistical methods and see how the results are impacted. We can also perform tests to

optimize the FDR. We used an extremely conservative FDR of 1×10^{-5}, in part because we had so many divergent loci and we wanted to narrow the search. However, in doing so we may have filtered loci that were likely under selection. This could be part of the reason for the dissimilarity between the replicate populations on the SNP level. It would be interesting to test how a lower threshold would affect the number of overlapping SNPs between replicates.

Functional genomic analysis of the larval fat body during pupariation

One interesting finding from the transcriptomic analysis of the larval fat body in the starvation-selected populations was the upregulation of genes associated with the spliceosome in response to pupariation. These findings warrant a follow-up analysis to look for differentially expressed splice variants between the populations at the different developmental timepoints. Differential splice variants of several transcription factors can lead to large changes in expression in developing tissues (Venables et al., 2012). It is possible that genes which appear to have similar expression levels in the current analysis are differentially spliced across selection treatments which could have a significant impact on the physiology of the larval fat body.

There were also many genes with unknown function that were identified as being highly up- or downregulated in response to both development and selection. Analysis of these genes affords the opportunity to discover new genes that are 20E-regulated as well as those that are altered in response to selection. To narrow the search, future studies could start with uncharacterized genes that were found to be under selection in the genomic analysis and differentially regulated in the transcriptomic analysis. These genes

could be knocked down or overexpressed in the larval fat body and screened for their effects on phenotypes such as development time, lipid accumulation or larval fat body dissociation.

Future studies may also combine the genomic and transcriptomic datasets to investigate relationships between the selected loci and changes in expression patterns. We can perform promoter analyses to test if selection has altered the binding sites for transcription factors associated with the expression of genes identified in the differential expression analysis. Because regulatory elements may exist at great distances from their actual target, we can perform the promoter analysis at different windows up- and downstream from the transcriptional start site to look for any significant associations. We can also search for over-represented sequences in the promoters of differentially expressed genes to try to find novel transcription factor binding sites.

5.3 Literature Cited

Aldrich, J.C., Maggert, K.A., 2015. Transgenerational Inheritance of Diet-Induced Genome Rearrangements in Drosophila. PLOS Genet. 11, e1005148. doi:10.1371/journal.pgen.1005148

Aw, W.C., Correa, C.C., Clancy, D.J., Ballard, J.W.O., 2011. Mitochondrial DNA variants in Drosophila melanogaster are expressed at the level of the organismal phenotype. Mitochondrion 11, 756–763. doi:10.1016/j.mito.2011.06.012

Brewer, M.L., 2013. Kinematic analysis of axial rotations and the effects of stress selection on takeoff flight performance. ThesesDissertationsProfessional Pap. Paper 1806.

Chien, C.-H., Chen, W.-W., Tsai, M.-J., Chang∗, T.-C., 2010. Investigation of the Lipid Metabolism during Drosophila Larva Development by Coherent Anti-Stokes Raman Scattering (CARS) Microscopy. Biophys. J. 98, 397a. doi:10.1016/j.bpj.2009.12.2140

Masek, P., Reynolds, L.A., Bollinger, W.L., Moody, C., Mehta, A., Murakami, K., Yoshizawa, M., Gibbs, A.G., Keene, A.C., 2014. Altered regulation of sleep and feeding contributes to starvation resistance in Drosophila melanogaster. J. Exp. Biol. 217, 3122–3132. doi:10.1242/jeb.103309

Paaby, A.B., Bergland, A.O., Behrman, E.L., Schmidt, P.S., 2014. A highly pleiotropic amino acid polymorphism in the *Drosophila* insulin receptor contributes to life-history adaptation: ADAPTIVE POLYMORPHISM AT *InR*. Evolution 68, 3395–3409. doi:10.1111/evo.12546

Poirier, P., 2006. Obesity and Cardiovascular Disease: Pathophysiology, Evaluation, and Effect of Weight Loss: An Update of the 1997 American Heart Association Scientific Statement on Obesity and Heart Disease From the Obesity Committee of the Council on Nutrition, Physical Activity, and Metabolism. Circulation 113, 898–918. doi:10.1161/CIRCULATIONAHA.106.171016

Reynolds, L.A., 2013. The Effects of Starvation Selection on Drosophila Melanogaster Life History and Development. UNLV ThesesDissertationsProfessional Pap. Paper 1876.

Venables, J.P., Tazi, J., Juge, F., 2012. Regulated functional alternative splicing in Drosophila. Nucleic Acids Res. 40, 1–10. doi:10.1093/nar/gkr648

Table S3.1 Proportion of variance explained and coordinates for each principal component

	PC1	**PC2**	**PC3**	**PC4**	**PC5**	**PC6**
Standard Deviation	0.6316	0.3148	0.2647	0.1942	0.1574	0.1235
Proportion of Variance	0.6177	0.1534	0.1085	0.0584	0.0384	0.0236
Cumulative Proportion	0.6177	0.7711	0.8796	0.938	0.9764	1

Principal Component Coordinates

Population	**PC1**	**PC2**	**PC3**	**PC4**	**PC5**	**PC6**
FA	0.3475	-0.2736	0.1977	-0.0561	-0.8729	-0.0123
FB	0.368	-0.3603	0.3562	0.0619	0.3262	0.7054
FC	0.3653	-0.3589	0.3374	0.0844	0.3389	-0.7085
SA	0.4258	-0.3129	-0.8453	-0.0155	0.077	0.0106
SB	0.4547	0.4751	0.0755	-0.7431	0.0972	-0.0124
SC	0.4714	0.5855	0.0054	0.6583	-0.0371	0.0098

Figure S3.1 Pearson product-moment correlation coefficient Matrix of r values and significance values

A Pearson Correlation Matrix (*r*)

	FA	FB	FC	SA	SB	SC
FA	1.00	0.72	0.71	0.54	0.51	0.47
FB	0.72	1.00	0.82	0.50	0.48	0.45
FC	0.71	0.82	1.00	0.51	0.48	0.46
SA	0.54	0.50	0.51	1.00	0.45	0.45
SB	0.51	0.48	0.48	0.45	1.00	0.71
SC	0.47	0.45	0.46	0.45	0.71	1.00

B Pearson Correlation Matrix (*p*)

	FA	FB	FC	SA	SB	SC
FA	$2e^{-16}$	$2e^{-16}$	$2e^{-16}$	$2e^{-16}$	$2e^{-16}$	$2e^{-16}$
FB	$2e^{-16}$	$2e^{-16}$	$2e^{-16}$	$2e^{-16}$	$2e^{-16}$	$2e^{-16}$
FC	$2e^{-16}$	$2e^{-16}$	$2e^{-16}$	$2e^{-16}$	$2e^{-16}$	$2e^{-16}$
SA	$2e^{-16}$	$2e^{-16}$	$2e^{-16}$	$2e^{-16}$	$2e^{-16}$	$2e^{-16}$
SB	$2e^{-16}$	$2e^{-16}$	$2e^{-16}$	$2e^{-16}$	$2e^{-16}$	$2e^{-16}$
SC	$2e^{-16}$	$2e^{-16}$	$2e^{-16}$	$2e^{-16}$	$2e^{-16}$	$2e^{-16}$

A **Figure S3.2 Total number of 100KB blocks with < 0.05 heterozygosity.**

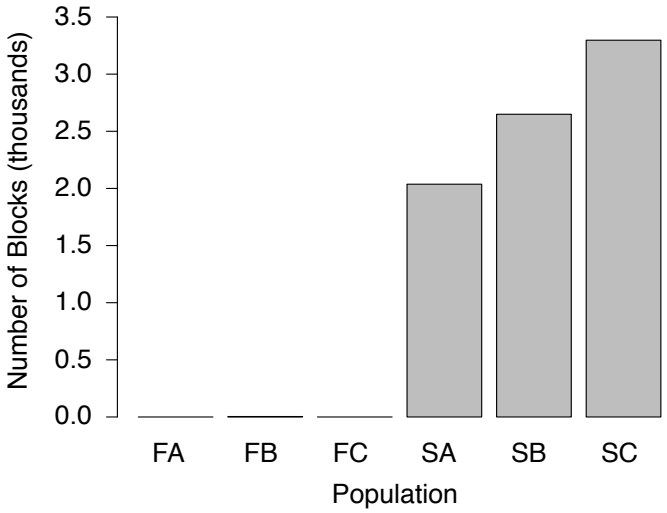

Table S3.2 List of genes in overlapping low heterozygosity windows

Name	Symbol	FlyBase Accession
Cytochrome P450-4g1	*Cyp4g1*	FBgn0010019
Protein O-mannosyltransferase 2	*tw*	FBgn0086368
Rab3 interacting molecule	*Rim*	FBgn0053547
Retinoblastoma-family protein	*Rbf*	FBgn0015799
Sec22 ortholog (S. cerevisiae)	*Sec22*	FBgn0260855
asense	*ase*	FBgn0000137
couch potato	*cpo*	FBgn0263995
ellipsoid body open	*ebo*	FBgn0266572
frizzled 3	*fz3*	FBgn0027343
lethal of scute	*l(1)sc*	FBgn0002561
pepsinogen-like	*pcl*	FBgn0011822
tincar	*tinc*	FBgn0261649
CG11663	uncharacterized	FBgn0029539
CG11664	uncharacterized	FBgn0040341
CG12347	uncharacterized	FBgn0038558
CG13358	uncharacterized	FBgn0026874
CG13359	uncharacterized	FBgn0025616
CG13360	uncharacterized	FBgn0025620
CG13373	uncharacterized	FBgn0029522
CG14634	uncharacterized	FBgn0040892
CG14635	uncharacterized	FBgn0029535
CG16989	uncharacterized	FBgn0025621
CG17801	uncharacterized	FBgn0038550
CG17802	uncharacterized	FBgn0038549
CG17803	uncharacterized	FBgn0038547
CG17806	uncharacterized	FBgn0038548
CG18012	uncharacterized	FBgn0038552
CG32816	uncharacterized	FBgn0052816
CG32817	uncharacterized	FBgn0052817
CG3713	uncharacterized	FBgn0040343
CG43445	uncharacterized	FBgn0263399
CG43867	uncharacterized	FBgn0264449
CG7357	uncharacterized	FBgn0038551
CR18166	uncharacterized	FBgn0029526
CR18275	uncharacterized	FBgn0029523
CR44469	uncharacterized	FBgn0265662

Figure S3.3 Comparison of drift threshold's obtained by Kimura algorithm versus Forward Simulation.

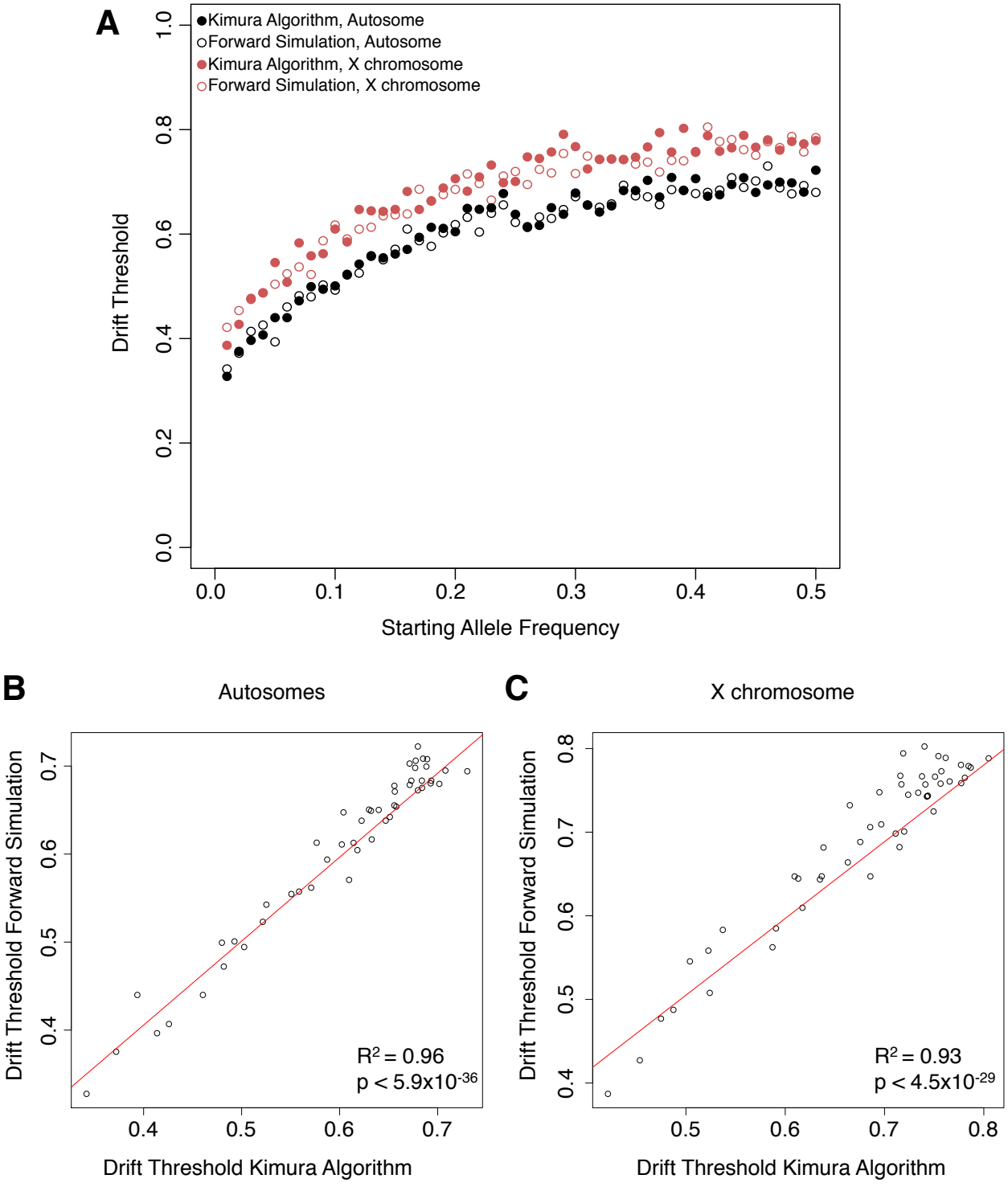

```
##### Estimate Ne #####

# Round the Favg to nearest 0.01
mafs[,FavgRound:=round(Favg,digits=2)]

# Loop over all starting allele frequencies from 0.01 to 0.5 and for each one compute the
variance of frequencies across all 3 replicates for all SNPs in that bin
# Store the results in a table
calculate.snp.variance <- function(data,chrType){
        if (chrType=="autosome"){data <- data[chr!="X",]}
        if (chrType=="x"){data <- data[chr=="X",]}
        snp.var<-data.frame(G0=numeric(), VAR=numeric())
        for(i in 1:50) {
                saf <- i/100
                saf.var <- var(unlist(data[FavgRound == saf,c("FA","FB","FC"),with=F]))
                snp.var[i,"G0"] <- saf
                snp.var[i,"VAR"] <- saf.var
        }
        return(as.data.table(snp.var))
}

# Equation 2 (Templeton, 2006)
estimate.Ne <- function(q0, t, obs.var) {
 x <- q0 * (1-q0)
 x <- obs.var / x
 x <- (1 - x) ** (1 / t)
 x <- 2 * (1 - x)
 x <- 1 / x
 return(x)
}

# Calculate variance and estimate effective population size for autosomes and x
chromsome
autosome.snp.var<-calculate.snp.variance(mafs,'autosome')
autosome.snp.var[,EstNe:=estimate.Ne(q0=G0, t=154, obs.var=VAR)]

x.snp.var<-calculate.snp.variance(mafs,'x')
x.snp.var[,EstNe:=estimate.Ne(q0=G0, t=154, obs.var=VAR)]

# Get medians - these tend to be robust to wonky estimates at the low starting allele
frequency
autosome.Ne <- median(autosome.snp.var$EstNe)
x.Ne <- median(x.snp.var$EstNe)
```

```
##### Use Equation 1 (Kimura, 1955), to generate a probability density function for
starting allele frequencies {0.01, 0.02 ... 0.50} #####

# Load package
require('rPython')

# kimuraDrift function takes p, Ne and t and returns area under distribution curve for each
value of x, requires python
kimuraDrift<-function(t,N,x,p){
# Supply all these input variables to python
python.assign("t",t)
python.assign("N",N)
python.assign("x",x)
python.assign("p",p)

python.exec(
"import scipy.special as ss
import math

def kimuraDrift(p):
        res=[0]*len(x)
        for i in range(1,51):
                a=p*(1-p)*i*(i+1)*((2*i)+1)
                b=ss.hyp2f1(1-i,i+2,2,p)
                c=math.exp((-i*(i+1)*float(t))/(4*float(N)))
                d=list()
                for xpos in x:
                        d.append(ss.hyp2f1(1-i,i+2,2,float(xpos))*a*b*c)
                res=[old + new for old, new in zip(res,d)]
        return(res)

out=list()
for i in p:
        out.append(kimuraDrift(float(i)))")

out<-python.get("out")
pdf<-do.call(cbind,out)
return(pdf)
}

# Input number of generations and effective population size
t<-154
x<-seq(0,1,length=1000)
```

```
p<-seq(0.01,0.5,by=0.01)

# Call kimuraDrift function
autosome.pdf<-kimuraDrift(t,autosome.Ne,x,p)
x.pdf<-kimuraDrift(t,x.Ne,x,p)

##### Use pdf to simulate drift and generate drift thresholdt #####

# The "realize" function, samples from the probability density function to realize n values
realize<-function(n,pval,chrType){
	if (chrType=="autosome"){data <- autosome.pdf}
	if (chrType=="x"){data <- x.pdf}
	pval<-which(p==pval)
	probs<-sapply(as.list(data[,pval]),function(x) abs(x))
	sample(x=x,size=n,prob=probs,replace=T)

}

# The "simulator" function calls the "realize" function to simulate user defined number of
"sims" for each population. It then creates a distribution of the absolute differences in allele
frequency and returns a user defined quantile value "quant".
simulator<-function(sims,pi,quant,chrType){
	cat(paste(pi,'\n',sep=""))
	FA<-realize(sims,pi,chrType)
	FB<-realize(sims,pi,chrType)
	FC<-realize(sims,pi,chrType)
	SA<-realize(sims,pi,chrType)
	SB<-realize(sims,pi,chrType)
	SC<-realize(sims,pi,chrType)

	Adiff<-abs(FA-SA)
	Bdiff<-abs(FB-SB)
	Cdiff<-abs(FC-SC)

	totDiff<-rbind(Adiff,Bdiff,Cdiff)

	return(quantile(totDiff,probs=c(quant)))
}

# Call the "simulator" function and return a data frame with drift threshold values for each
starting allele frequency. Specify the number of simulations and the desired quantile for the
drift threshold
number.of.simulations<-1e7
quantile.threshold<-0.99999

autosome.pi<-data.frame(pi=p)
```

```
autosome.pi$threshold<-apply(autosome.pi,1,function(x)
simulator(number.of.simulations,x[1],quantile.threshold,'autosome'))

x.pi<-data.frame(pi=p)
x.pi$threshold<-apply(x.pi,1,function(x)
simulator(number.of.simulations,x[1],quantile.threshold,'x'))
```

APPENDIX C. SUPPLEMENTARY GENE ONTOLOGY TABLE

Gene Ontology Terms	*GO Accession*	*p*
anatomical structure morphogenesis	GO:0009653	1.5E-36
organ development	GO:0048513	4.8E-34
organ morphogenesis	GO:0009887	1.1E-30
single-multicellular organism process	GO:0044707	5.4E-29
system development	GO:0048731	8.7E-29
post-embryonic organ development	GO:0048569	4.1E-27
multicellular organismal development	GO:0007275	7.1E-27
neuron differentiation	GO:0030182	7.2E-27
biological regulation	GO:0065007	1.2E-26
cell development	GO:0048468	1.6E-26
tissue morphogenesis	GO:0048729	2.1E-26
tube development	GO:0035295	3.4E-26
post-embryonic development	GO:0009791	1.2E-25
regulation of biological process	GO:0050789	2.0E-25
generation of neurons	GO:0048699	2.5E-25
morphogenesis of an epithelium	GO:0002009	5.5E-25
cellular component morphogenesis	GO:0032989	1.0E-24
locomotion	GO:0040011	1.4E-24
neuron development	GO:0048666	4.8E-24
metamorphosis	GO:0007552	5.9E-24
cell communication	GO:0007154	1.1E-23
instar larval or pupal morphogenesis	GO:0048707	1.7E-23
imaginal disc morphogenesis	GO:0007560	2.4E-23
post-embryonic organ morphogenesis	GO:0048563	2.4E-23
tube morphogenesis	GO:0035239	2.4E-23
imaginal disc development	GO:0007444	2.5E-23
post-embryonic morphogenesis	GO:0009886	4.6E-23
appendage morphogenesis	GO:0035107	7.0E-23
cell morphogenesis involved in differentiation	GO:0000904	1.0E-22
imaginal disc-derived appendage morphogenesis	GO:0035114	1.2E-22
regulation of multicellular organismal process	GO:0051239	1.9E-22
cell morphogenesis	GO:0000902	3.1E-22
instar larval or pupal development	GO:0002165	6.5E-22
post-embryonic appendage morphogenesis	GO:0035120	9.8E-22
cell morphogenesis involved in neuron differentiation	GO:0048667	3.0E-19
neuron projection morphogenesis	GO:0048812	4.0E-19
taxis	GO:0042330	4.3E-19
regulation of developmental process	GO:0050793	5.2E-19
signal transduction	GO:0007165	5.5E-19
neuron projection development	GO:0031175	7.4E-19

Gene Ontology Terms	*GO Accession*	*p*
axon development	GO:0061564	8.1E-19
axonogenesis	GO:0007409	9.1E-19
nervous system development	GO:0007399	1.5E-18
cell part morphogenesis	GO:0032990	5.9E-18
response to stimulus	GO:0050896	1.4E-17
imaginal disc-derived wing morphogenesis	GO:0007476	1.4E-17
cell projection morphogenesis	GO:0048858	3.1E-17
wing disc morphogenesis	GO:0007472	4.8E-17
behavior	GO:0007610	4.8E-17
wing disc development	GO:0035220	8.4E-17
chemotaxis	GO:0006935	2.4E-16
cell surface receptor signaling pathway	GO:0007166	1.3E-15
regulation of multicellular organismal development	GO:2000026	5.4E-15
axon guidance	GO:0007411	1.2E-14
sensory organ development	GO:0007423	1.2E-14
single-organism behavior	GO:0044708	4.9E-14
pattern specification process	GO:0007389	7.4E-14
compound eye morphogenesis	GO:0001745	2.3E-13
eye morphogenesis	GO:0048592	3.3E-13
sensory organ morphogenesis	GO:0090596	3.3E-13
eye development	GO:0001654	4.0E-13
regionalization	GO:0003002	8.5E-13
response to chemical	GO:0042221	9.2E-13
compound eye development	GO:0048749	1.3E-12
cell migration	GO:0016477	1.5E-12
regulation of cell differentiation	GO:0045595	2.3E-12
regulation of cell communication	GO:0010646	4.0E-12
localization	GO:0051179	4.6E-12
regulation of response to stimulus	GO:0048583	5.1E-12
regulation of signaling	GO:0023051	5.9E-12
cell motility	GO:0048870	6.2E-12
localization of cell	GO:0051674	9.7E-12
cellular response to stimulus	GO:0051716	1.4E-11
oogenesis	GO:0048477	2.7E-11
female gamete generation	GO:0007292	3.2E-11
response to external stimulus	GO:0009605	7.2E-11
regulation of nervous system development	GO:0051960	1.6E-10
regulation of biological quality	GO:0065008	1.9E-10
negative regulation of cellular process	GO:0048523	2.1E-10
sexual reproduction	GO:0019953	2.2E-10
reproductive process	GO:0022414	2.6E-10

Gene Ontology Terms	*GO Accession*	*p*
regulation of cell development	GO:0060284	2.7E-10
multi-organism reproductive process	GO:0044703	8.9E-10
actin cytoskeleton organization	GO:0030036	9.4E-10
regulation of cellular biosynthetic process	GO:0031326	1.1E-09
developmental process involved in reproduction	GO:0003006	1.1E-09
regulation of biosynthetic process	GO:0009889	1.1E-09
negative regulation of biological process	GO:0048519	1.3E-09
gamete generation	GO:0007276	1.4E-09
photoreceptor cell differentiation	GO:0046530	1.4E-09
single organism reproductive process	GO:0044702	1.6E-09
regulation of anatomical structure morphogenesis	GO:0022603	1.7E-09
multicellular organismal reproductive process	GO:0048609	1.7E-09
positive regulation of biological process	GO:0048518	1.7E-09
regulation of signal transduction	GO:0009966	1.9E-09
regulation of nitrogen compound metabolic process	GO:0051171	1.9E-09
respiratory system development	GO:0060541	2.7E-09
germ cell development	GO:0007281	2.9E-09
regulation of nucleobase-containing compound metabolic process	GO:0019219	4.3E-09
regulation of cellular metabolic process	GO:0031323	6.0E-09
learning or memory	GO:0007611	7.1E-09
cognition	GO:0050890	7.1E-09
regulation of RNA metabolic process	GO:0051252	7.9E-09
regulation of cellular macromolecule biosynthetic process	GO:2000112	8.6E-09
open tracheal system development	GO:0007424	9.9E-09
regulation of macromolecule biosynthetic process	GO:0010556	1.0E-08
gland development	GO:0048732	1.2E-08
single-organism localization	GO:1902578	1.3E-08
photoreceptor cell development	GO:0042461	1.3E-08
enzyme linked receptor protein signaling pathway	GO:0007167	1.6E-08
regulation of primary metabolic process	GO:0080090	2.4E-08
positive regulation of cellular process	GO:0048522	2.5E-08
eye photoreceptor cell differentiation	GO:0001754	3.2E-08
regulation of developmental growth	GO:0048638	4.1E-08
regulation of metabolic process	GO:0019222	4.1E-08
compound eye photoreceptor cell differentiation	GO:0001751	4.3E-08
cell-cell adhesion	GO:0098609	6.5E-08
system process	GO:0003008	7.6E-08
embryonic morphogenesis	GO:0048598	7.9E-08
negative regulation of multicellular organismal process	GO:0051241	1.1E-07
regulation of growth	GO:0040008	1.3E-07
single-organism transport	GO:0044765	1.4E-07

Gene Ontology Terms	*GO Accession*	*p*
leg disc development	GO:0035218	1.4E-07
imaginal disc-derived leg morphogenesis	GO:0007480	1.7E-07
eye photoreceptor cell development	GO:0042462	1.8E-07
regulation of gene expression	GO:0010468	2.1E-07
leg disc morphogenesis	GO:0007478	2.2E-07
regulation of transcription, DNA-templated	GO:0006355	2.4E-07
regulation of nucleic acid-templated transcription	GO:1903506	2.4E-07
regulation of RNA biosynthetic process	GO:2001141	2.4E-07
tissue migration	GO:0090130	2.6E-07
negative regulation of signaling	GO:0023057	3.0E-07
ameboidal-type cell migration	GO:0001667	3.1E-07
negative regulation of developmental process	GO:0051093	3.2E-07
compound eye photoreceptor development	GO:0042051	4.0E-07
establishment of localization	GO:0051234	4.6E-07
transport	GO:0006810	5.1E-07
negative regulation of cell communication	GO:0010648	5.3E-07
regulation of neurogenesis	GO:0050767	5.4E-07
regulation of cellular component organization	GO:0051128	5.4E-07
muscle organ development	GO:0007517	9.7E-07
positive regulation of metabolic process	GO:0009893	1.1E-06
anterior/posterior pattern specification	GO:0009952	1.2E-06
dendrite morphogenesis	GO:0048813	1.3E-06
epithelial cell migration	GO:0010631	1.7E-06
epithelium migration	GO:0090132	1.7E-06
multi-organism behavior	GO:0051705	1.8E-06
regulation of macromolecule metabolic process	GO:0060255	1.8E-06
heart development	GO:0007507	1.8E-06
cardiovascular system development	GO:0072358	1.8E-06
circulatory system development	GO:0072359	1.8E-06
negative regulation of signal transduction	GO:0009968	1.9E-06
cell-cell signaling	GO:0007267	2.6E-06
synaptic transmission	GO:0007268	2.9E-06
dendrite development	GO:0016358	3.2E-06
cell-cell adhesion via plasma-membrane adhesion molecules	GO:0098742	3.4E-06
regulation of synapse structure or activity	GO:0050803	3.4E-06
chemosensory behavior	GO:0007635	4.4E-06
salivary gland development	GO:0007431	4.5E-06
exocrine system development	GO:0035272	4.5E-06
embryonic pattern specification	GO:0009880	4.9E-06
RNA biosynthetic process	GO:0032774	5.1E-06
morphogenesis of a polarized epithelium	GO:0001738	5.1E-06

Gene Ontology Terms	*GO Accession*	*p*
negative regulation of biosynthetic process	GO:0009890	6.0E-06
negative regulation of cellular biosynthetic process	GO:0031327	6.0E-06
transcription, DNA-templated	GO:0006351	6.8E-06
nucleic acid-templated transcription	GO:0097659	6.8E-06
biological adhesion	GO:0022610	7.1E-06
larval development	GO:0002164	8.3E-06
learning	GO:0007612	8.9E-06
imaginal disc-derived wing vein morphogenesis	GO:0008586	9.2E-06
segmentation	GO:0035282	9.4E-06
motor neuron axon guidance	GO:0008045	1.0E-05
actomyosin structure organization	GO:0031032	1.2E-05
negative regulation of response to stimulus	GO:0048585	1.2E-05
establishment of planar polarity	GO:0001736	1.2E-05
establishment of tissue polarity	GO:0007164	1.2E-05
regulation of cell morphogenesis	GO:0022604	1.2E-05
chaeta morphogenesis	GO:0008407	1.3E-05
memory	GO:0007613	1.3E-05
positive regulation of cellular metabolic process	GO:0031325	1.3E-05
blastoderm segmentation	GO:0007350	1.4E-05
transmembrane receptor protein tyrosine kinase signaling pathway	GO:0007169	1.4E-05
negative regulation of cell differentiation	GO:0045596	1.4E-05
cell adhesion	GO:0007155	1.5E-05
epithelial cell development	GO:0002064	1.6E-05
embryonic development via the syncytial blastoderm	GO:0001700	1.7E-05
olfactory behavior	GO:0042048	1.8E-05
muscle cell development	GO:0055001	2.1E-05
striated muscle cell development	GO:0055002	2.1E-05
regulation of cell projection organization	GO:0031344	2.1E-05
central nervous system development	GO:0007417	2.3E-05
neuron recognition	GO:0008038	3.0E-05
regulation of neuron differentiation	GO:0045664	3.0E-05
regulation of cellular component biogenesis	GO:0044087	3.3E-05
negative regulation of macromolecule biosynthetic process	GO:0010558	3.5E-05
negative regulation of cellular macromolecule biosynthetic process	GO:2000113	3.5E-05
Wnt signaling pathway	GO:0016055	3.6E-05
regulation of cell morphogenesis involved in differentiation	GO:0010769	4.0E-05
olfactory learning	GO:0008355	4.1E-05
formation of organ boundary	GO:0010160	4.1E-05
ovarian follicle cell migration	GO:0007297	4.1E-05
mating behavior	GO:0007617	4.1E-05
regulation of cell fate commitment	GO:0010453	4.1E-05

Gene Ontology Terms	*GO Accession*	*p*
chaeta development	GO:0022416	4.3E-05
response to organic substance	GO:0010033	4.8E-05
wing disc dorsal/ventral pattern formation	GO:0048190	5.6E-05
negative regulation of nervous system development	GO:0051961	5.8E-05
negative regulation of cell fate commitment	GO:0010454	6.1E-05
border follicle cell migration	GO:0007298	6.2E-05
regulation of transcription from RNA polymerase II promoter	GO:0006357	6.2E-05
wing disc pattern formation	GO:0035222	6.5E-05
ommatidial rotation	GO:0016318	6.6E-05
ovarian follicle cell development	GO:0030707	6.7E-05
columnar/cuboidal epithelial cell development	GO:0002066	7.5E-05
imaginal disc pattern formation	GO:0007447	7.7E-05
muscle attachment	GO:0016203	7.8E-05
myofibril assembly	GO:0030239	7.8E-05
regulation of cell fate specification	GO:0042659	9.8E-05
associative learning	GO:0008306	1.0E-04
ion transport	GO:0006811	1.1E-04
regulation of neuron projection development	GO:0010975	1.1E-04
transmembrane receptor protein serine/threonine kinase signaling pathway	GO:0007178	1.1E-04
neurological system process	GO:0050877	1.1E-04
regulation of localization	GO:0032879	1.2E-04
salivary gland morphogenesis	GO:0007435	1.3E-04
gland morphogenesis	GO:0022612	1.3E-04
adult behavior	GO:0030534	1.3E-04
regulation of Wnt signaling pathway	GO:0030111	1.3E-04
dorsal/ventral pattern formation, imaginal disc	GO:0007450	1.4E-04
establishment of ommatidial planar polarity	GO:0042067	1.4E-04
negative regulation of cell fate specification	GO:0009996	1.5E-04
courtship behavior	GO:0007619	1.5E-04
regulation of synaptic growth at neuromuscular junction	GO:0008582	1.5E-04
mating	GO:0007618	1.5E-04
eye-antennal disc morphogenesis	GO:0007455	1.8E-04
homophilic cell adhesion via plasma membrane adhesion molecules	GO:0007156	2.1E-04
regulation of system process	GO:0044057	2.2E-04
R7 cell development	GO:0045467	2.4E-04
regulation of organ morphogenesis	GO:2000027	2.5E-04
post-embryonic hemopoiesis	GO:0035166	2.8E-04
larval lymph gland hemopoiesis	GO:0035167	2.8E-04
axon target recognition	GO:0007412	2.8E-04
negative regulation of nitrogen compound metabolic process	GO:0051172	2.8E-04
cyclic nucleotide metabolic process	GO:0009187	2.9E-04

Gene Ontology Terms	*GO Accession*	*p*
branching morphogenesis of an epithelial tube	GO:0048754	3.0E-04
branching involved in open tracheal system development	GO:0060446	3.0E-04
morphogenesis of a branching epithelium	GO:0061138	3.0E-04
dorsal/ventral pattern formation	GO:0009953	3.0E-04
positive regulation of developmental process	GO:0051094	3.0E-04
anterior/posterior axis specification	GO:0009948	3.1E-04
tripartite regional subdivision	GO:0007351	3.1E-04
anterior/posterior axis specification, embryo	GO:0008595	3.1E-04
cAMP metabolic process	GO:0046058	3.6E-04
regulation of synapse assembly	GO:0051963	3.8E-04
single organismal cell-cell adhesion	GO:0016337	3.8E-04
dorsal closure	GO:0007391	3.9E-04
single organism cell adhesion	GO:0098602	4.5E-04
positive regulation of biosynthetic process	GO:0009891	4.7E-04
positive regulation of cellular biosynthetic process	GO:0031328	4.7E-04
muscle system process	GO:0003012	4.7E-04
regulation of axonogenesis	GO:0050770	4.7E-04
R7 cell differentiation	GO:0045466	4.9E-04
lymph gland development	GO:0048542	4.9E-04
regulation of circadian rhythm	GO:0042752	4.9E-04
positive regulation of nitrogen compound metabolic process	GO:0051173	5.0E-04
positive regulation of macromolecule metabolic process	GO:0010604	5.5E-04
axis specification	GO:0009798	5.5E-04
morphogenesis of a branching structure	GO:0001763	5.9E-04
negative regulation of nucleobase-containing compound metabolic process	GO:0045934	6.0E-04
embryonic axis specification	GO:0000578	6.3E-04
actin filament organization	GO:0007015	6.3E-04
urogenital system development	GO:0001655	6.3E-04
epidermal growth factor receptor signaling pathway	GO:0007173	6.3E-04
ERBB signaling pathway	GO:0038127	6.3E-04
renal system development	GO:0072001	6.3E-04
germarium-derived egg chamber formation	GO:0007293	6.5E-04
antennal morphogenesis	GO:0048800	6.6E-04
positive regulation of multicellular organismal process	GO:0051240	6.7E-04
neuromuscular synaptic transmission	GO:0007274	6.8E-04
mesoderm morphogenesis	GO:0048332	7.6E-04
positive regulation of cellular component organization	GO:0051130	8.1E-04
multi-organism reproductive behavior	GO:0044705	8.1E-04
positive regulation of nucleobase-containing compound metabolic process	GO:0045935	8.2E-04
negative regulation of cellular metabolic process	GO:0031324	8.8E-04
short-term memory	GO:0007614	8.9E-04

Gene Ontology Terms	*GO Accession*	*p*
digestive tract development	GO:0048565	1.0E-03
digestive system development	GO:0055123	1.0E-03
regulation of cell proliferation	GO:0042127	1.0E-03
negative regulation of RNA metabolic process	GO:0051253	1.1E-03
gastrulation	GO:0007369	1.1E-03
G-protein coupled receptor signaling pathway	GO:0007186	1.1E-03
metal ion transport	GO:0030001	1.1E-03
peripheral nervous system development	GO:0007422	1.1E-03
renal tubule development	GO:0061326	1.1E-03
Malpighian tubule development	GO:0072002	1.1E-03
response to growth factor	GO:0070848	1.1E-03
negative regulation of transcription, DNA-templated	GO:0045892	1.2E-03
negative regulation of RNA biosynthetic process	GO:1902679	1.2E-03
negative regulation of nucleic acid-templated transcription	GO:1903507	1.2E-03
reproductive behavior	GO:0019098	1.2E-03
skeletal muscle organ development	GO:0060538	1.3E-03
morphogenesis of embryonic epithelium	GO:0016331	1.3E-03
regulation of synapse organization	GO:0050807	1.3E-03
decapentaplegic signaling pathway	GO:0008101	1.3E-03
establishment of mitotic spindle localization	GO:0040001	1.3E-03
organelle localization	GO:0051640	1.4E-03
intracellular signal transduction	GO:0035556	1.4E-03
eye-antennal disc development	GO:0035214	1.5E-03
negative regulation of Wnt signaling pathway	GO:0030178	1.5E-03
negative regulation of reproductive process	GO:2000242	1.5E-03
single-organism cellular localization	GO:1902580	1.6E-03
anterior Malpighian tubule development	GO:0061327	1.6E-03
locomotory behavior	GO:0007626	1.7E-03
heterophilic cell-cell adhesion via plasma membrane cell adhesion molecules	GO:0007157	1.7E-03
regulation of circadian sleep/wake cycle	GO:0042749	1.7E-03
compound eye retinal cell programmed cell death	GO:0046667	1.7E-03
establishment of spindle localization	GO:0051293	1.7E-03
spindle localization	GO:0051653	1.7E-03
aggressive behavior	GO:0002118	1.8E-03
determination of muscle attachment site	GO:0016204	1.9E-03
positive chemotaxis	GO:0050918	1.9E-03
vesicle localization	GO:0051648	2.0E-03
female meiosis chromosome segregation	GO:0016321	2.0E-03
synaptic vesicle localization	GO:0097479	2.0E-03
imaginal disc-derived wing margin morphogenesis	GO:0008587	2.2E-03
imaginal disc-derived wing hair organization	GO:0035317	2.2E-03

Gene Ontology Terms	*GO Accession*	*p*
establishment of organelle localization	GO:0051656	2.2E-03
hemopoiesis	GO:0030097	2.3E-03
negative regulation of decapentaplegic signaling pathway	GO:0090099	2.4E-03
organ growth	GO:0035265	2.4E-03
immune system development	GO:0002520	2.4E-03
hematopoietic or lymphoid organ development	GO:0048534	2.4E-03
regulation of intracellular signal transduction	GO:1902531	2.4E-03
actin filament bundle assembly	GO:0051017	2.4E-03
cellular response to growth factor stimulus	GO:0071363	2.5E-03
establishment of vesicle localization	GO:0051650	2.6E-03
cyclic purine nucleotide metabolic process	GO:0052652	2.7E-03
hair cell differentiation	GO:0035315	2.7E-03
regulation of transmembrane receptor protein serine/threonine kinase signaling	GO:0090092	2.7E-03
negative regulation of gene expression	GO:0010629	2.8E-03
negative regulation of cell development	GO:0010721	2.8E-03
inter-male aggressive behavior	GO:0002121	2.9E-03
response to endogenous stimulus	GO:0009719	3.0E-03
synaptic vesicle transport	GO:0048489	3.1E-03
establishment of synaptic vesicle localization	GO:0097480	3.1E-03
primary branching, open tracheal system	GO:0007428	3.2E-03
oocyte development	GO:0048599	3.3E-03
negative regulation of transcription from RNA polymerase II promoter	GO:0000122	3.4E-03
cellular response to organic substance	GO:0071310	3.4E-03
ovarian nurse cell to oocyte transport	GO:0007300	3.5E-03
potassium ion transport	GO:0006813	3.6E-03
regulation of synaptic transmission	GO:0050804	3.7E-03
positive regulation of gene expression	GO:0010628	3.7E-03
mitochondrion distribution	GO:0048311	3.8E-03
regulation of decapentaplegic signaling pathway	GO:0090097	3.8E-03
sleep	GO:0030431	3.8E-03
positive regulation of macromolecule biosynthetic process	GO:0010557	3.9E-03
anatomical structure homeostasis	GO:0060249	4.2E-03
maintenance of protein location	GO:0045185	4.2E-03
regulation of reproductive process	GO:2000241	4.2E-03
transcription from RNA polymerase II promoter	GO:0006366	4.4E-03
sarcomere organization	GO:0045214	4.4E-03
positive regulation of transcription, DNA-templated	GO:0045893	4.4E-03
positive regulation of RNA biosynthetic process	GO:1902680	4.4E-03
positive regulation of nucleic acid-templated transcription	GO:1903508	4.4E-03
salivary gland boundary specification	GO:0007432	4.5E-03
response to alcohol	GO:0097305	4.6E-03

Gene Ontology Terms	*GO Accession*	*p*
oocyte construction	GO:0007308	4.8E-03
endocytosis	GO:0006897	5.0E-03

APPENDIX D. DIFFERENTIALLY EXPRESSED GENES WITH A SIGNIFICANT DEVELOPMENT TERM

sym	*FBgn*	*Δlog2*	*padj*
a	FBgn0000008	2.15	7.4E-06
Aats-cys	FBgn0027091	-0.72	6.5E-05
Aats-gly	FBgn0027088	-0.55	3.3E-02
Aats-ile	FBgn0027086	-1.34	9.9E-09
Aats-val	FBgn0027079	-0.93	1.3E-05
aay	FBgn0023129	-0.93	1.9E-02
Ac3	FBgn0023416	-1.62	1.7E-02
Ac76E	FBgn0004852	-1.72	3.0E-05
ACC	FBgn0033246	-1.22	4.8E-02
AcCoAS	FBgn0012034	-1.45	8.2E-05
Acer	FBgn0016122	1.36	2.0E-04
Acox57D-d	FBgn0034629	-0.94	9.6E-03
Acp24A4	FBgn0051779	-1.96	2.0E-02
Act57B	FBgn0000044	-1.76	6.1E-03
ACXD	FBgn0040507	-1.25	1.9E-03
Adgf-A	FBgn0036752	0.62	1.8E-02
Adgf-D	FBgn0038172	-1.21	2.9E-02
Adk2	FBgn0283494	-1.31	1.1E-04
adp	FBgn0000057	-1.28	2.6E-04
AdSS	FBgn0027493	1.38	9.4E-04
Ady43A	FBgn0026602	-1.34	2.5E-03
Ag5r2	FBgn0020508	-4.01	3.0E-02
Ahcy89E	FBgn0015011	1.00	5.3E-03
Alas	FBgn0020764	-1.03	7.4E-04
alc	FBgn0260972	0.78	3.8E-03
Aldh	FBgn0012036	-2.00	4.2E-03
Alp1	FBgn0283479	-4.47	3.2E-08
alpha-Est2	FBgn0015570	-4.03	3.7E-16
alpha-Est5	FBgn0261393	-1.92	2.0E-06
alpha-Est7	FBgn0015575	1.50	6.4E-06
alpha-Est9	FBgn0015577	-2.56	1.6E-18
alphaCOP	FBgn0025725	-1.24	8.6E-04
alphagamma	FBgn0052865	-1.87	4.2E-02
Ama	FBgn0000071	1.44	2.9E-04
amn	FBgn0086782	-2.99	3.3E-02
Ance	FBgn0012037	1.33	1.7E-03
AOX1	FBgn0267408	-1.40	2.0E-02
AP-2sigma	FBgn0043012	0.62	2.1E-03
Aprt	FBgn0000109	1.48	1.7E-05
ArfGAP1	FBgn0020655	-0.73	3.0E-02
ArfGAP3	FBgn0037182	-0.77	1.3E-04
Arp2	FBgn0011742	0.82	2.5E-04
Art4	FBgn0037770	-0.94	6.1E-03
Ask1	FBgn0014006	1.02	2.6E-04
ASPP	FBgn0034606	-1.24	1.8E-02
Atf3	FBgn0028550	-1.67	5.7E-04
Atg18a	FBgn0035850	0.61	1.2E-02
Atg3	FBgn0036813	1.05	5.0E-06
Atg4b	FBgn0038325	0.71	1.7E-03
atl	FBgn0039213	-0.50	7.4E-03
AttD	FBgn0038530	3.29	1.0E-02
b	FBgn0000153	2.36	9.1E-04
B52	FBgn0004587	-0.61	1.6E-03
bam	FBgn0000158	0.97	2.2E-02
bchs	FBgn0043362	-1.11	3.6E-02
bdl	FBgn0028482	-2.02	1.6E-02
beat-IV	FBgn0039089	-1.82	3.5E-02
Bet1	FBgn0260857	-0.66	7.1E-03
beta-PheRS	FBgn0039175	-0.69	2.2E-04
beta'COP	FBgn0025724	-1.19	1.5E-03
betaTry	FBgn0010357	-5.80	2.3E-04
betaTub60D	FBgn0003888	0.97	7.7E-03
bgm	FBgn0027348	-3.04	9.1E-18
bi	FBgn0000179	-1.49	4.5E-04
bif	FBgn0014133	0.91	9.6E-05
bigmax	FBgn0039509	-2.12	4.6E-15
bin3	FBgn0263144	0.60	4.0E-02
Bmcp	FBgn0036199	1.22	2.0E-04
bowl	FBgn0004893	-0.90	1.1E-02
brat	FBgn0010300	-0.89	7.6E-03
bru-3	FBgn0264001	-1.55	3.2E-02
btl	FBgn0005592	1.47	1.4E-02
Bub3	FBgn0025457	-0.63	3.9E-02
bves	FBgn0031150	0.77	1.0E-02
Bx	FBgn0265598	-0.90	4.2E-03
by	FBgn0000244	-2.22	1.1E-15
byn	FBgn0011723	-2.83	4.9E-02
bys	FBgn0010292	-0.59	3.9E-02

sym	*FBgn*	*Δlog2*	*padj*
Arc1	FBgn0033926	1.94	1.6E-02
aret	FBgn0000114	0.93	2.5E-04
CadN	FBgn0015609	-1.13	2.2E-02
Caf1-55	FBgn0263979	-0.57	1.8E-02
CAH1	FBgn0027844	1.27	5.5E-04
CalpC	FBgn0260450	-0.78	3.4E-02
Calr	FBgn0005585	-0.86	2.6E-04
CapaR	FBgn0037100	-4.34	5.5E-10
cas	FBgn0004878	-2.93	1.5E-03
Cas	FBgn0022213	-0.55	4.3E-02
Cat	FBgn0000261	0.85	5.0E-03
cbt	FBgn0043364	-0.89	4.2E-02
Ccp84Ab	FBgn0004782	1.98	4.1E-02
Cct1	FBgn0041342	-0.69	1.8E-03
CD98hc	FBgn0037533	0.90	4.9E-04
Cda5	FBgn0051973	-2.02	6.1E-05
CDC45L	FBgn0026143	-1.08	8.1E-05
Cdc5	FBgn0265574	-0.53	5.8E-03
Cdc6	FBgn0035918	-0.82	1.2E-04
cDIP	FBgn0038865	-2.28	1.9E-05
Cdk5	FBgn0013762	0.48	2.4E-02
Ced-12	FBgn0032409	0.77	2.8E-02
CenB1A	FBgn0039056	0.70	2.1E-02
cer	FBgn0034443	1.96	1.4E-03
CG10005	FBgn0037972	2.77	4.7E-13
CG10019	FBgn0031568	1.44	4.0E-03
CG10026	FBgn0032785	-1.75	8.5E-08
CG10031	FBgn0031563	-3.80	4.2E-15
CG10053	FBgn0037490	0.68	3.5E-02
CG10062	FBgn0034439	1.73	4.6E-02
CG10073	FBgn0034440	-2.01	1.5E-02
CG10086	FBgn0037517	-1.05	1.3E-02
CG10166	FBgn0032799	-0.42	2.5E-02
CG10178	FBgn0032684	-2.57	8.3E-04
CG10211	FBgn0032685	-2.32	4.9E-04
CG10214	FBgn0039115	-1.16	2.2E-04
CG10237	FBgn0032783	-2.38	9.0E-06
CG10274	FBgn0035690	-0.52	1.4E-02
CG10286	FBgn0037439	-0.79	3.8E-04
CG10317	FBgn0038423	1.55	4.6E-02
CG10338	FBgn0032700	0.59	7.1E-03
C1GalTA	FBgn0032078	1.43	1.7E-05
C901	FBgn0021742	3.56	7.8E-03
CG10420	FBgn0039296	-1.23	1.9E-05
CG10433	FBgn0034638	-2.00	2.5E-05
CG10463	FBgn0032819	-1.30	1.0E-02
CG10467	FBgn0035679	1.18	1.5E-03
CG10469	FBgn0035678	1.14	2.0E-04
CG10494	FBgn0034634	-1.16	2.8E-04
CG10505	FBgn0034612	-3.68	1.7E-18
CG10513	FBgn0039311	-4.40	6.9E-13
CG10516	FBgn0036549	2.88	1.2E-09
CG10550	FBgn0039321	-4.85	1.1E-06
CG10555	FBgn0030034	-0.53	2.4E-02
CG10559	FBgn0039323	-1.67	4.0E-02
CG10560	FBgn0039325	-4.29	2.0E-04
CG10576	FBgn0035630	-1.04	3.0E-04
CG10660	FBgn0036288	0.98	2.8E-03
CG10747	FBgn0032845	0.64	2.2E-02
CG10822	FBgn0034478	2.40	1.7E-02
CG1090	FBgn0037238	1.59	2.2E-04
CG10910	FBgn0034289	-3.72	1.7E-03
CG1092	FBgn0037228	-0.99	9.5E-03
CG10960	FBgn0036316	1.80	9.1E-03
CG1103	FBgn0037235	0.97	2.7E-06
CG11030	FBgn0031736	-0.92	1.4E-03
CG11034	FBgn0031741	1.65	6.1E-03
CG1104	FBgn0037467	-0.77	5.1E-03
CG1105	FBgn0037465	-0.76	1.6E-02
CG11070	FBgn0028467	0.86	1.5E-03
CG11073	FBgn0034693	-2.56	7.5E-04
CG11123	FBgn0033169	-0.59	1.7E-02
CG11149	FBgn0031732	-5.69	6.3E-03
CG11151	FBgn0030519	-1.72	3.1E-06
CG11155	FBgn0039927	-0.85	3.2E-02
CG11168	FBgn0039249	-0.80	9.6E-03
CG11178	FBgn0030499	-0.43	6.0E-03
CG11192	FBgn0034507	5.36	5.2E-10
CG11226	FBgn0037195	1.22	1.7E-02
CG11236	FBgn0031860	-1.94	1.0E-03
CG11241	FBgn0037186	-2.00	3.1E-08
CG11257	FBgn0034442	0.87	3.3E-04

sym	*FBgn*	*Δlog2*	*padj*
CG10361	FBgn0036208	-2.44	2.7E-02
CG10365	FBgn0039109	-1.12	3.2E-02
CG10383	FBgn0032699	1.40	1.7E-04
CG10384	FBgn0034731	-3.21	3.4E-02
CG11340	FBgn0039840	-3.00	3.2E-05
CG11353	FBgn0035557	-2.74	2.3E-02
CG11367	FBgn0037185	0.98	1.4E-04
CG11377	FBgn0031217	-0.51	1.5E-02
CG11399	FBgn0037021	-0.62	2.5E-02
CG11406	FBgn0034990	4.31	1.5E-03
CG11414	FBgn0035024	-0.51	1.0E-02
CG11426	FBgn0037166	-2.04	6.5E-05
CG1143	FBgn0035359	-2.35	4.1E-02
CG11453	FBgn0038734	-2.36	1.8E-02
CG11456	FBgn0037031	-0.67	1.9E-02
CG11529	FBgn0036264	-4.24	1.4E-05
CG11537	FBgn0035400	-0.51	3.7E-02
CG11576	FBgn0039882	1.02	7.0E-03
CG11577	FBgn0036847	-0.91	7.8E-03
CG11583	FBgn0035524	-0.76	2.9E-02
CG11619	FBgn0036836	1.19	1.4E-02
CG11652	FBgn0036194	-0.87	1.5E-03
CG11658	FBgn0036196	0.94	1.6E-02
CG11672	FBgn0037563	-3.79	2.4E-02
CG1172	FBgn0264712	0.45	4.0E-02
CG11737	FBgn0037592	-0.86	6.2E-03
CG11739	FBgn0037239	1.18	2.2E-05
CG11816	FBgn0030495	4.19	1.4E-06
CG11837	FBgn0039627	-1.24	1.8E-02
CG11851	FBgn0039293	-0.95	5.4E-03
CG11857	FBgn0039303	-0.80	2.3E-03
CG11882	FBgn0039642	0.96	2.4E-02
CG11885	FBgn0031253	0.85	2.4E-06
CG11893	FBgn0039316	-2.91	4.1E-11
CG11920	FBgn0039274	-0.69	6.6E-03
CG11961	FBgn0034436	-0.69	4.7E-02
CG11975	FBgn0037648	0.53	1.7E-02
CG12009	FBgn0035430	1.89	2.2E-03
CG12034	FBgn0035421	0.44	5.1E-04
CG12071	FBgn0039808	-2.29	4.4E-02
CG1208	FBgn0037386	2.04	4.5E-04
CG11261	FBgn0036332	0.83	2.9E-02
CG11267	FBgn0036334	-0.59	2.9E-02
CG11309	FBgn0037070	-1.20	2.7E-03
CG11313	FBgn0039798	-2.71	1.3E-06
CG1218	FBgn0037377	0.57	2.3E-02
CG12207	FBgn0038220	0.85	5.9E-03
CG12224	FBgn0037974	2.49	2.2E-03
CG12239	FBgn0029810	-3.33	5.9E-04
CG12262	FBgn0035811	-1.63	2.9E-03
CG12301	FBgn0036514	-0.72	4.8E-02
CG12310	FBgn0036467	-3.45	1.7E-02
CG12321	FBgn0038577	0.68	4.8E-04
CG12325	FBgn0033557	-1.11	5.9E-04
CG12338	FBgn0033543	1.55	2.6E-05
CG12398	FBgn0030596	3.75	8.9E-03
CG12404	FBgn0032465	-0.46	1.1E-02
CG12428	FBgn0039543	-1.64	2.1E-05
CG12499	FBgn0038968	-0.80	4.5E-02
CG12512	FBgn0031703	-1.69	3.2E-02
CG12520	FBgn0036324	-2.39	2.1E-03
CG12531	FBgn0031064	-1.66	2.3E-02
CG12576	FBgn0031190	-0.49	8.9E-03
CG12608	FBgn0030630	-0.66	6.8E-03
CG12643	FBgn0040942	-0.94	9.4E-03
CG12655	FBgn0031080	2.66	3.4E-02
CG12715	FBgn0030443	-4.86	5.8E-06
CG12784	FBgn0038356	1.70	4.8E-02
CG12811	FBgn0037779	-0.81	1.2E-03
CG12825	FBgn0033221	-2.25	1.5E-10
CG12826	FBgn0033207	-3.79	2.8E-03
CG12868	FBgn0033945	1.54	9.6E-05
CG1299	FBgn0035501	-1.82	1.7E-02
CG13026	FBgn0036656	6.23	1.7E-07
CG13044	FBgn0036599	-4.05	1.8E-06
CG13077	FBgn0032810	-3.61	1.8E-06
CG13082	FBgn0032803	1.74	7.3E-03
CG13086	FBgn0032770	1.81	4.5E-04
CG13101	FBgn0032084	-2.35	8.6E-03
CG1311	FBgn0035523	-0.64	7.4E-03
CG13255	FBgn0040636	-1.99	2.8E-07
CG13272	FBgn0086673	-1.92	1.0E-02

sym	*FBgn*	*Δlog2*	*padj*
CG12104	FBgn0035238	0.98	3.4E-04
CG12116	FBgn0030041	-0.92	4.5E-02
CG12125	FBgn0030037	1.01	1.3E-02
CG1213	FBgn0037387	2.27	1.1E-03
CG12133	FBgn0033469	4.14	7.0E-07
CG12159	FBgn0033232	0.71	5.3E-03
CG13397	FBgn0014417	-2.10	1.9E-11
CG13460	FBgn0036471	-7.08	5.7E-06
CG13461	FBgn0036468	-6.59	1.7E-03
CG13488	FBgn0034670	-1.29	4.0E-02
CG13492	FBgn0034662	-3.73	2.0E-02
CG13560	FBgn0034899	-4.79	4.0E-02
CG13575	FBgn0034996	1.34	3.3E-02
CG13605	FBgn0039150	0.45	4.0E-02
CG13606	FBgn0039161	4.52	1.2E-07
CG13654	FBgn0039290	-1.29	1.0E-03
CG13678	FBgn0035859	-3.28	5.9E-04
CG13707	FBgn0035578	2.91	1.6E-06
CG13708	FBgn0035577	2.31	2.0E-03
CG13731	FBgn0036717	-5.21	5.4E-06
CG13748	FBgn0033355	2.37	3.5E-04
CG13784	FBgn0031897	1.34	1.6E-03
CG13806	FBgn0035325	-3.15	3.3E-02
CG13890	FBgn0035169	-1.19	3.3E-04
CG13900	FBgn0035162	-0.89	1.9E-02
CG13912	FBgn0035186	-1.70	1.6E-02
CG13947	FBgn0031277	-6.94	3.7E-03
CG13950	FBgn0031289	-3.35	6.7E-03
CG14040	FBgn0031676	1.89	7.1E-10
CG14062	FBgn0039592	4.14	1.1E-04
CG14100	FBgn0036889	-0.56	2.8E-02
CG14131	FBgn0036205	-1.04	2.2E-02
CG14132	FBgn0040817	1.35	2.7E-02
CG14135	FBgn0036193	0.68	2.6E-02
CG14160	FBgn0036066	-3.29	6.0E-03
CG14184	FBgn0036932	0.72	1.4E-02
CG14196	FBgn0031002	-1.26	9.8E-04
CG14207	FBgn0031037	-1.43	1.6E-06
CG14230	FBgn0031062	-0.72	3.0E-03
CG14234	FBgn0031065	-2.27	4.4E-02
CG14253	FBgn0039467	-1.58	5.9E-03
CG13283	FBgn0032613	-4.63	7.7E-11
CG13287	FBgn0035643	-3.33	2.6E-02
CG13311	FBgn0035929	-2.29	2.6E-03
CG13314	FBgn0035949	-2.46	1.3E-02
CG13322	FBgn0033784	0.69	1.7E-02
CG13360	FBgn0025620	-4.45	2.3E-28
CG14528	FBgn0039611	-0.83	2.2E-02
CG14569	FBgn0037123	1.73	2.1E-02
CG14570	FBgn0037122	2.29	8.7E-03
CG14606	FBgn0037485	-5.19	1.7E-08
CG14618	FBgn0031189	-0.70	1.2E-02
CG14650	FBgn0037252	-0.75	2.4E-02
CG14659	FBgn0037284	2.17	4.5E-02
CG14664	FBgn0040682	3.04	3.7E-02
CG14683	FBgn0037822	-0.65	3.6E-02
CG14688	FBgn0037819	-3.54	4.8E-15
CG14762	FBgn0033250	-2.70	6.4E-04
CG14803	FBgn0023513	-1.05	1.5E-06
CG14823	FBgn0035734	-2.43	2.1E-06
CG14850	FBgn0038239	-7.74	4.1E-03
CG14852	FBgn0038242	-6.20	2.2E-03
CG1486	FBgn0031174	-1.00	2.6E-05
CG14882	FBgn0038429	-1.38	7.8E-05
CG14931	FBgn0032374	1.51	4.1E-02
CG14995	FBgn0035497	1.50	3.8E-03
CG15011	FBgn0035518	-0.98	4.1E-05
CG15019	FBgn0035541	-1.09	3.8E-03
CG15096	FBgn0034394	-2.15	5.2E-04
CG15099	FBgn0034400	1.60	3.4E-04
CG1513	FBgn0033463	0.88	3.3E-03
CG15155	FBgn0032669	-3.11	1.7E-06
CG15170	FBgn0032733	-3.30	1.3E-02
CG1518	FBgn0031149	-0.90	4.6E-03
CG15199	FBgn0030270	-2.02	3.7E-03
CG15202	FBgn0030271	-1.84	7.3E-03
CG15203	FBgn0030261	-1.86	7.2E-12
CG15219	FBgn0040519	1.68	4.6E-02
CG15221	FBgn0030331	-3.49	9.0E-03
CG15279	FBgn0028886	-2.83	1.1E-07
CG15293	FBgn0028526	-4.46	9.8E-09
CG15330	FBgn0029987	2.53	2.4E-02

sym	*FBgn*	*Δlog2*	*padj*
CG14265	FBgn0040393	-6.29	1.5E-03
CG14282	FBgn0038685	1.83	3.2E-02
CG14302	FBgn0038647	-3.76	3.3E-02
CG14304	FBgn0038629	-3.79	1.4E-03
CG1440	FBgn0030038	0.82	2.1E-04
CG14515	FBgn0039648	3.15	1.8E-06
CG14523	FBgn0039612	1.52	3.6E-04
CG14526	FBgn0027578	1.07	8.7E-03
CG15528	FBgn0039742	-1.33	2.6E-02
CG15553	FBgn0039817	-1.23	4.4E-02
CG15556	FBgn0039821	-1.31	4.1E-02
CG15611	FBgn0034194	0.76	1.5E-02
CG15706	FBgn0034093	1.18	2.8E-02
CG15739	FBgn0030347	2.35	2.8E-10
CG15743	FBgn0030465	-0.89	1.5E-02
CG15756	FBgn0030493	2.89	3.0E-04
CG15772	FBgn0029799	-2.10	1.5E-03
CG15773	FBgn0029795	-2.85	2.1E-03
CG1578	FBgn0030336	0.60	4.0E-02
CG15784	FBgn0029766	-1.40	4.9E-04
CG15861	FBgn0035084	-0.93	3.7E-02
CG15863	FBgn0033467	1.58	4.8E-03
CG15879	FBgn0035309	-1.80	2.3E-03
CG15919	FBgn0040743	-3.23	4.8E-02
CG1607	FBgn0039844	2.24	7.0E-05
CG1636	FBgn0030030	-1.40	2.9E-06
CG1648	FBgn0033446	-2.96	3.3E-12
CG1657	FBgn0030286	-0.72	9.2E-03
CG1665	FBgn0033451	-1.12	3.5E-02
CG1671	FBgn0033454	-0.87	7.8E-03
CG16719	FBgn0036029	2.08	1.2E-02
CG16727	FBgn0038719	-3.92	1.1E-20
CG16743	FBgn0032322	-1.72	4.4E-07
CG16756	FBgn0029765	-3.24	2.8E-06
CG16762	FBgn0035343	-2.22	9.4E-05
CG16820	FBgn0032495	-2.33	1.7E-04
CG16898	FBgn0034480	-2.96	7.7E-04
CG16908	FBgn0037741	-0.64	1.6E-02
CG16926	FBgn0040732	0.94	1.1E-02
CG16964	FBgn0032385	1.71	3.7E-02
CG16995	FBgn0031412	2.60	1.8E-04
CG15369	FBgn0030105	-1.32	1.3E-02
CG1537	FBgn0030260	-2.70	7.6E-03
CG15404	FBgn0031512	-7.08	1.7E-09
CG15406	FBgn0031517	-1.38	3.2E-02
CG15408	FBgn0031523	-2.50	1.1E-03
CG15414	FBgn0031542	-2.61	3.9E-02
CG1545	FBgn0030259	-2.93	4.6E-02
CG15526	FBgn0039744	1.97	3.0E-02
CG17292	FBgn0032029	-1.20	1.5E-03
CG17322	FBgn0027070	-0.88	6.1E-03
CG17323	FBgn0032713	1.28	1.2E-04
CG17324	FBgn0027074	1.21	1.8E-02
CG17341	FBgn0028906	-2.58	1.2E-03
CG17362	FBgn0036393	-5.96	4.0E-04
CG17386	FBgn0033936	-3.53	1.3E-07
CG17549	FBgn0032774	-1.10	4.4E-02
CG17568	FBgn0032763	1.24	2.9E-04
CG17570	FBgn0260000	-3.40	9.5E-03
CG17571	FBgn0259998	-3.56	1.1E-02
CG17636	FBgn0025837	-2.25	2.2E-02
CG17681	FBgn0032668	0.84	3.5E-02
CG17698	FBgn0040056	-0.66	1.3E-02
CG17734	FBgn0037890	0.59	3.2E-02
CG17738	FBgn0038009	1.65	5.9E-05
CG1774	FBgn0039856	-1.53	9.1E-03
CG17746	FBgn0035425	0.53	1.6E-03
CG17751	FBgn0038717	-4.02	1.1E-15
CG17752	FBgn0038718	-4.44	1.4E-12
CG17754	FBgn0030114	1.26	2.1E-04
CG17760	FBgn0033756	1.51	1.6E-02
CG1785	FBgn0030061	-0.81	1.3E-03
CG17994	FBgn0033072	2.47	3.9E-02
CG18003	FBgn0061356	1.40	1.4E-02
CG18135	FBgn0036837	-1.15	6.8E-03
CG18179	FBgn0036023	6.98	7.1E-07
CG18249	FBgn0037553	0.70	3.0E-02
CG18268	FBgn0037520	-4.17	3.2E-04
CG18324	FBgn0033905	0.62	2.3E-02
CG18327	FBgn0033904	3.67	6.4E-12
CG1835	FBgn0031127	1.36	3.5E-02
CG18371	FBgn0033893	1.67	4.9E-02

sym	*FBgn*	*Δlog2*	*padj*
CG17003	FBgn0031082	1.64	4.8E-02
CG17026	FBgn0036550	-1.41	3.2E-03
CG1703	FBgn0030321	-0.54	1.4E-02
CG17036	FBgn0032449	1.59	5.2E-06
CG17075	FBgn0031239	-1.38	2.3E-02
CG17109	FBgn0039051	-2.07	2.1E-04
CG17145	FBgn0036953	-4.57	2.9E-02
CG17147	FBgn0260393	-4.45	2.2E-02
CG1718	FBgn0031170	-1.19	2.1E-02
CG17271	FBgn0038829	-1.18	5.9E-04
CG18788	FBgn0042126	2.31	3.7E-03
CG18815	FBgn0042138	-0.54	4.2E-03
CG1942	FBgn0033215	-3.47	1.2E-03
CG1971	FBgn0039881	0.98	3.5E-02
CG2016	FBgn0250839	2.01	2.9E-04
CG2070	FBgn0033203	3.59	3.0E-03
CG2145	FBgn0030251	-2.32	4.5E-08
CG2162	FBgn0035388	-0.55	7.6E-05
CG2187	FBgn0017448	-3.32	2.0E-05
CG2233	FBgn0029990	0.91	1.2E-02
Cg25C	FBgn0000299	-1.07	9.0E-06
CG2641	FBgn0037518	-1.40	8.9E-09
CG2691	FBgn0030504	-0.89	2.7E-03
CG2736	FBgn0035090	-1.56	1.6E-05
CG2767	FBgn0037537	-0.54	3.6E-02
CG2818	FBgn0031566	0.73	5.4E-04
CG2875	FBgn0029672	-0.89	1.1E-02
CG2918	FBgn0023529	-0.92	2.1E-02
CG2930	FBgn0028491	-2.65	2.1E-07
CG2972	FBgn0030177	-0.78	1.9E-02
CG2991	FBgn0031474	0.57	5.0E-02
CG30010	FBgn0050010	1.53	2.7E-08
CG30025	FBgn0050025	-4.21	1.2E-02
CG30033	FBgn0050033	-4.95	3.0E-03
CG30069	FBgn0050069	-1.15	2.9E-03
CG30083	FBgn0050083	1.43	3.1E-02
CG30088	FBgn0050088	2.15	8.0E-05
CG3009	FBgn0029720	-1.93	1.2E-02
CG30090	FBgn0050090	1.71	2.6E-02
CG30099	FBgn0050099	1.55	1.5E-02
CG30109	FBgn0050109	1.39	2.2E-05
CG18480	FBgn0028518	-1.53	1.1E-02
CG18528	FBgn0039189	1.02	2.9E-02
CG18547	FBgn0037973	1.61	9.7E-06
CG18622	FBgn0038460	0.99	7.8E-03
CG18635	FBgn0034279	-2.33	2.0E-02
CG18636	FBgn0032551	3.82	4.1E-07
CG18649	FBgn0036469	-3.80	3.3E-04
CG18659	FBgn0027561	0.97	1.4E-03
CG18745	FBgn0042102	-2.37	5.5E-05
CG18747	FBgn0042104	-2.52	5.1E-04
CG30463	FBgn0050463	-1.63	2.9E-03
CG3077	FBgn0031457	0.81	4.9E-03
CG31064	FBgn0051064	0.80	9.7E-06
CG31087	FBgn0051087	-4.32	1.1E-04
CG31103	FBgn0051103	-4.57	1.5E-03
CG31106	FBgn0051106	-1.72	2.7E-02
CG31126	FBgn0051126	1.33	1.0E-07
CG31226	FBgn0051226	2.00	2.4E-02
CG31259	FBgn0051259	-3.62	7.1E-05
CG31272	FBgn0051272	-3.70	1.4E-07
CG31323	FBgn0051323	-1.48	3.6E-04
CG31324	FBgn0051324	-1.13	1.6E-03
CG31344	FBgn0051344	1.36	2.6E-03
CG31368	FBgn0051368	-0.70	1.8E-02
CG31373	FBgn0051373	-0.97	3.5E-02
CG31380	FBgn0051380	-3.52	1.7E-07
CG31454	FBgn0051454	-1.40	2.2E-02
CG31496	FBgn0051496	-5.55	1.4E-05
CG31522	FBgn0051522	-0.92	4.8E-02
CG31606	FBgn0051606	3.00	2.2E-02
CG3163	FBgn0034961	0.70	4.6E-02
CG31633	FBgn0051633	1.45	5.4E-03
CG31636	FBgn0051636	2.82	6.0E-10
CG31659	FBgn0051659	2.05	4.0E-03
CG31663	FBgn0051663	0.92	2.3E-02
CG31664	FBgn0051664	-2.64	1.5E-03
CG3168	FBgn0029896	1.02	4.8E-02
CG31683	FBgn0051683	1.67	3.2E-02
CG31698	FBgn0051698	-7.17	7.5E-08
CG31741	FBgn0051741	-5.76	1.5E-02
CG31751	FBgn0086909	-0.88	4.1E-02

sym	*FBgn*	*Δlog2*	*padj*
CG30118	FBgn0050118	-1.03	1.0E-05
CG30122	FBgn0050122	-0.45	4.1E-02
CG30148	FBgn0050148	-1.45	8.4E-06
CG30187	FBgn0050187	-1.16	3.7E-03
CG30192	FBgn0050192	1.85	3.2E-02
CG30287	FBgn0050287	1.63	6.1E-03
CG30288	FBgn0050288	-2.68	2.0E-04
CG30345	FBgn0050345	-1.63	1.8E-05
CG30349	FBgn0050349	-0.70	3.1E-03
CG30371	FBgn0050371	-5.81	5.8E-17
CG30394	FBgn0050394	-1.32	7.1E-04
CG30431	FBgn0050431	1.27	1.4E-03
CG32107	FBgn0052107	-3.22	2.0E-02
CG32109	FBgn0052109	0.47	3.4E-02
CG32115	FBgn0052115	-2.27	4.1E-07
CG32164	FBgn0042177	-0.60	2.5E-02
CG32182	FBgn0052182	2.45	9.8E-05
CG32191	FBgn0052191	-3.74	1.5E-37
CG32198	FBgn0052198	-6.55	1.0E-03
CG32225	FBgn0052225	-3.15	3.6E-02
CG3224	FBgn0029885	-0.90	7.4E-04
CG32243	FBgn0052243	0.92	1.2E-03
CG32249	FBgn0052249	-3.06	3.1E-02
CG32344	FBgn0052344	-0.73	3.7E-04
CG32407	FBgn0052407	-2.29	2.7E-06
CG32425	FBgn0052425	-1.71	6.0E-07
CG32428	FBgn0052428	-2.02	1.3E-13
CG32512	FBgn0052512	-1.03	4.1E-02
CG32521	FBgn0052521	-0.57	3.8E-02
CG32588	FBgn0052588	1.72	4.8E-02
CG3264	FBgn0034712	-3.33	2.3E-04
CG32647	FBgn0052647	-3.80	4.0E-23
CG32669	FBgn0052669	-2.47	1.2E-04
CG3270	FBgn0033093	-1.58	2.1E-02
CG32732	FBgn0052732	-0.58	5.0E-03
CG32762	FBgn0052762	4.71	2.0E-04
CG32795	FBgn0040384	-0.43	1.4E-02
CG32815	FBgn0052815	-1.61	3.0E-02
CG3292	FBgn0034710	-5.17	1.3E-11
CG32982	FBgn0052982	2.09	6.6E-07
CG33052	FBgn0053052	-1.44	4.8E-07
CG3176	FBgn0029524	1.02	2.0E-02
CG31769	FBgn0051769	-2.35	3.7E-07
CG31777	FBgn0051777	2.11	6.9E-03
CG31792	FBgn0051792	-4.06	3.8E-08
CG31806	FBgn0051806	1.75	4.1E-02
CG31915	FBgn0051915	-0.69	6.7E-03
CG31918	FBgn0031678	-1.36	3.1E-06
CG31954	FBgn0051954	6.35	1.5E-04
CG31955	FBgn0051955	2.01	2.6E-07
CG31974	FBgn0051974	2.64	5.8E-10
CG32054	FBgn0052054	-3.00	3.6E-02
CG32066	FBgn0052066	0.88	7.2E-04
CG33998	FBgn0053998	7.76	2.6E-13
CG34007	FBgn0054007	1.49	3.1E-02
CG34010	FBgn0054010	2.35	9.8E-06
CG34043	FBgn0054043	-1.11	4.4E-02
CG34159	FBgn0085188	0.60	4.9E-02
CG34170	FBgn0085199	2.39	1.8E-03
CG34193	FBgn0085222	4.19	6.7E-05
CG34206	FBgn0085235	3.52	3.2E-07
CG34236	FBgn0085265	2.45	5.9E-06
CG34244	FBgn0085273	4.79	8.0E-09
CG34253	FBgn0085282	0.97	9.6E-03
CG34256	FBgn0085285	1.32	1.4E-02
CG34276	FBgn0085305	-4.95	3.2E-04
CG34278	FBgn0085307	-4.26	2.8E-02
CG34291	FBgn0085320	-1.60	1.4E-02
CG34296	FBgn0085325	1.50	1.8E-02
CG34301	FBgn0085330	-2.56	2.3E-02
CG34316	FBgn0085345	-2.70	2.4E-02
CG34325	FBgn0085354	2.54	2.3E-08
CG34331	FBgn0085360	-1.63	9.3E-08
CG34332	FBgn0085361	2.40	1.7E-02
CG34340	FBgn0085369	-2.71	4.2E-04
CG34370	FBgn0085399	-1.55	3.1E-02
CG34376	FBgn0085405	1.58	2.2E-07
CG34404	FBgn0085433	0.77	3.5E-02
CG34408	FBgn0085437	-0.60	9.2E-03
CG34426	FBgn0085455	-1.93	1.6E-02
CG34460	FBgn0085489	1.80	2.5E-02
CG3505	FBgn0038250	1.17	3.0E-04

sym	*FBgn*	*Δlog2*	*padj*
CG33056	FBgn0053056	-0.79	2.2E-02
CG33080	FBgn0053080	2.68	1.5E-17
CG33090	FBgn0028916	-0.83	2.8E-02
CG33123	FBgn0053123	-1.22	4.6E-06
CG33230	FBgn0053230	-0.63	3.5E-02
CG33281	FBgn0053281	-2.70	8.8E-06
CG33303	FBgn0053303	-1.13	1.9E-05
CG33307	FBgn0053307	-1.64	4.3E-04
CG3332	FBgn0031514	-3.05	1.9E-05
CG33332	FBgn0067629	-0.70	4.7E-02
CG3335	FBgn0036018	-0.77	1.1E-02
CG3348	FBgn0040609	-2.52	9.3E-07
CG3355	FBgn0031619	3.84	3.8E-05
CG33947	FBgn0083068	1.22	1.2E-02
CG3868	FBgn0036422	-3.09	5.9E-03
CG3902	FBgn0036824	-1.36	5.5E-04
CG3939	FBgn0040396	0.94	1.6E-02
CG3940	FBgn0037788	2.80	2.6E-06
CG3961	FBgn0036821	-1.54	1.2E-05
CG3984	FBgn0038291	-2.74	1.6E-11
CG4038	FBgn0011824	-1.07	4.7E-04
CG4050	FBgn0020312	-0.48	2.0E-02
CG4078	FBgn0029798	-0.80	6.8E-03
CG4133	FBgn0031257	-1.79	1.9E-02
CG4151	FBgn0029770	4.77	3.7E-05
CG42235	FBgn0250757	-3.05	4.7E-07
CG42237	FBgn0250862	-2.71	3.2E-02
CG42268	FBgn0259163	-1.27	1.8E-02
CG42322	FBgn0259222	-2.44	1.9E-03
CG42355	FBgn0259701	1.66	3.6E-02
CG42361	FBgn0259707	-1.64	2.6E-02
CG42365	FBgn0259711	0.78	5.9E-03
CG42369	FBgn0259715	-2.21	8.4E-03
CG4239	FBgn0030745	-0.70	1.4E-02
CG42395	FBgn0259741	0.90	3.7E-02
CG42489	FBgn0259992	-2.91	8.7E-05
CG42492	FBgn0259994	-2.01	4.6E-02
CG42514	FBgn0260388	-2.37	3.3E-11
CG42524	FBgn0260429	-1.20	1.2E-03
CG42535	FBgn0260643	1.60	4.9E-02
CG42675	FBgn0261561	1.43	1.5E-02
CG3520	FBgn0034859	-0.62	3.9E-03
CG3529	FBgn0035995	-0.62	2.5E-02
CG3570	FBgn0035035	-0.82	2.3E-02
CG3588	FBgn0025643	-2.73	2.5E-03
CG3597	FBgn0031417	1.76	1.6E-02
CG3604	FBgn0031562	1.89	4.3E-02
CG3635	FBgn0032981	-2.26	9.1E-03
CG3662	FBgn0031285	-0.48	2.6E-02
CG3687	FBgn0034097	1.73	3.7E-02
CG3699	FBgn0040349	3.73	6.6E-16
CG3700	FBgn0034796	1.78	1.9E-03
CG3714	FBgn0031589	-1.56	6.9E-10
CG3726	FBgn0029824	1.48	3.1E-05
CG3775	FBgn0030425	-4.62	4.4E-22
CG42847	FBgn0262036	1.48	4.8E-05
CG42867	FBgn0262141	2.36	1.6E-03
CG42876	FBgn0262150	2.27	1.4E-04
CG4293	FBgn0024983	-1.05	4.2E-07
CG4301	FBgn0030747	-1.87	3.3E-04
CG4306	FBgn0036787	-0.84	3.7E-02
CG43061	FBgn0262363	1.94	3.0E-02
CG43078	FBgn0262508	-1.32	1.7E-03
CG43082	FBgn0262528	6.67	1.0E-06
CG43083	FBgn0262529	-3.17	1.5E-02
CG43085	FBgn0262531	-2.15	2.1E-03
CG43103	FBgn0262563	1.10	1.8E-03
CG43107	FBgn0262567	1.44	1.8E-02
CG43109	FBgn0262569	-2.08	6.0E-03
CG43139	FBgn0262613	-4.17	3.5E-02
CG43153	FBgn0262683	-2.33	1.2E-02
CG43165	FBgn0262721	-2.57	7.7E-05
CG43179	FBgn0262808	2.96	4.1E-05
CG43248	FBgn0262893	-2.15	3.1E-02
CG4325	FBgn0026878	-1.22	5.8E-04
CG43291	FBgn0262983	-1.98	8.6E-03
CG43313	FBgn0263005	-1.25	3.2E-04
CG43315	FBgn0263020	-6.82	3.2E-03
CG4332	FBgn0030456	-0.76	5.7E-04
CG43335	FBgn0263040	2.80	2.1E-03
CG43336	FBgn0263041	3.18	1.8E-03
CG4335	FBgn0038795	-1.63	1.6E-03

sym	*FBgn*	*Δlog2*	*padj*
CG42680	FBgn0261566	5.69	3.9E-14
CG4269	FBgn0034741	1.11	3.8E-05
CG42694	FBgn0261584	1.55	9.6E-09
CG42711	FBgn0261628	2.19	9.0E-03
CG42713	FBgn0261630	4.82	4.5E-03
CG42716	FBgn0261633	4.30	4.6E-02
CG42717	FBgn0261634	6.60	4.1E-11
CG42729	FBgn0261682	-4.58	1.5E-04
CG42733	FBgn0261686	1.88	3.8E-02
CG42748	FBgn0261802	-1.08	9.1E-03
CG42792	FBgn0261925	3.63	2.9E-05
CG42806	FBgn0261975	-1.01	2.9E-04
CG42807	FBgn0261989	1.52	1.3E-02
CG42817	FBgn0261999	1.85	1.8E-06
CG42832	FBgn0262021	-5.72	2.5E-02
CG42841	FBgn0262030	1.88	4.0E-02
CG44037	FBgn0264829	1.68	4.0E-02
CG4407	FBgn0030431	1.67	8.2E-06
CG44098	FBgn0264907	-2.38	8.1E-04
CG4433	FBgn0038763	-0.56	1.9E-02
CG44403	FBgn0265576	1.68	3.1E-02
CG44475	FBgn0265668	4.40	9.1E-06
CG4452	FBgn0035981	-0.89	4.7E-13
CG4462	FBgn0038752	-2.28	7.7E-03
CG4465	FBgn0038750	-2.94	3.2E-02
CG44956	FBgn0266261	-6.89	1.1E-07
CG4500	FBgn0028519	-2.55	1.7E-05
CG4502	FBgn0031896	0.97	4.9E-07
CG45057	FBgn0266417	-2.84	7.4E-04
CG45076	FBgn0266446	-2.19	2.1E-02
CG45081	FBgn0266456	6.48	3.0E-11
CG45486	FBgn0267042	1.95	2.5E-02
CG4554	FBgn0034734	-0.92	1.1E-02
CG4562	FBgn0038740	1.50	4.1E-03
CG4585	FBgn0025335	1.02	1.3E-06
CG4587	FBgn0028863	-1.87	2.7E-02
CG4607	FBgn0029932	-0.91	2.1E-02
CG4610	FBgn0034735	-0.47	4.2E-02
CG4615	FBgn0029935	-1.12	2.1E-03
CG4619	FBgn0032166	-1.14	3.3E-03
CG4702	FBgn0037992	2.10	4.8E-03
CG43394	FBgn0263256	-1.37	1.3E-02
CG43427	FBgn0263346	-1.36	3.4E-04
CG43446	FBgn0263400	1.94	3.2E-03
CG43618	FBgn0263596	2.50	3.8E-02
CG4362	FBgn0038784	3.69	1.3E-04
CG4363	FBgn0034663	-4.08	4.1E-02
CG43693	FBgn0263776	-1.83	7.8E-03
CG43737	FBgn0263994	-2.59	3.7E-02
CG43742	FBgn0263999	-3.46	8.4E-09
CG4375	FBgn0031295	1.63	4.3E-02
CG43778	FBgn0264308	-2.73	3.6E-03
CG43897	FBgn0264489	-1.54	2.8E-06
CG43921	FBgn0264542	-1.83	1.8E-02
CG4393	FBgn0039075	1.18	4.5E-03
CG44006	FBgn0264748	1.27	4.7E-02
CG44014	FBgn0264776	1.31	3.3E-04
CG5080	FBgn0031313	-1.06	5.6E-03
CG5096	FBgn0032235	-1.65	4.9E-02
CG5150	FBgn0035620	-5.43	3.2E-04
CG5151	FBgn0036576	-1.44	1.8E-03
CG5177	FBgn0031908	-1.83	3.7E-02
CG5191	FBgn0038803	1.02	1.7E-02
CG5210	FBgn0013763	-2.28	2.5E-06
CG5214	FBgn0037891	0.51	4.0E-05
CG5290	FBgn0036772	-1.46	2.2E-03
CG5321	FBgn0030575	-1.50	2.2E-02
CG5361	FBgn0037786	-1.80	4.0E-02
CG5377	FBgn0038974	0.83	1.1E-03
CG5391	FBgn0038943	-3.93	2.7E-03
CG5402	FBgn0039521	-3.71	8.6E-03
CG5404	FBgn0038354	-2.09	4.0E-02
CG5421	FBgn0032434	1.24	4.1E-02
CG5484	FBgn0039450	-0.64	6.4E-03
CG5493	FBgn0034364	0.76	3.1E-02
CG5527	FBgn0039564	-2.36	2.8E-05
CG5554	FBgn0034914	1.15	1.0E-02
CG5561	FBgn0031333	2.16	4.5E-02
CG5589	FBgn0036754	-0.98	3.4E-02
CG5618	FBgn0036975	1.74	2.2E-04
CG5697	FBgn0038846	5.58	1.5E-20
CG5707	FBgn0026593	-1.75	9.6E-04

sym	*FBgn*	*Δlog2*	*padj*
CG4716	FBgn0033820	-1.67	9.3E-04
CG4721	FBgn0039024	-3.02	2.5E-09
CG4723	FBgn0039023	-1.74	1.3E-10
CG4725	FBgn0039022	-3.70	2.7E-33
CG4752	FBgn0034733	-2.20	1.6E-06
CG4781	FBgn0035043	-1.68	7.2E-03
CG4793	FBgn0028514	-2.58	5.2E-10
CG4806	FBgn0260456	-0.63	1.4E-02
CG4835	FBgn0035607	-3.90	6.9E-03
CG4847	FBgn0034229	-3.10	1.6E-02
CG4968	FBgn0032214	0.51	3.6E-02
CG4995	FBgn0032219	-0.98	4.3E-02
CG5004	FBgn0260748	1.39	9.4E-05
CG5011	FBgn0040723	-4.99	9.2E-03
CG5022	FBgn0032225	-1.43	4.3E-02
CG5023	FBgn0038774	-3.21	2.0E-03
CG5033	FBgn0028744	-0.89	4.2E-03
CG5044	FBgn0038326	0.53	1.7E-02
CG6142	FBgn0039415	-3.27	4.1E-03
CG6175	FBgn0036152	0.67	4.2E-02
CG6178	FBgn0039156	-1.03	2.8E-02
CG6225	FBgn0038072	1.37	4.8E-02
CG6287	FBgn0032350	1.23	1.3E-03
CG6295	FBgn0039471	-5.26	2.0E-02
CG6296	FBgn0039470	-6.81	2.9E-04
CG6356	FBgn0039178	-2.33	5.9E-08
CG6357	FBgn0033875	1.44	3.0E-02
CG6415	FBgn0032287	-2.48	3.0E-05
CG6426	FBgn0034162	-3.05	3.3E-07
CG6428	FBgn0029689	-1.21	1.1E-03
CG6465	FBgn0037818	-1.57	1.5E-03
CG6574	FBgn0037846	-1.48	2.9E-05
CG6650	FBgn0036402	0.64	2.9E-05
CG6664	FBgn0036685	0.34	1.4E-02
CG6674	FBgn0036063	0.73	7.5E-04
CG6695	FBgn0039215	-0.60	4.7E-03
CG6701	FBgn0033889	0.80	2.6E-02
CG6707	FBgn0036058	0.92	1.6E-03
CG6712	FBgn0032408	-1.03	5.9E-03
CG6830	FBgn0037934	-2.85	1.6E-03
CG6836	FBgn0036834	1.96	3.2E-03
CG5724	FBgn0038082	-3.56	2.9E-03
CG5728	FBgn0039182	-0.79	4.3E-02
CG5746	FBgn0039186	-0.52	4.9E-02
CG5756	FBgn0034301	-5.12	3.2E-02
CG5781	FBgn0032448	1.82	4.5E-02
CG5789	FBgn0039207	-2.69	2.1E-09
CG5793	FBgn0038858	2.14	5.5E-05
CG5819	FBgn0034717	-1.40	1.7E-02
CG5885	FBgn0025700	-1.34	1.5E-09
CG5902	FBgn0039136	0.66	2.9E-03
CG5910	FBgn0036993	2.15	3.4E-09
CG5938	FBgn0046247	1.07	4.2E-07
CG5991	FBgn0026576	-0.96	2.6E-02
CG6006	FBgn0063649	-2.18	1.7E-02
CG6024	FBgn0036202	-2.02	2.3E-02
CG6067	FBgn0029828	1.00	4.5E-03
CG6084	FBgn0086254	0.97	7.7E-03
CG6091	FBgn0036180	0.51	2.7E-02
CG7252	FBgn0036226	-5.55	9.2E-05
CG7255	FBgn0036493	-3.70	1.7E-33
CG7265	FBgn0038272	-1.42	2.7E-02
CG7272	FBgn0036501	-2.31	3.5E-08
CG7276	FBgn0036499	1.91	2.9E-02
CG7298	FBgn0036948	-3.92	1.9E-02
CG7299	FBgn0032282	-3.44	6.7E-03
CG7320	FBgn0036782	-1.04	6.9E-03
CG7357	FBgn0038551	-0.40	2.5E-02
CG7367	FBgn0031976	2.16	4.7E-03
CG7369	FBgn0037188	-0.92	9.5E-04
CG7381	FBgn0038098	-2.61	2.2E-03
CG7402	FBgn0036768	-5.25	3.7E-07
CG7408	FBgn0036765	-1.07	5.5E-03
CG7456	FBgn0032258	-0.47	7.2E-03
CG7458	FBgn0037144	-1.74	1.4E-03
CG7460	FBgn0036749	0.77	2.9E-02
CG7523	FBgn0038533	-0.66	1.1E-03
CG7530	FBgn0038256	1.05	1.4E-02
CG7587	FBgn0038523	-6.68	8.8E-09
CG7606	FBgn0040565	-4.95	3.1E-05
CG7627	FBgn0032026	1.60	4.5E-05
CG7702	FBgn0038638	-0.86	1.2E-02

sym	*FBgn*	*Δlog2*	*padj*
CG6870	FBgn0032652	-3.07	1.3E-11
CG6891	FBgn0030955	1.23	1.7E-02
CG6910	FBgn0036262	-4.44	5.5E-20
CG6912	FBgn0038290	-2.10	6.7E-04
CG6933	FBgn0036952	-4.95	3.6E-04
CG6937	FBgn0038989	-0.74	4.9E-02
CG6961	FBgn0030959	0.64	4.7E-02
CG6966	FBgn0038286	0.83	4.8E-02
CG7016	FBgn0039238	-1.46	2.6E-10
CG7059	FBgn0038957	1.52	8.4E-03
CG7071	FBgn0260467	3.15	3.7E-11
CG7084	FBgn0038938	3.30	7.1E-07
CG7139	FBgn0027532	-0.79	1.7E-02
CG7149	FBgn0031948	-1.22	6.6E-05
CG7220	FBgn0033544	1.23	7.7E-03
CG7222	FBgn0033551	1.31	2.1E-06
CG7227	FBgn0031970	3.13	5.8E-10
CG7231	FBgn0031968	0.97	3.5E-03
CG7246	FBgn0030081	-0.94	3.3E-03
CG7248	FBgn0036229	-4.81	1.9E-03
CG8128	FBgn0030668	1.84	5.8E-11
CG8157	FBgn0034010	-2.12	3.2E-04
CG8160	FBgn0034011	-3.60	1.4E-08
CG8176	FBgn0037702	0.62	4.9E-02
CG8230	FBgn0027607	-1.11	2.2E-07
CG8249	FBgn0034045	2.26	3.9E-05
CG8299	FBgn0034052	2.23	2.8E-02
CG8311	FBgn0034141	-0.82	3.3E-02
CG8323	FBgn0033903	2.54	1.7E-14
CG8329	FBgn0036022	8.31	2.2E-04
CG8358	FBgn0037727	2.30	5.7E-05
CG8389	FBgn0034063	-0.96	4.8E-02
CG8405	FBgn0034071	1.02	4.4E-02
CG8412	FBgn0037743	-0.74	9.2E-03
CG8420	FBgn0037664	1.41	1.0E-02
CG8501	FBgn0033724	1.19	8.0E-05
CG8539	FBgn0035791	3.67	5.3E-15
CG8547	FBgn0033919	-1.81	2.2E-05
CG8550	FBgn0033742	-2.64	2.2E-09
CG8602	FBgn0035763	0.42	1.4E-02
CG8611	FBgn0027602	-0.72	2.2E-02
CG7728	FBgn0036686	-0.70	1.6E-02
CG7737	FBgn0033584	1.22	6.0E-03
CG7739	FBgn0036509	0.55	2.3E-02
CG7778	FBgn0032025	2.83	3.4E-04
CG7781	FBgn0032021	-1.82	1.4E-03
CG7845	FBgn0033059	-0.79	1.3E-02
CG7872	FBgn0030658	-0.83	7.9E-03
CG7906	FBgn0036417	4.50	3.0E-06
CG7924	FBgn0036416	5.26	6.2E-09
CG7968	FBgn0028532	-3.90	3.2E-02
CG7991	FBgn0035260	-1.44	3.2E-02
CG7992	FBgn0031004	-1.78	7.5E-04
CG8008	FBgn0033387	1.64	9.1E-03
CG8031	FBgn0038110	0.79	3.0E-02
CG8036	FBgn0037607	-1.14	1.4E-05
CG8046	FBgn0033388	1.82	7.1E-03
CG8083	FBgn0025709	-1.97	1.4E-06
CG8100	FBgn0036410	0.95	1.7E-02
CG8108	FBgn0027567	1.22	3.4E-04
CG8112	FBgn0037612	-1.18	2.8E-03
CG9259	FBgn0032913	-4.68	1.3E-23
CG9270	FBgn0032908	1.79	5.7E-05
CG9281	FBgn0030672	-0.67	5.7E-03
CG9286	FBgn0038183	-0.84	7.8E-03
CG9297	FBgn0038181	-2.74	5.7E-04
CG9304	FBgn0034674	0.95	2.3E-02
CG9305	FBgn0032512	-0.57	3.6E-02
CG9331	FBgn0032889	-1.94	2.6E-04
CG9394	FBgn0034588	-4.39	1.9E-02
CG9413	FBgn0030574	-2.33	4.0E-04
CG9426	FBgn0032485	0.42	1.6E-02
CG9447	FBgn0033110	-1.82	1.9E-02
CG9449	FBgn0036875	-1.32	3.5E-03
CG9497	FBgn0031800	3.19	3.2E-10
CG9505	FBgn0031805	-1.25	1.6E-02
CG9507	FBgn0031808	-2.40	9.8E-03
CG9522	FBgn0030587	1.94	4.7E-03
CG9527	FBgn0031813	-0.97	1.7E-04
CG9547	FBgn0031824	1.25	2.8E-02
CG9629	FBgn0036857	1.39	2.6E-04
CG9630	FBgn0037561	-0.72	6.9E-03

sym	*FBgn*	*Δlog2*	*padj*
CG8613	FBgn0033924	-0.79	6.0E-06
CG8641	FBgn0035733	-3.28	3.4E-06
CG8642	FBgn0033312	-1.43	2.7E-02
CG8665	FBgn0032945	-3.44	4.5E-10
CG8735	FBgn0033309	-0.72	4.9E-02
CG8738	FBgn0033321	2.15	2.0E-03
CG8740	FBgn0027585	-1.32	1.2E-03
CG8771	FBgn0033766	-0.88	6.1E-03
CG8773	FBgn0038135	-4.21	2.0E-03
CG8814	FBgn0031478	-0.75	4.2E-03
CG8854	FBgn0033702	3.39	2.0E-04
CG8888	FBgn0033679	-4.18	1.7E-04
CG8909	FBgn0030706	-1.75	4.7E-02
CG8939	FBgn0030720	-0.98	1.1E-03
CG9008	FBgn0028540	-1.83	1.0E-05
CG9040	FBgn0036394	-4.48	3.3E-04
CG9098	FBgn0031762	-2.31	1.1E-02
CG9175	FBgn0031779	-0.74	1.7E-02
CG9220	FBgn0030662	-1.71	2.3E-07
CG9246	FBgn0032925	-0.90	1.5E-03
CG9253	FBgn0032919	-0.92	2.0E-03
CG9257	FBgn0032916	-0.74	8.2E-03
CngB	FBgn0266346	-1.52	2.2E-02
CNMa	FBgn0035282	-2.37	1.5E-04
cnn	FBgn0013765	1.46	6.2E-07
Cog3	FBgn0031536	-0.74	2.5E-05
Cont	FBgn0037240	-0.73	7.3E-03
cora	FBgn0010434	-0.91	1.2E-03
Corin	FBgn0033192	1.48	9.9E-03
corn	FBgn0259173	-1.62	9.2E-06
coro	FBgn0265935	0.98	1.5E-08
corto	FBgn0010313	-0.62	3.4E-02
cpa	FBgn0034577	0.62	6.2E-03
cpb	FBgn0011570	0.72	1.3E-03
cpo	FBgn0263995	-1.13	3.9E-02
Cpr	FBgn0015623	0.88	4.6E-03
Cpr11A	FBgn0030394	-5.41	2.1E-04
Cpr49Ac	FBgn0033725	-1.24	1.1E-03
Cpr64Aa	FBgn0035510	-6.31	2.5E-04
Cpr67B	FBgn0035985	-4.36	3.6E-05
cpx	FBgn0041605	-1.48	2.6E-02
CG9650	FBgn0029939	-1.39	1.5E-02
CG9669	FBgn0036667	-0.69	1.5E-03
CG9674	FBgn0036663	-2.65	3.3E-19
CG9701	FBgn0036659	4.04	2.8E-06
CG9801	FBgn0037623	1.72	1.2E-04
CG9812	FBgn0034860	2.51	2.0E-04
CG9839	FBgn0037633	-1.16	1.0E-03
CG9849	FBgn0034803	-0.70	4.8E-04
CG9855	FBgn0037242	0.29	3.6E-02
CG9864	FBgn0034490	-2.48	1.4E-03
CG9896	FBgn0034808	-1.81	2.9E-02
CG9903	FBgn0030756	-3.04	2.3E-02
CG9928	FBgn0032472	-2.43	1.0E-02
CG9932	FBgn0262160	-1.03	3.4E-02
CG9990	FBgn0039594	-0.91	2.2E-02
CG9992	FBgn0030744	0.54	1.7E-02
cher	FBgn0014141	-2.83	3.2E-18
Cht4	FBgn0022700	3.02	4.5E-02
cib	FBgn0026084	1.41	2.8E-04
CkIIbeta2	FBgn0026136	1.76	4.8E-02
cln3	FBgn0036756	-1.40	4.2E-02
clumsy	FBgn0026255	-1.70	9.2E-03
CR44390	FBgn0265540	1.32	5.7E-04
CR44414	FBgn0265587	4.33	4.2E-03
CR44510	FBgn0265703	-2.02	2.5E-04
CR44599	FBgn0265810	-1.43	4.1E-02
CR44602	FBgn0265813	2.60	1.6E-02
CR44616	FBgn0265827	2.49	2.9E-02
CR44632	FBgn0265843	-3.51	2.5E-10
CR44640	FBgn0265851	-4.53	6.6E-03
CR44727	FBgn0265940	2.24	1.4E-02
CR44756	FBgn0265977	2.58	1.3E-02
CR44846	FBgn0266140	2.73	4.6E-02
CR44912	FBgn0266217	4.23	3.6E-05
CR44977	FBgn0266312	1.72	3.4E-02
CR44987	FBgn0266322	-1.63	3.5E-02
CR45004	FBgn0266356	4.06	8.4E-05
CR45007	FBgn0266359	-3.74	7.7E-03
CR45018	FBgn0266376	1.09	7.3E-03
CR45043	FBgn0266403	5.35	2.6E-03
CR45048	FBgn0266408	0.94	4.6E-02

sym	*FBgn*	*Δlog2*	*padj*
CR31144	FBgn0051144	2.04	2.3E-02
CR31781	FBgn0051781	-1.75	1.9E-02
CR32194	FBgn0052194	1.05	2.9E-02
CR34044	FBgn0054044	-2.39	6.5E-03
CR42746	FBgn0261709	2.89	1.2E-02
CR42791	FBgn0261924	3.29	2.6E-03
CR43279	FBgn0262968	1.71	4.1E-02
CR43283	FBgn0262972	-2.44	1.7E-02
CR43297	FBgn0262989	1.82	5.0E-02
CR43300	FBgn0262992	1.95	7.5E-03
CR43428	FBgn0263376	5.83	7.7E-04
CR43451	FBgn0263405	2.84	5.0E-02
CR43459	FBgn0263413	-1.96	7.2E-04
CR43493	FBgn0263504	-1.45	5.6E-03
CR43626	FBgn0263617	-1.40	1.0E-02
CR43641	FBgn0263650	2.53	3.2E-05
CR43727	FBgn0263975	0.88	1.4E-02
CR43751	FBgn0265017	1.89	3.7E-02
CR43808	FBgn0264352	-3.90	1.8E-02
CR43864	FBgn0264446	-1.88	2.9E-03
CR43928	FBgn0264549	-2.06	2.5E-03
CR44135	FBgn0264984	2.02	1.4E-05
CR44179	FBgn0265068	-0.84	1.8E-02
CR44192	FBgn0265081	-2.54	3.7E-02
csul	FBgn0015925	-0.65	1.7E-02
Ctr1A	FBgn0062413	0.77	4.0E-02
cu	FBgn0261808	1.57	2.4E-04
cue	FBgn0011204	-1.42	6.3E-05
Cul1	FBgn0015509	0.72	1.3E-03
Cul2	FBgn0032956	-0.99	1.5E-03
CYLD	FBgn0032210	0.85	2.2E-03
Cyp12a5	FBgn0038680	-3.88	3.5E-08
Cyp12b2	FBgn0034387	-1.54	3.5E-02
Cyp12e1	FBgn0037817	-0.97	2.9E-02
Cyp28a5	FBgn0028940	-3.99	1.3E-20
Cyp304a1	FBgn0038095	-1.89	3.1E-05
Cyp309a1	FBgn0031432	2.00	3.0E-03
Cyp309a2	FBgn0041337	1.58	3.2E-02
Cyp4aa1	FBgn0034053	2.68	4.7E-04
Cyp4ac1	FBgn0031693	-3.95	1.8E-18
Cyp4ac2	FBgn0031694	-4.36	6.4E-07
CR45108	FBgn0266577	-2.37	4.3E-03
CR45145	FBgn0266638	4.86	1.9E-11
CR45242	FBgn0266777	-3.20	1.4E-02
CR45264	FBgn0266802	1.31	2.1E-02
CR45265	FBgn0266803	3.66	7.6E-04
CR45321	FBgn0266860	1.45	2.2E-02
CR45382	FBgn0266931	-1.91	3.7E-02
CR45397	FBgn0266946	2.95	2.6E-02
CR45424	FBgn0266973	2.47	7.1E-03
CR45431	FBgn0266980	3.31	2.4E-02
CR45445	FBgn0266994	-1.94	8.2E-03
CR45522	FBgn0267078	4.86	2.3E-02
CR45593	FBgn0267153	1.74	9.1E-04
CR45722	FBgn0267286	3.70	2.4E-05
CR45755	FBgn0267319	-2.66	4.7E-02
CrebA	FBgn0004396	-1.55	2.2E-07
CREG	FBgn0025456	0.76	4.1E-02
CRMP	FBgn0023023	1.88	7.3E-05
crq	FBgn0015924	0.95	2.0E-04
cry	FBgn0025680	2.23	1.2E-03
Crz	FBgn0013767	-2.20	4.7E-02
CrzR	FBgn0036278	-2.47	1.8E-03
CS-2	FBgn0029091	-1.64	2.7E-02
CSN7	FBgn0028836	0.39	5.4E-03
dco	FBgn0002413	0.53	3.1E-02
Dd	FBgn0029067	0.95	5.4E-03
Decay	FBgn0028381	-2.44	9.0E-06
Def	FBgn0010385	5.03	3.2E-04
Desat1	FBgn0086687	-1.71	1.8E-05
Df31	FBgn0022893	-0.91	2.0E-02
Dh31-R	FBgn0052843	-1.26	1.4E-02
Dh44-R2	FBgn0033744	-1.29	2.6E-02
dia	FBgn0011202	1.11	1.6E-02
Dip-B	FBgn0000454	1.16	4.8E-02
dmGlut	FBgn0010497	5.15	2.5E-26
Dmtn	FBgn0037443	0.97	2.2E-02
dpp	FBgn0000490	1.96	1.2E-07
dpr12	FBgn0085414	-2.41	3.4E-05
Drat	FBgn0033188	-0.83	3.3E-02
drd	FBgn0260006	-2.73	3.7E-04
dre4	FBgn0002183	-0.44	3.7E-02

sym	*FBgn*	*Δlog2*	*padj*
Cyp4ac3	FBgn0031695	-3.37	2.7E-04
Cyp4ad1	FBgn0033292	-2.05	5.1E-09
Cyp4d2	FBgn0011576	-1.36	3.6E-02
Cyp4e3	FBgn0015035	-3.36	3.7E-03
Cyp4g15	FBgn0030304	-3.68	8.5E-04
Cyp4p1	FBgn0015037	-1.95	7.1E-05
Cyp4p2	FBgn0033395	-3.08	4.6E-04
Cyp4p3	FBgn0033397	-2.17	3.9E-04
Cyp4s3	FBgn0030615	-2.05	1.2E-04
Cyp6a18	FBgn0039519	-3.38	1.5E-04
Cyp6a23	FBgn0033978	-2.19	4.2E-06
Cyp6a9	FBgn0013771	-2.30	3.5E-05
Cyp6g1	FBgn0025454	-2.85	3.0E-10
Cyp6g2	FBgn0033696	-1.54	2.4E-04
Cyp6t3	FBgn0033697	-5.43	4.6E-08
Cyp6w1	FBgn0033065	-3.88	9.0E-06
Cyp9b1	FBgn0015038	-3.07	2.4E-09
Cyp9b2	FBgn0015039	-1.90	1.9E-03
Cyp9f2	FBgn0038037	-2.25	1.1E-06
Cys	FBgn0004629	2.01	4.6E-06
D2hgdh	FBgn0023507	1.91	3.0E-03
dac	FBgn0005677	-0.88	4.8E-02
Dad	FBgn0020493	-0.63	4.6E-02
Dak1	FBgn0028833	-0.81	8.4E-03
Dap160	FBgn0023388	-0.60	2.9E-02
daw	FBgn0031461	-1.01	4.3E-03
egh	FBgn0001404	-0.70	4.9E-02
egr	FBgn0033483	-1.65	9.6E-09
eIF-2alpha	FBgn0261609	-0.63	4.5E-02
eIF-2beta	FBgn0004926	-0.96	6.0E-05
eIF-2gamma	FBgn0263740	-0.89	2.0E-03
eIF3-S9	FBgn0034237	-0.56	1.3E-02
Eig71Ea	FBgn0004588	5.56	3.5E-09
Eig71Eb	FBgn0004589	5.79	8.2E-08
Eig71Ec	FBgn0004590	5.57	6.8E-05
Eig71Ed	FBgn0004591	5.52	2.9E-06
Eig71Ee	FBgn0004592	-6.73	3.0E-11
Eig71Ef	FBgn0004593	7.65	8.4E-12
Eig71Eg	FBgn0004594	5.62	2.7E-07
Eig71Eh	FBgn0014848	9.67	6.1E-07
Eig71Ei	FBgn0014849	8.18	2.4E-07

sym	*FBgn*	*Δlog2*	*padj*
Dref	FBgn0015664	-0.75	5.1E-03
Drep1	FBgn0024732	1.00	1.0E-02
drk	FBgn0004638	-1.56	7.8E-09
Dronc	FBgn0026404	1.63	9.8E-08
drosha	FBgn0026722	-0.42	4.3E-02
Drs	FBgn0283461	2.36	4.5E-04
Drsl1	FBgn0052274	-4.41	4.6E-03
Drsl2	FBgn0052279	4.98	5.2E-06
Drsl5	FBgn0035434	2.15	3.3E-04
Dscam2	FBgn0265296	-2.55	1.7E-02
Dtg	FBgn0038071	1.76	5.8E-06
dve	FBgn0020307	-1.67	1.1E-02
Dyb	FBgn0033739	-0.91	3.5E-03
Dyrk2	FBgn0016930	2.50	2.2E-07
dysc	FBgn0264006	-1.62	5.9E-03
e	FBgn0000527	3.29	4.1E-05
E(spl)m5-HLH	FBgn0002631	-1.38	2.4E-02
E2f1	FBgn0011766	-0.68	7.8E-03
Eaat1	FBgn0026439	-4.94	6.8E-32
eag	FBgn0000535	-1.88	2.3E-02
eater	FBgn0243514	-2.30	1.1E-05
Eb1	FBgn0027066	0.79	3.6E-03
EcR	FBgn0000546	-2.32	8.3E-10
edl	FBgn0023214	-1.07	7.3E-03
eEF1delta	FBgn0032198	-0.56	3.5E-02
Efr	FBgn0029849	-1.23	6.7E-03
FoxP	FBgn0262477	-2.25	4.6E-02
Fpps	FBgn0025373	-0.75	1.1E-02
frma	FBgn0029769	-2.60	7.0E-05
fru	FBgn0004652	-1.81	3.8E-05
Fst	FBgn0037724	-2.40	6.3E-04
FucTA	FBgn0036485	-2.61	1.6E-02
Fur1	FBgn0004509	1.02	1.4E-02
fus	FBgn0023441	1.04	7.8E-03
fuss	FBgn0039932	1.11	4.1E-02
futsch	FBgn0259108	-1.40	4.3E-02
Gad1	FBgn0004516	-2.41	8.4E-03
Gadd34	FBgn0034948	0.52	3.9E-02
Gal	FBgn0001089	2.06	1.7E-04
galectin	FBgn0031213	-0.80	8.4E-03
Galphai	FBgn0001104	2.00	8.7E-17

sym	*FBgn*	*Δlog2*	*padj*
Eip71CD	FBgn0000565	1.07	5.4E-03
Eip93F	FBgn0264490	3.60	3.1E-12
Elk	FBgn0011589	-2.15	3.2E-03
Elp2	FBgn0033540	-0.71	1.3E-02
emp	FBgn0010435	0.63	4.4E-03
endos	FBgn0061515	0.53	1.6E-03
ergic53	FBgn0035909	-1.04	1.1E-03
erm	FBgn0031375	-2.80	3.3E-02
Est-6	FBgn0000592	-2.08	1.4E-04
Est-Q	FBgn0037090	-3.53	7.0E-09
Exn	FBgn0261547	1.15	6.7E-04
Exo84	FBgn0266668	0.49	2.9E-02
Ext2	FBgn0029175	0.67	1.6E-03
ey	FBgn0005558	-1.19	4.0E-03
Fak	FBgn0020440	1.37	1.5E-04
FASN1	FBgn0283427	-3.06	7.1E-10
fbl	FBgn0011205	-0.91	5.8E-04
Fbp2	FBgn0000640	1.15	8.7E-03
Fcp3C	FBgn0000644	1.34	3.6E-03
fd59A	FBgn0004896	-3.70	2.5E-02
Fer1HCH	FBgn0015222	0.99	2.1E-03
Fgop2	FBgn0031871	0.66	9.4E-04
Fim	FBgn0024238	1.07	4.7E-05
FK506-bp1	FBgn0013269	-0.74	7.1E-04
Flo2	FBgn0264078	-0.62	2.5E-02
Fmo-2	FBgn0033079	3.30	2.8E-05
fok	FBgn0263773	2.38	1.6E-06
fon	FBgn0032773	-2.71	1.5E-06
GstD1	FBgn0001149	1.32	2.6E-02
GstD5	FBgn0010041	2.93	5.8E-05
GstE10	FBgn0063499	-3.35	1.3E-06
GstE3	FBgn0063497	-1.97	4.6E-04
GstE7	FBgn0063493	-1.59	2.2E-02
GstZ2	FBgn0037697	-2.04	3.3E-02
GXIVsPLA2	FBgn0036545	-0.75	3.6E-02
Hdc	FBgn0005619	3.17	7.4E-07
hebe	FBgn0033448	-1.40	2.2E-02
Hex-C	FBgn0001187	2.69	3.9E-03
HisCl1	FBgn0037950	2.82	1.5E-07
Hml	FBgn0029167	-3.43	5.4E-13
Hmx	FBgn0264005	-2.98	4.0E-02
gammaCOP	FBgn0028968	-0.72	4.5E-02
Gapdh2	FBgn0001092	0.94	6.2E-03
Gasp	FBgn0026077	1.48	4.2E-03
Gat	FBgn0039915	-1.29	1.0E-03
GATAe	FBgn0038391	-1.63	2.2E-03
Gbp	FBgn0034199	1.98	2.9E-06
Gbs-76A	FBgn0036862	-1.13	4.3E-03
gcl	FBgn0005695	0.78	7.4E-04
Gclc	FBgn0040319	-1.18	7.0E-04
GCS2beta	FBgn0032643	-0.52	3.0E-02
Gdap1	FBgn0035587	1.51	2.9E-02
Gie	FBgn0037551	0.90	1.4E-03
GIIIspla2	FBgn0030013	-1.28	5.1E-06
gish	FBgn0250823	0.59	4.8E-02
glob3	FBgn0037385	1.64	3.7E-02
GLS	FBgn0261625	-2.31	2.0E-08
GM130	FBgn0034697	-0.92	1.0E-03
Gmer	FBgn0267823	-0.84	3.3E-04
Gnmt	FBgn0038074	-1.77	4.4E-02
Got2	FBgn0001125	1.16	6.6E-03
Gp210	FBgn0266580	-0.78	6.7E-04
Gp93	FBgn0039562	-1.29	1.8E-05
Gpo-1	FBgn0022160	1.76	4.3E-03
Gr97a	FBgn0041224	2.45	6.6E-03
Grasp65	FBgn0036919	-1.02	3.0E-04
Grip	FBgn0029830	1.27	4.3E-03
Grip91	FBgn0001612	-0.92	3.0E-03
Gs2	FBgn0001145	-2.15	1.3E-04
Ir54a	FBgn0034272	2.24	4.5E-02
Irk1	FBgn0265042	1.93	3.3E-09
Irk3	FBgn0032706	-3.43	6.9E-15
Irp-1B	FBgn0024957	1.47	3.3E-04
IscU	FBgn0037637	0.82	3.0E-04
Itgbn	FBgn0010395	-1.97	1.4E-03
Jafrac1	FBgn0040309	0.81	1.6E-02
jagn	FBgn0037374	-0.54	1.4E-02
jdp	FBgn0027654	-1.28	4.4E-07
Jhe	FBgn0010052	-1.51	3.1E-03
Jhedup	FBgn0034076	-3.69	4.0E-05
JhI-1	FBgn0028426	-0.61	9.7E-03
Jon25Bii	FBgn0031654	-4.41	6.0E-03

sym	*FBgn*	*Δlog2*	*padj*
Ho	FBgn0037933	0.59	1.9E-02
Hph	FBgn0264785	-0.60	1.4E-03
Hr46	FBgn0000448	2.11	5.0E-04
Hr78	FBgn0015239	-0.50	2.9E-03
Hsc70-4	FBgn0266599	-0.47	2.6E-02
Hsp23	FBgn0001224	1.38	7.3E-03
Hsp68	FBgn0001230	-2.11	3.0E-03
Hsp70Ba	FBgn0013277	-3.58	6.8E-05
Hsp70Bb	FBgn0013278	-3.22	4.1E-04
Hsp70Bbb	FBgn0051354	-3.39	1.8E-04
Hsp83	FBgn0001233	-0.92	4.7E-02
HtrA2	FBgn0038233	0.64	3.3E-03
hyx	FBgn0037657	-0.58	2.7E-02
Ibf1	FBgn0037670	-0.66	4.8E-02
Idgf4	FBgn0026415	-1.23	6.8E-04
Idgf5	FBgn0064237	-2.33	3.8E-04
if	FBgn0001250	-0.85	2.1E-03
Ih	FBgn0263397	0.91	3.0E-02
IKKbeta	FBgn0024222	0.74	2.3E-02
Ilp8	FBgn0036690	3.71	1.5E-04
imd	FBgn0013983	0.86	7.3E-03
ImpL1	FBgn0001256	2.71	1.9E-02
ImpL2	FBgn0001257	-2.83	1.9E-21
Indy	FBgn0036816	1.02	3.4E-02
Inos	FBgn0025885	-1.49	2.2E-03
insc	FBgn0011674	1.95	1.3E-05
IntS2	FBgn0030858	-1.04	3.1E-06
Inx5	FBgn0030989	1.62	3.9E-02
IP3K1	FBgn0032147	-0.73	4.9E-02
Ipk1	FBgn0050295	-1.06	5.8E-04
Lac	FBgn0010238	-1.16	5.6E-04
lace	FBgn0002524	0.85	4.2E-03
LamC	FBgn0010397	-2.18	3.3E-17
lap	FBgn0086372	0.77	2.9E-02
laza	FBgn0037163	-2.09	3.3E-11
lbk	FBgn0034083	-1.84	6.0E-15
Lcp1	FBgn0002531	-5.77	9.6E-09
Lcp2	FBgn0002533	-4.51	1.1E-05
Lcp4	FBgn0002535	-3.67	4.4E-04
lcs	FBgn0028583	-4.68	2.2E-03
Letm1	FBgn0019886	0.69	2.9E-02

sym	*FBgn*	*Δlog2*	*padj*
Jon25Biii	FBgn0031653	-4.64	1.2E-02
Jon65Aiii	FBgn0035665	-3.71	2.0E-02
Jon65Aiv	FBgn0250815	-3.32	4.1E-02
Jon66Ci	FBgn0035886	-4.80	1.0E-02
Jon66Cii	FBgn0035887	-4.86	5.5E-03
Jon74E	FBgn0023197	-7.49	2.8E-07
jumu	FBgn0015396	-1.06	3.9E-03
Jupiter	FBgn0051363	1.23	1.4E-05
Kal1	FBgn0039155	-2.53	6.2E-33
kappaB-Ras	FBgn0040513	-1.83	1.2E-02
Karybeta3	FBgn0087013	-0.63	6.9E-03
Kat60	FBgn0040208	-0.65	8.0E-03
Kaz-m1	FBgn0002578	-4.66	4.1E-03
KFase	FBgn0031821	-1.73	2.7E-02
kn	FBgn0001319	-1.00	2.4E-02
ko	FBgn0020294	-0.94	3.6E-03
Kr-h2	FBgn0266449	-0.43	7.6E-03
kz	FBgn0001330	-0.84	7.5E-03
l(1)G0007	FBgn0026713	-0.92	2.8E-02
l(1)G0020	FBgn0027330	-0.92	2.7E-03
l(1)G0193	FBgn0027280	1.15	1.2E-06
l(1)G0196	FBgn0027279	-1.67	1.7E-08
l(1)G0320	FBgn0028327	-1.20	3.0E-06
l(2)34Fd	FBgn0261535	-1.03	6.7E-03
l(2)efl	FBgn0011296	-2.70	1.0E-03
l(2)k01209	FBgn0022029	-0.75	4.2E-02
l(2)k09022	FBgn0086451	-0.91	6.8E-03
l(2)k12914	FBgn0263852	-0.65	4.8E-02
l(3)07882	FBgn0010926	-0.77	3.7E-02
l(3)72Dn	FBgn0263605	-0.84	2.7E-02
meigo	FBgn0250820	-1.36	8.2E-09
Mekk1	FBgn0024329	-0.61	1.9E-02
melt	FBgn0023001	-1.35	1.1E-02
Meltrin	FBgn0265140	1.56	1.6E-05
Membrin	FBgn0260856	-0.91	1.1E-02
Men	FBgn0002719	1.40	4.5E-02
mesh	FBgn0051004	-1.25	4.3E-02
mew	FBgn0004456	-0.87	6.1E-03
mex1	FBgn0004228	-2.38	3.0E-02
Mf	FBgn0038294	-2.31	3.2E-04
mfas	FBgn0260745	1.51	8.9E-04

sym	*FBgn*	*Δlog2*	*padj*
Lgr1	FBgn0016650	-2.18	5.0E-03
lin-28	FBgn0035626	-2.13	2.0E-02
Lint-1	FBgn0030274	1.11	2.1E-02
Lip3	FBgn0023495	-3.73	2.4E-04
List	FBgn0034381	2.14	5.0E-03
lost	FBgn0263594	-0.61	2.3E-04
LpR1	FBgn0066101	-1.07	2.1E-02
lqfR	FBgn0261279	-0.65	1.4E-03
Lrt	FBgn0034540	-2.05	2.7E-11
Lsp1alpha	FBgn0002562	-1.84	3.3E-02
Lsp1beta	FBgn0002563	-3.03	1.7E-16
Lsp1gamma	FBgn0002564	-2.22	4.1E-08
Lst	FBgn0034140	-1.53	5.0E-04
ltl	FBgn0268063	-1.06	3.7E-03
lva	FBgn0029688	-0.94	3.4E-02
LysB	FBgn0004425	-4.98	6.0E-03
LysD	FBgn0004427	-4.47	2.1E-03
LysP	FBgn0004429	-3.75	3.5E-02
mag	FBgn0036996	-7.91	1.1E-05
MAGE	FBgn0037481	-0.73	3.9E-02
magu	FBgn0262169	-1.78	2.1E-05
mahj	FBgn0034641	-0.72	9.1E-03
Mal-A1	FBgn0002570	-4.53	4.8E-03
Mal-A7	FBgn0033296	3.01	8.7E-06
Manf	FBgn0027095	-0.83	5.4E-03
Mat1	FBgn0024956	-0.68	3.1E-05
Mct1	FBgn0023549	-1.58	1.4E-06
Mdh2	FBgn0262559	-0.85	8.6E-03
Mdr49	FBgn0004512	0.99	1.6E-02
Mdr50	FBgn0010241	-2.33	1.5E-02
Mdr65	FBgn0004513	-2.34	4.2E-03
mei-41	FBgn0004367	-0.79	6.0E-03
Msr-110	FBgn0015766	-1.55	3.4E-05
Mst87F	FBgn0002862	1.71	1.9E-05
mtd	FBgn0013576	1.39	9.8E-09
mth	FBgn0023000	0.65	6.2E-05
mthl15	FBgn0051720	-1.38	4.5E-02
mthl6	FBgn0035789	-3.55	1.2E-04
Muc11A	FBgn0052656	-2.72	4.3E-08
Muc26B	FBgn0040950	-5.04	4.1E-02
Muc68Ca	FBgn0036181	-6.22	2.0E-08
mfrn	FBgn0039561	1.25	3.9E-05
MFS12	FBgn0033234	2.03	1.3E-03
MFS14	FBgn0010651	1.05	5.1E-03
MFS18	FBgn0025684	-1.65	3.2E-07
Mgat1	FBgn0034521	-0.76	9.9E-03
Mhc	FBgn0264695	-2.16	1.2E-03
mi	FBgn0261786	-0.71	3.1E-02
mib2	FBgn0086442	0.66	1.7E-02
Mid1	FBgn0053988	-2.00	2.0E-02
mip120	FBgn0033846	-0.72	1.5E-02
mip40	FBgn0034430	0.94	1.6E-02
miple2	FBgn0029002	1.26	1.1E-03
mir-2a-1	FBgn0262377	-4.05	5.1E-05
mir-2a-2	FBgn0262460	-2.22	8.3E-05
Mlc1	FBgn0002772	-1.66	3.4E-02
Mlf	FBgn0034051	0.46	3.9E-03
Mlp60A	FBgn0259209	-2.25	3.2E-02
Mmp1	FBgn0035049	1.34	2.9E-03
Mmp2	FBgn0033438	2.64	2.4E-08
Mnn1	FBgn0031885	-0.58	1.6E-02
Mob2	FBgn0259481	-0.69	2.0E-02
mod	FBgn0002780	-0.82	3.8E-02
modSP	FBgn0051217	1.27	1.9E-06
Moe	FBgn0011661	-0.79	2.7E-04
Mon1	FBgn0031640	0.48	4.1E-02
mor	FBgn0002783	-0.45	6.8E-03
Mp	FBgn0260660	1.29	2.4E-03
Mp20	FBgn0002789	-2.74	3.6E-04
Mppe	FBgn0259985	-0.80	1.4E-03
mrj	FBgn0034091	0.93	5.5E-05
MRP	FBgn0032456	1.48	7.5E-04
msk	FBgn0026252	-0.90	6.8E-04
Nop60B	FBgn0259937	-0.94	8.6E-03
Nopp140	FBgn0037137	-0.64	1.1E-02
Nost	FBgn0259734	-1.32	1.7E-04
Nox	FBgn0085428	-1.59	2.1E-02
Npc2a	FBgn0031381	1.41	8.8E-03
Npc2c	FBgn0037783	-7.31	2.6E-03
Npc2g	FBgn0039800	-0.90	1.8E-02
Npc2h	FBgn0039801	-2.86	6.8E-11
NPF	FBgn0027109	-3.05	1.5E-02

sym	*FBgn*	*Δlog2*	*padj*
Muc96D	FBgn0051439	-5.86	7.2E-07
Myc	FBgn0262656	-1.45	3.9E-07
Myo28B1	FBgn0040299	-1.50	3.0E-02
Mys45A	FBgn0033379	-0.67	1.7E-02
nab	FBgn0259986	-2.00	1.6E-02
nAChRbeta3	FBgn0031261	1.73	6.1E-03
Nap1	FBgn0015268	-0.74	2.3E-02
Nbr	FBgn0032924	-0.37	2.5E-02
Nc73EF	FBgn0010352	-0.74	2.2E-02
Ncc69	FBgn0036279	-0.96	1.0E-02
ncm	FBgn0086707	-0.87	1.8E-03
Ndae1	FBgn0259111	-2.11	2.0E-07
Ndc1	FBgn0039125	-0.46	2.8E-02
neb	FBgn0004374	2.24	3.5E-04
nerfin-1	FBgn0028999	-3.10	1.4E-02
ng2	FBgn0010294	-5.82	3.6E-03
Nha2	FBgn0263390	-2.76	1.8E-08
NHP2	FBgn0029148	-0.88	4.1E-02
NijA	FBgn0036101	1.29	1.2E-02
niki	FBgn0045980	-2.70	3.0E-08
NimB5	FBgn0028936	-2.17	1.9E-11
NimC3	FBgn0001967	1.40	3.9E-02
NimC4	FBgn0260011	5.13	2.0E-03
ninaC	FBgn0002938	-3.13	1.7E-02
ninaD	FBgn0002939	-3.33	2.6E-05
NKAIN	FBgn0085442	0.98	1.9E-02
NLaz	FBgn0053126	2.16	2.7E-05
Nlp	FBgn0016685	-0.88	1.3E-03
Nmd3	FBgn0023542	-0.78	1.1E-02
Nmdmc	FBgn0010222	1.83	4.1E-05
Nmnat	FBgn0039254	0.46	1.9E-02
noc	FBgn0005771	-0.58	2.8E-02
nom	FBgn0037617	0.73	3.4E-02
nop5	FBgn0026196	-0.79	3.6E-02
Papss	FBgn0020389	-1.06	3.3E-03
PCB	FBgn0027580	-1.07	2.5E-02
Pde6	FBgn0038237	-0.91	2.2E-02
Pdfr	FBgn0260753	-2.34	1.8E-04
Pdi	FBgn0014002	-1.50	9.0E-06
Pdk1	FBgn0020386	-1.44	6.4E-08
pdm3	FBgn0261588	-1.03	2.7E-02
Nplp4	FBgn0040717	-2.54	9.3E-03
Nrg	FBgn0264975	-1.34	5.8E-09
nrv3	FBgn0032946	-2.33	3.7E-03
Ns2	FBgn0034243	-0.56	4.0E-03
Ns3	FBgn0266284	-0.86	3.1E-05
Ns4	FBgn0032882	-0.43	1.6E-02
Nup154	FBgn0021761	-0.63	1.0E-02
Nup205	FBgn0031078	-0.86	6.2E-03
Nup50	FBgn0033264	-0.57	6.1E-03
Nup93-1	FBgn0027537	-0.60	1.6E-02
Oatp30B	FBgn0032123	1.06	1.0E-02
Oatp58Db	FBgn0034715	-2.14	1.3E-06
Obp49a	FBgn0050052	-2.24	2.4E-03
Obp56d	FBgn0034470	2.91	4.7E-03
obst-H	FBgn0053983	-1.91	3.5E-02
Odc1	FBgn0013307	-1.24	5.7E-03
Odc2	FBgn0013308	-2.00	3.2E-06
onecut	FBgn0028996	-1.93	3.3E-02
Or10a	FBgn0030298	-3.74	4.2E-03
Orc2	FBgn0015270	-0.94	8.8E-03
Ork1	FBgn0017561	1.90	1.6E-02
Oscillin	FBgn0031717	-1.80	2.2E-09
Osi15	FBgn0037424	4.24	7.6E-03
Osi7	FBgn0037414	2.92	4.4E-02
OstDelta	FBgn0034277	-1.19	3.2E-06
Ostgamma	FBgn0032015	-0.92	1.7E-04
OstStt3	FBgn0011336	-1.32	5.9E-11
out	FBgn0259834	0.87	8.4E-03
p120ctn	FBgn0260799	0.49	3.7E-02
p24-1	FBgn0030341	-0.85	4.8E-04
P58IPK	FBgn0037718	-1.14	4.1E-05
Pabp2	FBgn0005648	-0.76	1.9E-02
Pak	FBgn0267698	1.23	3.4E-05
PAPLA1	FBgn0031990	-1.01	1.8E-02
Poxm	FBgn0003129	1.21	8.4E-03
Ppa	FBgn0020257	0.89	9.0E-03
ppk10	FBgn0065110	1.22	5.9E-03
ppk19	FBgn0039679	-2.40	3.5E-03
ppk22	FBgn0051105	1.80	7.5E-03
pr	FBgn0003141	-0.81	2.5E-02
Prm	FBgn0003149	-1.93	9.0E-03

sym	*FBgn*	*Δlog2*	*padj*
peb	FBgn0003053	-1.04	4.7E-02
per	FBgn0003068	-2.48	8.9E-04
Pex14	FBgn0037020	-0.65	1.6E-02
Pfk	FBgn0003071	1.19	7.2E-04
pgant3	FBgn0027558	-0.40	4.7E-02
pgant6	FBgn0035375	-0.98	7.5E-04
PGRP-LA	FBgn0035975	1.58	4.0E-04
PGRP-LC	FBgn0035976	1.29	1.2E-05
PGRP-LD	FBgn0260458	-2.45	1.5E-03
PGRP-SB1	FBgn0043578	1.40	4.9E-02
PGRP-SB2	FBgn0043577	5.08	1.3E-04
PH4alphaPV	FBgn0051015	-2.78	5.3E-03
PH4alphaSG1	FBgn0051014	-5.39	1.2E-03
PH4alphaSG2	FBgn0039779	-6.33	9.9E-04
Phae2	FBgn0263235	-3.33	4.4E-03
PHGPx	FBgn0035438	0.67	1.9E-02
PI31	FBgn0033669	0.60	5.7E-04
pic	FBgn0260962	-0.35	1.5E-02
Piezo	FBgn0264953	-2.01	3.0E-11
Pig1	FBgn0003086	-5.02	6.0E-05
Pino	FBgn0016926	-1.69	3.4E-09
PIP4K	FBgn0039924	0.47	9.9E-03
pit	FBgn0266581	-0.76	1.6E-02
pk	FBgn0003090	-1.23	1.1E-02
PKD	FBgn0038603	-0.78	6.7E-03
Pkg21D	FBgn0000442	-2.48	9.1E-07
ple	FBgn0005626	4.36	5.1E-09
Plp	FBgn0086690	1.41	3.4E-03
Pmm45A	FBgn0033377	0.88	1.3E-03
Pmp70	FBgn0031069	-1.50	6.7E-05
pncr002:3R	FBgn0063127	-2.05	3.3E-02
pncr015:3L	FBgn0063083	4.57	8.6E-05
pnt	FBgn0003118	-1.46	1.1E-09
pog	FBgn0051660	-2.41	3.0E-03
Pomp	FBgn0032884	0.76	1.3E-05
POSH	FBgn0040294	-0.45	4.8E-02
RasGAP1	FBgn0004390	-0.74	1.6E-02
raw	FBgn0003209	-1.49	5.1E-04
Rbf2	FBgn0038390	-0.81	4.9E-02
Rbm13	FBgn0030067	-0.98	2.3E-02
Rbp6	FBgn0260943	-2.09	2.6E-02
pros	FBgn0004595	-2.06	3.1E-02
Prosalpha2	FBgn0086134	0.60	2.1E-02
Prosalpha6	FBgn0250843	0.57	4.6E-03
Prosap	FBgn0040752	-0.93	2.6E-02
Prosbeta2	FBgn0023174	0.66	6.2E-03
Prosbeta4	FBgn0032596	0.61	1.5E-02
Prp19	FBgn0261119	-0.58	7.3E-04
prt	FBgn0043005	-2.99	8.3E-03
psh	FBgn0030926	-1.09	5.3E-03
Ptp4E	FBgn0004368	-0.73	1.4E-02
Ptpmeg	FBgn0261985	0.86	2.6E-03
Ptpmeg2	FBgn0028341	1.18	1.6E-03
Pvf3	FBgn0085407	-0.72	3.3E-02
PVRAP	FBgn0052406	-1.86	4.7E-02
pyd3	FBgn0037513	0.85	3.4E-02
PyK	FBgn0267385	1.73	6.2E-05
pzg	FBgn0259785	-0.51	4.6E-02
r	FBgn0003189	-1.52	1.6E-04
Rab19	FBgn0015793	1.21	4.8E-08
Rab21	FBgn0039966	0.88	1.9E-05
Rab26	FBgn0086913	-3.35	1.8E-04
Rab3-GAP	FBgn0027505	0.58	2.6E-02
Rab3-GEF	FBgn0030613	-2.18	1.1E-02
Rab39	FBgn0029959	0.87	6.5E-04
Rab5	FBgn0014010	0.55	3.1E-02
Rab6	FBgn0015797	-0.60	7.2E-03
Rab7	FBgn0015795	0.72	1.7E-02
Rab9	FBgn0032782	-2.04	1.8E-04
RAF2	FBgn0036624	-0.65	7.6E-03
RagA-B	FBgn0037647	0.51	6.9E-03
Rala	FBgn0015286	1.01	2.0E-03
Ran	FBgn0020255	-0.53	1.3E-02
RanGAP	FBgn0003346	-0.57	3.8E-02
rap	FBgn0262699	-1.48	3.5E-09
Rap2l	FBgn0025806	0.67	5.9E-04
RapGAP1	FBgn0264895	0.94	3.1E-03
Rrp1	FBgn0004584	-0.71	3.1E-04
Rrp47	FBgn0030711	0.96	3.0E-03
run	FBgn0003300	-2.41	7.8E-03
S	FBgn0003310	-0.44	4.6E-02
sage	FBgn0037672	-4.53	1.0E-06

sym	*FBgn*	*Δlog2*	*padj*
rdgB	FBgn0003218	0.87	9.2E-03
Rdl	FBgn0004244	-1.71	4.7E-02
Reck	FBgn0036463	1.12	3.8E-03
Reep1	FBgn0261564	0.56	6.6E-04
Ret	FBgn0011829	-1.48	2.0E-02
Rgk1	FBgn0264753	4.54	4.5E-30
Rgl	FBgn0026376	-2.22	1.3E-03
rgr	FBgn0267792	1.04	7.6E-03
RhoGAP15B	FBgn0030808	1.11	2.0E-02
RhoGAP71E	FBgn0036518	0.74	2.0E-03
RhoGAP92B	FBgn0038747	0.68	2.2E-02
RhoGDI	FBgn0036921	0.78	7.7E-04
RhoGEF4	FBgn0035761	-1.20	2.3E-02
RhoU	FBgn0083940	-0.61	4.3E-02
Ric	FBgn0265605	-0.68	2.1E-04
Rim2	FBgn0031359	-1.82	5.1E-09
Rint1	FBgn0035762	-0.49	3.7E-02
RIOK2	FBgn0039306	-0.55	3.1E-02
Rip11	FBgn0027335	-2.09	5.5E-22
Rm62	FBgn0003261	-0.61	7.5E-04
rn	FBgn0267337	-1.41	3.3E-02
RN-tre	FBgn0020620	1.02	1.3E-03
RNaseX25	FBgn0010406	-0.60	2.2E-02
RnrS	FBgn0011704	-0.62	4.2E-02
robo3	FBgn0041097	-1.81	4.8E-02
rogdi	FBgn0036697	2.17	4.5E-20
rost	FBgn0011705	1.10	2.8E-04
RpI1	FBgn0019938	-0.87	3.7E-03
RpI135	FBgn0003278	-0.79	3.4E-02
RpIII128	FBgn0004463	-0.63	7.6E-03
RpLP0-like	FBgn0033485	-0.80	7.8E-03
Rpn1	FBgn0028695	0.56	1.4E-02
Rpn10	FBgn0015283	0.67	1.7E-04
Rpn9	FBgn0028691	0.67	3.9E-03
Rpt1	FBgn0028687	0.74	4.8E-03
Rpt3	FBgn0028686	0.76	3.6E-02
Rpt4	FBgn0028685	0.68	3.6E-04
Rpt5	FBgn0028684	0.66	2.6E-04
shot	FBgn0013733	-1.74	1.8E-04
Shroom	FBgn0085408	1.14	2.1E-05
Sid	FBgn0039593	1.08	1.9E-02
salt	FBgn0039872	-5.44	1.3E-10
Sam-S	FBgn0005278	-1.26	4.5E-03
santa-maria	FBgn0025697	2.16	3.8E-04
Sar1	FBgn0038947	-0.79	1.1E-05
sas	FBgn0002306	-1.21	1.7E-02
SCAP	FBgn0033052	-1.38	8.1E-06
scat	FBgn0011232	-0.79	1.4E-02
SclB	FBgn0266492	-3.17	3.5E-03
Scp2	FBgn0020907	-3.55	1.2E-09
scramb1	FBgn0052056	1.00	4.2E-03
scro	FBgn0028993	-1.97	2.4E-02
scrt	FBgn0004880	-2.33	2.1E-02
sda	FBgn0015541	-1.53	4.5E-13
SdhA	FBgn0261439	0.65	4.1E-02
sdk	FBgn0021764	1.13	2.2E-03
Sec22	FBgn0260855	-0.71	4.2E-03
Sec24CD	FBgn0262126	-1.26	4.9E-04
Sec31	FBgn0033339	-1.59	3.4E-12
Sec61alpha	FBgn0086357	-1.38	3.0E-08
Sec61beta	FBgn0010638	-1.03	2.2E-04
Sec61gamma	FBgn0031049	-1.34	3.7E-03
sel	FBgn0263260	-1.44	1.4E-06
Sema-1b	FBgn0016059	0.87	8.0E-03
Sema-5c	FBgn0250876	0.92	1.6E-02
sens	FBgn0002573	-2.80	7.4E-04
Ser	FBgn0004197	-1.25	6.5E-03
Ser6	FBgn0011834	-3.97	9.8E-03
Sesn	FBgn0034897	1.72	2.1E-04
Set	FBgn0014879	-0.54	4.9E-02
SF1	FBgn0025571	-0.52	1.4E-03
sfl	FBgn0020251	1.81	1.6E-03
Sgs1	FBgn0003372	-7.74	1.4E-11
Sgs3	FBgn0003373	-8.25	1.1E-16
Sgs4	FBgn0003374	-7.45	1.0E-12
Sgs5	FBgn0003375	-6.87	1.6E-09
shd	FBgn0003388	-5.40	######
shf	FBgn0003390	0.95	1.8E-02
shg	FBgn0003391	1.28	9.4E-03
ssp7	FBgn0052667	-2.17	1.7E-03
SsRbeta	FBgn0011016	-1.16	2.6E-07
Stat92E	FBgn0016917	1.39	2.8E-04

sym	*FBgn*	*Δlog2*	*padj*
sif	FBgn0085447	-1.61	3.4E-02
Sik2	FBgn0025625	-1.50	2.0E-02
sing	FBgn0261245	1.66	4.6E-02
Sirup	FBgn0031971	-1.53	3.1E-04
sisA	FBgn0003411	-5.62	4.0E-04
sky	FBgn0032901	1.40	1.5E-03
slam	FBgn0043854	-0.94	3.2E-02
sll	FBgn0038524	-0.60	8.0E-03
smp-30	FBgn0038257	-2.26	1.3E-02
Snap25	FBgn0011288	-1.35	2.6E-02
sno	FBgn0265630	0.89	1.8E-02
snoRNA:Psi1	FBgn0083039	-3.62	3.0E-03
Snp	FBgn0265192	1.88	3.5E-06
Sobp	FBgn0033654	2.07	1.4E-05
Sod3	FBgn0033631	-1.65	2.2E-13
Sodh-1	FBgn0024289	-2.01	4.6E-02
SP1173	FBgn0035710	-3.62	5.7E-11
Sp212	FBgn0053329	2.37	1.9E-04
SP2637	FBgn0034371	0.96	7.7E-06
Spase12	FBgn0040623	-0.90	1.3E-02
Spase25	FBgn0030306	-1.01	1.6E-05
Spat	FBgn0014031	-2.63	8.8E-06
Spec2	FBgn0044823	0.82	4.6E-02
SPH93	FBgn0032638	2.01	3.0E-07
Sply	FBgn0010591	-0.72	3.3E-03
Spn	FBgn0010905	-1.47	5.0E-06
Spn43Ab	FBgn0024293	-2.29	1.9E-09
Spn43Ad	FBgn0044011	-2.04	1.4E-03
Spp	FBgn0031260	-1.78	1.0E-09
Sps2	FBgn0032224	-0.56	4.6E-03
Spt5	FBgn0040273	-0.33	2.3E-02
sqa	FBgn0259678	-1.85	4.5E-02
sqd	FBgn0263396	-0.72	3.7E-03
sra	FBgn0086370	1.11	1.6E-03
srl	FBgn0037248	-0.95	2.2E-03
SRm160	FBgn0036340	-0.35	4.9E-02
Srp54k	FBgn0010747	-0.70	2.9E-03
Srp68	FBgn0035947	-1.13	1.8E-06
Srp72	FBgn0038810	-0.79	3.2E-04
SrpRbeta	FBgn0011509	-1.20	6.0E-05
tim	FBgn0014396	-1.75	1.3E-04
stc	FBgn0001978	-0.51	2.0E-02
ste24a	FBgn0034176	-0.48	1.9E-02
stops	FBgn0086704	-1.21	3.8E-02
stumps	FBgn0020299	0.77	5.0E-02
stv	FBgn0086708	-1.90	2.4E-03
sty	FBgn0014388	-1.01	1.0E-03
su(f)	FBgn0003559	-0.54	2.2E-02
su(r)	FBgn0086450	-2.08	4.7E-04
sud1	FBgn0265189	-0.55	2.5E-02
sug	FBgn0033782	-1.20	1.7E-02
Sur-8	FBgn0038504	1.48	1.3E-11
Surf6	FBgn0038746	-1.06	3.2E-03
swi2	FBgn0034262	-2.28	7.2E-04
Swip-1	FBgn0032731	1.63	8.3E-05
syd	FBgn0024187	0.84	1.3E-02
Syn	FBgn0004575	-1.70	4.3E-02
Syn1	FBgn0037130	-1.60	1.9E-02
Syt1	FBgn0004242	0.93	1.2E-03
Sytalpha	FBgn0261089	-2.52	1.1E-04
Syx13	FBgn0036341	1.65	3.0E-05
Syx17	FBgn0035540	0.46	4.7E-02
Syx18	FBgn0039212	-0.60	4.0E-02
t	FBgn0086367	0.46	1.3E-02
Taf2	FBgn0011836	-0.62	3.6E-03
Tailor	FBgn0037470	0.43	8.0E-03
Takl1	FBgn0046689	-3.16	5.9E-06
tamo	FBgn0041582	0.50	2.5E-02
Tapdelta	FBgn0021795	-1.00	3.5E-03
Tdc1	FBgn0259977	-1.75	2.0E-03
Tdrd3	FBgn0036450	-0.53	2.3E-02
Tep1	FBgn0041183	1.11	1.8E-02
Tep4	FBgn0041180	-1.42	6.0E-08
TER94	FBgn0261014	0.54	1.3E-02
TfIIA-L	FBgn0011289	0.43	1.2E-02
Tg	FBgn0031975	-3.60	3.2E-05
Tgi	FBgn0036373	0.37	4.8E-02
thetaTry	FBgn0011555	-6.25	4.3E-02
Thor	FBgn0261560	-1.17	4.2E-03
Tie	FBgn0014073	-1.85	5.5E-03
Tig	FBgn0011722	-2.01	4.8E-07
Uro	FBgn0003961	-5.83	4.3E-14

sym	*FBgn*	*Δlog2*	*padj*
Timp	FBgn0025879	1.46	1.6E-03
Tina-1	FBgn0035083	-1.57	4.1E-05
Tm2	FBgn0004117	-2.35	1.5E-03
TM9SF3	FBgn0035622	-0.78	1.5E-04
tomb	FBgn0031715	1.82	1.8E-02
Tomosyn	FBgn0030412	0.95	2.2E-02
TotB	FBgn0038838	3.74	8.8E-06
TotZ	FBgn0044809	3.67	2.2E-03
TpnC73F	FBgn0010424	-2.36	3.9E-04
Traf-like	FBgn0030748	-0.98	2.9E-02
TRAM	FBgn0040340	-1.66	2.9E-03
Tre1	FBgn0046687	1.42	7.6E-05
Tsf2	FBgn0036299	0.52	2.0E-02
Tsf3	FBgn0034094	1.06	1.3E-02
tsh	FBgn0003866	-0.67	1.9E-02
Tsp29Fa	FBgn0032074	-2.85	5.4E-04
Tsp3A	FBgn0040334	0.76	1.1E-02
Tsp42Ed	FBgn0029507	1.04	1.5E-03
Tsp42Eg	FBgn0033128	-1.97	2.0E-04
Tsp42Ei	FBgn0033130	1.09	2.1E-02
Tsp42Eq	FBgn0033138	-3.08	1.3E-09
Tsp86D	FBgn0037848	0.61	2.5E-02
Tsp96F	FBgn0027865	1.24	1.7E-02
Tsp97E	FBgn0039465	1.36	3.2E-05
Tsr1	FBgn0037073	-0.78	4.3E-03
tty	FBgn0015558	-1.62	1.8E-02
Tudor-SN	FBgn0035121	-1.50	6.6E-08
TwdlE	FBgn0031957	1.37	1.5E-02
twin	FBgn0011725	0.58	1.9E-02
twr	FBgn0262801	-1.14	6.4E-03
TyrR	FBgn0038542	-3.51	7.5E-13
U4-U6-60K	FBgn0036733	-0.41	3.5E-02
UbcE2M	FBgn0035853	0.50	1.0E-02
Ube3a	FBgn0061469	0.54	9.7E-03
Ugt	FBgn0014075	-0.73	1.1E-02
Ugt35a	FBgn0026315	-4.88	1.5E-08
Ugt36Ba	FBgn0040262	-3.47	4.0E-03
Ugt86Dh	FBgn0040252	-4.27	6.1E-03
Ugt86Dj	FBgn0040250	-3.53	3.1E-03
Unc-13-4B	FBgn0266719	-0.81	1.8E-02
Unc-89	FBgn0053519	-1.76	4.1E-02
up	FBgn0004169	-2.44	4.3E-04
VAChT	FBgn0270928	-2.59	2.5E-02
Vap-33B	FBgn0053523	0.58	4.1E-03
vfl	FBgn0259789	-1.09	2.2E-02
Vha100-2	FBgn0028670	-0.97	2.8E-03
Vha100-5	FBgn0032373	-1.40	7.6E-03
Vha44	FBgn0262511	-0.34	2.3E-02
vkg	FBgn0016075	-1.01	4.3E-03
vri	FBgn0016076	-0.56	3.6E-02
Vsx1	FBgn0263511	-2.50	4.4E-02
Vsx2	FBgn0263512	-2.33	4.9E-02
wake	FBgn0266418	-0.69	4.1E-02
wcd	FBgn0262560	-0.94	2.5E-02
wdp	FBgn0034718	-0.80	4.4E-02
wit	FBgn0024179	-1.71	9.8E-07
wol	FBgn0261020	-0.65	4.4E-03
wor	FBgn0001983	-3.38	7.1E-03
wupA	FBgn0283471	-2.35	3.2E-03
yellow-f2	FBgn0038105	-3.32	8.2E-06
yin	FBgn0265575	-1.75	2.8E-02
yip7	FBgn0040060	-5.06	3.2E-04
Zasp52	FBgn0265991	-1.14	3.5E-04
zfh2	FBgn0004607	-1.13	4.6E-02
Zip48C	FBgn0033665	0.61	1.5E-03
Zip88E	FBgn0038312	-2.23	7.9E-07
ZnT63C	FBgn0035432	0.45	4.1E-02
ZnT77C	FBgn0037000	-0.84	6.0E-03
ZnT86D	FBgn0037875	1.87	1.1E-06
zye	FBgn0036985	-2.97	8.9E-04

APPENDIX E. DIFFERENTIALLY EXPRESSED GENES WITH A SIGNIFICANT SELECTION TERM

sym	*FBgn*	*Δlog2*	*padj*	*sym*	*FBgn*	*Δlog2*	*padj*
Acox57D-d	FBgn0034629	0.96	4.0E-02	CG15097	FBgn0034396	-1.41	1.1E-02
Adk3	FBgn0042094	1.05	7.8E-05	CG15879	FBgn0035309	1.80	9.8E-04
alpha-Est4	FBgn0015572	1.22	4.9E-02	CG16704	FBgn0031558	-1.73	3.2E-02
alpha-Est5	FBgn0261393	1.24	2.4E-02	CG16762	FBgn0035343	-1.61	4.9E-02
aralar1	FBgn0028646	-1.18	2.5E-02	CG17778	FBgn0023534	3.80	3.7E-04
AttC	FBgn0041579	2.03	1.9E-02	CG18467	FBgn0034218	2.98	4.0E-02
bab1	FBgn0004870	-1.34	2.4E-02	CG18473	FBgn0037683	1.28	3.4E-02
baz	FBgn0000163	-0.85	4.2E-02	CG18744	FBgn0042101	1.95	1.4E-02
BEAF-32	FBgn0015602	-0.60	2.0E-03	CG18746	FBgn0042103	-1.87	3.9E-02
Best1	FBgn0040238	-0.61	2.0E-02	CG2064	FBgn0033205	1.58	7.0E-03
blot	FBgn0027660	-1.37	2.1E-03	CG2909	FBgn0030189	0.89	1.2E-02
brv3	FBgn0040333	2.63	2.5E-02	CG30082	FBgn0050082	3.31	3.5E-03
bt	FBgn0005666	1.80	3.2E-02	CG30088	FBgn0050088	-1.66	3.1E-02
btsz	FBgn0266756	-0.94	8.0E-03	CG30287	FBgn0050287	-2.85	1.9E-06
cbx	FBgn0011241	-0.77	4.0E-02	CG30463	FBgn0050463	-1.81	7.0E-03
CCDC53	FBgn0031979	-1.32	3.8E-02	CG31097	FBgn0051097	-1.73	1.6E-02
CG10073	FBgn0034440	2.14	6.9E-03	CG31326	FBgn0051326	4.28	1.2E-03
CG10405	FBgn0038431	-2.77	3.4E-03	CG31547	FBgn0051547	-1.60	1.1E-02
CG10420	FBgn0039296	1.29	2.4E-05	CG31777	FBgn0051777	2.13	4.0E-02
CG10671	FBgn0035586	0.79	2.0E-02	CG31808	FBgn0062978	-1.05	4.2E-02
CG10725	FBgn0036362	-3.75	2.4E-03	CG3277	FBgn0031518	-2.10	1.1E-02
CG10814	FBgn0033830	6.41	4.6E-16	CG32795	FBgn0040384	0.46	3.9E-02
CG10962	FBgn0030073	1.52	6.9E-03	CG32813	FBgn0052813	-1.29	2.0E-02
CG11236	FBgn0031860	-1.67	3.6E-02	CG33111	FBgn0053111	0.90	4.1E-03
CG11257	FBgn0034442	0.73	2.4E-02	CG34034	FBgn0054034	-2.20	3.1E-02
CG11313	FBgn0039798	-3.33	1.4E-08	CG34291	FBgn0085320	-1.84	2.4E-02
CG11406	FBgn0034990	-4.07	3.6E-02	CG34437	FBgn0085466	-1.60	2.6E-02
CG12133	FBgn0033469	-3.72	2.5E-03	CG3631	FBgn0038268	0.81	1.1E-02
CG12721	FBgn0030373	1.87	2.4E-03	CG3857	FBgn0023520	-1.02	5.4E-03
CG13323	FBgn0033788	-1.99	3.3E-02	CG42711	FBgn0261628	2.42	2.3E-02
CG13962	FBgn0032824	-1.87	6.7E-04	CG42817	FBgn0261999	-1.40	1.1E-02
CG13982	FBgn0031811	2.21	4.8E-02	CG42876	FBgn0262150	-1.85	3.2E-02
CG14102	FBgn0036906	-1.27	2.3E-03	CG43125	FBgn0262588	-1.67	1.1E-02
CG14285	FBgn0038674	2.85	6.0E-03	CG4335	FBgn0038795	1.46	3.2E-02
CG14357	FBgn0038204	-3.63	3.7E-02	CG4408	FBgn0039073	-1.15	6.7E-05
CG14529	FBgn0039609	-1.49	5.3E-03	CG45071	FBgn0266441	2.19	2.1E-03
CG14692	FBgn0037836	6.25	4.6E-08	CG4607	FBgn0029932	-1.18	1.1E-02
CG14693	FBgn0037837	2.31	5.0E-02	CG4629	FBgn0031299	-1.49	2.3E-05
CG14933	FBgn0040968	3.48	2.0E-02	CG6244	FBgn0036531	2.85	6.3E-03

sym	*FBgn*	*Δlog2*	*padj*
CG14963	FBgn0035409	-1.61	1.5E-02
CG15067	FBgn0034331	3.39	3.2E-02
CG7567	FBgn0039670	-3.48	3.0E-03
CG8299	FBgn0034052	4.39	6.1E-06
CG8642	FBgn0033312	-1.67	4.4E-02
CG9509	FBgn0030594	-2.31	3.9E-04
CG9717	FBgn0039789	-1.53	2.1E-02
CG9766	FBgn0037229	3.54	1.7E-04
chinmo	FBgn0086758	1.83	3.1E-02
clumsy	FBgn0026255	-1.74	4.2E-02
corto	FBgn0010313	-0.82	2.0E-02
Cpr47Eg	FBgn0086519	3.82	4.9E-02
cpx	FBgn0041605	1.97	1.1E-02
CR42874	FBgn0262148	1.44	2.0E-02
CR43166	FBgn0262722	-2.14	6.8E-03
CR43933	FBgn0264554	-2.00	4.5E-02
CR44031	FBgn0264823	-1.95	3.3E-04
CR44077	FBgn0264886	4.22	2.1E-02
CR44186	FBgn0265075	-2.06	4.0E-02
CR44510	FBgn0265703	-3.10	4.6E-08
CR44964	FBgn0266279	-1.71	5.0E-02
CR45139	FBgn0266632	-1.49	4.5E-02
CR45194	FBgn0266704	5.13	3.3E-17
CR45469	FBgn0267025	3.91	2.4E-02
CTPsyn	FBgn0266452	1.22	3.1E-02
Cyp28a5	FBgn0028940	1.42	2.4E-02
Cyp4ad1	FBgn0033292	2.12	2.2E-09
Cyp4d8	FBgn0015033	1.26	4.0E-02
Cyp4e3	FBgn0015035	3.95	4.0E-03
Cyp9b1	FBgn0015038	2.04	2.3E-04
dpr4	FBgn0053512	4.79	4.3E-06
Dr	FBgn0000492	-0.85	3.6E-02
Dys	FBgn0260003	-1.10	7.8E-03
edl	FBgn0023214	-1.14	2.4E-02
Fic	FBgn0263278	0.90	2.4E-03
Gat	FBgn0039915	-2.05	1.9E-07
glob1	FBgn0027657	1.43	3.2E-03
GstD2	FBgn0010038	4.35	1.4E-05
GstD6	FBgn0010042	2.67	2.4E-02
GstE3	FBgn0063497	1.69	2.5E-02
GstE7	FBgn0063493	-2.58	4.3E-04

sym	*FBgn*	*Δlog2*	*padj*
CG6424	FBgn0028494	-0.86	1.2E-02
CG6475	FBgn0038886	-1.98	3.1E-02
ine	FBgn0011603	-1.83	1.1E-02
Inos	FBgn0025885	1.31	5.0E-02
IP3K1	FBgn0032147	-1.15	5.2E-03
Ir76a	FBgn0260874	-2.19	1.4E-05
Iris	FBgn0031305	2.44	7.0E-03
kdn	FBgn0261955	-1.00	1.1E-02
klu	FBgn0013469	-1.63	1.9E-03
lin-28	FBgn0035626	-3.57	6.4E-04
LManVI	FBgn0032069	5.03	1.8E-07
mew	FBgn0004456	-0.89	3.2E-02
MRE23	FBgn0262741	-1.75	1.5E-02
mtd	FBgn0013576	-0.86	1.1E-02
mthl15	FBgn0051720	-2.10	7.1E-03
Muc96D	FBgn0051439	-3.91	1.8E-02
NetA	FBgn0015773	-0.90	1.2E-02
Nlg1	FBgn0051146	3.03	1.1E-04
nompC	FBgn0016920	2.60	2.8E-05
p38c	FBgn0267339	1.58	2.1E-03
P58IPK	FBgn0037718	0.81	4.0E-02
Pdcd4	FBgn0030520	-0.63	3.6E-02
peb	FBgn0003053	-1.67	3.4E-03
PGRP-SB1	FBgn0043578	-3.84	4.9E-10
PHGPx	FBgn0035438	0.88	9.1E-03
pigs	FBgn0029881	2.37	3.3E-02
Pmp70	FBgn0031069	1.25	1.1E-02
Ppa	FBgn0020257	-0.95	3.6E-02
Ppt2	FBgn0032358	0.78	4.8E-02
Prosbeta4	FBgn0032596	-0.75	1.2E-02
r2d2	FBgn0031951	0.50	3.3E-02
Rgk1	FBgn0264753	-1.48	2.2E-02
rut	FBgn0003301	-1.10	2.0E-02
sda	FBgn0015541	-0.68	2.7E-02
sdt	FBgn0261873	-1.01	8.0E-03
Sec22	FBgn0260855	0.67	4.6E-02
sel	FBgn0263260	1.44	1.8E-05
Swip-1	FBgn0032731	-1.39	1.1E-02
Syx7	FBgn0267849	0.64	4.5E-02
TotC	FBgn0044812	-2.32	3.6E-02
Tsp42Ed	FBgn0029507	1.00	2.0E-02

sym	*FBgn*	*Δlog2*	*padj*
GXIVsPLA2	FBgn0036545	0.90	3.9E-02
hoe1	FBgn0041150	1.92	1.3E-09
inaD	FBgn0001263	5.04	1.1E-02
ine	FBgn0011603	-1.83	1.1E-02
Inos	FBgn0025885	1.31	5.0E-02
IP3K1	FBgn0032147	-1.15	5.2E-03
Ir76a	FBgn0260874	-2.19	1.4E-05
Iris	FBgn0031305	2.44	7.0E-03
kdn	FBgn0261955	-1.00	1.1E-02
klu	FBgn0013469	-1.63	1.9E-03
lin-28	FBgn0035626	-3.57	6.4E-04
LManVI	FBgn0032069	5.03	1.8E-07
mew	FBgn0004456	-0.89	3.2E-02
MRE23	FBgn0262741	-1.75	1.5E-02
mtd	FBgn0013576	-0.86	1.1E-02
mthl15	FBgn0051720	-2.10	7.1E-03
Muc96D	FBgn0051439	-3.91	1.8E-02
NetA	FBgn0015773	-0.90	1.2E-02
Nlg1	FBgn0051146	3.03	1.1E-04
nompC	FBgn0016920	2.60	2.8E-05
p38c	FBgn0267339	1.58	2.1E-03
P58IPK	FBgn0037718	0.81	4.0E-02
Pdcd4	FBgn0030520	-0.63	3.6E-02
peb	FBgn0003053	-1.67	3.4E-03
PGRP-SB1	FBgn0043578	-3.84	4.9E-10
PHGPx	FBgn0035438	0.88	9.1E-03
pigs	FBgn0029881	2.37	3.3E-02
Pmp70	FBgn0031069	1.25	1.1E-02
Ppa	FBgn0020257	-0.95	3.6E-02
Ppt2	FBgn0032358	0.78	4.8E-02
Prosbeta4	FBgn0032596	-0.75	1.2E-02
r2d2	FBgn0031951	0.50	3.3E-02
Rgk1	FBgn0264753	-1.48	2.2E-02
rut	FBgn0003301	-1.10	2.0E-02
sda	FBgn0015541	-0.68	2.7E-02
sdt	FBgn0261873	-1.01	8.0E-03
Sec22	FBgn0260855	0.67	4.6E-02
sel	FBgn0263260	1.44	1.8E-05
Swip-1	FBgn0032731	-1.39	1.1E-02
Syx7	FBgn0267849	0.64	4.5E-02
TotC	FBgn0044812	-2.32	3.6E-02

sym	*FBgn*	*Δlog2*	*padj*
Tsp42Ed	FBgn0029507	1.00	2.0E-02
Victoria	FBgn0053117	-4.73	2.8E-05
wb	FBgn0261563	-0.98	3.7E-02
wtrw	FBgn0260005	-1.05	2.6E-02
Zip88E	FBgn0038312	-1.53	1.2E-02
ZnT63C	FBgn0035432	-0.62	2.0E-02

APPENDIX F. DIFFERENTIALLY EXPRESSED GENES WITH A SIGNIFICANT INTERACTION TERM

		F3IN vs. S3IN		*F3IN vs. FWPP*		*S3IN vs. SWPP*		*FWPP vs. SWPP*	
sym	*FBgn*	*Δlog2*	*padj*	*Δlog2*	*padj*	*Δlog2*	*padj*	*Δlog2*	*padj*
7B2	FBgn0041707	-2.05	5.8E-02	-1.98	**1.3E-02**	1.60	**3.9E-02**	1.53	6.6E-02
Aats-his	FBgn0027087	-0.07	1.0E+00	-0.87	3.0E-01	1.94	**2.6E-03**	2.74	**5.2E-05**
Aats-lys	FBgn0027084	-0.44	7.8E-01	-0.95	**4.7E-02**	0.62	2.0E-01	1.13	**1.1E-02**
Acox57D-p	FBgn0034628	0.48	7.2E-01	1.20	**2.2E-03**	-0.51	2.7E-01	-1.23	**2.1E-03**
Adh	FBgn0000055	-0.58	7.6E-01	-0.50	4.6E-01	-2.94	**5.2E-07**	-3.01	**2.0E-06**
Ag5r	FBgn0015010	-2.70	**1.3E-02**	1.09	3.1E-01	4.67	**1.1E-09**	0.88	4.3E-01
Ald	FBgn0000064	0.06	9.9E-01	0.12	8.5E-01	-1.32	**2.1E-04**	-1.39	**2.8E-04**
alpha-PheRS	FBgn0030007	-0.22	9.6E-01	-0.49	5.8E-01	1.88	**1.6E-03**	2.15	**6.2E-04**
AMPdeam	FBgn0052626	0.46	4.8E-01	-0.95	**4.6E-04**	-2.13	**5.1E-19**	-0.71	**1.5E-02**
Aos1	FBgn0029512	-0.37	8.5E-01	-0.42	5.4E-01	1.50	**1.8E-03**	1.54	**2.4E-03**
Argk	FBgn0000116	-0.61	7.8E-01	-0.14	9.0E-01	2.20	**1.2E-04**	1.73	**5.4E-03**
Arp10	FBgn0031050	0.02	1.0E+00	-0.17	9.0E-01	2.58	**1.4E-04**	2.77	**1.4E-04**
Arp8	FBgn0030877	-0.03	1.0E+00	-0.28	8.1E-01	2.04	**1.4E-03**	2.29	**6.6E-04**
Arpc3B	FBgn0065032	-0.58	8.3E-01	0.46	6.5E-01	3.82	**4.1E-10**	2.78	**5.5E-05**
Arpc4	FBgn0031781	-0.35	9.2E-01	0.13	9.2E-01	2.80	**1.5E-06**	2.33	**2.8E-04**
Art8	FBgn0032329	-0.30	9.1E-01	-1.13	5.6E-02	0.84	1.3E-01	1.67	**1.6E-03**
aru	FBgn0029095	-0.17	9.7E-01	-0.33	7.2E-01	1.97	**4.3E-04**	2.14	**3.6E-04**
ATPCL	FBgn0020236	1.65	**1.9E-11**	-1.40	**5.1E-09**	-2.58	**1.0E-30**	0.47	1.2E-01
awd	FBgn0000150	-0.24	9.6E-01	-0.49	5.6E-01	1.93	**7.7E-04**	2.18	**3.5E-04**
babos	FBgn0034724	-0.82	4.7E-01	0.39	5.5E-01	2.23	**4.7E-07**	1.01	5.4E-02
Best2	FBgn0035696	-0.90	**1.7E-03**	-0.62	**1.9E-02**	0.52	**4.4E-02**	0.24	4.9E-01
beta3GalTII	FBgn0033315	-0.37	9.3E-01	0.36	7.5E-01	2.93	**5.0E-06**	2.21	**1.8E-03**
betaTub56D	FBgn0003887	-0.52	8.0E-01	-0.86	2.3E-01	1.92	**4.6E-04**	2.26	**1.0E-04**
Bgb	FBgn0013753	-0.43	8.5E-01	-0.46	5.6E-01	1.92	**3.0E-04**	1.94	**6.1E-04**
blow	FBgn0004133	-0.39	8.6E-01	0.02	9.9E-01	2.17	**1.0E-05**	1.76	**9.9E-04**
bmm	FBgn0036449	0.18	9.4E-01	0.12	8.5E-01	-1.27	**3.0E-04**	-1.22	**1.3E-03**
boca	FBgn0004132	0.09	9.9E-01	-0.68	3.8E-01	1.45	**1.5E-02**	2.22	**2.6E-04**
c11.1	FBgn0040236	0.49	4.7E-01	0.06	9.1E-01	-0.98	**3.8E-04**	-0.56	8.8E-02
Cand1	FBgn0027568	-0.05	9.8E-01	0.51	**4.8E-02**	-0.31	2.6E-01	-0.87	**2.4E-04**
cbc	FBgn0033842	-0.12	9.8E-01	-0.08	9.6E-01	2.49	**1.5E-04**	2.45	**5.4E-04**
CBP	FBgn0026144	-0.80	5.0E-01	-0.30	6.9E-01	1.53	**9.3E-04**	1.03	5.1E-02
Cbs	FBgn0031148	0.36	9.4E-01	-0.32	8.1E-01	2.79	**1.5E-04**	3.47	**9.7E-06**
CCKLR-17D3	FBgn0030954	-0.82	7.7E-01	-1.22	2.1E-01	1.58	**4.1E-02**	1.98	**1.5E-02**
Cct5	FBgn0010621	-0.12	9.8E-01	-0.43	6.2E-01	1.86	**1.2E-03**	2.18	**3.4E-04**
Cctgamma	FBgn0015019	-0.19	9.5E-01	-0.46	4.4E-01	1.15	**1.1E-02**	1.42	**2.4E-03**
Cda9	FBgn0034197	-3.12	**2.7E-02**	-3.02	**5.4E-03**	1.77	1.2E-01	1.66	1.7E-01
cert	FBgn0027569	0.48	5.1E-01	0.86	**4.7E-03**	-0.24	5.8E-01	-0.61	5.7E-02
CG10098	FBgn0037472	0.03	1.0E+00	-0.03	9.9E-01	1.94	**1.1E-04**	2.00	**2.1E-04**

		F3IN vs. S3IN		*F3IN vs. FWPP*		*S3IN vs. SWPP*		*FWPP vs. SWPP*	
sym	*FBgn*	*Δlog2*	*padj*	*Δlog2*	*padj*	*Δlog2*	*padj*	*Δlog2*	*padj*
CG10131	FBgn0033949	-0.07	1.0E+00	-0.35	8.2E-01	4.37	**1.5E-07**	4.65	**2.1E-07**
CG10140	FBgn0036363	-3.09	**2.5E-03**	-0.81	4.6E-01	3.45	**1.7E-05**	1.18	2.4E-01
CG10418	FBgn0036277	-0.41	8.9E-01	-0.58	5.2E-01	2.13	**5.6E-04**	2.30	**4.8E-04**
CG10635	FBgn0035603	-0.17	9.8E-01	0.08	9.6E-01	3.30	**4.5E-07**	3.04	**2.4E-05**
CG10932	FBgn0029969	0.18	9.8E-01	0.09	9.6E-01	3.05	**2.7E-05**	3.14	**6.3E-05**
CG10939	FBgn0010620	-1.06	3.1E-01	-2.16	**2.7E-05**	-0.27	7.8E-01	0.83	1.9E-01
CG11069	FBgn0039244	-0.69	7.0E-01	-0.83	2.1E-01	1.16	**3.2E-02**	1.30	**2.2E-02**
CG11077	FBgn0039930	-1.14	1.6E-01	-0.05	9.7E-01	1.77	**1.7E-04**	0.68	2.4E-01
CG11109	FBgn0037200	-0.09	9.8E-01	-0.69	2.9E-01	1.24	**1.6E-02**	1.84	**4.4E-04**
CG11137	FBgn0037199	-0.08	1.0E+00	0.13	9.2E-01	3.02	**4.4E-06**	2.81	**9.0E-05**
CG11425	FBgn0037167	-1.33	5.7E-01	-2.02	**3.5E-02**	1.32	1.8E-01	2.01	**3.2E-02**
CG11438	FBgn0037164	-0.23	9.7E-01	0.24	8.6E-01	3.08	**1.2E-05**	2.61	**6.1E-04**
CG11594	FBgn0035484	0.10	9.9E-01	-1.54	1.1E-01	1.75	**3.5E-02**	3.39	**3.5E-05**
CG11788	FBgn0034495	-0.41	9.3E-01	-0.33	8.1E-01	2.87	**9.9E-05**	2.79	**4.4E-04**
CG12014	FBgn0035445	-1.16	8.2E-02	-1.83	**3.8E-05**	-0.11	9.1E-01	0.55	3.6E-01
CG12038	FBgn0035179	-0.84	7.8E-01	-1.06	3.0E-01	1.87	**1.9E-02**	2.09	**1.3E-02**
CG12056	FBgn0030099	-0.34	9.3E-01	-0.65	4.6E-01	2.41	**8.2E-05**	2.72	**3.8E-05**
CG12134	FBgn0033471	-0.19	9.7E-01	-0.77	3.9E-01	2.25	**5.7E-04**	2.84	**4.7E-05**
CG12194	FBgn0031636	0.34	8.4E-01	2.08	**4.8E-08**	0.11	9.0E-01	-1.63	**1.0E-04**
CG12237	FBgn0031048	0.07	1.0E+00	-0.17	8.9E-01	2.44	**2.1E-04**	2.68	**1.5E-04**
CG12268	FBgn0039131	-0.67	8.5E-01	-1.78	9.7E-02	1.39	1.5E-01	2.50	**7.9E-03**
CG12279	FBgn0038080	-0.02	1.0E+00	-0.27	8.1E-01	2.36	**1.8E-04**	2.61	**1.1E-04**
CG1265	FBgn0035517	-0.18	9.6E-01	-0.89	1.0E-01	0.85	7.5E-02	1.56	**8.3E-04**
CG12708	FBgn0030666	-0.94	7.1E-01	-2.16	**1.0E-02**	0.97	2.7E-01	2.18	**8.9E-03**
CG12730	FBgn0029771	-0.25	9.5E-01	-0.12	9.1E-01	1.87	**3.8E-04**	1.74	**2.1E-03**
CG12880	FBgn0046258	-0.91	5.4E-01	-0.22	8.2E-01	1.95	**3.2E-04**	1.26	**4.1E-02**
CG12948	FBgn0037739	-0.06	1.0E+00	0.07	9.6E-01	2.13	**4.6E-05**	2.00	**3.9E-04**
CG13053	FBgn0040801	-0.03	1.0E+00	-0.59	6.8E-01	2.76	**1.1E-03**	3.32	**2.8E-04**
CG13102	FBgn0032088	-1.22	7.0E-01	-1.33	2.5E-01	2.20	**1.7E-02**	2.31	**1.8E-02**
CG13117	FBgn0032140	-0.27	9.6E-01	0.00	1.0E+00	3.10	**1.7E-06**	2.83	**6.4E-05**
CG1315	FBgn0026565	-1.45	5.2E-01	-2.33	**1.6E-02**	1.01	3.7E-01	1.89	6.0E-02
CG1317	FBgn0035333	0.07	9.7E-01	0.54	**3.6E-02**	-0.28	3.2E-01	-0.76	**1.6E-03**
CG13285	FBgn0035611	-1.56	5.5E-01	-1.86	1.2E-01	2.04	**4.7E-02**	2.34	**3.0E-02**
CG13315	FBgn0040827	-0.82	4.8E-01	-2.12	**3.8E-06**	-0.27	7.5E-01	1.03	5.5E-02
CG13321	FBgn0033787	-1.41	1.5E-01	-0.04	9.9E-01	2.26	**8.4E-05**	0.89	2.1E-01
CG13795	FBgn0031937	0.41	7.6E-01	-1.76	**2.5E-07**	-3.38	**3.7E-26**	-1.21	**1.7E-03**
CG14015	FBgn0031716	-1.15	7.5E-01	-1.59	2.0E-01	1.93	5.7E-02	2.37	**2.6E-02**
CG14079	FBgn0036849	-0.77	8.0E-01	0.01	9.9E-01	3.09	**5.0E-05**	2.30	**4.9E-03**
CG14118	FBgn0036323	-2.48	7.9E-02	-2.32	**2.5E-02**	1.35	2.2E-01	1.20	3.1E-01
CG14141	FBgn0036146	-0.71	8.7E-01	-2.61	**2.5E-02**	1.07	4.2E-01	2.97	**7.3E-03**

		F3IN vs. S3IN		*F3IN vs. FWPP*		*S3IN vs. SWPP*		*FWPP vs. SWPP*	
sym	*FBgn*	*Δlog2*	*padj*	*Δlog2*	*padj*	*Δlog2*	*padj*	*Δlog2*	*padj*
CG14210	FBgn0031040	-0.32	9.3E-01	-0.67	4.1E-01	2.00	**7.9E-04**	2.35	**2.1E-04**
CG14247	FBgn0039454	-1.63	5.1E-01	-2.54	**2.2E-02**	1.52	1.8E-01	2.42	**2.8E-02**
CG14257	FBgn0039479	-0.74	7.8E-01	-1.19	1.9E-01	1.45	**4.9E-02**	1.91	**1.2E-02**
CG14270	FBgn0029665	-0.06	1.0E+00	-0.12	9.3E-01	2.90	**1.1E-05**	2.96	**3.6E-05**
CG14275	FBgn0032022	-0.37	9.3E-01	-0.85	3.8E-01	1.86	**9.0E-03**	2.34	**1.9E-03**
CG14464	FBgn0033000	-0.36	8.9E-01	-0.15	8.8E-01	1.95	**3.7E-04**	1.74	**3.3E-03**
CG14544	FBgn0039407	-0.61	7.8E-01	-0.52	5.3E-01	1.60	**5.2E-03**	1.51	**1.5E-02**
CG14636	FBgn0037217	-2.52	**2.9E-02**	-2.55	**3.6E-03**	1.55	9.3E-02	1.58	1.0E-01
CG14853	FBgn0038246	-1.12	7.2E-01	-3.05	**1.7E-03**	0.08	9.7E-01	2.02	6.2E-02
CG14946	FBgn0032405	0.52	8.5E-01	1.23	1.5E-01	4.16	**1.5E-11**	3.46	**4.2E-07**
CG14961	FBgn0035439	1.90	**5.6E-04**	0.49	4.6E-01	-1.89	**4.4E-05**	-0.49	4.7E-01
CG15068	FBgn0040733	-1.21	6.5E-01	-3.65	**3.7E-05**	0.01	1.0E+00	2.45	**1.3E-02**
CG15145	FBgn0032649	1.58	2.2E-01	1.87	**1.7E-02**	-0.71	4.6E-01	-1.01	2.5E-01
CG15423	FBgn0031580	-2.46	1.4E-01	-2.91	**8.8E-03**	2.12	5.4E-02	2.57	**2.3E-02**
CG1552	FBgn0030258	-0.77	8.5E-01	-2.36	**4.7E-02**	1.96	7.3E-02	3.55	**9.4E-04**
CG15537	FBgn0039770	-1.12	7.1E-01	-1.80	9.2E-02	1.40	1.5E-01	2.08	**3.4E-02**
CG15890	FBgn0030576	-1.87	1.0E-01	-2.24	**4.0E-03**	0.74	4.6E-01	1.11	2.2E-01
CG15891	FBgn0029860	-0.35	9.2E-01	-0.35	7.3E-01	1.99	**8.9E-04**	1.99	**1.9E-03**
CG15922	FBgn0040575	-0.40	9.2E-01	0.11	9.5E-01	3.37	**7.8E-07**	2.85	**1.4E-04**
CG16836	FBgn0040735	-0.55	8.8E-01	-1.10	3.0E-01	1.95	**2.1E-02**	2.50	**3.8E-03**
CG16890	FBgn0028932	-0.12	8.5E-01	0.12	6.2E-01	0.70	**9.2E-07**	0.46	**3.6E-03**
CG16903	FBgn0040394	-0.11	9.8E-01	-0.38	6.5E-01	1.59	**3.6E-03**	1.85	**1.2E-03**
CG17121	FBgn0039043	-1.29	7.4E-02	-0.84	1.5E-01	1.58	**7.5E-04**	1.13	**3.1E-02**
CG17141	FBgn0039020	-0.70	5.7E-01	-0.72	2.0E-01	1.03	**2.4E-02**	1.05	**3.2E-02**
CG17259	FBgn0031497	-0.13	9.8E-01	-1.00	1.5E-01	1.12	5.9E-02	1.99	**6.0E-04**
CG17265	FBgn0031488	-0.83	1.3E-01	-0.32	4.9E-01	1.14	**6.6E-04**	0.63	1.0E-01
CG17266	FBgn0033089	-0.09	9.9E-01	-0.37	7.4E-01	2.13	**1.0E-03**	2.40	**4.9E-04**
CG17360	FBgn0037949	0.31	7.6E-01	0.38	2.7E-01	-0.58	**4.1E-02**	-0.65	**2.8E-02**
CG1738	FBgn0030291	-0.54	7.3E-01	-0.52	3.6E-01	1.04	**1.7E-02**	1.02	**3.1E-02**
CG1749	FBgn0030305	-0.48	8.5E-01	-1.41	**4.9E-02**	1.39	**3.1E-02**	2.32	**3.2E-04**
CG1824	FBgn0030403	-0.14	9.8E-01	0.06	9.8E-01	2.36	**1.1E-04**	2.16	**1.0E-03**
CG1969	FBgn0039690	-1.16	2.3E-01	-1.58	**5.2E-03**	1.25	**2.4E-02**	1.67	**3.0E-03**
CG2021	FBgn0035271	-0.26	9.3E-01	0.01	9.9E-01	1.90	**9.0E-05**	1.63	**2.0E-03**
CG2200	FBgn0030447	-0.40	8.4E-01	-0.31	6.9E-01	1.49	**1.9E-03**	1.40	**6.6E-03**
CG2678	FBgn0014931	1.01	1.5E-01	0.90	7.7E-02	-0.72	1.4E-01	-0.61	2.5E-01
CG2915	FBgn0033241	-0.18	9.7E-01	-0.57	5.0E-01	1.77	**3.6E-03**	2.17	**6.5E-04**
CG2975	FBgn0031468	-2.17	**2.7E-02**	-2.29	**2.4E-03**	0.41	7.5E-01	0.52	6.6E-01
CG3008	FBgn0031643	0.34	4.1E-01	0.52	**9.3E-03**	-0.18	4.9E-01	-0.36	9.8E-02
CG30172	FBgn0050172	-0.14	9.8E-01	-2.34	**2.1E-03**	1.16	1.4E-01	3.35	**8.8E-06**
CG30344	FBgn0050344	-0.12	9.6E-01	-0.33	5.4E-01	1.21	**9.7E-04**	1.41	**2.8E-04**

		F3IN vs. S3IN		*F3IN vs. FWPP*		*S3IN vs. SWPP*		*FWPP vs. SWPP*	
sym	*FBgn*	*Δlog2*	*padj*	*Δlog2*	*padj*	*Δlog2*	*padj*	*Δlog2*	*padj*
CG30392	FBgn0050392	-0.31	9.3E-01	0.03	9.9E-01	2.38	**5.6E-05**	2.03	**1.5E-03**
CG30423	FBgn0050423	-0.09	9.9E-01	0.30	7.9E-01	2.61	**1.3E-05**	2.22	**6.5E-04**
CG30456	FBgn0050456	-1.24	**2.6E-03**	0.14	8.1E-01	1.38	**2.2E-05**	0.00	1.0E+00
CG3097	FBgn0029804	-0.86	7.2E-01	0.54	5.6E-01	3.01	**8.9E-07**	1.62	**1.9E-02**
CG31030	FBgn0051030	-0.40	9.4E-01	-1.82	8.2E-02	2.57	**2.5E-03**	3.99	**9.6E-06**
CG31121	FBgn0051121	-0.51	8.5E-01	-0.19	8.7E-01	2.16	**5.3E-04**	1.83	**6.7E-03**
CG31235	FBgn0051235	-1.08	7.7E-01	-1.83	1.4E-01	2.15	**3.5E-02**	2.90	**5.6E-03**
CG31337	FBgn0051337	-0.28	9.3E-01	0.64	3.5E-01	2.60	**1.2E-07**	1.68	**2.2E-03**
CG31460	FBgn0051460	-0.06	9.9E-01	-0.74	2.1E-01	0.94	5.1E-02	1.61	**7.6E-04**
CG31516	FBgn0051516	-3.50	**1.0E-02**	-3.15	**4.6E-03**	1.29	3.3E-01	0.94	5.4E-01
CG31549	FBgn0051549	0.13	9.8E-01	0.14	9.2E-01	3.04	**1.4E-05**	3.03	**6.4E-05**
CG31706	FBgn0051706	-1.07	7.3E-01	-2.37	**1.6E-02**	0.84	4.7E-01	2.15	**3.1E-02**
CG31715	FBgn0051715	-0.17	9.7E-01	0.36	7.3E-01	2.62	**1.3E-05**	2.09	**1.4E-03**
CG31728	FBgn0051728	-0.48	8.1E-01	0.09	9.4E-01	1.96	**1.1E-04**	1.39	**1.3E-02**
CG31793	FBgn0051793	-0.13	9.6E-01	0.46	3.5E-01	-1.43	**1.7E-04**	-2.03	**2.4E-07**
CG31810	FBgn0051810	-2.47	**4.8E-02**	-2.94	**9.8E-04**	1.20	2.5E-01	1.67	1.0E-01
CG3184	FBgn0029892	-0.11	9.9E-01	-0.24	8.5E-01	2.41	**2.6E-04**	2.53	**3.4E-04**
CG31922	FBgn0051922	-0.36	9.2E-01	-0.11	9.3E-01	2.33	**1.7E-04**	2.09	**1.9E-03**
CG31957	FBgn0051957	-0.03	1.0E+00	0.34	7.7E-01	3.10	**1.1E-06**	2.73	**9.0E-05**
CG32069	FBgn0052069	-0.23	9.6E-01	-0.25	8.3E-01	2.40	**2.1E-04**	2.41	**5.0E-04**
CG32174	FBgn0052174	-0.83	7.9E-01	0.30	8.4E-01	3.42	**2.9E-05**	2.29	**1.1E-02**
CG32187	FBgn0052187	-1.04	7.0E-01	-2.23	**1.2E-02**	1.78	**2.7E-02**	2.98	**4.4E-04**
CG32354	FBgn0052354	-1.40	7.8E-02	-1.07	8.8E-02	0.82	1.8E-01	0.49	5.1E-01
CG33977	FBgn0053977	-0.15	9.8E-01	-0.47	6.1E-01	2.19	**2.6E-04**	2.52	**9.0E-05**
CG33993	FBgn0053993	-0.78	7.9E-01	0.12	9.5E-01	3.21	**2.0E-05**	2.32	**4.8E-03**
CG34112	FBgn0086608	-0.83	7.5E-01	-2.28	**1.9E-03**	0.23	8.7E-01	1.69	**3.4E-02**
CG34163	FBgn0085192	-0.09	9.9E-01	-0.42	6.6E-01	2.06	**6.6E-04**	2.39	**2.0E-04**
CG34183	FBgn0085212	-0.40	7.8E-01	-0.61	2.2E-01	0.92	**1.6E-02**	1.13	**5.4E-03**
CG34251	FBgn0085280	-1.51	4.6E-01	-1.81	7.9E-02	1.76	5.6E-02	2.05	**3.1E-02**
CG34279	FBgn0085308	-2.41	1.2E-01	-4.24	**8.2E-06**	0.29	8.9E-01	2.12	5.5E-02
CG34284	FBgn0085313	-1.30	4.4E-01	-2.98	**5.1E-05**	-0.24	8.7E-01	1.44	1.0E-01
CG3548	FBgn0035033	-0.36	7.9E-01	-0.41	3.9E-01	1.13	**1.4E-03**	1.18	**1.8E-03**
CG3603	FBgn0029648	0.07	1.0E+00	-0.29	8.1E-01	2.45	**2.7E-04**	2.81	**9.0E-05**
CG3609	FBgn0031418	-0.51	8.4E-01	-0.69	3.9E-01	2.24	**1.3E-04**	2.43	**1.1E-04**
CG3649	FBgn0034785	-0.36	9.5E-01	-1.35	2.1E-01	2.20	**7.8E-03**	3.20	**2.5E-04**
CG3689	FBgn0035987	-0.30	5.7E-01	-0.61	**2.7E-03**	0.19	4.7E-01	0.49	**2.1E-02**
CG3814	FBgn0025692	-1.49	5.8E-02	-0.69	3.1E-01	1.59	**2.7E-03**	0.79	2.1E-01
CG3880	FBgn0035057	-0.42	9.4E-01	-1.29	2.7E-01	2.19	**1.7E-02**	3.06	**1.2E-03**
CG3909	FBgn0027524	-0.20	9.6E-01	-0.18	8.7E-01	2.07	**4.0E-04**	2.05	**1.0E-03**
CG40228	FBgn0063670	0.06	1.0E+00	0.00	1.0E+00	2.09	**2.0E-05**	2.15	**5.2E-05**

		F3IN vs. S3IN		*F3IN vs. FWPP*		*S3IN vs. SWPP*		*FWPP vs. SWPP*	
sym	*FBgn*	*Δlog2*	*padj*	*Δlog2*	*padj*	*Δlog2*	*padj*	*Δlog2*	*padj*
CG40472	FBgn0085736	-0.04	1.0E+00	-0.03	9.9E-01	2.33	**9.8E-05**	2.32	**3.1E-04**
CG41128	FBgn0069923	-0.30	9.4E-01	0.05	9.8E-01	2.35	**6.6E-05**	2.01	**1.7E-03**
CG42249	FBgn0259101	-0.87	7.7E-01	-3.06	**1.7E-04**	0.09	9.6E-01	2.28	**9.5E-03**
CG42259	FBgn0266569	-0.22	9.7E-01	-0.28	8.3E-01	3.10	**8.4E-06**	3.16	**3.2E-05**
CG42327	FBgn0259227	0.18	8.9E-01	0.33	3.6E-01	-0.69	**1.7E-02**	-0.84	**4.6E-03**
CG42382	FBgn0259728	-0.46	8.0E-01	-0.08	9.5E-01	1.90	**7.2E-05**	1.51	**3.5E-03**
CG43133	FBgn0262607	0.94	3.3E-01	2.53	**8.7E-09**	0.56	3.5E-01	-1.03	5.3E-02
CG43236	FBgn0262881	-0.54	9.0E-01	-1.37	2.2E-01	2.35	**8.1E-03**	3.17	**5.3E-04**
CG43324	FBgn0263029	-1.20	5.1E-01	-0.80	3.9E-01	1.77	**1.5E-02**	1.37	9.0E-02
CG4409	FBgn0034128	-1.12	6.9E-01	-0.85	4.5E-01	2.40	**3.5E-03**	2.13	**1.7E-02**
CG44250	FBgn0265185	-0.76	8.0E-01	-0.06	9.9E-01	3.89	**1.8E-07**	3.19	**1.0E-04**
CG44625	FBgn0265836	-1.56	6.3E-01	-1.63	2.3E-01	3.32	**1.3E-03**	3.39	**2.1E-03**
CG4570	FBgn0037844	-0.85	7.2E-01	-1.06	2.1E-01	1.66	**1.3E-02**	1.86	**8.2E-03**
CG4646	FBgn0033810	-0.23	9.7E-01	-0.46	6.9E-01	2.70	**1.3E-04**	2.93	**1.0E-04**
CG4741	FBgn0035040	-1.17	**4.0E-03**	-0.72	6.0E-02	0.72	**4.0E-02**	0.28	5.7E-01
CG4860	FBgn0037999	0.18	9.8E-01	0.41	7.5E-01	3.23	**1.1E-05**	3.00	**1.8E-04**
CG5002	FBgn0034275	-0.22	9.4E-01	-1.36	**5.4E-03**	0.29	6.9E-01	1.43	**3.1E-03**
CG5013	FBgn0038396	-0.12	9.9E-01	0.21	8.7E-01	3.13	**4.9E-06**	2.79	**1.8E-04**
CG5084	FBgn0034288	-4.32	**3.1E-04**	-4.54	**9.4E-06**	0.35	8.7E-01	0.58	7.5E-01
CG5261	FBgn0031912	0.29	4.7E-01	0.23	2.8E-01	-0.63	**9.0E-05**	-0.58	**1.0E-03**
CG5282	FBgn0036986	-1.13	6.5E-01	-1.80	5.5E-02	1.36	1.2E-01	2.03	**2.1E-02**
CG5382	FBgn0038950	-0.11	9.8E-01	-0.63	3.2E-01	1.14	**2.5E-02**	1.65	**1.2E-03**
CG5397	FBgn0031327	0.19	9.7E-01	0.09	9.6E-01	3.45	**2.3E-07**	3.55	**7.6E-07**
CG5399	FBgn0038353	-1.46	2.5E-01	0.47	6.5E-01	3.20	**7.2E-07**	1.26	1.1E-01
CG5412	FBgn0038806	-0.11	9.9E-01	-0.15	9.1E-01	2.80	**2.0E-05**	2.83	**6.7E-05**
CG5522	FBgn0034158	0.26	8.6E-01	0.33	5.1E-01	-0.97	**7.7E-03**	-1.04	**6.8E-03**
CG5525	FBgn0032444	-0.14	9.8E-01	-0.50	6.0E-01	2.19	**4.8E-04**	2.55	**1.3E-04**
CG5535	FBgn0036764	-0.10	9.9E-01	-1.25	7.3E-02	0.91	1.7E-01	2.06	**7.3E-04**
CG5715	FBgn0039180	7.57	**9.0E-20**	1.11	3.7E-01	-1.78	5.4E-02	4.68	**2.1E-07**
CG5721	FBgn0034315	-0.02	1.0E+00	0.38	7.1E-01	2.66	**1.2E-05**	2.26	**6.5E-04**
CG5767	FBgn0034292	-3.88	**3.0E-03**	-3.89	**3.0E-04**	1.01	5.0E-01	1.02	4.9E-01
CG5770	FBgn0034291	-3.37	**1.1E-02**	-3.13	**3.5E-03**	1.30	3.1E-01	1.07	4.4E-01
CG5773	FBgn0034290	0.49	7.6E-01	-1.11	**1.6E-02**	-2.99	**2.4E-15**	-1.38	**1.8E-03**
CG5846	FBgn0032171	-0.39	9.3E-01	-0.10	9.5E-01	3.10	**5.8E-06**	2.81	**1.6E-04**
CG6180	FBgn0032453	0.10	9.9E-01	0.01	1.0E+00	3.01	**2.7E-05**	3.10	**6.4E-05**
CG6195	FBgn0038723	-0.31	9.3E-01	-0.28	7.9E-01	1.95	**7.5E-04**	1.91	**2.0E-03**
CG6236	FBgn0038318	0.17	9.7E-01	-0.38	6.9E-01	1.88	**1.9E-03**	2.43	**1.2E-04**
CG6414	FBgn0029690	-0.38	9.5E-01	-1.64	1.3E-01	2.09	**1.7E-02**	3.35	**2.1E-04**
CG6495	FBgn0027550	-0.71	8.5E-01	-2.42	**1.7E-02**	1.06	3.5E-01	2.77	**4.4E-03**
CG6610	FBgn0035675	-0.23	9.6E-01	-0.36	7.5E-01	2.27	**5.9E-04**	2.41	**6.1E-04**

		F3IN vs. S3IN		F3IN vs. FWPP		S3IN vs. SWPP		FWPP vs. SWPP	
sym	*FBgn*	*Δlog2*	*padj*	*Δlog2*	*padj*	*Δlog2*	*padj*	*Δlog2*	*padj*
CG6617	FBgn0030944	-0.37	9.0E-01	0.19	8.5E-01	2.41	**2.0E-05**	1.85	**2.7E-03**
CG6833	FBgn0036405	-0.47	7.5E-01	-0.15	8.2E-01	1.23	**1.3E-03**	0.91	**3.3E-02**
CG7006	FBgn0039233	-0.26	9.6E-01	-0.69	4.2E-01	2.10	**7.0E-04**	2.53	**1.2E-04**
CG7048	FBgn0038976	-0.19	9.5E-01	0.01	9.9E-01	1.56	**1.9E-04**	1.36	**2.8E-03**
CG7101	FBgn0030963	-0.54	6.9E-01	-1.07	**1.9E-02**	0.45	3.8E-01	0.99	**3.3E-02**
CG7646	FBgn0036926	-0.69	7.0E-01	-0.68	3.1E-01	1.63	**1.2E-03**	1.63	**2.5E-03**
CG7985	FBgn0028499	0.04	1.0E+00	-1.01	2.9E-01	2.20	**2.0E-03**	3.25	**1.8E-05**
CG8010	FBgn0031008	0.02	1.0E+00	-0.45	6.2E-01	1.71	**4.3E-03**	2.18	**4.9E-04**
CG8078	FBgn0033375	0.10	9.9E-01	-0.10	9.5E-01	2.72	**6.1E-05**	2.92	**6.4E-05**
CG8111	FBgn0035825	0.20	9.7E-01	-0.09	9.5E-01	2.22	**2.4E-04**	2.50	**1.0E-04**
CG8273	FBgn0037716	0.47	2.9E-01	0.39	1.8E-01	-0.48	5.4E-02	-0.39	1.6E-01
CG8321	FBgn0033677	-0.68	3.3E-01	-0.51	2.5E-01	0.80	**2.4E-02**	0.63	1.1E-01
CG8386	FBgn0034061	-0.18	9.7E-01	-0.26	8.2E-01	2.27	**1.9E-04**	2.36	**3.0E-04**
CG8399	FBgn0034067	-0.72	7.2E-01	-1.53	**1.2E-02**	0.81	2.2E-01	1.62	**6.9E-03**
CG8635	FBgn0033317	-0.13	9.8E-01	-0.26	8.2E-01	2.13	**6.0E-04**	2.26	**6.1E-04**
CG8675	FBgn0030834	-0.31	8.9E-01	-0.43	5.2E-01	1.41	**3.1E-03**	1.54	**2.3E-03**
CG8778	FBgn0033761	-0.07	1.0E+00	0.05	9.9E-01	2.88	**6.9E-05**	2.76	**4.1E-04**
CG8837	FBgn0031520	-1.12	2.6E-01	-2.04	**1.4E-04**	0.47	5.4E-01	1.39	**1.9E-02**
CG8952	FBgn0030688	-1.55	1.9E-01	-2.68	**8.7E-05**	0.42	7.1E-01	1.55	**4.7E-02**
CG9034	FBgn0040931	0.04	1.0E+00	0.03	9.9E-01	3.34	**4.8E-06**	3.35	**2.6E-05**
CG9135	FBgn0031769	-0.59	6.5E-01	-0.77	1.2E-01	0.87	**4.4E-02**	1.05	**1.8E-02**
CG9149	FBgn0035203	-0.19	9.7E-01	-0.01	9.9E-01	2.70	**5.8E-05**	2.52	**5.0E-04**
CG9338	FBgn0032899	-0.59	8.2E-01	-0.57	5.5E-01	2.48	**1.3E-04**	2.46	**4.2E-04**
CG9372	FBgn0036891	0.07	1.0E+00	0.13	9.2E-01	3.23	**2.8E-07**	3.18	**3.9E-06**
CG9422	FBgn0033092	-0.14	9.5E-01	-0.79	**3.2E-02**	0.52	1.5E-01	1.17	**6.0E-04**
CG9427	FBgn0037721	-0.75	7.9E-01	0.20	8.8E-01	3.06	**2.0E-05**	2.11	**7.8E-03**
CG9452	FBgn0036877	0.36	9.6E-01	1.30	2.8E-01	5.18	**1.8E-09**	4.24	**1.2E-05**
CG9521	FBgn0030588	-0.21	9.8E-01	-1.13	3.8E-01	2.73	**3.2E-03**	3.65	**2.6E-04**
CG9593	FBgn0038365	-0.92	7.6E-01	-1.26	2.3E-01	2.00	**1.4E-02**	2.34	**6.5E-03**
CG9682	FBgn0039760	-3.67	**9.7E-04**	-3.09	**1.6E-03**	1.37	2.2E-01	0.78	5.7E-01
CG9686	FBgn0030158	-0.98	4.5E-01	0.82	2.4E-01	2.84	**2.4E-08**	1.05	9.6E-02
CG9689	FBgn0030159	-0.43	9.3E-01	0.20	8.9E-01	3.96	**4.1E-08**	3.33	**3.3E-05**
CG9769	FBgn0037270	-0.06	1.0E+00	-0.37	7.3E-01	2.11	**7.8E-04**	2.41	**2.9E-04**
CG9914	FBgn0030737	-0.27	8.9E-01	1.96	**7.9E-07**	0.04	9.7E-01	-2.19	**2.2E-07**
CHOp24	FBgn0029709	-0.05	1.0E+00	-0.49	6.4E-01	2.13	**1.6E-03**	2.57	**2.9E-04**
Chrac-16	FBgn0043001	-0.05	1.0E+00	-0.38	7.1E-01	2.07	**8.5E-04**	2.39	**2.9E-04**
Cht2	FBgn0022702	-0.25	9.6E-01	-0.46	6.9E-01	2.89	**2.6E-05**	3.09	**3.3E-05**
Cog7	FBgn0051040	-0.50	4.5E-01	-0.87	**3.7E-03**	0.46	1.6E-01	0.83	**7.0E-03**
colt	FBgn0019830	-0.19	9.6E-01	-0.52	5.2E-01	1.60	**5.8E-03**	1.92	**1.4E-03**
COX5A	FBgn0019624	-0.03	1.0E+00	0.07	9.8E-01	2.82	**3.7E-05**	2.72	**2.4E-04**

		F3IN vs. S3IN		F3IN vs. FWPP		S3IN vs. SWPP		FWPP vs. SWPP	
sym	*FBgn*	*Δlog2*	*padj*	*Δlog2*	*padj*	*Δlog2*	*padj*	*Δlog2*	*padj*
CR30055	FBgn0050055	-0.45	6.2E-01	-0.08	8.8E-01	1.08	**1.3E-04**	0.71	**2.3E-02**
CR32111	FBgn0052111	-1.22	4.6E-01	-1.51	7.0E-02	1.49	**4.1E-02**	1.78	**2.1E-02**
CR32207	FBgn0052207	1.05	6.6E-01	-0.31	8.1E-01	2.47	**6.1E-04**	3.83	**2.3E-07**
CR42491	FBgn0259993	-0.33	8.8E-01	-0.78	2.1E-01	1.46	**2.3E-03**	1.91	**1.5E-04**
CR43264	FBgn0262945	-0.17	9.8E-01	0.54	6.1E-01	3.22	**1.2E-06**	2.52	**5.7E-04**
CR43957	FBgn0264617	-0.62	8.4E-01	0.04	9.9E-01	3.85	**1.6E-08**	3.19	**2.6E-05**
CR43995	FBgn0264727	-0.52	8.4E-01	-0.82	3.2E-01	1.60	**1.3E-02**	1.90	**4.6E-03**
CR44145	FBgn0264994	-1.88	5.4E-02	-0.52	5.8E-01	2.40	**2.0E-04**	1.03	1.8E-01
CR45140	FBgn0266633	-1.17	4.9E-01	-1.71	**3.3E-02**	1.48	**4.1E-02**	2.02	**7.3E-03**
crok	FBgn0032421	-0.20	9.6E-01	0.27	8.1E-01	2.69	**5.8E-06**	2.22	**6.0E-04**
Csat	FBgn0024994	-0.65	1.8E-01	-1.14	**5.2E-05**	-0.11	8.4E-01	0.38	3.0E-01
Cyp12a4	FBgn0038681	-1.13	8.2E-02	-2.99	**1.8E-14**	-1.00	**2.6E-02**	0.86	9.2E-02
Cyp28d1	FBgn0031689	0.22	9.1E-01	-1.35	**3.2E-04**	-2.81	**4.8E-17**	-1.24	**1.8E-03**
Cyp4d14	FBgn0023541	0.85	3.3E-01	0.40	5.1E-01	-1.17	**7.4E-03**	-0.72	1.6E-01
dbe	FBgn0020305	-0.25	8.8E-01	-0.48	3.1E-01	0.88	**1.6E-02**	1.11	**3.4E-03**
Dbp21E2	FBgn0086130	-0.17	8.7E-01	-1.13	**6.7E-06**	0.04	9.5E-01	1.00	**2.7E-04**
dgt2	FBgn0032390	-0.40	9.0E-01	-0.21	8.5E-01	2.35	**1.1E-04**	2.16	**9.6E-04**
Dhfr	FBgn0004087	0.28	9.6E-01	0.02	9.9E-01	3.13	**4.4E-06**	3.40	**3.9E-06**
Dip-C	FBgn0000455	0.01	1.0E+00	0.35	7.5E-01	2.74	**9.9E-06**	2.40	**3.8E-04**
dj-1beta	FBgn0039802	0.36	9.4E-01	-0.04	9.9E-01	2.72	**1.5E-04**	3.12	**5.2E-05**
Doc2	FBgn0035956	-0.80	7.6E-01	-1.52	6.8E-02	1.18	1.2E-01	1.90	**1.2E-02**
Doc3	FBgn0035954	-1.11	2.8E-01	-0.85	2.1E-01	1.21	**3.0E-02**	0.95	1.3E-01
Dph5	FBgn0024558	0.01	1.0E+00	-0.54	5.6E-01	1.94	**2.2E-03**	2.50	**1.8E-04**
Dpit47	FBgn0266518	-0.26	9.3E-01	-0.56	4.0E-01	1.48	**2.5E-03**	1.78	**5.3E-04**
dpr7	FBgn0053481	-0.56	8.9E-01	-1.98	5.1E-02	1.44	1.4E-01	2.86	**1.8E-03**
dUTPase	FBgn0250837	-0.46	8.6E-01	-0.65	4.6E-01	2.37	**1.2E-04**	2.56	**1.1E-04**
E(spl)m2-BFM	FBgn0002592	-0.82	6.9E-01	-0.75	3.4E-01	1.47	**1.6E-02**	1.40	**3.4E-02**
E(spl)m3-HLH	FBgn0002609	-0.92	4.8E-01	-0.66	3.4E-01	1.44	**7.0E-03**	1.18	**4.7E-02**
E(spl)mdelta-HLH	FBgn0002734	-0.95	6.8E-01	-1.60	**4.8E-02**	0.90	2.8E-01	1.55	**4.9E-02**
e(y)2	FBgn0000618	-0.13	9.8E-01	0.12	9.3E-01	2.60	**2.1E-05**	2.35	**4.0E-04**
Eh	FBgn0000564	-1.21	7.6E-01	-2.00	1.3E-01	2.25	**4.5E-02**	3.03	**7.3E-03**
elB	FBgn0004858	-1.15	8.9E-02	-1.52	**9.4E-04**	0.34	6.3E-01	0.70	2.0E-01
epsilonCOP	FBgn0027496	-0.27	9.6E-01	-0.42	7.3E-01	2.91	**5.1E-05**	3.06	**7.8E-05**
ETHR	FBgn0038874	-2.73	**2.9E-03**	-4.25	**9.5E-09**	-0.83	4.3E-01	0.69	5.8E-01
FER	FBgn0000723	-0.98	1.0E-01	-1.03	**1.6E-02**	0.68	1.2E-01	0.72	1.1E-01
Fib	FBgn0003062	-0.18	9.7E-01	-0.63	5.1E-01	2.13	**1.7E-03**	2.59	**3.1E-04**
fsd	FBgn0033813	-0.04	1.0E+00	0.17	8.9E-01	2.93	**9.0E-06**	2.71	**1.5E-04**
Fuca	FBgn0036169	0.27	8.4E-01	0.08	8.9E-01	-1.29	**7.3E-05**	-1.09	**1.9E-03**
FucT6	FBgn0030327	-0.20	9.6E-01	-0.93	2.0E-01	1.30	**3.0E-02**	2.03	**6.9E-04**
fy	FBgn0001084	-0.66	5.7E-01	-0.48	3.9E-01	1.29	**1.5E-03**	1.10	**1.3E-02**

		F3IN vs. S3IN		F3IN vs. FWPP		S3IN vs. SWPP		FWPP vs. SWPP	
sym	*FBgn*	*Δlog2*	*padj*	*Δlog2*	*padj*	*Δlog2*	*padj*	*Δlog2*	*padj*
Gale	FBgn0035147	-0.68	6.0E-01	-1.73	**6.6E-05**	0.07	9.4E-01	1.12	**1.9E-02**
GILT1	FBgn0038149	-0.48	8.3E-01	-1.09	1.1E-01	1.43	**1.3E-02**	2.05	**5.0E-04**
Glg1	FBgn0264561	0.24	7.5E-01	-0.07	8.4E-01	-0.80	**2.2E-05**	-0.50	**2.1E-02**
Gpdh	FBgn0001128	0.45	7.7E-01	-0.02	9.9E-01	-1.79	**3.4E-06**	-1.32	**2.0E-03**
grnd	FBgn0032682	-0.74	6.8E-01	-0.92	1.7E-01	1.25	**2.2E-02**	1.43	**1.2E-02**
grp	FBgn0261278	-0.41	7.5E-01	-0.59	1.7E-01	0.71	5.0E-02	0.89	**1.7E-02**
GstE13	FBgn0033381	0.35	9.2E-01	-0.77	3.4E-01	2.05	**6.2E-04**	3.17	**2.4E-07**
GstS1	FBgn0010226	0.08	9.6E-01	-0.07	8.4E-01	-0.87	**1.3E-05**	-0.71	**9.9E-04**
Gtp-bp	FBgn0010391	-0.13	9.8E-01	-1.27	1.4E-01	1.75	**1.3E-02**	2.89	**5.2E-05**
Gycalpha99B	FBgn0013972	-0.25	9.6E-01	-1.56	**4.3E-02**	0.77	3.2E-01	2.09	**2.9E-03**
Hakai	FBgn0032812	-0.39	8.4E-01	-0.65	3.0E-01	1.18	**1.6E-02**	1.44	**4.4E-03**
He	FBgn0028430	-0.05	1.0E+00	-0.96	3.5E-01	2.15	**6.5E-03**	3.05	**1.8E-04**
Hel25E	FBgn0014189	-0.18	9.1E-01	-0.48	2.1E-01	0.62	5.4E-02	0.92	**3.7E-03**
Herp	FBgn0031950	0.61	1.0E-01	-0.44	1.5E-01	-1.34	**2.6E-09**	-0.29	3.6E-01
His4r	FBgn0013981	-0.34	9.2E-01	-0.24	8.2E-01	2.32	**6.1E-05**	2.22	**3.7E-04**
hng1	FBgn0034599	0.03	1.0E+00	-0.03	9.9E-01	2.84	**2.7E-05**	2.90	**7.9E-05**
hoe2	FBgn0031649	-2.85	**4.1E-03**	-4.42	**7.5E-09**	-1.08	2.9E-01	0.49	7.3E-01
hoip	FBgn0015393	-0.29	9.2E-01	-0.84	1.9E-01	1.07	**4.6E-02**	1.61	**2.5E-03**
HP1b	FBgn0030082	-0.27	9.3E-01	-0.56	4.0E-01	1.64	**7.7E-04**	1.94	**1.8E-04**
HP1c	FBgn0039019	-0.37	9.2E-01	-0.19	8.7E-01	2.42	**1.0E-04**	2.24	**8.1E-04**
Hs3st-B	FBgn0031005	-0.90	7.9E-01	-2.38	**2.6E-02**	1.25	2.6E-01	2.73	**7.2E-03**
Hsc70-3	FBgn0001218	0.71	5.4E-01	-0.14	8.6E-01	-1.79	**1.9E-05**	-0.94	5.5E-02
Hsc70-5	FBgn0001220	0.51	1.9E-01	-0.02	9.7E-01	-0.91	**2.0E-05**	-0.39	1.4E-01
HSPC300	FBgn0061198	-0.18	9.7E-01	0.46	6.4E-01	2.96	**1.4E-06**	2.31	**5.9E-04**
ImpE3	FBgn0001255	-0.87	7.5E-01	-0.02	9.9E-01	3.04	**6.8E-06**	2.19	**3.2E-03**
in	FBgn0001259	-0.57	8.2E-01	-0.97	2.4E-01	1.53	**1.9E-02**	1.93	**4.4E-03**
iPLA2-VIA	FBgn0036053	1.36	**1.3E-06**	-0.20	6.2E-01	-1.37	**7.7E-08**	0.19	6.6E-01
lpod	FBgn0030187	1.15	5.0E-01	0.51	6.2E-01	-2.40	**7.6E-04**	-1.77	**3.0E-02**
jbug	FBgn0028371	-0.82	3.0E-01	-1.29	**2.3E-03**	0.16	8.4E-01	0.63	2.0E-01
Jhl-21	FBgn0028425	-0.53	6.7E-01	-0.75	1.0E-01	0.64	1.3E-01	0.86	**4.1E-02**
kar	FBgn0001296	-1.36	**3.0E-03**	0.08	9.1E-01	1.80	**3.0E-07**	0.37	4.7E-01
l(2)34Fc	FBgn0261534	-0.32	9.6E-01	0.58	6.4E-01	3.71	**1.3E-06**	2.81	**8.1E-04**
l(2)35Be	FBgn0261881	0.02	1.0E+00	0.03	9.9E-01	2.65	**5.0E-05**	2.64	**1.8E-04**
l(3)01239	FBgn0010741	-0.27	8.6E-01	-0.29	5.8E-01	1.15	**8.9E-04**	1.17	**1.6E-03**
Lcp3	FBgn0002534	-0.93	8.0E-01	-4.32	**4.7E-06**	-0.25	9.0E-01	3.15	**2.3E-03**
LKRSDH	FBgn0025687	0.81	5.8E-02	-0.68	**3.9E-02**	0.54	8.5E-02	2.04	**5.4E-14**
Lmpt	FBgn0261565	-1.19	**2.4E-05**	0.29	3.9E-01	-1.15	**9.8E-06**	-2.63	**8.9E-29**
Lon	FBgn0036892	0.23	7.8E-01	0.31	2.7E-01	-0.47	**4.1E-02**	-0.56	**2.1E-02**
Lpin	FBgn0263593	0.60	4.9E-01	0.21	7.1E-01	-1.30	**1.3E-04**	-0.92	**1.6E-02**
LSm7	FBgn0261068	-0.19	9.7E-01	-0.34	7.7E-01	2.81	**1.9E-05**	2.97	**3.3E-05**

		F3IN vs. S3IN		*F3IN vs. FWPP*		*S3IN vs. SWPP*		*FWPP vs. SWPP*	
sym	*FBgn*	*Δlog2*	*padj*	*Δlog2*	*padj*	*Δlog2*	*padj*	*Δlog2*	*padj*
mab-21	FBgn0029003	-0.86	7.1E-01	-1.05	2.1E-01	1.83	**5.3E-03**	2.02	**3.3E-03**
mAChR-B	FBgn0037546	0.89	7.2E-01	1.98	**5.0E-03**	-1.70	**2.7E-02**	-2.79	**2.1E-04**
Mcm3	FBgn0024332	-0.48	8.7E-01	-0.26	8.3E-01	2.34	**3.9E-04**	2.13	**2.8E-03**
Mco1	FBgn0032116	0.76	6.6E-01	1.72	**1.5E-03**	-0.65	3.4E-01	-1.61	**3.7E-03**
Mctp	FBgn0034389	0.39	8.3E-01	1.92	**2.0E-05**	-0.09	9.3E-01	-1.61	**8.2E-04**
MED21	FBgn0040020	-0.18	9.4E-01	-0.26	6.6E-01	1.31	**2.7E-04**	1.39	**3.2E-04**
MED4	FBgn0035754	0.06	1.0E+00	-0.01	9.9E-01	2.49	**7.9E-05**	2.56	**1.6E-04**
MFS9	FBgn0038799	-1.60	3.7E-01	-4.70	**6.4E-09**	0.06	9.7E-01	3.15	**5.4E-04**
Mipp2	FBgn0026060	0.18	8.7E-01	0.46	1.5E-01	-0.55	**4.8E-02**	-0.83	**2.7E-03**
mira	FBgn0021776	-0.70	8.4E-01	-3.01	**6.1E-04**	0.03	9.9E-01	2.34	**1.3E-02**
mnd	FBgn0002778	-0.91	1.3E-01	-1.13	**5.0E-03**	0.60	1.7E-01	0.81	5.9E-02
Mocs1	FBgn0263241	-0.10	9.7E-01	0.77	**3.2E-02**	-0.60	1.1E-01	-1.47	**1.8E-05**
MRE16	FBgn0267910	-0.05	1.0E+00	0.25	8.6E-01	4.26	**1.1E-08**	3.96	**1.1E-06**
mrn	FBgn0261109	-0.02	1.0E+00	-0.26	8.2E-01	2.16	**7.3E-04**	2.40	**4.2E-04**
mRpL2	FBgn0036135	-0.13	9.8E-01	-0.17	9.0E-01	2.59	**1.2E-04**	2.63	**2.9E-04**
mRpL20	FBgn0036335	-0.14	9.7E-01	-0.43	5.1E-01	1.28	**5.5E-03**	1.58	**1.1E-03**
mRpL21	FBgn0036853	-0.30	9.3E-01	-0.10	9.3E-01	1.97	**4.1E-04**	1.77	**3.2E-03**
mRpL23	FBgn0035335	-0.27	8.9E-01	-0.45	4.3E-01	1.06	**1.2E-02**	1.23	**5.4E-03**
mRpL27	FBgn0053002	-0.31	9.5E-01	-0.33	7.9E-01	2.63	**9.8E-05**	2.65	**2.7E-04**
mRpL30	FBgn0029718	0.00	1.0E+00	-0.07	9.7E-01	2.48	**9.2E-05**	2.55	**1.8E-04**
mRpL34	FBgn0083983	-0.18	9.8E-01	0.16	9.2E-01	3.26	**6.5E-06**	2.93	**2.0E-04**
mRpL36	FBgn0042112	-0.09	9.9E-01	0.10	9.5E-01	2.53	**8.7E-05**	2.34	**7.4E-04**
mRpL4	FBgn0001995	-0.24	9.5E-01	-0.51	4.9E-01	1.45	**5.8E-03**	1.72	**1.8E-03**
mRpL40	FBgn0037892	-0.19	9.6E-01	-0.14	9.0E-01	2.10	**1.7E-04**	2.05	**6.5E-04**
mRpL42	FBgn0033480	-0.34	9.3E-01	0.01	9.9E-01	2.39	**8.7E-05**	2.03	**2.1E-03**
mRpL46	FBgn0035272	0.10	9.9E-01	0.07	9.8E-01	3.05	**1.5E-05**	3.08	**5.5E-05**
mRpL49	FBgn0030433	-0.40	8.9E-01	-0.53	5.5E-01	2.18	**2.7E-04**	2.30	**3.2E-04**
mRpL51	FBgn0032053	-0.19	9.7E-01	-0.23	8.3E-01	1.96	**6.8E-04**	2.00	**1.1E-03**
mRpL52	FBgn0033208	-0.16	9.7E-01	0.14	9.0E-01	2.41	**2.9E-05**	2.11	**7.3E-04**
mRpS14	FBgn0044030	-0.36	9.3E-01	0.20	8.7E-01	2.80	**1.4E-05**	2.23	**1.5E-03**
mRpS21	FBgn0044511	-0.17	9.7E-01	0.04	9.9E-01	2.74	**1.9E-05**	2.53	**2.8E-04**
mRpS25	FBgn0030572	-0.13	9.8E-01	-0.02	9.9E-01	2.50	**5.2E-05**	2.39	**3.4E-04**
mRpS26	FBgn0036774	-0.26	9.6E-01	-0.54	6.0E-01	2.42	**3.1E-04**	2.69	**1.7E-04**
msd1	FBgn0035209	-0.50	8.5E-01	-0.16	8.9E-01	2.34	**1.7E-04**	2.00	**3.0E-03**
msd5	FBgn0035210	-0.38	9.2E-01	-0.31	7.9E-01	2.22	**4.7E-04**	2.15	**1.6E-03**
mthl9	FBgn0035131	-0.92	5.7E-02	-1.23	**2.5E-04**	0.03	9.7E-01	0.33	4.9E-01
ND-30	FBgn0266582	-0.10	9.9E-01	0.08	9.7E-01	2.94	**1.8E-05**	2.76	**2.0E-04**
ND-AGGG	FBgn0058002	-0.23	9.6E-01	0.10	9.4E-01	2.36	**4.5E-05**	2.03	**1.2E-03**
ND-B12	FBgn0034645	-0.07	1.0E+00	0.22	8.7E-01	3.46	**1.5E-06**	3.16	**5.8E-05**
ND-B14.5A	FBgn0025839	-0.18	9.8E-01	0.07	9.8E-01	3.47	**1.8E-06**	3.23	**5.2E-05**

		F3IN vs. S3IN		F3IN vs. FWPP		S3IN vs. SWPP		FWPP vs. SWPP	
sym	*FBgn*	*Δlog2*	*padj*	*Δlog2*	*padj*	*Δlog2*	*padj*	*Δlog2*	*padj*
ND-B14.5B	FBgn0031505	-0.03	1.0E+00	0.10	9.6E-01	3.60	**1.5E-06**	3.47	**2.4E-05**
ND-B18	FBgn0030605	-0.19	9.7E-01	0.07	9.7E-01	2.59	**6.1E-05**	2.33	**8.4E-04**
ND-PDSW	FBgn0021967	-0.17	9.7E-01	-0.14	9.2E-01	2.44	**1.7E-04**	2.41	**5.7E-04**
Nep1	FBgn0029843	-1.22	3.0E-01	-1.70	**9.7E-03**	0.54	5.3E-01	1.02	1.6E-01
Nep3	FBgn0031081	-0.83	1.4E-01	-2.08	**3.6E-10**	-0.57	1.6E-01	0.68	1.1E-01
ng3	FBgn0010295	-1.90	4.6E-01	-3.03	**8.5E-03**	1.07	4.6E-01	2.19	7.1E-02
NimB1	FBgn0027929	-0.58	8.6E-01	-0.22	8.8E-01	3.11	**2.6E-05**	2.75	**6.1E-04**
NimB2	FBgn0028543	-0.12	9.9E-01	-2.01	**7.9E-03**	0.61	5.5E-01	2.50	**6.7E-04**
Nle	FBgn0021874	-0.11	9.8E-01	-0.87	2.8E-01	1.49	**2.1E-02**	2.24	**6.0E-04**
Not10	FBgn0260444	0.03	1.0E+00	-0.29	8.0E-01	2.20	**6.6E-04**	2.52	**2.5E-04**
Nup37	FBgn0039301	-0.54	7.2E-01	-0.66	2.1E-01	0.82	6.2E-02	0.95	**4.2E-02**
Nup43	FBgn0038609	-0.09	9.9E-01	-0.51	6.5E-01	2.96	**1.8E-05**	3.38	**5.7E-06**
Obp99a	FBgn0039678	-0.06	1.0E+00	-2.35	**1.1E-02**	1.20	2.4E-01	3.49	**9.0E-05**
obst-B	FBgn0027600	-0.79	7.5E-01	0.08	9.6E-01	2.68	**1.9E-05**	1.81	**9.2E-03**
obst-J	FBgn0036940	-3.03	**2.8E-02**	-2.11	7.5E-02	2.60	**1.0E-02**	1.69	1.5E-01
Orct2	FBgn0086365	-0.60	7.8E-01	-1.27	5.9E-02	0.79	2.4E-01	1.46	**2.0E-02**
oxt	FBgn0015360	0.20	8.6E-01	0.40	2.5E-01	-0.67	**1.6E-02**	-0.87	**2.4E-03**
Pal2	FBgn0262728	-0.86	7.7E-01	-1.66	7.9E-02	1.18	2.0E-01	1.98	**2.2E-02**
Pbgs	FBgn0036271	-0.07	1.0E+00	-1.21	1.5E-01	1.23	9.0E-02	2.37	**6.5E-04**
pch2	FBgn0051453	-0.13	9.7E-01	-0.15	8.7E-01	2.08	**1.5E-05**	2.10	**5.6E-05**
Pebp1	FBgn0038973	-2.41	1.3E-01	-2.90	**5.7E-03**	2.04	5.3E-02	2.53	**1.8E-02**
Pex19	FBgn0032407	0.28	9.5E-01	-0.21	8.5E-01	2.16	**6.0E-04**	2.66	**6.8E-05**
Pex7	FBgn0035922	-1.28	6.9E-01	-2.87	**6.0E-03**	0.50	7.7E-01	2.09	6.3E-02
Pgam5	FBgn0023517	-0.28	9.5E-01	-0.24	8.4E-01	2.19	**4.7E-04**	2.14	**1.4E-03**
Pgant35A	FBgn0001970	-0.21	9.7E-01	-0.17	8.9E-01	2.62	**3.6E-05**	2.58	**1.7E-04**
PIG-C	FBgn0035435	-0.01	1.0E+00	1.26	**1.2E-05**	0.03	9.7E-01	-1.25	**5.5E-05**
pncr013:4	FBgn0262731	0.06	1.0E+00	-0.12	9.0E-01	1.79	**3.4E-04**	1.97	**2.4E-04**
pnut	FBgn0013726	-0.52	3.3E-01	-0.16	7.1E-01	0.88	**6.3E-04**	0.52	8.2E-02
Prosbeta6	FBgn0002284	-0.11	8.8E-01	0.59	**2.6E-04**	-0.02	9.6E-01	-0.72	**1.8E-05**
Prp38	FBgn0050342	-0.16	9.7E-01	-0.17	8.8E-01	2.23	**1.5E-04**	2.24	**4.0E-04**
PSR	FBgn0038948	-0.23	9.6E-01	-0.08	9.6E-01	2.26	**3.3E-04**	2.11	**1.9E-03**
r-l	FBgn0003257	-0.50	7.6E-01	-0.81	1.3E-01	0.81	8.4E-02	1.11	**1.8E-02**
Rab23	FBgn0037364	-0.95	4.9E-01	-1.03	1.4E-01	1.11	6.3E-02	1.19	6.0E-02
RabX1	FBgn0015372	-0.70	6.5E-01	-1.35	**1.2E-02**	0.54	4.0E-01	1.18	**3.1E-02**
Rae1	FBgn0034646	-0.14	9.8E-01	-0.17	8.7E-01	1.84	**8.0E-04**	1.87	**1.4E-03**
Rbp1	FBgn0260944	-0.34	8.9E-01	-0.08	9.5E-01	1.91	**2.1E-04**	1.64	**3.3E-03**
rdgBbeta	FBgn0027872	0.62	4.7E-01	0.91	**2.0E-02**	-0.51	2.2E-01	-0.80	**4.3E-02**
ref(2)P	FBgn0003231	0.28	8.1E-01	0.08	8.8E-01	-1.03	**7.4E-04**	-0.83	**1.3E-02**
regucalcin	FBgn0030362	-0.12	9.8E-01	-0.75	4.3E-01	2.18	**1.7E-03**	2.81	**1.2E-04**
RNASEK	FBgn0262116	-0.21	9.6E-01	-0.03	9.9E-01	2.67	**2.0E-05**	2.48	**2.6E-04**

		F3IN vs. S3IN		F3IN vs. FWPP		S3IN vs. SWPP		FWPP vs. SWPP	
sym	*FBgn*	*Δlog2*	*padj*	*Δlog2*	*padj*	*Δlog2*	*padj*	*Δlog2*	*padj*
robl	FBgn0024196	-0.38	9.1E-01	0.08	9.6E-01	2.76	**6.5E-06**	2.30	**5.8E-04**
roX2	FBgn0019660	-0.60	8.3E-01	-0.56	5.9E-01	2.21	**1.7E-03**	2.16	**3.8E-03**
RPA3	FBgn0266421	0.08	9.9E-01	-0.37	7.1E-01	2.15	**4.1E-04**	2.60	**6.1E-05**
RpII18	FBgn0003275	-0.32	9.3E-01	-0.54	5.3E-01	2.00	**8.4E-04**	2.22	**5.0E-04**
RpII33	FBgn0026373	-0.65	7.0E-01	-0.29	7.0E-01	1.44	**2.7E-03**	1.09	**4.2E-02**
RpL11	FBgn0013325	-0.09	9.9E-01	-0.16	9.1E-01	2.47	**4.9E-04**	2.54	**7.6E-04**
RpL13A	FBgn0037351	0.10	9.9E-01	-0.21	8.7E-01	2.53	**3.8E-04**	2.84	**1.8E-04**
RpL23	FBgn0010078	0.06	1.0E+00	-0.10	9.6E-01	3.20	**2.1E-05**	3.36	**3.5E-05**
RpL27A	FBgn0261606	-0.06	1.0E+00	-0.27	8.3E-01	2.29	**7.1E-04**	2.50	**5.0E-04**
RpL36	FBgn0002579	0.05	1.0E+00	-0.11	9.5E-01	3.14	**2.1E-05**	3.31	**3.5E-05**
RpL38	FBgn0040007	0.09	9.9E-01	0.03	9.9E-01	2.73	**5.2E-05**	2.79	**1.2E-04**
RpL41	FBgn0066084	-0.02	1.0E+00	-0.21	8.6E-01	2.23	**8.0E-04**	2.42	**6.1E-04**
Rpn2	FBgn0028692	-0.09	9.4E-01	0.55	**4.5E-03**	-0.20	4.0E-01	-0.83	**9.6E-06**
Rpn5	FBgn0028690	-0.14	8.8E-01	0.73	**5.5E-04**	-0.03	9.4E-01	-0.91	**3.3E-05**
Rpn6	FBgn0028689	-0.20	7.6E-01	0.85	**4.1E-07**	0.20	3.9E-01	-0.85	**2.3E-06**
RpS12	FBgn0260441	-0.09	9.9E-01	-0.31	8.1E-01	2.45	**5.1E-04**	2.67	**3.9E-04**
RpS14b	FBgn0004404	0.04	1.0E+00	-0.16	9.0E-01	2.38	**4.6E-04**	2.59	**3.5E-04**
RpS15Ab	FBgn0033555	0.01	1.0E+00	-0.47	2.2E-01	0.66	**3.8E-02**	1.15	**3.0E-04**
Rrp4	FBgn0034879	-0.33	9.4E-01	-0.80	3.9E-01	2.28	**9.0E-04**	2.75	**1.6E-04**
Rrp40	FBgn0260648	-0.33	9.3E-01	-0.97	2.3E-01	1.64	**8.2E-03**	2.28	**4.5E-04**
Rsf1	FBgn0011305	-0.58	6.0E-01	-0.42	4.0E-01	1.09	**3.4E-03**	0.94	**2.2E-02**
rtet	FBgn0028468	-0.38	8.5E-01	-0.03	9.9E-01	2.20	**6.8E-07**	1.85	**1.4E-04**
rtv	FBgn0261277	-0.09	9.9E-01	0.06	9.8E-01	3.12	**7.3E-06**	2.97	**9.0E-05**
Sans	FBgn0033785	-0.97	4.9E-01	-0.40	6.4E-01	1.77	**1.4E-03**	1.20	5.7E-02
SC35	FBgn0265298	-0.20	9.7E-01	-0.25	8.4E-01	2.65	**3.8E-05**	2.70	**1.0E-04**
scb	FBgn0003328	-0.65	2.0E-01	-0.93	**2.1E-03**	0.25	5.5E-01	0.53	1.2E-01
Sce	FBgn0003330	-0.41	8.6E-01	-0.08	9.5E-01	2.03	**1.4E-04**	1.70	**3.3E-03**
Scgbeta	FBgn0038042	-0.78	8.0E-01	-2.22	**1.7E-02**	1.99	**1.8E-02**	3.43	**9.0E-05**
SdhC	FBgn0037873	-0.22	9.6E-01	0.05	9.8E-01	2.47	**1.1E-04**	2.20	**1.5E-03**
Sec13	FBgn0024509	-0.10	9.9E-01	-0.96	1.8E-01	1.11	7.0E-02	1.98	**8.4E-04**
SelG	FBgn0030350	-0.25	9.6E-01	-0.30	8.1E-01	2.66	**1.0E-04**	2.71	**2.5E-04**
sesB	FBgn0003360	-0.18	9.6E-01	-1.09	**4.3E-02**	0.79	1.3E-01	1.70	**4.9E-04**
Sgf11	FBgn0036804	-0.09	9.8E-01	-0.47	3.9E-01	1.16	**4.1E-03**	1.53	**2.9E-04**
Sgs7	FBgn0003377	-1.98	3.5E-01	-4.86	**5.0E-07**	-1.31	3.0E-01	1.58	2.0E-01
Sgs8	FBgn0003378	-1.67	5.6E-01	-3.78	**2.9E-04**	-0.11	9.7E-01	1.99	9.6E-02
Ski6	FBgn0032487	-0.23	9.6E-01	-0.15	9.0E-01	2.27	**3.0E-04**	2.19	**1.1E-03**
slif	FBgn0037203	-0.55	8.5E-01	-1.47	7.7E-02	1.06	1.9E-01	1.98	**7.6E-03**
slv	FBgn0025469	-0.65	4.4E-01	-0.51	2.7E-01	0.92	**1.2E-02**	0.78	5.4E-02
SmB	FBgn0262601	-0.10	9.9E-01	-0.44	7.1E-01	3.15	**7.9E-06**	3.49	**4.3E-06**
SmD2	FBgn0261789	-0.30	9.2E-01	-0.25	7.8E-01	1.76	**4.6E-04**	1.71	**1.6E-03**

		F3IN vs. S3IN		F3IN vs. FWPP		S3IN vs. SWPP		FWPP vs. SWPP	
sym	*FBgn*	*Δlog2*	*padj*	*Δlog2*	*padj*	*Δlog2*	*padj*	*Δlog2*	*padj*
SmF	FBgn0000426	-0.36	8.4E-01	-0.54	3.5E-01	1.17	**8.1E-03**	1.35	**3.4E-03**
Smyd5	FBgn0038869	0.37	8.8E-01	-1.06	1.1E-01	0.97	1.0E-01	2.39	**2.4E-05**
sol	FBgn0003464	-1.17	**7.7E-03**	-1.66	**4.2E-07**	0.04	9.6E-01	0.53	2.1E-01
Spase22-23	FBgn0039172	-0.39	7.0E-01	-0.95	**1.3E-03**	0.15	7.7E-01	0.71	**2.4E-02**
Spc25	FBgn0087021	-0.86	3.8E-01	-0.57	3.4E-01	1.51	**7.4E-04**	1.22	**1.3E-02**
spi	FBgn0005672	-0.93	**2.5E-02**	-1.81	**9.6E-11**	-0.19	7.0E-01	0.68	**4.6E-02**
SREBP	FBgn0261283	0.49	5.6E-01	0.24	5.9E-01	-0.97	**1.3E-03**	-0.72	**3.4E-02**
Srp19	FBgn0015298	-0.56	5.2E-01	-0.54	2.1E-01	0.78	**2.5E-02**	0.76	**4.4E-02**
Ssk	FBgn0036945	-1.14	3.4E-01	-0.39	6.6E-01	1.72	**2.8E-03**	0.97	1.5E-01
sta	FBgn0003517	-0.02	1.0E+00	-0.38	7.7E-01	2.47	**7.8E-04**	2.83	**2.9E-04**
sun	FBgn0014391	-0.26	9.6E-01	-0.10	9.5E-01	2.63	**4.2E-05**	2.47	**3.8E-04**
sut2	FBgn0028562	-0.23	9.7E-01	-2.07	**2.6E-02**	1.61	5.5E-02	3.44	**5.6E-05**
Syx16	FBgn0031106	-0.33	9.5E-01	0.16	9.1E-01	3.60	**7.6E-07**	3.11	**1.0E-04**
Syx8	FBgn0036643	-0.34	9.2E-01	-0.30	7.6E-01	1.84	**1.5E-03**	1.80	**3.5E-03**
T-cp1	FBgn0003676	-0.21	9.6E-01	-0.39	6.6E-01	2.11	**2.2E-04**	2.29	**1.8E-04**
Tace	FBgn0039734	-0.40	9.5E-01	-1.22	3.0E-01	2.05	**2.7E-02**	2.87	**2.3E-03**
tap	FBgn0015550	-1.10	7.8E-01	-3.00	**6.6E-03**	0.51	7.8E-01	2.41	**3.6E-02**
tko	FBgn0003714	-0.28	9.1E-01	-0.13	8.7E-01	1.61	**4.6E-04**	1.46	**3.1E-03**
toe	FBgn0036285	-2.12	8.9E-02	-2.32	**8.9E-03**	1.01	3.3E-01	1.21	2.4E-01
Tom	FBgn0026320	-0.64	8.0E-01	-0.63	5.1E-01	1.91	**5.7E-03**	1.90	**9.8E-03**
Tsp26A	FBgn0031760	-0.71	1.2E-01	-0.32	4.0E-01	0.77	**8.7E-03**	0.38	2.9E-01
Tsp2A	FBgn0024361	-0.88	5.2E-01	-0.38	6.3E-01	1.62	**2.1E-03**	1.12	6.1E-02
Tsp42Ea	FBgn0029508	-0.99	5.8E-01	-0.24	8.3E-01	2.34	**1.1E-04**	1.60	**1.9E-02**
Tspo	FBgn0031263	0.38	9.2E-01	-0.57	5.5E-01	1.95	**3.4E-03**	2.90	**2.9E-05**
TwdlG	FBgn0037225	0.01	1.0E+00	0.87	4.5E-01	-2.12	**3.0E-02**	-2.98	**2.2E-03**
Uhg4	FBgn0083124	-0.53	8.0E-01	-0.75	3.1E-01	1.59	**4.9E-03**	1.81	**2.3E-03**
Updo	FBgn0033428	-0.19	9.7E-01	-0.13	9.3E-01	2.70	**7.0E-05**	2.65	**2.9E-04**
UQCR-6.4	FBgn0034245	-0.18	9.6E-01	-0.10	9.3E-01	1.86	**4.9E-04**	1.78	**1.8E-03**
Usp14	FBgn0032216	-0.04	9.8E-01	0.73	**1.2E-03**	-0.06	8.9E-01	-0.83	**2.9E-04**
Vha36-1	FBgn0022097	-0.13	9.8E-01	-0.17	8.9E-01	2.55	**7.1E-05**	2.59	**1.8E-04**
Vmat	FBgn0260964	-0.70	8.5E-01	-2.00	5.6E-02	1.28	2.1E-01	2.58	**6.7E-03**
Vps45	FBgn0261049	-0.03	1.0E+00	-0.09	9.3E-01	1.83	**9.8E-05**	1.89	**1.9E-04**
wbl	FBgn0004003	-0.48	8.8E-01	-0.05	9.9E-01	2.54	**2.0E-04**	2.11	**4.4E-03**
WDR79	FBgn0031782	0.09	9.9E-01	-0.29	8.2E-01	2.59	**1.6E-04**	2.96	**5.7E-05**
wuho	FBgn0029857	-0.11	9.9E-01	-0.17	8.9E-01	2.76	**2.5E-05**	2.83	**6.4E-05**
x16	FBgn0028554	-0.35	8.0E-01	-0.63	1.7E-01	0.94	**1.2E-02**	1.22	**1.5E-03**
Xrp1	FBgn0261113	0.41	7.7E-01	0.89	**4.0E-02**	-0.64	1.4E-01	-1.11	**5.7E-03**
yellow-e2	FBgn0038151	-0.48	9.2E-01	-0.98	3.7E-01	2.14	**9.3E-03**	2.64	**2.3E-03**
YT521-B	FBgn0027616	-0.21	9.2E-01	-0.47	3.3E-01	0.87	**2.4E-02**	1.13	**4.0E-03**

CURRICULUM VITAE

Christopher Hardy, Ph.D.

christopher.hardy@unlv.edu
(858) 229-3658

Education

2004-2008	B.S. in Biological Sciences from the University of California, Irvine
2010-2016	Ph.D. in Biology from the University of Nevada, Las Vegas

Publications

2015	**Hardy CM, Birse RT, Wolf MJ, Yu L, Bodmer R, Gibbs AG**. Obesity-associated cardiac dysfunction in starvation-selected *Drosophila melanogaster*. *American Journal of Physiology - Regulatory, Integrative and Comparative Physiology* 309: R658–R667, 2015.
2016	(Submitted) **Hardy CM, Burke M, Han M, Everett L, Lantz K, Gibbs AG.** Genome-wide Analysis of Starvation-selected *Drosophila melanogaster*- a Genetic Model of Obesity.

Employment

2002-2005	Physics Tutor MESA Program (Mathematics Engineering Science Achievement Program for educationally underrepresented students), Santa Ana Community College
2007-2008	Physics Tutor at the UC Irvine Learning and Academic Resource Center
2008-2010	Laboratory Manager at Genescient Biotech: designed and performed experiments to find preventative medicines for aging, Huntington Beach CA.
2010-2014	Graduate Assistant, BIOL 196, BIOL 189 and BIOL 100, University of Nevada Las Vegas
2014-2016	Research Assistant, University of Nevada Las Vegas

Invited Talks

2015	56th Annual Drosophila Research Conference, Genetics Society of America, Chicago IL.
2015	Graduate College Research Reception, University of Nevada Las Vegas

Programming Languages

Python, R, UNIX-based command line tools

Honors/Awards

2006	Outstanding Team Captain, UC Irvine Rugby Organization
2007	Summer Undergraduate Research Program Fellow, University of California Irvine
2007-2008	Undergraduate Research Opportunity Program Fellow, University of California Irvine
2012	Phi Kappa Phi Chapter 100 Honors Fellow
2012	Graduate & Professional Student Association Grant Recipient, University of Nevada Las Vegas
2013	Graduate & Professional Student Association Research Forum Outstanding Presentation Award
2013	Graduate & Professional Student Association Grant Recipient, University of Nevada Las Vegas
2014	Terry Evans Scholarship Recipient
2014	Abstract-based Travel Award, American Physiological Society Intersociety Meeting: Comparative Approaches to Grand Challenges in Physiology.
2014	2nd Place Best Poster Competition, (75 Applicants) American Physiological Society Intersociety Meeting: Comparative Approaches to Grand Challenges in Physiology
2014	3rd Place Rebel Grad Slam Finalist, (64 Applicants). Present your thesis in 3 minutes or less to a general audience.
2015	UNLV Summer Session Scholarship
2015	Patricia Sastaunik Scholarship
2015	3rd Place Rebel Grad Slam Finalist, (70 Applicants). Present your thesis in 3 minutes or less to a general audience.

Poster Presentations

2014	**Hardy CM, Birse RT, Wolf MJ, Yu L, Bodmer R, Gibbs AG** "Obesity-associated Cardiac Dysfunction in Starvation-selected *Drosophila melanogaster*" American Physiological Society Intersociety Meeting: Comparative Approaches to Grand Challenges in Physiology.
2014	**Lantz K, Hardy CM, Andres A** "Rab GTPases and their role in glue secretion in the larval salivary gland." 55th Annual *Drosophila* Research Conference, Genetics Society of America.

Experience

2006-2010	University of California Irvine Science Internship: Laboratory Manager, Experiment Leader, Lab of Dr. Michael Rose
2012	Completed specialized course in RNA-Seq Bioinformatics Analysis, University of California Davis
2012-2014	President of BIOS, the School of Life Sciences Graduate Student Organization, University of Nevada Las Vegas.
2015	Student panelist at the UNLV graduate student orientation

Community Outreach

2005-2006	HOAG Hospital Clinical Care Extender Program
2011	Festival of Communities, showcased the advantages of *Drosophila* research to children (ages 5-18), University of Nevada Las Vegas
2012	Science Fair Judge for the Beal Bank USA Southern Nevada Regional Science & Engineering Fair (Elementary to High School aged participants).
2012	Hosting Calvary Chapel Christian High School students at University of Nevada Las Vegas, tour of the campus and educational outreach through discussion of personalized genetic medicine and individual DNA extraction experiment.
2013	Lectured on personalized genomic medicine and performed DNA isolation experiment with MESA (Math, Engineering and Science Achievement) student at Santa Ana Community College.
2014	"Genius Hour" Participant. Advised 4-5th grade students on their science projects.
2014	Lectured on personalized genetic medicine and performed sheep heart dissection with Biology Club at Clark High School, Las Vegas Nevada.
2014-2015	Teaming up with the Y.O.U. organization to help elementary school students at Zel & Mary Lowman Elementary School (Las Vegas, Nevada) enter and compete in local science fairs.
2015	Hosted Clark High School students at UNLV, tour of the campus and educational outreach through discussion of personalized genetic medicine and individual DNA extraction experiment.
2015	Interviewed by Las Vegas News Channel KSNV for story discussing results from "Obesity-induced Cardiac Dysfunction in Starvation-selected *Drosophila melanogaster*"
2014-Present	Founding member of Science Café Las Vegas, an organization dedicated to promoting scientific discussion on current events with the community.